Regulation of Skeletal Muscle Proteolysis

by
Adrian Slee

Thesis submitted to the
University of Nottingham
for the degree of
Doctor of Philosophy

January 2005

Division of Nutritional Sciences
School of Biosciences
University of Nottingham
Sutton Bonington Campus
Loughborough
Leicestershire
LE12 5RD

ACKNOWLEDGEMENTS

I wish to express my deep gratititude towards a number of people who have made this thesis possible.

First and foremost, my supervisor Dr Tim Parr for his continuous help, guidance and support over the past four years. His knowledge and understanding has been invaluable to me.

I wish to thank Professor Peter Buttery for the use of the Division of Nutritional Sciences laboratory and practical equipment and to Dr. G. Lee for use of the calf LD samples. I wish to also thank Dr. Ron Bardsley and Dr. Paul Sensky for use of the porcine LD samples.

I would also like to extend my thanks to all those at the Division of Nutritional Sciences, who have always been happy and willing to help me with my efforts and their friendship has made my time here a most enjoyable one.

I am also grateful to all my closest friends who I have met along the journey and who have reminded me of what is important in life. Finally, I am indebted to my parents for their lifelong support in all my endeavours in life.

ABSTRACT

Proteolysis is a component of protein turnover, controlled by multiple proteolytic systems. Alterations in system components within skeletal muscle has been associated with hypertrophy, remodelling, atrophy, apoptosis and metabolic dysregulation. Key components may have novel regulatory roles, e.g. calpain-3 and cathepsin-L. Experiments described within this thesis investigated the hypothesis that the gene expression of specific proteolytic system components within skeletal muscle may be co-ordinately regulated and altered during nutritional and pharmacological states known to modify protein turnover and induce muscle growth.

Gene expression for multiple components of the calpain system was analysed in calf LD (*Longissmus Dorsi*) by Quantitative Real-Time PCR in a plane of nutrition trial. There were three groups: low (LOW), high (HIGH) plane of nutrition and LOW to HIGH (REFED). Half of each group were slaughtered 48 hrs after refeeding, whilst the remainder were slaughtered 13 days later. Total RNA yield/g LD increased ($P < 0.05$) across all groups between slaughter dates. Calpain-3 expression increased in LOW and REFED and calpastatin in all groups between slaughter dates, with a trend towards significance ($P = 0.073$, $P = 0.085$, respectively). In the 1st slaughter, calpain-3 expression had a trend to be lower in the LOW group and values for REFED were similar to HIGH value level.

cDNA probes for unique and novel proteolytic system components were generated by RT-PCR and used to investigate the effects of acute and chronic β-adrenergic stimulation, on the gene expression of those specific components in pig LD, by northern blotting.

The β_2-adrenergic agonist clenbuterol (5 ppm) decreased glycogen levels (mg/g LD) ($P < 0.001$), increased cathepsin-L expression ($P < 0.001$) and increased E2G1 values numerically within 24 hrs of treatment. Cathepsin-L was unchanged by adrenaline administration. Calpain-3 was unchanged with either clenbuterol or adrenaline treatment.

The significance and implications of the data are discussed.

PUBLICATION

JONES SW, STEENAGE GR, SLEE A, SIMPSON EJ, BARDSLEY RG, PARR T and GREENHAFF PL. (2002) Resistance training induces the expression of calpain protease inhibitor calpastatin in human. *The Journal of Physiology* **543P** 86P.

TABLE OF CONTENTS

TABLE OF FIGURES

TABLE OF TABLES

ABBREVIATIONS

%	percentage
mg	milligram
g	gram
kg	kilogram
µg	microgram
w/v	weight per volume
kDa	kilo daltons
M	molar
mM	millimolar
µM	micromolar
ml	millilitre
µl	microlitre
mm	millimetre
cm	centimetre
cm^3	cubic centimetre
nm	nanometre
ME	metabolisable energy
rpm	revolutions per minute
°C	degrees celcius
OD	optical density
min	minute
sec	second
hr	hours
V	volts
NaOH	sodium hydroxide
NaCl	sodium chloride
Ca^{2+}	calcium ion
Tris	2 amino-2-(hydroxymethyl)-propane-1,3-diol
SDS	sodium dodecyl sulphate
β-ME	beta-mercaptoethanol
DMSO	dimethyl sulfoxide

DNA	deoxyribonucleic acid
dsDNA	double-stranded DNA
cDNA	complementary DNA
mRNA	messenger ribonucleic acid
PCR	polymerase chain reaction
RT-PCR	reverse-transcriptase PCR
LD	longissmus dorsi
α	alpha
β	beta

CHAPTER 1 INTRODUCTION

This thesis examines the effects of nutritional and pharmacological treatments-known to alter protein turnover and muscle growth, on the mRNA expression of various proteolytic system components within skeletal muscle. In addition it explores the development of experimental techniques to quantify the mRNA expression of a range of specific proteolytic system components within bovine and porcine skeletal muscle.

Skeletal muscle is a large functional metabolic tissue with a continuous flow and turnover of substrates and amino acids. The constituent cellular proteins exist in a dynamic state and are subject to characteristic turnover rates (Garrow, James and Ralph, 2000 c). Their 'steady-state' levels are thus maintained by a delicate balance of both protein synthesis and degradation (Doherty and Mayer, 1992 a). Intracellular protein degradation is a tightly controlled and highly regulated process, with multiple protease systems and their endogenous inhibitors working in concert to bring about the net process of cellular protein degradation.

Intracellular proteases involved in protein degradation, and thereby turnover have been identified within skeletal muscle and shown to play a role in the processes of muscle growth, wasting, remodelling and balance between life and death of the cell. The four intracellular protease systems to be discussed within this thesis include the lysosomal-cathepsin, calpain, ubiquitin-proteasome and caspase systems. Each system has specific roles within the cell selectively degrading proteins of intracellular, membrane and extracellular origin.

The lysosomal cathepsin system is predominantly involved in the bulk degradation of sarcoplasmic proteins whole to amino acids. Within the acidic environment of the lysosome there are a number of cathepsin endo-proteases that act on proteins in co-ordination with exopeptidases and di-and tri-peptidases (Doherty and Mayer, 1992 c). Under catabolic conditions the system may play a role in the degradation of cleaved myofibrillar proteins within skeletal muscle, leading ultimately to atrophy.

The calpain system comprises of non-lysosomal, calcium-dependent, neutral, cysteine proteases in skeletal muscle. The calpains are involved in specific cleavage events as opposed to bulk degradation of proteins whole to amino acids (Goll *et al*, 2003). Proteins of interest (within the scope of this thesis) degraded include cytoskeletal and myofibrillar proteins along with regulatory proteins. It has been suggested that the calpains may act as the rate-limiting step in myofibrillar breakdown (Goll *et al*, 2003). This process is altered during hypertrophy, remodelling and catabolic-atrophic conditions, in co-ordination with changes in the calpain system (Thompson and Palmer, 1998, Goll *et al*, 1998, Goll *et al*, 2003).

The ubiquitin-proteasome system degrades a large number of proteins whole to amino acids. Specific proteins targeted for degradation are 'tagged' with ubiquitin and transported to the proteasome (a multi-protease complex), with the aid of specific ubiquitin conjugation and ligase enzymes (Ciechanover *et al*, 2000, Glickman and Ciechanover, 2002). Within muscle, cleaved myofibrillar units are degraded by the system, with various system components up-regulated during catabolic, atrophic and remodelling conditions (Lecker *et al*, 1999, Jagoe and Goldberg, 2001).

The caspase system is composed of a number of highly specific cysteine proteases that are involved in the process of controlled cell death, apoptosis (Grimm, 2003d). The caspases cleave a number of regulatory and cytoskeletal proteins. They are constitutively expressed as inactive precursors and activated by caspase-mediated cleavage or autocleavage. Caspases are activated by diverse signals including: extracellular mediators (e.g. TNFα), mitochondrial and sarcoplasmic reticulum stress. This leads to the activation of the downstream caspases, that initiate the apoptotic pathway. Within skeletal muscle, the system may be activated under catabolic, atrophic and pathophysiological conditions, including myopathies and muscular dystrophies (Sandri and Carraro, 1999).

Experiments carried out within this thesis examined different methods to quantitatively measure mRNA gene expression changes within skeletal muscle of different species including: Real-Time Quantitative RT-PCR and the development of cDNA probes with the aim of utilising them in northern blot hybridisation's and/or a global approach like cDNA macroarrays.

Altered levels of dietary feeding and hence 'plane of nutrition' can have a significant effect on protein deposition in rapidly growing farm animals (Lee, 2001, Kristensen *et al*, 2002, Kristensen *et al*, 2004) During rapid growth phases where there is a high level of muscle remodelling and hypertrophy taking place, nutrition can have a sensitive effect on these processes. Of interest within the scope of this thesis is how an altered plane of nutrition alters proteolytic systems, which in turn may contribute to a net effect on protein -turnover and -deposition. Initial experiments carried out in this thesis were concerned specifically with the effects of altered plane of nutrition in growing calves on the mRNA gene expression of components of the calpain system within skeletal muscle.

The beta-adrenergic agonist class of compounds are known to act as nutrient repartitioning agents, inducing skeletal muscle hypertrophy and fat loss in adipose tissue when administered in chronic high doses in farm animals (Mersmann, 1998). It is believed that beta-adrenergic agonists such as clenbuterol achieve increases in muscle protein accretion through primarily decreasing cellular protein degradation. Alterations in the calpain-calpastatin system have been observed with beta-agonist treatment (Mersmann, 1998, Navegantes *et al*, 2002). There is limited information whether other proteolytic system components are altered with treatment and in turn how this may alter protein turnover and the hypertrophy process. Later experiments carried out in this thesis examined whether beta-adrenergic agonist administration would specifically alter the mRNA expression of key components of specific proteolytic systems within porcine skeletal muscle.

CHAPTER 2 LITERATURE REVIEW

2.1 INTRODUCTION

The area investigated within this thesis is that proteolytic systems within skeletal muscle are to some degree co-ordinately regulated in response to stimuli which alter muscle growth. Therefore, this review of the literature will firstly consider the structure, function and metabolic role of skeletal muscle. This leads to a description of the signals which alter muscle protein metabolism, with particular reference to those which affect muscle-protein catabolism. There is then an examination of the proteolytic systems which are likely to play a key role in skeletal muscle proteolysis.

2.2 SKELETAL MUSCLE STRUCTURE, FUNCTION AND PROTEIN METABOLISM

2.2.1 The Dual Function of Skeletal Muscle Tissue

Skeletal muscle may be viewed as possessing two separate functional roles controlled ultimately by the process of protein turnover; the balance between protein synthetic and protein degradative processes (Rooyackers and Nair, 1997, Liu and Barrett, 2002).

The first and most obvious function of skeletal muscle is that of its critical role in allowing biomechanical joint movement, force production and protection of organs/tissues (Voet and Voet, 1995a, Garrow, James and Ralph, 2000 a). Skeletal muscle is the largest tissue of the human body comprising ~40-45% of total body weight, ~50% of total body protein and ~70-80% of the cell mass (Rooyackers and Nair, 1997). It is made unique amongst other cell types by the presence of a network of structural proteins arranged in a fibrillar, 'lattice-like' structure. These proteins and the overall complex cell architecture act in concert to allow contractile activity and force production in response to neural stimuli from the neuro-muscular junction.

The second function is that skeletal muscle can be viewed in parallel as a large, dynamic, functional, metabolic pool/temporary store of amino acids that can be utilised

and partitioned into various pathways during daily functioning, stress and immune responses/reactions, cell damage and various pathophysiological conditions.

2.2.2 Cell Architecture

Many of the proteins that form the complex muscle cell architecture and are essential for contractile and regulatory functions are substrates for intracellular protease systems; and are possible substrates for subsequent amino acid repartitioning pathways.

Skeletal muscle consists of long cylindrical multinucleate cells called muscle fibers/myofibers, arranged in parallel. A single myofiber is composed of a number of parallel contractile myofibrillar subunits which in turn consist of sarcomere units, repeated longitudinally (see Figure 2.2.2-1). This 'myofibrillar lattice' consists of numerous structural proteins but there is three main fractions: 1) actin associated with tropomyosin and troponin (thin filament), 2) myosin (thick filament), and 3) titin and nebulin making up the cytoskeletal structure mainly (Voet and Voet, 1995a). Each sarcomere unit is bound at either end by a Z disk/Z line composed of α-actinin. The actin myofilaments are anchored and extend out from the Z line in both directions. The thick myosin filaments interdigitate with thin filaments, are able to slide over each other and have a point of contact via myosin head cross bridges. Myosin filaments are anchored centrally within the sarcomere to the M disk, composed of myosin, C-protein, and M-protein. Titin, (~3600-kD), extends from the thick filament, and M-disk, to the Z-line and may act as a 'spring' to keep thick filaments centered, and 'mechanical sensor'. Nebulin (~800-kD), is thought to 'wind' along the whole length of the thin filament, join to the Z line and may function as a thin filament 'length controller' (Voet and Voet, 1995a).

The contractile apparatus is linked to the extracellular matrix (ECM) and periphery by a number of cytoskeletal proteins and the dystrophin-associated protein complex (DAPC) (see figure 2.2.2-1). The cytoskeletal costameres consist of focal adhesion proteins including vinculin, talin, α-actinin, and β_1 integrins (Ervasti, 2003). Muscle costameres contain γ-actin, spectrin, desmin, vimentin, clathrin, ankyrin, and technically dystrophin (Taylor *et al*, 1995). They are subsarcolemmal protein assemblies that physically couple peripheral myofibrils to the sarcolemma via interacting with

the Z line. It is suggested that they may be responsible for transducing contractile forces laterally from sarcomeres, across the sarcolemma to the ECM and neighbouring myofibers (Taylor *et al*, 1995, Ervasti, 2003). They may play a role in sarcolemmal stabilisation and have greater functions in linking mechanotransduction signalling to the regulation of gene expression (Sadoshima and Izumo, 1997, Carson and Wei, 2000, Rennie and Tipton, 2000, Kääriäinen *et al*, 2001, Ervasti, 2003, Katsumi *et al*, 2004).

The DAPC plays a key structural link between the ECM and F-actin thin filaments (see figure 2.2.2-1); and may stabilise the sarcolemma (Ervasti, 2003), transduce force from sarcomeres to ECM and be involved in cell signalling (Brown *et al*, 1997, Ono *et al*, 1999, Tkatchenko *et al*, 2001, Ehmsen *et al*, 2002, Kumar *et al*, 2004). Dystrophin binds to actin at its N-terminus, associating with dystrobrevin at its C-terminus, in turn, interacting with α- and β-syntrophins. α- and β-dystroglycans make the link between laminin connecting to the ECM and subsarcolemmal dystrophin. There are five transmembrane sarcoglycans, α, β, γ, δ and ε., and a transmembrane protein called sarcospan. Other proteins known to be associated with the DAPC include syncoilin, laminin-2, caveolin-3, nNOS (neuronal nitric oxide synthase) and sodium channels (Ehmsen *et al*, 2002). The absence/downregulation of one or more of many of these structural proteins may initiate muscular dysfunction, disorders, and proteolytic system activation.

Figure 2.2.2-1. Diagrammatic representation of the dystrophin-associated complex (DAPC) connecting the myofibrillar apparatus to the extracellular matrix (ECM).

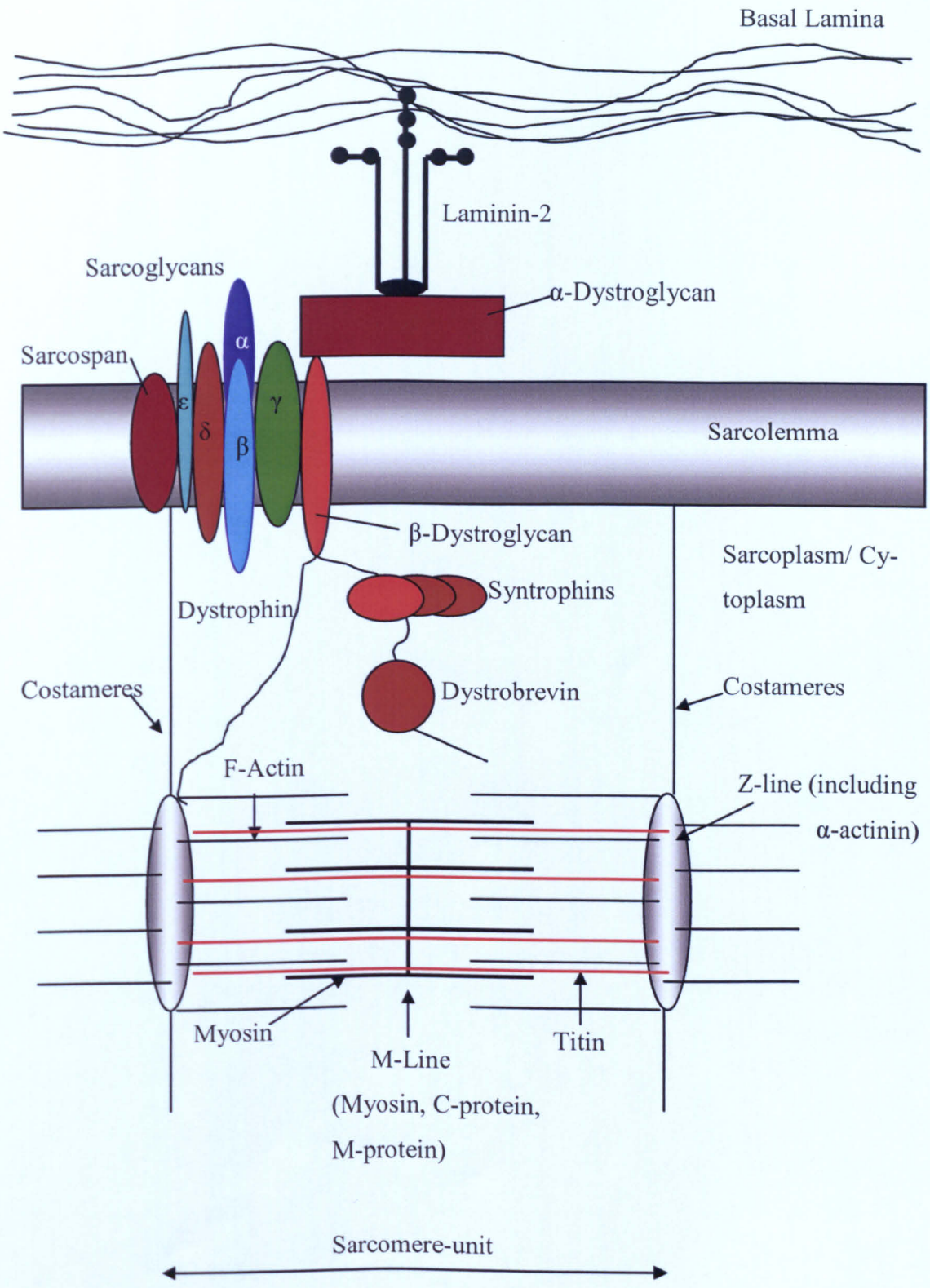

2.2.3 Skeletal Muscle Fiber Types

The relevance muscle fiber type has to this thesis subject is that there are fiber type dependent variations in function and metabolism which influence the processes of muscle atrophy and hypertrophy; which may relate to variability in proteolytic systems contained within these differing fiber types.

Mammalian skeletal muscle consists of a mosaic of different fiber types that are versatile and adapt in response to different functional and mechanical demands (Maltin *et al*, 2001, Spangenburg and Booth, 2003). They accomplish this by adjusting their phenotypic properties (Spangenburg and Booth, 2003). Fiber types may be characterised by physiological, metabolic and molecular markers. In general, studies based on myosin heavy chain (MHC) isoform profiles, show there to be at least four types of fibers. More types have been suggested and 'hybrid-fibers' detected, which co-express two or more MHC isoforms within the same fiber (Pette and Staron, 2000, Spangenburg and Booth, 2003).

Type I, red, or slow-oxidative fibers have been characterised as being slow-twitch, fatigue-resistant, containing slow isoform contractile proteins, high volume-density of mitochondria, high levels of myoglobin, high oxidative enzyme capacity, high capillary density and small fiber CSA (Cross Sectional Area).

Type IIA, red, fast-oxidative fibers are fast-contracting, relatively fatigue resistant with high oxidative capacity and medium fiber CSA.

Type IIX and IIB are white, fast-glycolytic fibers with increased contraction rate, low fatigue-resistance, containing increased expression of fast contractile protein isoforms, high myosin ATPase activity, low mitochondrial volume-density, high glycolytic enzyme capacity and large CSA.

Literature suggests that muscle fiber type expression is regulated by multiple signalling pathways and transcription factors as opposed to a single controlling pathway (Swoap et al, 2000, Pette and Staron, 2000, Maltin *et al*, 2001, Spangenburg and Booth, 2003). Certain physiological and pathological stimuli are known to influence

fiber type gene expression, transformation and myosin heavy chain transitions (Pette and Staron, 2000, Maltin *et al*, 2001, Spangenburg and Booth, 2003). These include hormonal administration, mechanical loading, innervation, aging, atrophy, muscle disease and cachexia (Sultan *et al*, 2001, Maltin *et al*, 2001, Diffee *et al*, 2002, Stevenson *et al*, 2003). Intracellular Ca^{2+} concentration ($[Ca^{2+}]i$) homeostasis may have a prominent role in fiber type regulation (Pette and Staron, 2000, Allen and Leinwand, 2002, Spangenburg and Booth, 2003).

There are vast variations in the phenotypic expression of proteins within type I and type II fibers (Cambell et al, 2001). Some authors have suggested from animal growth promoter studies, medical cachexia and sarcopenia studies that type II fibers have greater 'plasticity', adaptive potential and are more susceptible to atrophy and hypertrophy (Pette and Staron, 2000, Maltin *et al*, 2001, Spangenburg and Booth, 2003).

2.2.4 Subcellular Protein Compartments and Myofibrillar Turnover

Roughly 30-35% of all proteins within the muscle cell comprise of cytoplasmic, short-lived, moderate-to-rapidly turning over proteins (see figure 2.2.4-1) (Goll *et al*, 2003). This subfraction of 'sarcoplasmic' non-myofibrillar proteins consists of metabolic enzymes and regulatory proteins. Slowly turning over myofibrillar proteins within skeletal muscle constitute 55-65% of the total protein content (Goll *et al*, 1998 Goll *et al*, 2003). Individual myofibrillar units may have different turnover rates. For skeletal muscles to function properly as contractile tissue, the myofibrils must remain intact. It has been suggested contractile proteins are able to move between myofilaments, move to the periphery of the myofibril, interact with degrading system(s) and be exchanged for newly synthesised myofilaments. Research suggests the presence of a separate identified protein fraction of myofibrillar origin, with a higher turnover rate, accounting for ~5-10% of total protein in cell (Goll *et al*, 1998, Thompson and Palmer, 1998). This small fraction of 'easily releasable myofilaments' (ERMs), that exist on the periphery of the myofibril, would contain newly synthesised, and partially degraded myofilaments (Goll *et al*, 1998, Thompson and Palmer, 1998).

Figure 2.2.4-1. A schematic diagram of the proposed flow of amino acids within skeletal muscle. *Amino acids flow from the free intracellular pool to other dynamic protein compartments, with different turnover rates.*

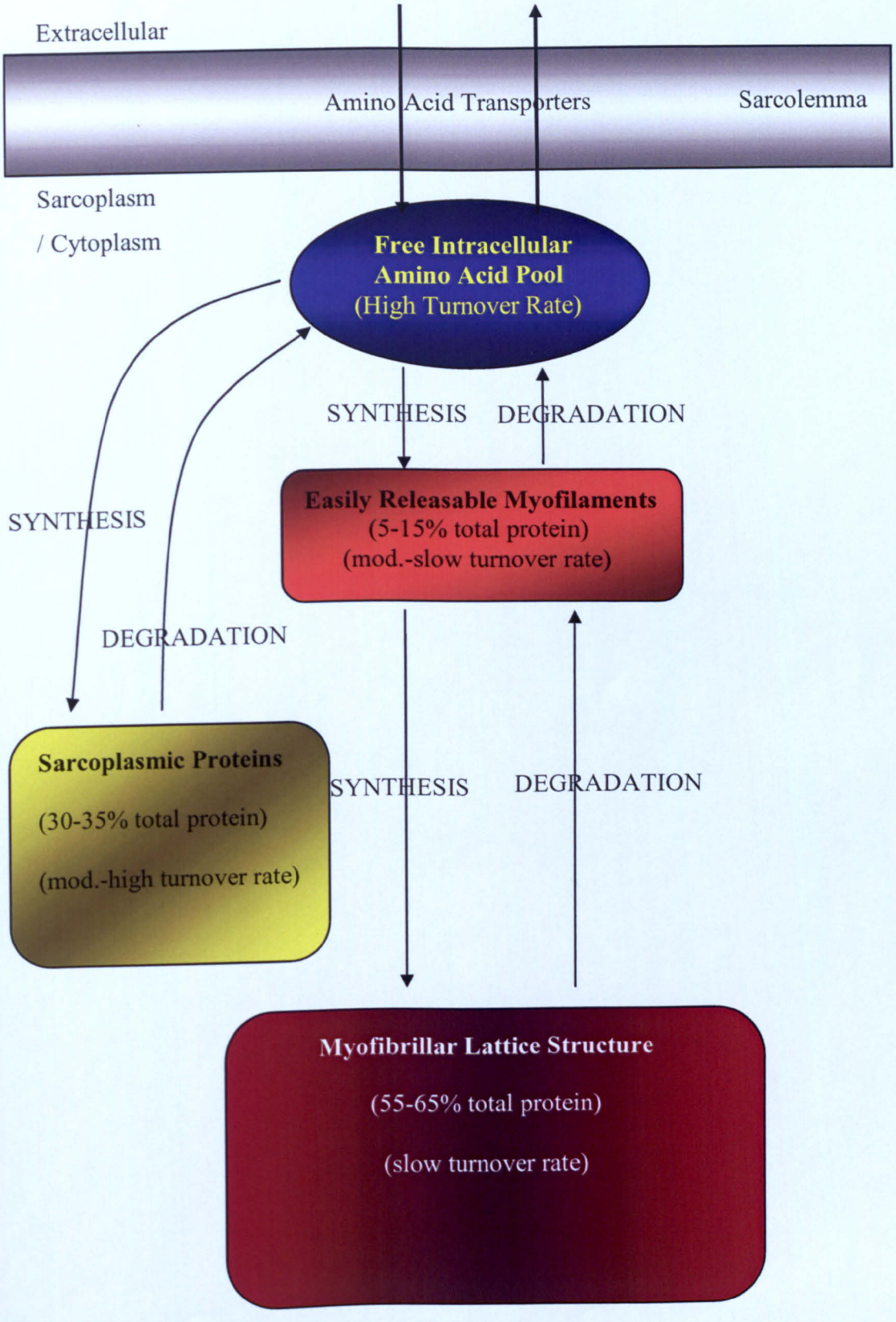

Myofibrillar turnover is dependent on the proteolysis of specific myofibrillar protein substrates. It has been suggested that this is primarily through a calcium-dependent, calpain-protease mediated mechanism (Goll *et al*, 2003) (discussed in later calpain Section 2.6.3) (see Figure 2.2.4-2). Nebulin and Titin, which stretches across filaments to the Z-line, is degraded by calpain-protease action on the surface of the myofibril at the point where they enter the the Z-line. This severs attachment of the Z-line proteins to the remainder of the myofibril, releasing the Z-line proteins like α-actinin and releasing myosin (thick) and actin (thin) filaments from the surface of the myofibril (see 1. of Figure 2.2.4-2). After the release of a single 'layer' of filaments, the remaining myofibril is narrowed by one thick filament and two thin filaments but is otherwise unchanged and functionally able to contract. The released filaments can reassemble back onto the surface of the myofibril, or additional degradation of troponin and tropomyosin (Tm) (on thin filament) and C-protein (on thick filament), results in disassociation of thick and thin filaments to myosin and actin molecules, respectively (see 2. of Figure 2.2.4-2). The myosin and actin molecules and polypeptide fragments of other calpain-degradaded proteins (i.e. titin, nebulin, desmin, troponin, tropomyosin and C-protein) are degraded to amino acids by the proteasome, cellular peptidases and possibly lysosomal-cathepsin proteolysis (Goll *et al* 2003) (see 3. of Figure 2.2.4-2). The relevant protease systems are introduced and described in great detail in later sections.

A final point of discussion with the model presented for myofibrillar turnover, is that only surface myofibrillar proteins appear able to turnover. The myofibrillar proteins within a myofibril would not be turned over as they are not accessible, according to this model. The only way to initiate turnover would involve 'opening' the myofibril up to allow the release of myofibrillar proteins. This leaves the question as to whether this model is valid and whether only surface myofibrillar proteins on a myofibril turnover.

Figure 2.2.4-2. A schematic diagram of a proposed model of myofibrillar turnover/degradation. *Adapted from Goll et al, 2003. See Figure. 2.2.2-1 for identification of specific proteins.*

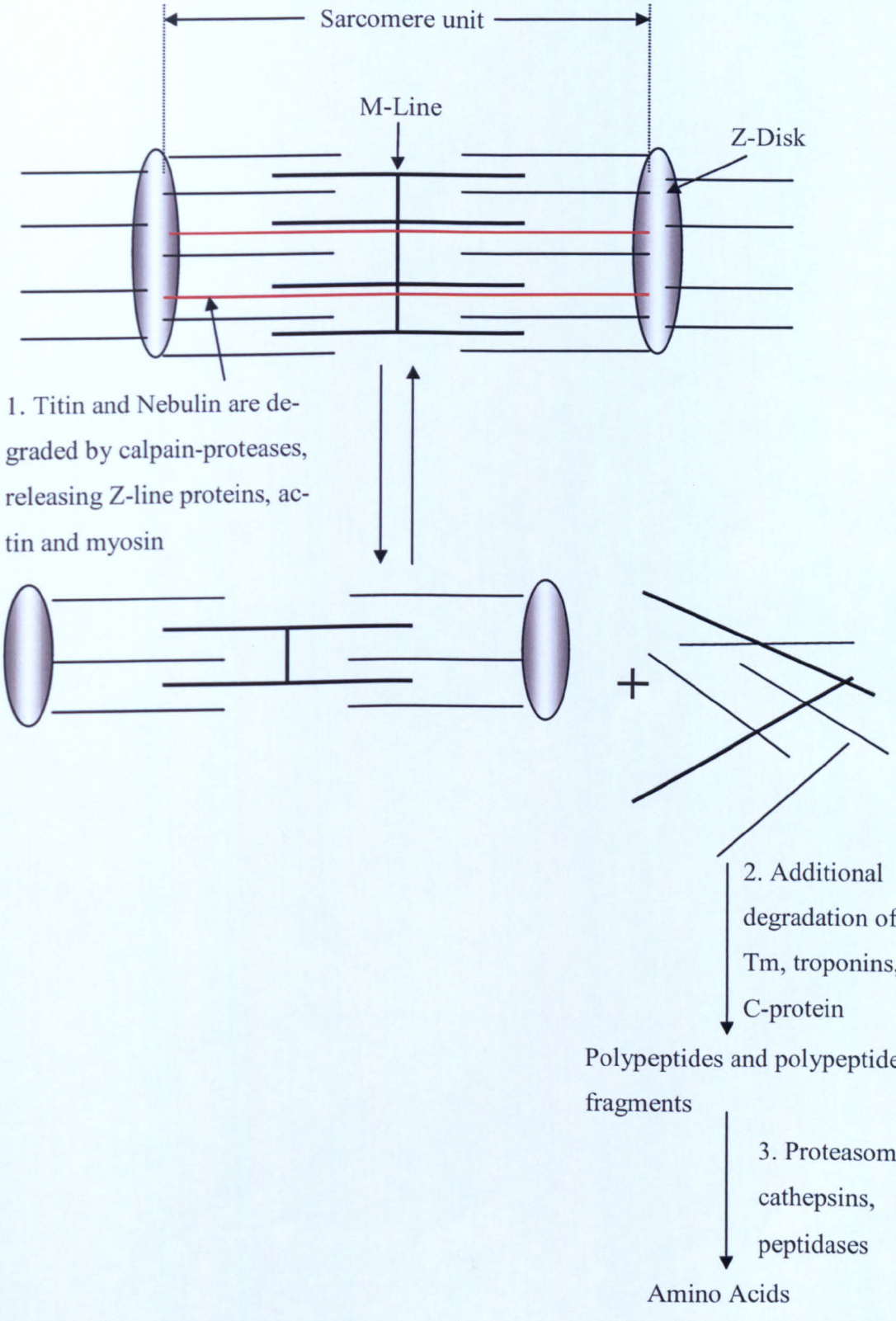

2.2.5 Amino Acid Repartitioning

As already indicated skeletal muscle acts as a large metabolic pool/ temporary dynamic store of amino acids that can be repartitioned into a number of essential pathways and processes that require specific amino acids (Rooyackers and Nair, 1997, Rennie and Tipton, 2000) The source of amino acids required for various pathways may come from the breakdown of proteins of myofibrillar and non-myofibrillar origin; a coordinated process controlled by multiple protease systems. Essential metabolic pathways that require amino acids include:

BCAA (Branched Chain Amino Acid) synthesis and oxidation.

Glutamine synthesis with subsequent uptake and utilisation by the gut, immune system, liver and kidneys.

Glutamine and Alanine release with subsequent partitioning towards gluconeogenic pathways.

Partitioning of amino acids towards hepatic synthesis of acute phase reactants.

Sulphur containing amino acids, eg. Cysteine is required for glutathione synthesis.

The processes and pathways listed above are up-regulated differentially during fasting, stress, illness and infection (discussed in Section 2.4), leading to an increased demand for amino acids. Hence, raised net skeletal muscle protein degradation satisfy's much of the raised demand (see Figure. 2.2.5-1).

Figure 2.2.5-1 The balance of supply and demand on the plasma amino acid pool during stress and infection.

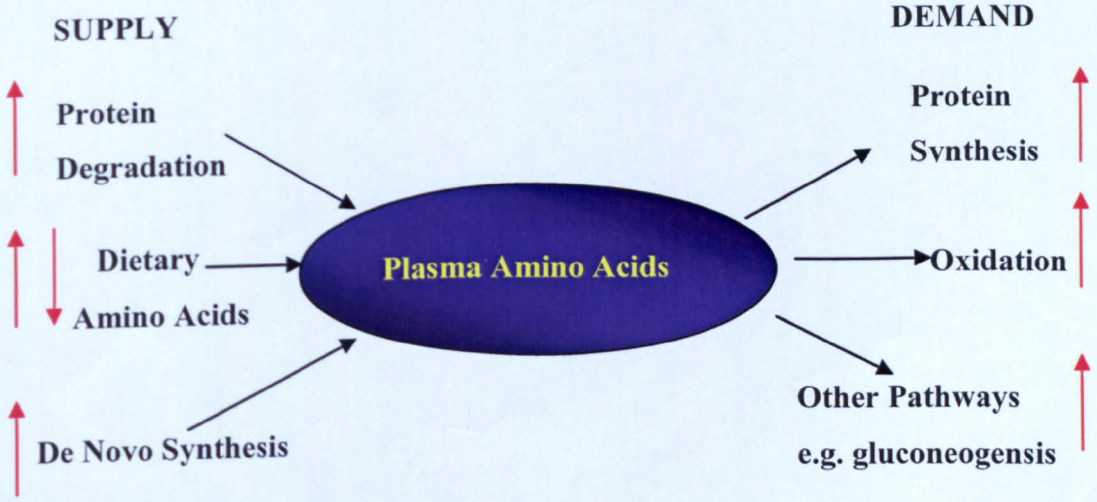

2.2.6 Protein Metabolism Studies

Skeletal muscle protein metabolism has been studied in animals, humans, incubated muscle and cell cultures. The majority of the research effects have focused on the process of protein synthesis (Thompson and Palmer, 1998, Liu and Barrett, 2002). The process of proteolysis/protein degradation has yet to be as well understood. Previously proteolysis has been viewed as a bulk process with no definite, specific pathway of degradation. This is in part a reflection of the complexity of this process.

Clinical methods proven to be useful in evaluating protein metabolism and proteolysis include: Amino acid kinetics studies which allow estimations of protein turnover at a whole-body level and within individual tissues/organs (Liu and Barrett, 2002). Muscle tissue release of tyrosine, phenylalanine and leucine has been used as a measure of cell proteolysis. Phenylalanine and tyrosine are neither catabolised nor synthesised within skeletal muscle, therefore the rate of appearance (R_a) of these amino acids is a good estimate of protein degradation and amino acid release (Liu and Barrett, 2002). Researchers have also focused on other markers including, muscle glutamine and alanine release, BCAA release and uptake (Ohara *et al*, 1995) and plasma glutamine. During illness and metabolic stress there is a raised requirement for glutamine which correlates with increased plasma glutamine, leucine R_a and muscle degradation (Yarasheki *et al*, 1998, Claeyssens *et al*, 2000). Although 70% of overall glutamine comes from muscle tissue, it is not an estimate of muscle proteolysis however, as much of glutamine tissue release (~87%) is believed to be satisfied by de novo synthesis (Kuhn *et al*, 1999, Claeyssens *et al*, 2000). Level of 3-methylhistidine (3-MH) release from muscle cells enables the determination of the specific rate of myofibrillar breakdown (Liu and Barrett, 2002, Rooyackers and Nair, 1997). 3MH is a post-translationally modified amino acid derived from myofibrillar proteins (actin and myosin), is not reincorporated into other protein pools but released from the cell and excreted (although the estimation of smooth muscle contribution to 3-MH is not accurately known).

There are many types of proteolytic events taking place over multiple time courses and subcellular compartments. For example, there may be an increase in overall intracellular proteolytic cleavage events, but no complete degradation of the proteins,

subsequent conversion to free amino acids and release from the cell. This is a likely occurrence during growth and remodelling events. Therefore researchers have focused attention towards non-tracer methods, measuring mRNA, protein levels and activities of components of specific identified proteolytic systems within skeletal muscle (Thompson and Palmer, 1998). Specific substrate cleavage by proteases has also been focused on, e.g. those that are regulatory or cytoskeletal proteins.

2.2.7 Summary

Skeletal muscle makes up a large proportion of total body weight (~40-45%) and total body protein (~50%). The overall intracellular architecture within skeletal muscle is highly complex, with subcellular protein compartments with different turnover rates and functional activities. The myofibrillar proteins that make up to 55-60% of the proteins within skeletal muscle are required to be functionally intact to allow contractile activity. Therefore, myofibrillar turnover is a highly regulated process that has been suggested to involve calpain proteases. Both the sarcoplasmic and myofibrillar proteins can be degraded completely to amino acids by protease systems, to satisfy increased demands for amino acids for different pathways and processes; many of which are up-regulated during stress, illness and infection.

2.3 REGULATION OF PROTEIN TURNOVER

2.3.1 Introduction

Protein turnover within skeletal muscle is regulated by a number of diverse signals including nutrients, hormones, autocrine/paracrine factors and stretch- /mechanical loading- induced pathways (Rooyackers and Nair, 1997, Thompson and Palmer, 1998, Rennie and Tipton, 2000). This thesis is predominantly concerned with the effects of specific dietary and a pharmacological treatment (β-adrenergic agonists) known to alter muscle growth/hypertrophy and how specific proteolytic systems may be involved in these processes. Therefore, within the scope of this literature review the topics to be covered in this section include muscle growth so as to describe the general cellular growth process and importance of remodelling and proteolysis. A

description of the GH-IGF-1 endocrine axis then follows as the GH-IGF axis is the major controller of cell growth, known to alter in many states including during altered planes of nutrition. An in depth description of the β-adrenergic agonists and their effects on muscle growth is included to provide an understanding of how these growth-promoting agents may alter specific signalling pathways and induce changes in proteolytic systems. The effects of nutrition/feeding and various hormones on protein turnover, hypertrophy and proteolysis then follows. This was important so as to indicate that during feeding and altered planes of nutrition a myriad of endocrine and cellular signalling pathways are altered, which leads to various global effects on proteolysis. A description of the importance of proteolytic systems with regards to severe catabolic, stress, infection and atrophy states follows in Section 2.4.

2.3.2 Muscle Growth

Cellular growth requires the organism to sustain a phase of net gain of cellular components, i.e. a net positive protein-energy anabolic state. For an increase in protein constituents at a cellular level there must be a net increase in protein synthesis to lead to protein accretion. This may be accomplished by increasing protein synthesis and/or decreasing protein breakdown (Rooyackers and Nair, 1997). Skeletal myocellular hypertrophy (defined as an increase in size of myofibers with an increase in protein content, cytoplasm, nuclei and myofibrils) and at specific times hyperplasia (increase in cell number) collectively leads to whole muscle increases in protein content, cross sectional area (CSA) and mass (Paul and Rosenthal, 2002).

Presumably for skeletal muscle cell and tissue growth to occur there must be a huge co-ordination of processed effort to allow growth to occur (Maltin *et al*, 2001, Paul and Rosenthal, 2002). This is accomplished by remodelling and modifying the internal cell environment/architecture and extracellular components (Maltin *et al*, 2001, Paul and Rosenthal, 2002, Kristensen *et al*, 2002, Féasson *et al*, 2002). Remodelling has been suggested to be important during 'catch-up' growth after a nutrient-feed restiction (Kristensen *et al*, 2002, Kristensen *et al*, 2004), muscle recovery during reloading after unloading-induced atrophy (Taillandier *et al*, 2003) and eccentric-contraction exercise (Féasson *et al*, 2002). Remodelling may involve an increase in myofibrillar and cytoskeletal re-arrangement and net protein synthesis; and increase

in sarcoplasmic protein pool turnover (Kristensen *et al*, 2002, Féasson *et al*, 2002, Taillandier *et al*, 2003, Kristensen *et al*, 2004). These processes are likely to require an increase in specific proteolytic cleavage events, but not bulk degradation of proteins to amino acids and concomitant release of amino acids into the bloodstream. It has been confirmed that protease activity and protein degradation is heightened during periods of 'catch-up' growth, muscle recovery and remodelling (Kristensen *et al*, 2002, Féasson *et al*, 2002, Taillandier *et al*, 2003, Kristensen *et al*, 2004).

2.3.3 Growth Hormone (GH)

The GH-IGF (Growth Hormone-Insulin-Like Growth Factor) hypothalamic-pituitary-axis (also involving hepatic and local tissues) acts as a major controller of cell and tissue growth. GH-IGF axis activity is greatest during early life cycle growth phases in animals and humans, rises during puberty and decreases in adults. The axis has complex coordinated, regulatory feed-back relationships with the hypothalamic-pituitary-testicular axis (HPTA), androgens, estradiol, thyroid hormones, insulin, glucocorticoids, noradrenaline and neurotransmitters (Lackey *et al*, 1999).

Circulating GH, secreted by the pituitary gland is known to directly bind to GH receptors (GHR) on skeletal muscle and stimulate protein synthesis, but studies regarding muscle protein breakdown are unclear (Rooyackers and Nair, 1997, Garlick *et al*, 1998, Breier, 1999, Vann *et al*, 2000). The main anabolic effects of GH are through the stimulation of hepatic-systemic and local tissue production of IGF-1 (Rooyackers and Nair, 1997, Garlick *et al*, 1998, Lackey *et al*, 1999, Breier, 1999). IGF-1 increases protein synthesis and decreases protein degradation, in addition to stimulating satellite cell proliferation and differentiation (Bass *et al*, 1999, Liu and Barrett, 2002). The biological effects of IGF-1 are modulated by specific IGFBP's (Insulin-like Growth Factor Binding Proteins), which are known to alter during dietary and pharmacological treatments (Vestergaard *et al*, 2003). A specific skeletal muscle specific isoform of IGF-1 (termed mechano-growth factor) has recently been found which only appears to be produced by damaged or loaded muscle (Adams, 2002, Spangenburg, 2003).

Figure 2.3.3-1 illustrates a simplified model of how the GH-IGF axis interacts with skeletal muscle and alters protein turnover and hypertrophy. GH may directly bind to GH receptors (GHR) on skeletal muscle cells, stimulating protein synthesis and the local production of IGF-1. GH also stimulates hepatic IGF-1 secretion and modulates hepatic IGFBP production. Hepatic-systemic IGF-1 travels to skeletal muscle in the circulation bound to specific IGFBPs. In reality there a number of IGFBPs known to have positive and negative effects on IGF-1 activity, relationships too complex to go into detail within this literature review however. The IGF-1-IGFBP complex may be disassociated by protease actions on IGFBPs, thus releasing IGF-1. Released IGF-1 may subsequently bind to IGF-1 receptors on skeletal muscle cells, stimulate protein synthesis and decrease protein degradation. Mechanical damage may stimulate the local production of a muscle-specifc isoform of IGF-1. Systemic, locally produced and muscle-specifc IGF-1 may stimulate satellite cell proliferation and differentiation. The net effect of these stimuli is an increase in protein accretion, increase in myonuclei and increase in hypertrophy.

Nutritional and metabolic-endocrine status has important complex regulatory effects on the GH-IGF axis (Breier, 1999). Increased protein intake in steers has been shown to increase GH pulse frequency and level of nutrition positively correlate with hepatic GHR (Breier, 1999). Thyroid hormones, dependent on nutritional-micronutrient status, protein and carbohydrate intake, affect GH-IGF axis activity and 'anabolic-effectiveness' of GH (Lackey *et al*, 1999). For example, normal/normal-high range of T_3, thyroid hormones are known to increase the mRNA levels of GHR and IGF-1 in fetal sheep skeletal muscle (Forhead *et al*, 2002). Insulin, also dependent on macronutrient-calorie intake is known to have a permissive regulatory role in IGF-1 secretion. Insulin increases IGF-1 levels and regulates the expression of the IGF-1 receptor (IGF-1R) (Lackey *et al*, 1999). Androgens increase GH concentrations by modulating pulse amplitude and frequency of GH secretions from the pituitary gland. This is thought to be directly linked to the aromatisation of androgens to estrogens (Lackey *et al*, 1999). Androgens may also up-regulate the expression of IGF-1 and down-regulate the expression of IGFBP-4 in muscle (Bhasin *et al*, 2001). Glucocorticoids have negative effects on the GH-IGF-1 axis. In excess they can decrease GH and IGF-1 levels and thought to also modulate IGF-R and IGFBP (Lackey *et al*, 1999).

Figure 2.3.3-1. A simplified proposed model of the actions of the GH-IGF axis on skeletal muscle protein turnover and hypertrophy.

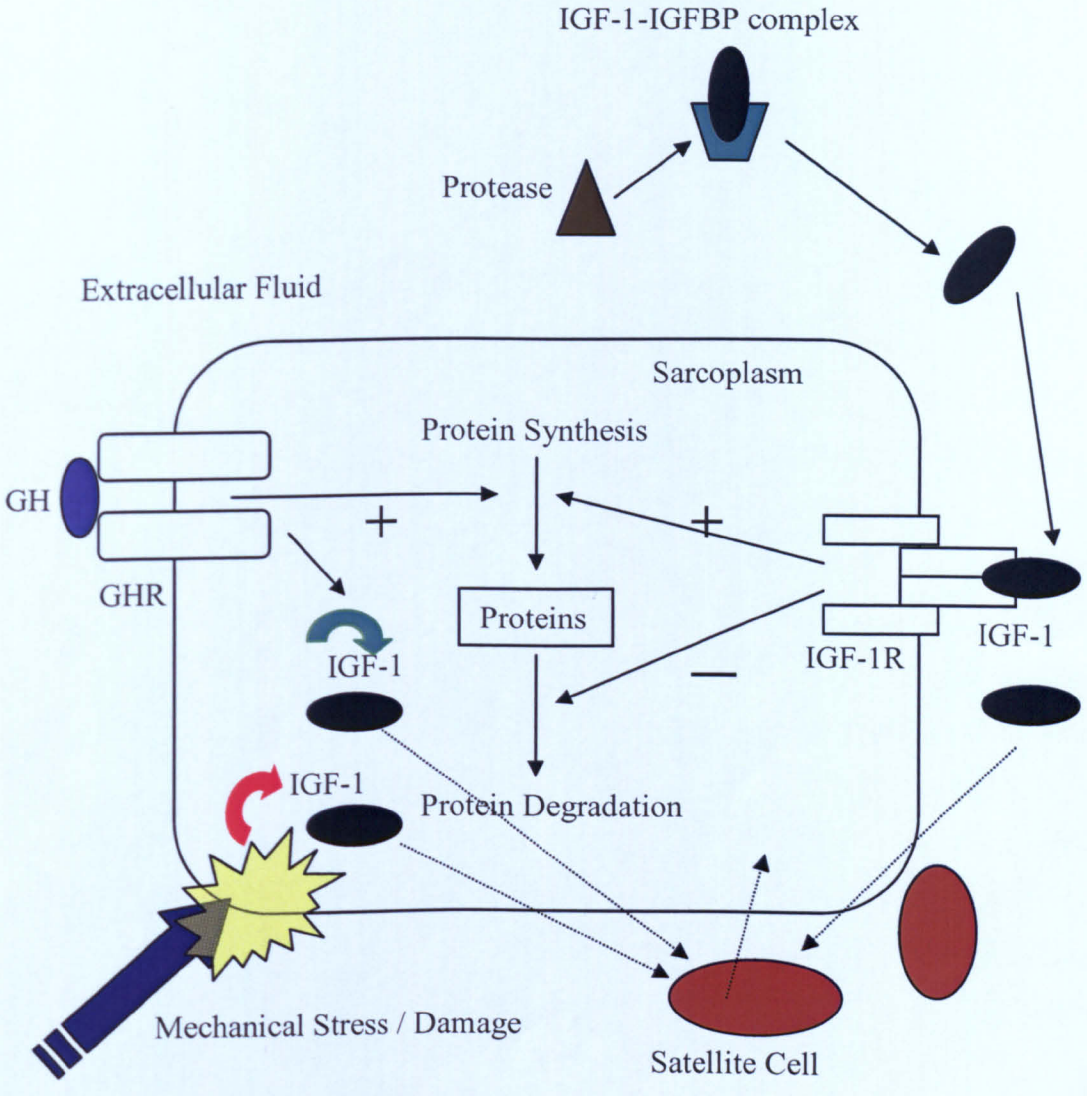

High GH levels in the 'fed state' acts as a protein-anabolic hormone, as all the regulatory hormones described above that affect GHR, IGF-1, IGF-1R and IGFBP's are all affected and up-regulated (note that the IGFBPs are differentialy regulated); and glucocorticoids decreased (see Section 2.3.5.3 for information about hormonal response to feeding). In the 'fasted state', GH secretion increases and acts to increase fat mobilisation and metabolism and may have a protein sparring effect aiding in preventing muscle protein catabolism. However, during fasting a degree of hepatic GH resistance takes place and systemic IGF-1 secretion is dramatically reduced (Henricks *et al*, 1994, Breier, 1999, Vestergaard *et al*, 2003).

GH administration has been well researched and widely used as a growth-promoting agent in livestock production (Bell *et al*, 1998, Breier, 1999, Vann *et al*, 2000, Vestergaard *et al*, 2003), treatment for catabolic wasting conditions (Garlick, 1998, Mann, 1999, Kotler, 2000) and in performance enhancement as a protein-anabolic and lipolytic agent (Sonksen, 2001). Chronic high dose administration of GH in fed, growing animals is known to act as a nutrient repartitioning agent, increasing lean body mass and decreasing fat mass (Bell *et al*, 1998, Breier, 1999, Vann *et al* 2000). Studies in humans are less conclusive and suggest that tissues other than skeletal muscle may be more sensitive to the protein-anabolic effect of GH (Rooyackers and Nair, 1997). Zhang *et al*, 1999 showed evidence that GH administration does not stimulate muscle protein anabolism directly in rabbit muscle. The lack of conclusive evidence in humans of GH acting as a potent anabolic agent may also be due to dose treatment patterns, time length of treatment and dose concentrations, along with species variability. In catabolic patients, GH has had a positive effect in myotonic dystrophy but some negative effects in the critically ill (Rooyackers and Nair, 1997, Herrington and Su, 2001). It has been suggested that GH administration during an acute-phase response to infection/illness may disturb the hepatic synthesis of acute-phase proteins and may increase mortality rates (Kotler, 2000).

In summary, GH acts as a protein-anabolic agent in the fed state, when other hormonal factors are in place (i.e. insulin, thyroid hormones and sex steroids in particular). Much of its positive effects are through the stimulation of hepatic and local production of IGF-1. In this state there is a potent suppression of proteolysis, rise in protein synthesis and protein accretion, which may lead to myofiber hypertrophy.

2.3.4 Beta-Adrenergic Agonists

2.3.4.1 Introduction

A major part of this thesis work involves the effects of beta-adrenergic stimulation on proteolytic systems, therefore this section contains a more detailed examination of these growth promoting effects.

The beta-adrenergic agonist (βAA) class of compounds are chemically and physiologically based on the endogenous catecholamines, adrenaline, secreted systemically by the adrenal medulla and noradrenaline, secreted by the sympathetic nervous system (SNS) through adrenergic terminals (Frayn, 1997b, Frayn, 1997g, Mersmann, 1998). They are classically thought of as counter-regulatory stress hormones (Rooyackers and Nair, 1997, Frayn, 1997b, Frayn, 1997g). They have actions on alpha (α) and beta (β) adreno-receptors (AR) throughout the body (Frayn, 1997b, Mersmann, 1998). A number of synthetic phenethanolamine derivative compounds have been developed with varying drug half-lives and specificities/affinities for different beta receptor types. Examples, include the β_2-specific-agonists clenbuterol, salbutamol (albuterol), ractopamine ('Paylean'®), fenoterol and the non-specific agonist ephedrine (Mersmann, 1998). βAAs have been used clinically in medicine at low doses as bronchodilators, alleviating asthma symptoms. (Mersmann, 1998, Pellegrino *et al*, 2003)

2.3.4.2 βAA Effects on Muscle Metabolism

The βAAs, including the endogenous catecholamines noradrenaline and adrenaline, are known to have a general catabolic effect on lipid and glucose metabolism promoting degradation, mobilisation and oxidation, but an anabolic effect on protein metabolism in skeletal muscle (Rooyackers and Nair, 1997, Mersman *et al*, 1998, Navegantes *et al*, 2002). The beta-adrenergic system has been characterised and shown to have a positive effect on lean-muscle tissue deposition in a number of species, including humans (Kissel *et al*, 2001, Fowler *et al*, 2004), mice (Pellegrino *et al*, 2003), rats (Cardoso *et al*, 1998), horses (Kearns *et al*, 2001) and recently fish (Lortie *et al*, 2003), but effects are most prominent in farm-meat animals (Mersmann,

1998, Bell *et al*, 1998). βAAs have been studied extensively for use as growth-promoting/modifying agents in livestock (Mersmann, 1998, Bell *et al*, 1998). βAAs improve feed conversion, increase the rate and efficiency of protein deposition in lean tissues and decrease fat deposition (Mersmann, 1998, Bell *et al*, 1998). They induce increases in protein accretion, CSA and glycolytic capacity/fast-twitch charcteristics. There effects are to increase the proportion of type 2B and fast-twitch fibers, in a 'time- and dose-dependent' manner, through altering the myosin heavy chain isoform content, increasing glycolytic (e.g. PFK and LDH) and decreasing mitochondrial oxidative enzyme activities (e.g. CS and COX) (Rajab *et al*, 2000, Depreux *et al*, 2002, Pellegrino *et al*, 2003).

βAAs have also been shown to decrease muscle protein loss during protein-catabolic conditions including denervation-induced atrophy (Sneddon *et al*, 2000), food restriction (Cardoso *et al*, 1998), glucoccorticoid-induced atrophy (Pellegrino *et al*, 2003), aging (Ryall *et al*, 2003), injury (Beitzel *et al*, 2004) and muscular dystrophy (Lynch *et al*, 2001). βAA like clenbuterol potentially could be utilised in clinical settings as a possible means of reducing skeletal muscle protein loss/depletion in conditions such as cancer cachexia, AIDS wasting and age-related sarcopenia (Kotler 2000, Ryall *et al*, 2003). A trial using albuterol in child patients with Duchenne and Becker muscular dystrophies showed that there was an increase in strength and muscle function over a 3 month treatment period (Fowler *et al*, 2004).

The βAAs have come to be regarded as 'nutrient repartitioning' agents (Bell *et al*, 1998, Kearns *et al*, 2001). βAAs have in turn been used/abused by athletes and bodybuilders for a number of years to enhance muscle growth, muscle function and fat loss (Grundig and Bachmann, 1995, Duchaine, 1996, Dawson, 2001). Elite power athletes and sprinters have relied on it not only due to its repartitioning effects, but due to its potential fiber type switching properties (slow to fast), which are particularly suited to higher intensities of exercise (based on power output).

2.3.4.3 Potential Mechanisms for βAA Induced Hypertrophy

The effects of βAAs on overall animal performance and nutrient repartitioning are well documented, but the exact underlying mechanism of their action within skeletal muscle has yet to be clarified.

In terms of specific actions on protein turnover, studies suggest βAA are able to stimulate skeletal muscle protein synthesis (Bell *et al*, 1998, Mersmann *et al*, 1998, McDonagh *et al*, 1999, Sneddon *et al*, 2001) and increase the abundance of mRNA for muscle specific proteins, although increased synthesis hasn't been consistently proven (Bell *et al*, 1998, Mersmann *et al*, 1998, Navegantes *et al*, 2002). Other studies strongly suggest that they are able to decrease proteolysis (Bell *et al*, 1998, Navegantes *et al*, 1999, Navegantes *et al* 2001, Navegantes *et al*, 2002). McDonagh *et al*, 1999, showed an increase in synthesis, but no decrease in degradation, despite a decrease in calpain protease system activity. McDonagh suggested that there was no decrease in net cell degradation as myofibrillar degradation may be independently regulated to sarcoplasmic proteins degradation.

It is thought that βAAs exert most of their effects in skeletal muscle via the β_2-receptor (β_2-AR). Although β_1 and β_3 have been detected, β_2 is the predominant receptor type in muscle tissue (Mersmann, 1998).

Activation of the G-protein linked/coupled β_2-ARs increases cAMP (cyclic adenosine monophosphate) production from ATP (adenosine triphosphate) through adenylate cyclase (AC) activation (see Figure. 2.3.4.3-1) (Mersmann, 1998, Navegantes *et al*, 2002). Protein kinase A (PKA) then becomes activated by cAMP. PKA is the main effector of β-AR activation responses/functions. PKA is then able to phosphorylate a number of intracellular proteins to activate/deactivate them accordingly. In terms of gene transcription, PKA once activated can activate the cAMP response element binding protein (CREB), which subsequently binds to a cAMP response element (CRE) in the regulatory part of a specific gene (Navegantes *et al*, 2002).

Figure 2.3.4.3-1. A proposed scheme of the mechanism of action of βAAs in skeletal muscle. *Adapted from Navegantes et al, 2002.*

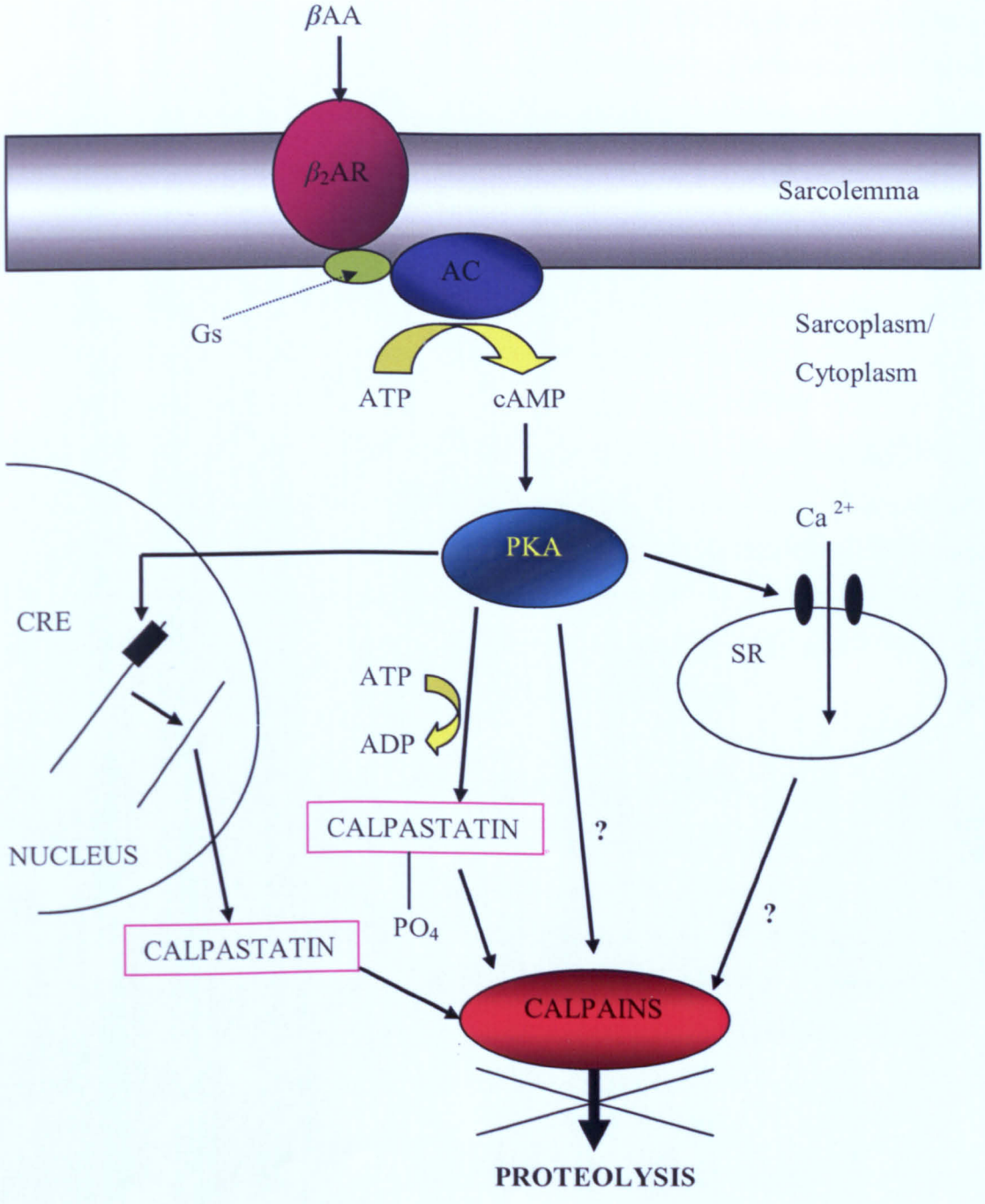

One mechanism by which βAAs decrease protein degradation is through the inhibition of calpain-dependent proteolysis by increasing the mRNA and activity of calpastatin (Parr *et al*, 1992, Bardsley *et al*, 1992, Speck *et al*, 1993, Sensky *et al*, 1996, Mc Donagh *et al*, 1999), an endogenous inhibitor of the calpains, through a cAMP-dependent mechanism. Phosphorylation of calpastatin and calpains by PKA has also been suggested to act as a controller of activity (Navegantes *et al*, 2002). This topic is also covered in detail in the calpain system, Section 2.8. The βAAs may also affect sarcoplasmic reticulum (SR) calcium sequesteration which may in turn affect proteolysis (Navegantes *et al*, 2002). Figure 2.3.4.3-1 illustrates the proposed scheme of βAA action.

The adrenoceptors vary in number and type amongst tissues, species and muscle fiber types (Mersmann, 1998). Slow twitch fibers have been reported to contain more β-receptors than fast twitch fibers (Ryall *et al*, 2002, Ryall *et al*, 2003).

The regulation of functional membrane β-AR number/density, down-regulation and internalisation is determined principally by key metabolic hormones and mediators. Thyroid hormones, GH, sex steroids, glucocorticoids, insulin, and βAA may affect receptor sensitivity and/or regulation. In human epidermoid carcinoma cells, insulin and βAAs have been shown to internalise the β_2-G-protein-coupled receptor through distinct and separate cytoskeletal pathways (Shumay *et al*. 2004).

Glucocorticoids are able to induce muscle atrophy and fast to slow fiber type transformations, whereas βAAs have the opposite effects and can antagonize glucocorticoid-induced atrophy and fiber type transformation (Pellegrino *et al*, 2003). However, glucocorticoids may also potentiate the effects of βAAs by possibly preventing desensitisation and down regulation, through a reduction in β-AR phosphorylation (reduction in desensitisation) and acting on GRE (Glucocorticoid Response Element) sequence in β_2-AR gene (oppose downregulation).

Some researchers have suggested that as growth occurs predominantly in fast fibers and fast fibers have a lower receptor density than slow twitch fibers, this indicates that there is little relationship between receptor density/distribution and muscle hypertrophy, suggesting other pathways of action (Ryall *et al*, 2002, Ryall *et al*, 2003).

However, studies show that optimal repartitioning occurs within the first 2 weeks of administration, leveling off thereafter in a number of species (Bell *et al*, 1998, Mersmann, 1998, Kearns *et al*, 2001). This is thought to be directly related to the rapid downregulation and desensitisation of the β-AR in response to chronic agonist stimulation, suggesting repartitioning is β-AR dependent. In terms of proteolysis, Navegantes *et al*, 2002, makes convincing arguments that the decrease in proteolysis is β-AR, cAMP, and Ca^{2+}-dependent. Also, rather than a fast twitch specific protein-anabolic response, it may be that βAA increase muscle growth by modifying fiber type composition, i.e. they stimulate to a greater degree slower fibers with higher β-AR densities and induce fast-twitch fiber modifications. In turn this increases the proportion of fast fibers, protein content and CSA. However, the connection between CSA, hypertrophy and fiber type can only be taken as a hypothetical view, as many studies suggest that slow to fast transformations take place during atrophy in rats (Stevenson *et al*, 2003, Casse *et al*, 2003), spaceflight in rats (Fitts *et al*, 2000), cachexia in mice (Diffee *et al*, 2002) and mechanical unloading (Pette *et al*, 2000). Fiber typing of muscle fibers varies immensely across species as discussed earlier in Section 2.2.3 (Pette *et al*, 2000, Spangenburg and Booth, 2003), so we cannot make any true judgements relating to human muscle tissue. It is unknown in humans whether a slow to fast transformation is indicative of a catabolic, pathological state or an anabolic state.

Other suggested mechanisms of action of βAA and/or β-AR activation are that they may modulate other anabolic hormone pathways/receptor sensitivities. There maybe a potential role played by PKC and specific isoforms. PKC-α and PKC-θ have been suggested to play potential roles in the action of clenbuterol on amelioration of denervation-induced atrophy in rats (Sneddon *et al*, 2000). It has also been reported that the Gβ/γ proteins (of the G-protein-coupled β-AR) activate the PI(3)K/Akt (PKB) pathway (Glass, 2003); the same pathway utilised by IGF-1. Other studies suggest a possible interaction between the IGF system and clenbuterol administration. Cardoso *et al*, in 1998 showed that serum IGF-1 increased (110%) in food-restricted, clenbuterol-treated rats. More recently, Sneddon *et al*, in 2001 showed an elevation in the neurotrophic agents IGF-II and H19 transcripts and phosphorylation of 4E-BP1 and $p70^{S6k}$ in rat plantaris muscle undergoing clenbuterol-induced anabolism. Awede *et al*, in 2002, measured a fivefold increase in local IGF-1 mRNA, eightfold increase in

IGFBP-4, fivefold increase in IGFBP-5 mRNA and increase in IGF-1 content in rat soleus muscle after clenbuterol administration.

Additional effects on calcium homeostasis and activation of other pathways has been suggested. βAA may decrease cytosolic Ca^{2+} by possibly affecting sarcoplasmic reticulum Ca^{2+} sequesteration and in turn decrease calcium-dependent proteolytic activity (Navegantes *et al*, 2002) (see Figure 2.3.4.3-1). However, Kearns *et al*, 2001 commented that clenbuterol is highly lipophylic, can enter muscle tissue and increase passive Ca^{2+} release from the SR of single fibers. If true this may explain why there is reports of an increase in *m*-calpain (*m*-calpain is a calcium-dependent protease discussed in Section 2.8, activated at higher calcium concentrations) protease activity with βAA administration (Parr *et al* 1992).

A Ca^{2+}-mediated pathway may very well be implicated in clenbuterol and βAA-induced hypertrophy considering the possible effects of clenbuterol and βAA on protein kinase activation (PK's can affect Ca^{2+} homeostasis and some are dependent on Ca^{2+}), IGF pathways, calcium-dependent protease pathways and fiber type transformations. The Ca^{2+}/calmodulin –dependent protein phosphatase calcineurin has been linked to IGF-mediated hypertrophy and fiber-type transformations (Semsarian *et al*, 1999, Olson and Williams, 2000, Swoap *et al*, 2000, Mitchell *et al*, 2002). If βAA initiate hypertrophy along with fiber type transformations which are known to be calcium-dependent/regulated events controlled by a host of signalling pathways including, calcineurin and calpains, then it points the way to a more complex control of hypertrophy.

2.3.4.4 Summary

βAA have potent nutrient repartioning effects, inducing muscle hypertrophy and fat mobilisation and oxidation, when administered in chronic and relatively high doses. The positive effects of βAAs on muscle protein turnover and hypertrophy makes them important potential agents for the meat and livestock industry, but also for clinical applications in treating catabolic wasting disorders.

The mechanism by which they induce hypertrophy and protein accretion in skeletal muscle is not completely resolved but is thought to primarily involve a decrease in protein degradation. The decrease in protein degradation has been linked to increases in βAR binding to receptor followed by their activation and subsequent cAMP formation, and PKA activation. A component of this response are alterations in the mRNA and activity of components of the calpain-calpastatin system. The net effect is thought to be a decrease in calcium/calpain-dependent proteolysis (to be described in detail in Section 2.8).

2.3.5 Dietary Feeding and Plane of Nutrition

2.3.5.1 Introduction

Feeding and alterations in the level of daily dietary nutritional, calorie and protein intake, relative to daily total energy expenditure (TEE), can have a profound effect on metabolism and lean and fat tissue deposition / loss in many organisms; including humans and farm animals (Henricks *et al*, 1994, Frayn, 1997f, Garrow, James and Ralph, 2000b, Costa *et al*, 2004, Kristensen *et al*, 2004). Nutritional intake of macro- and micro-nutrients affects levels of metabolic hormones, mediators, degradatory products (metabolites) and metabolic processes, systemically and within skeletal muscle tissue (Frayn, 1997a, Frayn, 1997c, Rooyackers and Nair, 1997, Rennie and Tipton, 2000, Garrow, James and Ralph, 2000b). This leads to alterations in whole-body and skeletal muscle protein turnover and regulation of protease-system pathways.

2.3.5.2 Plane of Nutrition

The level of dietary-nutritional calorie and protein intake relative to the total energy expenditure (TEE), or 'plane of nutrition', will dictate whether an organism is in net gain or loss of lean body/fat tissue mass (Frayn, 1997f).

A high plane of nutrition above the daily TEE, i.e. a nutrient-calorie excess, in humans/farm animals leads to specific adaptations to switch to a mode of metabolic inefficiency (upregulated thermo-genic/-regulatory pathways) and nutrient deposition

(as lean and fat tissues) (Frayn, 1997f). The level of lean tissue gain, skeletal muscle protein accretion and ratio of lean gain : fat gain, may depend on a number of complex factors known to alter endocrine pathways and protein turnover. These may include the age, sex, pre-set genetic factors, health (exposure to stress, infections, trauma etc.), physical activity and pre-existing bodyfat level of the subject; along with macro/micro-nutrient composition of high-plane diet and how long the dietary intervention takes place (Henricks *et al*, 1994, Frayn, 1997f, Rooyackers and Nair, 1997, Roubenoff, 1997, Biolo *et al*, 1997, Raina and Jeejeebhoy, 1998, Bistrian, 1999, Rennie and Tipton, 2000, Garrow, James and Ralph, 2000e, Kotler, 2000, Pi-Sunyer, 2000, Lee, 2001, Maltin *et al*, 2001).

A low plane of nutrition relative to daily TEE would be in negative energy balance. This would initiate nutrient depletion and up-regulation in metabolic efficiency. This is characterised by losses of fat and lean body mass and down-regulation of thermoregulatory pathways (Frayn, 1997d, Frayn, 1997f, Lee, 2001, Costa *et al*, 2004). The ratio of lean tissue loss : fat loss may depend on the same factors as listed above.

2.3.5.3 Feeding and Protein Turnover

There are profound differences between the 'fasting' and 'fed state', with regards to skeletal muscle protein metabolism and turnover. In brief, the 'fed-state' is thought to be a protein-anabolic state where net protein synthesis may be stimulated and net protein degradation reduced. The 'fasting' state is known as a protein-catabolic state where net protein synthesis is reduced, net protein degradation is increased and amino acids are readily re-partitioned into pathways and processes mentioned in Section 2.2.5 (Rooyackers and Nair, 1997, Rennie and Tipton, 2000). Obviously this process is exacerbated greatly during prolonged fasting, leading to starvation. The metabolic hormone mediators of the protein-anabolic response to feeding (increase in protein synthesis and/or decrease in protein degradation) and protein-catabolic response to fasting (decrease in protein synthesis and/or increase protein degradation) is summarised in Table 2.3.5.3-1 (Symonds *et al*, 1989, Henricks *et al*, 1994, Frayn, 1997a, Frayn, 1997b, Frayn, 1997c, DeFeo, 1998, Lackey *et al*, 1999, Liu and Barrett, 2002, Vestergaard *et al*, 2003, Kiyma *et al*, 2004). The endocrine mediators in Table 2.3.5.3-1, respond at different time frames. For example, thyroid hormones,

androgens and IGF-1 form part of a long-term response to feeding on muscle protein turnover, where as insulin is a classical short term response. Feeding and fasting may also affect endocrine mediator receptor levels and/or binding proteins. An example discussed in Section 2.3.3 includes the increase in GH that has been observed with both feeding (although some studies show a decrease in GH) and fasting. During the fasting state, hepatic GHR and heptic IGF-1 activity is down-regulated so GH acts predominantly as a fat mobilising hormone.

Nutrients may also have direct effects on protein turnover within skeletal muscle. Amino acids have been shown to directly stimulate protein synthesis (Rennie and Tipton, 2000, Greiwe *et al*, 2001, Balage *et al*, 2001), possibly lower degradation (Balage *et al*, 2001) and may also down-regulate lysosomal proteolysis (Busquets *et al*, 2000).

Table 2.3.5.3-1. A summary of the main protein -anabolic and –catabolic endocrine responses to feeding and fasting, that alter skeletal muscle protein turnover.

Protein-anabolic response to feeding	Protein-catabolic response to fasting
↑ insulin	↓ insulin
↑/ ↓ GH	↑ GH
↑ T_3-thyroid hormone	↓ T_3-thyroid hormone
↑ IGF-1	↓ IGF-1
↑ androgens	↓ androgens
↓ glucocorticoids	↑ glucocorticoids

Excess nutrients stored within myofibers include fats stored as intracellular triglycerides, glucose as glycogen and a raised free amino acid pool (post-prandial). The subsequent increased water drawn into the cell due to nutrient excess leads to an increased cell hydration state. Increased hydration state alone may decrease proteolysis (Vomdahl and Haussinger, 1996).

2.3.5.4 Endocrine Mediators and Proteolysis Influenced by Fed/Fasted State

Specifically with regards to skeletal muscle protein breakdown, insulin and IGF-1 are known to decrease net cellular protein degradation and have strong anti-proteolytic effects, possibly inhibiting lysosomal-cathepsin proteolysis and ubiquitin-proteasome system activity (Liu and Barrett, 2002) (systems discussed in detail in Sections 2.7 and 2.9, respectively). Insulin is known to rapidly and potently decrease protein breakdown post-meal, although the protein pools affected are thought to be of non-myofibrillar origin, i.e. sarcoplasmic proteins (Rooyackers and Nair, 1997). A dramatic and rapid decrease in proteolysis would obviously affect fast-turnover proteins of sarcoplasmic origin, a process thought to predominantly involve lysosomal-cathepsin proteolysis (described in Section 2.7). Fasting increases mRNA and/or activity of components of both the lysosomal-cathepsin system (Doherty and Mayer, 1992c, Thompson and Palmer, 1998, Mosoni *et al*, 1999, Jagoe *et al*, 2002, Lecker *et al*, 2004) and the ubiquitin-proteasome system (Mosoni *et al*, 1999, Jagoe *et al*, 2002, Lecker *et al*, 2004). It is thought that this response is attributed mainly to low insulin, IGF-1 and raised glucocorticoids.

GH is described in detail in Section 2.3.3. Its effects on proteolysis are unclear. Excess T_3, for example during hyperthyroidism, increases degradation (Rooyackers and Nair, 1997). Androgens are known to increase protein synthesis but effects on bulk degradation are unclear (Bhasin *et al*, 2001). Many of the long-term effects of androgens on muscle protein turnover and proteolysis may involve alterations in the GH-IGF axis (Bhasin *et al*, 2001). Catecholamines are increased in response to fasting (Frayn, 1997g). As described in Section 2.3.4, the endogenous catecholamines (noradrenaline and adrenaline) are known to decrease protein degradation, believed to be mediated in part through down-regulating calcium-calpain dependent proteolysis (Rooyackers and Nair, 1997, Navegantes *et al*, 2002).

2.4 SEVERE CATABOLIC STATES AND THE STRESS REACTION

2.4.1 Introduction

During catabolic states including; prolonged fasting and malnutrition, illness, infection, trauma, pathophysiological disorders and severe stress the mammalian organism responds to the stimuli by mounting a stress response (Biolo *et al*, 1997, Ingenbleek and Bernstein, 1999). This may generate a whole body catabolic response, with increased amino acid and energy requirements (hypermetabolism) and upregulation of the previously mentioned amino acid partitioning processes (see Section 2.2.5) (Biolo *et al*, 1997, Ingenbleek and Bernstein, 1999, Jackson *et al*, 1999). There is a characteristic fall in nitrogen balance and loss of lean body mass (LBM) / body cell mass (BCM). This is a purposeful response to promote survival. The level of the stress response and its protein-catabolic effects ultimately depends on the intensity and duration of the insult/stimuli (Biolo *et al*, 1997, Ingenbleek and Bernstein, 1999). In the long term the greater the loss and rate of loss of LBM/BCM, the higher the levels of morbidity and mortality, which is a considerable clinical problem in states such as sepsis, cancer cachexia and HIV/AIDS wasting (Kotler, 2000). The intracellular proteolytic systems may act in co-ordination to control amino acid production and mobilisation from myofibrillar and sarcoplasmic protein pools (Hasselgren and Fischer, 2001). Therefore, it is appropriate for the purposes of this literature review to discuss this area of research.

2.4.2 Relevant Clinical Catabolic Conditions

There are three known classifications of protein-catabolic states that exhibit skeletal muscle depletion and loss. They tend to follow different patterns and pathways of loss and have different effects on skeletal muscle proteolysis.

1) Wasting: Involuntary weight loss, generally driven by inadequate dietary intake (Roubenhoff, 1997). In general, although protein degradation is increased, inadequate dietary intake doesn't evoke an intense stress reaction and massive rise in skeletal muscle proteolysis (Bistrian, 1999).

2) Cachexia: A state of intense protein loss (depending on the severity of the insult) during chronic or end stage diseases, due to the impact of an immune/acute-phase response/stress reaction and its encompassing hormonal and peptide mediators on protein turnover (Biolo *et al*, 1997, Roubenhoff, 1997, Kotler, 2000). Examples of conditions include: Burns, trauma, post-operative stress, cancer, infections/sepsis, AIDS/HIV, heart failure, rheumatoid arthritis, tuberculosis, chronic obstructive pulmonary disease (COPD), and other inflammatory and autoimmune disorders (Biolo *et al*, 1997, Yarasheki *et al*, 1998, Kotler and Heymsfield, 1998, Macallan, 1999, Libera, 1999, Tisdale, 1999, Vescovo, *et al*, 2000, Baracos, 2000, Tisdale, 2000, Kotler, 2000).

3) Sarcopenia: An involuntary loss of muscle mass that may be an intrinsic part of aging (Roubenoff, 1999). Thought to be due to primarily alterations in hormonal output and balance. Studies have linked sarcopenia and aging to decreased levels of GH, sex steroids (testosterone etc.), IGF-1, possibly T_3 and possibly decreased α-motorneuron activity, along with a simultaneous rise in catecholamines, glucocorticoids and cytokines (Proctor *et al*, 1998, Roubenoff, 1999, Yeh and Schuster, 1999). Conditions classified under sarcopenic states, but not intrinsic with ageing include, disuse atrophy and weightlessness (Fitts *et al*, 2000, Adams *et al*, 2003).

Other examples, that fall outside the main classifications include:

A) Direct local damage/trauma, including eccentric contraction induced damage to musculoskeletal tissues activates proteolysis directly and indirectly via the systemic stress response initiated in hypothalamic-pituitary glands and immune system (Mansoor *et al* 1996, Biolo *et al*, 1997, Sandri and Carraro, 1999, Farges *et al*, 2002, Stupka *et al*, 2001, Féasson *et al*, 2002). There will be varying effects on total cell damage and proteolysis depending on the type and intensity of trauma.

B) Muscular dystrophy (MD) and limb girdle muscular dystrophies (LGMDs) are debilitating conditions, causing decreased muscle function, pain and disability, due to genetic defects in expression of skeletal muscle specific proteins (Brown, 1997, Bushby, 1999). Absence of proteins involved in sarcolemma stabilisation, force transduction/transmission and possible regulatory roles (e.g. sarcoglycans and dys-

trophin) gives rise to duchenne and LGMDs. This causes impaired contractile activity/force production, increased susceptibility to muscle injury, sarcolemmal destabilisation and dysregulation in cytoplasmic calcium homeostasis (Tidball and Spencer, 2000, Lynch *et al*, 2001, Spencer and Mellgren, 2002). Clinical features can include increased proteolysis, muscle atrophy, apoptosis, and necrosis (Baghdiguian *et al*, 1999, Engvall and Wewer, 2003). As will be discussed in later sections, protease systems play a key role in the pathogenesis of these conditions.

C) A rise in proteolysis and possibly muscle atrophy may occur in other diverse settings including: Kidney dysfunction and uremic states (Mitch, 1997), Type I and Type II diabetes (Rooyackers and Nair, 1997, De Feo, 1998), Cushings syndrome/glucocorticoid treatment (Rooyackers and Nair, 1997, Claeyssens *et al*, 2000), obesity (Argilés *et al*, 1999), hyperthyroidism-denervation (Authier *et al*, 1997, Llovera *et al*, 1999).

In summary, diverse signals may induce similar end results, i.e. muscle atrophy through activation of the stress reaction and/or similar degradatory pathways.

2.4.3 The Stress Reaction and Other Stress-Related Factors on Muscle Proteolysis

The stress reaction encompasses a large spectrum of metabolic, endocrine and immune alterations developed by the injured body in response to varying causal agents (Biolo *et al*, 1997, Ingenbleek and Bernstein, 1999). The reaction to stress and acute injury is primarily characterised by the release of cytokines by activated macrophages/monocytes or other reacting cells. They are regarded as major autocrine, paracrine and endocrine orchestrators of the stress response (Biolo *et al*, 1997, Ingenbleek and Bernstein, 1999). Interleukin-1, -6 (IL-1 and Il-6) and Tumour necrosis factor-α (TNF-α) reveal prominent activities, notably enhanced production of counterregulatory hormones (cortisol, catecholamines and glucagon). GH and thyroid hormones adapt to these metabolic adjustments along complex regulatory mechanisms, too complex to be discussed in detail in this review. A brief indication of the factors and resulting effects of 'the stress reaction' on skeletal muscle are described below.

In skeletal muscle during a stress reaction/immune response there is a characteristic depression of anabolic processes and responsiveness (Biolo *et al*, 1997, Ingenbleek and Bernstein, 1999). For example, a development of insulin and GH resistance, and probably IGF-1 resistance. The effects of hyper-cortisolaemia, -glucagonemia, and –catecholemia, along with cytokine overproduction enforces this state of anabolic depression/refraction/resistance, general catabolism, fuel mobilisation, protein catabolism and amino acid mobilisation. This is compounded by an increased demand for specific limiting amino acids to synthesise acute-phase reactants (APRs) during an acute phase response. These APRs tend to have unusual amino acid compositions. For example, elevated fibrinogen synthesis in cancer patients with an acute phase response has been reported (Preston, 1998). It was suggested that to synthesise 1g of fibrinogen it may require 2.6g of muscle protein (12g skeletal muscle tissue), due to requirement for limiting aromatic amino acids.

Proteolytic systems within skeletal muscle become upregulated by the effects of hormones and cytokine interactions with receptors, activation of intracellular pathways and concomitant rise in gene transcription and post-translational modifying activation of systems (Hasselgren and Fischer, 2001). The key activating cytokines include IL-1, IL-6, TNF-α and interferon-γ (IFN-γ) (Roubenoff, 1997, Kotler, 2000, Baracos, 2000). Prostaglandin E2 (PGE2) may also be implicated as a key factor (Thompson and Palmer, 1998, Tisdale, 2000).

Evidence points towards induction of proteases and pro-apoptotic responses (i.e. promotion of cell death, a topic discussed in Section 2.10) during diverse catabolic, stress and immuno-inflammatory responses. Overproduction of proinflammatory cytokines, in particular TNFα is suggested to be a key stimulus. The generation of reactive oxygen species (ROS) and activation of the NF-κB (Nuclear-Factor kappa B) transcription factor pathway is reported to be involved and affect proteolysis. Kumar and Boriek, reported an increase in NFκB activation in mechanically stretched diaphragm muscle from normal and *mdx* (dystrophic) mice (Kumar and Boriek, 2003). The basal level of NFκB activity was higher in *mdx* mice and mechanical stress further upregulated activity. They found that activity is dependent on free radical production and is Ca^{2+}-independent. The increase in activity concided with increased

expression of IL-1β and TNF-α, which preceeded muscular dystrophy in the *mdx* mice.

The function of increased NF-κB activity is to promote cell survival initially and inhibit apoptosis (Grimm, 2003e). Insulin, known for its metabolic and anti-proteolytic effects in muscle, has been observed to have an anti-apoptotic function in cells, possibly through activation of NF-κB and NF-κB-dependent survival genes, like TRAF2 (Tumour Necrosis Factor Receptor-associated Factor 2) and Mn-SOD (Manganese-superoxide Dismutase) (Bertrand *et al*, 1998, Bertrand *et al*, 1999). In support of this role it should be noted that a total loss of NF-κB activity in human skeletal muscle promotes myoapoptosis (see LGMD2A in calpain Section 2.8.4). Proinflammatory cytokines up-regulated in the NF-κB 'survival' response may have important effects on proliferation and differentiation of satellite cells (Alvarez *et al*, 2002), which in turn, allows muscle fiber regeneration after injury (Mitchell and Pavlath, 2001, Grounds *et al*, 2002), which is important during MDs. Ladner *et al*, 2003, reported a biphasic activation of NF-κB in skeletal muscle cells in response to prolonged exposure to TNFα. The first phase was "potent but transient", but the second was suggested to be a 'persistent' signal (lasting additional 24-36 hours), due to a long-term exposure to TNFα, which lead to loss of muscle gene products. In basal situations the effects of TNFα is to induce an apoptotic (via. Death receptor) and anti-apoptotic (via. NF-κB) effect through its receptors, leading to an eventual cancelling out of responses (possibly occuring in initial cachexia). However, during high chronic levels of TNFα (and other inflammatory mediators), muscle fibers may be more sensitive to the pro-apoptotic effects and protease activation.

During cellular dysfunction (e.g. during MDs) and excessive and prolonged inflammatory stimulation, a positive feedback mechanism may function. Increased cell damage and free radical production increases NFκB activity, in turn, increasing pro-inflammatory cytokine production, inflammatory mediators and ROS production. This increases further inflammation, cell damage and intracellular protease and NFκB activation (Ladner *et al*, 2003). Increased oxidation of membrane lipids (peroxidation), proteins and DNA (Macdonald *et al*, 2003) can lead to ubiquitin-proteasome system activation (Merker *et al*, 2001) and further trigger cell death pathways. It is interesting to note that a number of genes that have NF-κB binding

sites in their promoter regions include cytokines, calpain proteases, ubiquitin-proteasome system components and a number of inflammatory mediators (Hasselgren and Fischer, 2001, Penner *et al*, 2002, Macdonald *et al*, 2003).

The transcription factors AP-1, C/EBP-β and -δ are also associated with inflammatory responses, have binding sites in the promoter regions of members of the calpain and ubiquitin-proteasome systems and are up-regulated in muscle during sepsis (Thompson and Palmer, 1998, Hasselgren and Fischer, 2001, Penner *et al*, 2002, Macdonald *et al*, 2003). Penner *et al*, 2002, reported that the up-regulation in C/EBP-β and δ was partly glucocorticoid-dependent. Previously Penner *et al*, 2001, suggested NF-κB and AP-1 are differentially regulated during sepsis. He found that using the glucocorticoid receptor antagonist RU38486, sepsis-induced AP-1 activity dropped but increased NF-κB activity. This is an important finding as glucocorticoids are thought to have an anti-inflammatory effect (decreasing NF-κB activity) and have been implicated in the atrophy response to many stimuli but never fully proven (Thompson and Palmer, 1998, Raillière *et al*, 1997). Partly, because researchers have focused on genes containing the GRE (Glucocorticoid Response Element) previously, with no success (Thompson and Palmer, 1998). Interestingly also, GH which is generally elevated during stress responses and plays a key metabolic role during many of the conditions discussed, is thought to regulate the transcription factors, C/EBP-β and –δ and glucocorticoid receptor (Herrington and Su, 2001).

In summary, muscle protein loss is a serious concern affecting morbidity and mortality in many clinical situations and states that involve stress/immuno-inflammatory responses, e.g. cachexia. Much is known about the stress reaction and its mediators, yet the precise effects on intracellular protease systems within skeletal muscle is unclear and may involve complex mechanisms. The pro-inflamatory cytokines, glucocorticoid receptor and transcription factors NF-κB, AP-1 C/EBP-β and –δ, altered during stress/immuno-inflammatory responses may play key roles in the induction of protease systems.

Clinical research has recently been driven towards investigating the use of anti-inflammatory and anti-cytokine compounds, and nutrients, including: protein and amino acids, anti-oxidants and n-3 fatty acids (Mayer *et al*, 1998, Bistrian, 1999, Yeh

and Schuster, 1999, Tisdale, 1999, Kotler, 2000, Baud *et al*, 2001, Grimble, 2003, Grounds and Torrisi, 2004); in many stress reaction/immuno-inflammatory conditions. The aim being to reduce inflammation, oxidant stress, tissue damage and in turn reduce lean body mass loss.

2.5 SUMMARY OF THE RELEVANCE OF SKELETAL MUSCLE PROTEOLYSIS

Skeletal muscle tissue has a dual role. Firstly, it is required for muscle contractile activity and secondly, due to its mass, composition and energy expenditure it is important for amino acid repartitioning, glucose and lipid clearance (Rennie and Tipton, 2000). It is therefore important to maintain muscle tissue for optimal physical health. Conditions that induce muscle wasting/atrophy are associated with decreased muscle function, increased disability, debilitation, morbidity and mortality (Roubenoff, 1999, Tisdale, 1999, Tisdale, 2000, Kotler, 2000). Proteolytic systems within skeletal muscle are activated during many catabolic states and may act as the primary mechanism in myofibrillar degradation (Hasselgren and Fischer, 2001, Goll *et al*, 2003).

The medical application of growth-promoting/nutrient-repartitioning agents like testosterone analogues, GH, IGF-1, insulin, insulin-sensitisers and β-adrenergic agonists has been to attempt to drive anabolism and/or prevent/reduce catabolism; and thereby combat muscle wasting/atrophy in a number of animal models and clinical settings (Rooyackers and Nair, 1997, Garlick et al, 1998, Mann, 1999, Yeh and Schuster, 1999, Bistrian, 1999, Kotler, 2000, Fowler *et al*, 2004). Many have been utilised and studied extensively in farm animals and shown to increase lean body mass and efficiency of growth (Grant and Gerrard, 1998, Bell *et al*, 1998, McDonagh *et al*, 1999). The different pharmacological agents are known to have variable suppressing effects on proteolysis. Proteolytic system inhibitors have been suggested by both the livestock industry (Goll, *et al*, 1998) and in clinical medicine to potentially have a beneficial effect on muscle growth and protein accretion in a number of catabolic states indicated in Section 2.4.2.

Proteolysis and specific intracellular protease systems are also involved in the meat tenderisation process and meat quality (Taylor *et al*, 1995, McDonagh *et al*, 1999,

Hopkins and Thompson, 2001a, Hopkins and Thompson, 2001b, Hopkins and Thompson, 2001c). This has important commercial implications for the livestock industry. Meat tenderness post-slaughter is dependent on the rate of proteolysis of myofibrillar and cytoskeletal proteins within skeletal muscle (process described in Section 2.2.4). Studies suggest that for an increase in muscle growth, a decrease in proteolysis is favourable, whereas for meat tenderisation, an increase in proteolysis pre-slaughter is favourable. This contradiction makes the use of pharmacological growth-promoting agents difficult in the livestock industry. Therefore, a greater understanding of the significance of the individual proteolytic systems in muscle may allow manipulation which will enhance muscle growth, but not have a negative effect on the proteolytic dependent process of tenderisation.

2.6 INTRODUCTION TO THE PROTEOLYTIC PATHWAYS

Proteolysis in skeletal muscle serves 3 major functions:-

1) Protein turnover at steady state conditions.
2) Muscle wasting/compartmental depletion under catabolic conditions.
3) Sarcomeric remodelling, related to adaptive responses.e.g. during growth.

Research suggests that these functions are achieved within skeletal muscle through coordinate interactions between four major intracellular proteolytic systems, other intracellular (local, independent, mitochondrial and sarcoplasmic reticulum proteases may function) and extracellular proteases and endogenous, intracellular protease inhibitors (Doherty and Mayer, 1992c, Thompson and Palmer, 1998, Jagoe *et al*, 2002, Stevenson *et al*, 2003, Lecker *et al*, 2004). It has been suggested that the vast majority, if not all proteolysis is ATP-dependent. Although peptide hydrolysis by many proteases does not require energy, ATP is required for various activation steps, ion pump functioning and possible catalysis and protein transport mechanisms (Doherty and Mayer, 1992c). An important source of proteases during inflammatory/immune responses and local trauma is white mononuclear cells, which may invaginate muscle cells and subsequently release proteases, including cathepsins (Farges *et al*, 2002).

The four major intracellular proteolytic systems operating within skeletal muscle tissue include:

Lysosomal-Cathepsin protease system,

ATP-dependent Ubiquitin-Proteasome system,

Calpain system,

Caspase pathway.

All four systems have individual importance in regulating specific proteolytic events within skeletal muscle, under different nutritional, metabolic, endo-, para- and autocrine influences, and pharmacological and pathological conditions.

Protease systems have been implicated not only in intracellular protein turnover but also highly specific 'recycling' functions, sarcoplasmic and myofibrillar remodelling and repartitioning (Glickman and Ciechanover, 2002, Goll *et al*, 2003). Whole cell protein turnover in basal cell turnover conditions, cancer growth, excessive cell loss/death during apoptotic and apoptotic-like and necrotic states are all dependent on regulation of protease system activation (Sandri and Carraro, 1999, Tidball and Spencer, 2000, Grimm, 2003a). More recently, as will be described, various proteases have been linked to myocellular glucose and fat metabolism, or the dysregulation of, and pathological states such as diabetes (Baier *et al*, 2000, Walder *et al*, 2002, Huang *et al*, 2003). This is an unexpected role for enzymes which were traditionally associated with gross protein turnover.

2.7 THE LYSOSOMAL CATHEPSIN PROTEASE SYSTEM

2.7.1 Structure and Function

Lysosomes are located in the interior of irregular, single-membrane bound, vesicular structures found ubiquitously in the cytoplasm of mammalian cells. Lysosomes are more acidic than the cytoplasm and contain a variety of enzymes that are responsible for 'digesting' various cell materials (Doherty and Mayer, 1992c, Voet and Voet, 1995b). The lysosome is responsible for degrading extracellular proteins (e.g. plasma lipoproteins and hormones) and phagocytosed bacteria after undergoing endocytosis. The endosome-lysosome pathway is also responsible for peptide generation to the immune system and turnover of cell membrane proteins. Some cytosolic proteins are

also degraded through a process involving engulfing in autophagic vacuoles and eventual fusion with the lysosome (Doherty and Mayer, 1992c, Voet and Voet, 1995b). The numerous functions of the system are limited however to individual cell types, such that for example, mature myofibers would be incapable of phagocytosing bacteria.

Lysosomes are capable of the rapid breakdown of intact cytoplasmic and extracellular proteins completely to amino acids, through a combined action of cathepsin endoproteases (which cleave internal peptide bonds of proteins), exopeptidases (carboxypeptidases A and B and aminopeptidases) and di- and tripeptidases (Doherty and Mayer, 1992c). The acid proteases of the lysosomal compartment are most active at a low pH and thus a low pH is maintained by an ATP-dependent H^+ pump.

Cathepsins are classified on the basis of the important amino acid at the active site. Cathepsins B, H and L have cysteine, D, aspartate and G, serine (see Table 2.7.1-1). They are thought to be activated by auto-proteolysis in acidic pH or by proteolysis by other proteases (Grimm, 2003a). For example, cathepsin D can activate B and L. Ceramide is also reported to bind and promote proteolytic activation of cathepsin D (Grimm, 2003a). A number of endogenous inhibitors for the cathepsins have been identified termed the 'cystatin superfamily', although little is known about their function within skeletal muscle (Auerswald *et al*, 1996, Grimm, 2003a, Stevenson *et al*, 2003).

Table 2.7.1-1. Lysosomal-cathepsin proteases. *Cathepsins B, D, L and H are main enzymes identified in skeletal muscle.*

Enzyme	Essential active site residue	Presence in skeletal muscle
Cathepsin B	Cysteine	Yes
Cathepsin D	Aspartate	Yes
Cathepsin G	Serine	?
Cathepsin H	Cysteine	Yes
Cathepsin L	Cysteine	Yes

Due to the nature of autophagy, lysosomal proteolysis was originally viewed as a 'bulk' non-specific protein degrading system, incapable of degrading short-lived, unstable regulatory proteins. Several mechanisms operate with regards to sequesteration of cytoplasmic proteins which can impart (Doherty and Mayer, 1992c, Voet and Voet, 1995b). Bulk non-selective autophagy is accomplished by macroautophagy (known to be able to sequester whole organelles). Microautophagy is thought to be a more selective process involving multivesicular body (containing protein aggregates) invagination. Heterophagy (internalisation of extracellular materials into the lysosome-related system) is important for cellular homeostasis, nutrition, hormone and growth factor action. Secretion-coupled degradation involves the lysosomal system in regulation of the rate of secretion of various secretory proteins. Examples are that of casein secretion from mammary glands (Doherty and Mayer, 1992c). It would be interesting to know whether the lysosomal system plays a role in regulation of autocrine and paracrine secretion of growth factors, including IGF-1, FGF and TGF-β, from skeletal muscle cells. Another point of interest is that older studies suggested ubiquitin has a minor role in lysosomal proteolysis during nutrient deprivation and heat stress (Doherty and Mayer, 1992c). This may suggest another pathway for specificity control or 'cross-over' of system pathways. However, the primary mechanism of selective sequesteration of certain proteins (including possibly some that are unstable and short-lived) is through recognition of proteins containing a certain pentapeptide motif, Lys-phe-Glu-Arg-Gln (KFERQ) or a closely related sequence. The KFERQ motif (or similar) containing protein is recognised and bound in the cytosol by prp73 (73-kDa peptide recognition protein), a member of the 70-kD heat shock protein (hsp70) family; and subsequently targeted to the lysosome (Doherty and Mayer, 1992c, Doherty and Mayer, 1992d,Voet and Voet, 1995b).

2.7.2 Metabolic Role in Skeletal Muscle

Lysosomes and lysosomal cathepsin proteases are detected in skeletal muscle (see Table 2.7.1-1) (Thompson and Palmer, 1998). It is known that lysosomes degrade many intact cellular proteins (e.g. membrane and soluble proteins) completely to amino acids, but thought to only play a minor role in myofibrillar degradation under basal and catabolic conditions (roles thought to be attributed to calpain and ubiquitin-proteasome systems) (Farges *et al*, 2002). The lysosomal-cathepsin system is unable

to directly degrade intact myofibrillar proteins, only cleaved myofilament units. This is thought to be due to their cellular location, i.e. outside the periphery of the myofibrillar apparatus (Doherty and Mayer, 1992e).

The lysosomal system is thought to be regulated by specific nutrients, hormones and nutritional feeding and fasting (Doherty and Mayer, 1992c, Doherty and Mayer, 1992d, Voet and Voet, 1995b). BCAAs may decrease activity of lysosomal proteases (Busquets *et al*, 2000) and insulin may inhibit lysosomal proteolysis possibly due to a reduction in autophagic vacuole formation and/or decrease in lysosomal fragility (Thompson and Palmer, 1998). As described in Section 2.3.5.4, the rapid and potent decrease in protein breakdown post-meal is thought to be attributed to a rise in insulin (and probably amino acids) and affect proteins of non-myofibrillar origin (Rooyackers and Nair, 1997). Therefore, it is likely that any rapid and potent decrease in protein breakdown and rise in lysosomal proteolysis indicates that the lysosomal-cathepsin system may play a major role in 'bulk' sarcoplasmic proteolysis (note: in co-ordination with the ubiquitin-proteasome system).

Serum and nutrient deprivation of cells leads to a rapid rise in non-selective macroautophagy. During prolonged nutrient deprivation (e.g. starvation) a rise in selective uptake of proteins takes place via the KFERQ-motif recognition-prp73 mechanism, which may function to spare essential and recycle non-essential proteins (Doherty and Mayer, 1992d, Voet and Voet, 1995b).

The lysosomal-cathepsin system has been suggested to play a role in the induction of the proteolytic response in muscle during a number of diverse catabolic-atrophic states (Tsujinaka *et al*, 1996, Tsujinaka *et al*, 1997, Farges *et al*, 2002, Deval *et al*, 2001, Stevenson *et al*, 2003), the pathogenesis of degenerative myopathies (Weinstein *et al*, 1997) and involved in cell death, apoptosis and necrosis (Grimm, 2003a).

Table 2.7.2-1 indicates the various conditions and states that have been reported to affect the lysosomal enzymes in skeletal muscle. In nearly all catabolic states listed there is a loss of muscle weight (of studied organism), increase in protein degradation and common increase in cathepsin-L mRNA and/or activity. Many of the states

affect whole body proteolysis and involve stress-immune responses as described in Section 2.4. For example, Mansoor *et al*, 1996 (see Table 2.7.2-1) observed increases in whole-body and myofibrillar breakdown, cortisol excretion, IL-1β, IL-6 and proteolytic system activities in human head trauma patients; in addition to an increase in cathepsin-D mRNA. An important observation to note with many of the studies is that there is an associated rise in pro-inflammatory cytokines. Interestingly, the increase in cathepsin-B and -L mRNA and activities observed in IL-6 transgenic mice and during abcess formation in mice, was inhibited using an IL-6 receptor antibody (Tsujinaka *et al*, 1996 and Tsujinaka *et al*, 1997).

Therefore, under catabolic-atrophic conditions lysosomal proteolysis may play a greater role in muscle and myofibrillar protein breakdown (Weinstein *et al*, 1997). It is possible that specific cathepsins up-regulated during these states, in particular cathepsin-L, may play a role in this response (Deval *et al*, 2001, Stevenson *et al*, 2003).

In Table 2.7.2-1, Féasson *et al*, 2002 observed an increase in activities of cathepsins B and L after a bout of eccentric exercise in humans. This is obviously interesting as it may implicate the cathepsins in a possible coordinated remodelling response to exercise-induced muscle damage.

In Table 2.7.2-1, Huang *et al*, 2003 found that cathepsin-L mRNA may play a role in glucose metabolism in skeletal muscle in humans. An impairment in an insulin-mediated rise in cathepsin-L mRNA was associated with a diabetic state. This is the first study to suggest that lysosomal-cathepsin proteolysis, in particular, cathepsin-L activity is involved in myocellular glucose metabolism and/or insulin signalling.

From Table 2.7.2-1 it can be seen that much is known about conditions that alter mRNA levels of cathepsins during various catabolic-atrophic stimuli, yet little is known about their transcriptional control. Similar regulators may be involved as described in Section 2.4.3, i.e. the glucocorticoid receptor, NF-κB, AP-1, C/EBP-β and –δ, which are known to alter during stress/immuno-inflammatory responses. Further studies would need to confirm these theories.

Table 2.7.2-1. Reported effects of various conditions and states on cathepsins in skeletal muscle.

Condition or state	Effect on Lysosomal Cathepsin system	Reference
Fasting	↑ / ↔ mRNA for Cathepsins. ↑ mRNA Cathepsin L is consistant finding.	Thompson and Palmer, 1998, Mosoni *et al*, 1999, Jagoe *et al*, 2002, Lecker *et al*, 2004.
Dis-use/unloading/microgravity	↑ / ↔ mRNA for Cathepsins. ↑ mRNA Cathepsin L is consistant finding. ↑ mRNA Cystatin C.	Ikemoto *et al*, 2001, .Stevenson *et al*, 2003.
Head trauma.	↑ Cathepsin D mRNA.	Mansoor *et al*, 1996.
Local blunt trauma.	↑ Cathepsin B activity and mRNA for Cathepsins B, L, H and C. Cathepsin B Located to mononuclear cells.	Farges *et al*, 2002
Distal and proximal denervation.	↑ protein degradation and DECLINE in lysosomal latency (indication of increased lysosomal response).	Weinstein *et al*, 1997.
Diabetes mellitus and Uremia.	↑ Cathepsin L (2-3 fold) mRNA, no change in other Cathepsins.	Lecker *et al*, 2004.
Sepsis Dexamethasone treatment	↑ Cathepsin-L mRNA and protein. Others components INCREASE up to 4-fold. ↑ Cathepsin-L mRNA.	Deval *et al*, 2001.
Cancer cachexia	↑ Cathepsin-L mRNA and activity.	Deval *et al*, 2001, Lecker *et al*, 2004.
Il-6 transgenic mice.	↑ Cathepsin-B and -L mRNA and activities, inhibited by MR 16-1 (IL-6 receptor antibody) treatment.	Tsujinaka, 1996.
Inflammation and abcess formation.	↑ Cathepsin-B and -L mRNA and activities, inhibited by MR 16-1 (IL-6 receptor antibody) treatment.	Tsujinaka, 1997.
Eccentric exercise bout.	↑ apoptotic markers and loss of dystrophin. ↑ in Cathepsins B and L activities	Birai *et al*, 2000, Féasson *et al*, 2002
Diabetes and control subjects.	↑ Cathepsin L mRNA correlated with insulin-mediated glucose uptake, glucose oxidation, and fasting glucose concentrations.	Huang *et al*, 2003

	Impaired in diabetic subjects.	

2.7.3 SUMMARY

A number of specific cathepsin proteases function in co-ordination with exopeptidases and di- and tri- peptidases, within the acidic lysosomal compartment, to completely degrade in an ATP-driven process, proteins of intracellular and extracellular origin within skeletal muscle. Under basal conditions the system may play a key role in 'relatively non-selective' bulk sarcoplasmic protein degradaton (in co-ordination with the ubiquitin-proteasome system), but a limited role in the degradation of cleaved-myofibrillar units.

Evidence suggests the lysosomal-cathepsin system has a role in fasting-, denervation-, disuse/microgravity-, trauma-, sepsis-, cancer- and cytokine-induced rises in muscle proteolysis and atrophy. Other diverse conditions like age-related sarcopenia, uremia, type I and II diabetes and glucose intolerance may also be affected. Studies indicate that cathepsin L is the key functioning lysosomal protease in nearly all of the studied states. This suggests that during such states the system may play a more selective role in proteolysis.

Evidence suggests a strong regulatory role played by various mediators of the stress and immune response, with regards to cathepsin regulation. Cytokines and glucocorticoids are potentially implicated, in particular the proinflammatory cytokines, IL-6 and TNF-α. Regulation of cathepsin gene transcription is under regulatory control, but it is unknown which factors are involved. It may involve a number of factors associated in immuno-inflammatory/stress responses.

2.8 THE CALPAIN SYSTEM

2.8.1 Structure and Activity

The calpains are calcium-dependent, neutral, cysteine, intracellular, non-lysosomal proteases. The first characterised vertebrate calpains were the ubiquitous μ- (micro) and m- (milli) calpains, with repsective requirements for μ- and m- concentrations of

calcium ions for activation (Sazontova *et al*, 1999, Goll *et al*, 2003). The calpains have been found to be a complex family with at least 11 different calpain genes now identified (Huang and Wang, 2001). In skeletal muscle, the calpains of importance include μ- and *m*-calpain, a skeletal muscle specific calpain known as calpain 3 or p94 and more recently identified, calpain 10 (Goll *et al*, 1998, Sazontova *et al*, 1999, Tidball and Spencer, 2000, Huang and Wang, 2001, Ma *et al*, 2001, Goll *et al*, 2003)

In terms of structure μ-(Aoki *et al*, 1986)- and *m*-(Imajoh *et al*, 1998)- calpain (or calpains 1 and 2), were found to consist of a different large 80kDa and small 28 kDa subunit that associate non-covalently. The large subunit contains four different distinct domains. Domain 1 may be a regulatory domain cleaved during calpain activation (autolytic activation). Domain 2 acts as the proteolytic domain, similar to other cysteine proteases (cysteine catalytic site). Domain 3 may be involved in binding phospholipids and regulating calpain activity by electrostatic interactions (Goll *et al*, 2003). Domain 4 is the calcium binding domain similar to calmodulin, with five EF-hand structures. The small subunit, contains domains 5 and 6. Domain 5 being important in enabling calpain association with membrane phospholipids. Domain 6 contains four calcium binding domains homologous to domain 4. Figure 2.8.1-1, illustrates the domain structures of the ubiquitous μ- and *m*-calpains. Calpain 3/p94 (94 kDa protein) contains four distinct domains and has 50% sequence homology with the ubiquitous μ- and *m*-calpains. It is different in structure in that it has no small subunit and presence of three additional insertion sequence regions (NS, IS1 and IS2), with expected functional importance (Sorimachi *et al*, 1989). IS1 has three autolytic sites, S1, S2, and S3. The IS2 sequence is capable of associating with titin. In immunostained myofibrils it is located along the N2 and Z-line *in vivo*. Within the IS2 region there is a potential nuclear translocation signal (NTS) (Goll *et al*, 2003). Figure 2.8.1-1, illustrates the domain structures of calpain-3, in relation to the ubiquitous μ- and *m*-calpains.

Calpain 3 has an unknown function and activation mechanism due to its instability in muscle extracts. It has been suggested that Calpain 3 is produced as an inactive zymogen, similar to the Caspase family and has a proteolytic activity that is activated on autolytic cleavage in the IS1 region (Taveau *et al*, 2003).

Figure 2.8.1-1. Schematic structures of A) ubiquitous *μ*-and *m*-calpain and B) muscle-specific calpain-3. *The large catalytic subunit and small regulatory subunits are indicated for the ubiquitous calpains and muscle-specific calpain-3. The four domains (I, II, III and IV) are indicated with three specific regions of muscle-specific calpain-3 (NS, IS1 and IS2). The Nuclear Localisation Signal (NLS) is indicated within IS2. The size scale in number of amino acids is indicated at either end of the sequence. μ- Calpain is 714 amino acids long and m-calpain, 699. Calpain-3 is as described 821 amino acids long and 94 kDa in mass.*

A) Ubiquitous *μ*-and *m*-Calpain

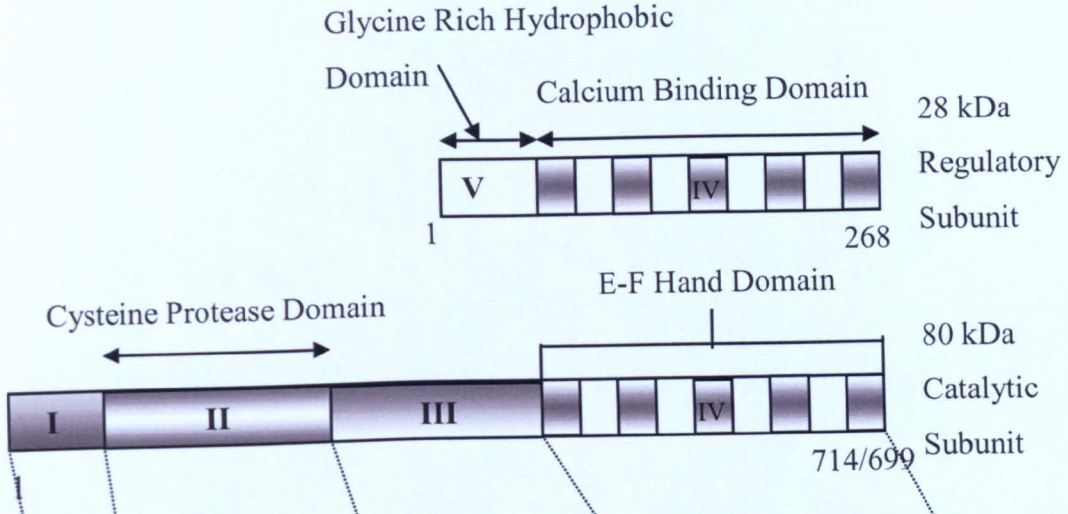

B) Muscle-Specific Calpain-3

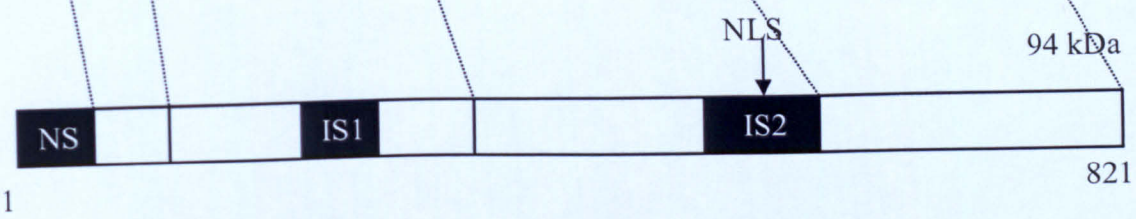

Calpain 10 has recently been characterised, found to be ubiquitously expressed and linked to insulin dependent glucose metabolism (Ma *et al*, 2001). It is thought to be a novel calpain, found in many cell types in human, mouse and rat. It is devoid of a calmodulin domain and exhibits a nuclear localisation capability (Ma *et al*, 2001).

The calpains are regulated in activities by a complex number of interactions and requirements (Sazontova *et al*, 1999, Perrin and Huttenlocher, 2002). These include, whole cell and near-membrane intracellular Ca^{2+} ion concentrations. The calpains interact with the endogenous inhibitor calpastatin (see below). Regulation of calpain gene transcription has not been fully characterised at present, but may involve a number of factors involved in inflammatory/stress responses. Binding sites for the transcription factors NF-κB, AP-1, C/EBP-β and -δ in the promoter region for members of the calpain system have been found. (Sorimachi *et al*, 1996, Penner *et al*, 2002).

Calpains are also known to be regulated in activation by translocation to the plasma membrane, subsequent binding with specific phospholipids and activation (Perrin and Huttenlocher, 2002). Calpains may be regulated by phosphorylation state. Activator proteins for the calpains have also been identified and are thought to function attached to the plasma membrane (Sazontova *et al*, 1999). It has been speculated that *μ*- and *m*- calpains are in their active state prior to autolysis, where as calpain 3 has been suggested to be activated on autolysis. In vivo $[Ca^{2+}]$ and the presence of calpastatin suggests that true in vivo basal activity for *μ*- and *m*- calpain is low.

Calpastatin is the specific endogenous inhibitor of *μ*- and *m*- calpains which does not modulate the activity of any other proteases. It is thought to be regulated by phosphorylation state and Ca^{2+} ions, and may be inactivated by calpain- or caspase-mediated cleavage (Sazontova *et al*, 1999, Goll *et al*, 2003). Calpastatin protein is heterogenous in size across species and tissue and this heterogeneity is thought to be due to alternative splicing and post-translational processing. Different isoforms are expressed in cardiac and skeletal muscle and may have differential effects on calpain activity (Goll *et al*, 1998, Parr *et al*, 2000, Parr *et al*, 2001). Gene expression may be regulated in part through actions on a cAMP-responsive element (confirmed in bovine) (Cong *et al*, 1998) by CREB. Activity may be regulated by PKA-mediated

phosphorylation, as PKA phosphorylation sites have been identified in the XL domain (see Figure 2.8.1-2.) (Goll *et al*, 2003).

Figure 2.8.1-2. Schematic structure of calpastatin. *Calpastatin consists of a non-inhibitory N-terminal XL and leader domain (L), followed by four inhibitory domains (I, II, III and IV). Bovine cardiac calpastatin is 786 amino acids long and has all domains present. Other species have different size sequences.*

Calpastatin

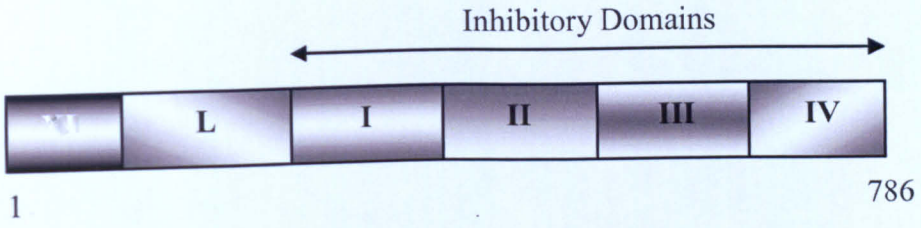

2.8.2 Calpain Function

The precise physiological function of the calpains is not known. They are believed to be involved in processes such as exocytosis, cell fusion, differentiation, apoptosis, proliferation, metabolism, myofibrillar, cytoskeletal and sarcoplasmic protein pool turnover (Sazontova *et al*, 1999, Goll *et al*, 2003).

The calpains do not degrade intact proteins into amino acids like the lysosomal and ATP-dependent ubiquitin proteasome system, but instead cleave specific proteins. The list of proteins that undergo proteolytic cleavage includes: cytoskeletal and myofibrillar proteins, transcription factors and their inhibitors, e.g. IκBα, ion channels, protein kinases, glycolytic and other metabolic enzymes and membrane bound proteins, like Ca^{2+}-ATPases (Verret *et al*, 1999, Krebs and Graves, 2000, Chen *et al*, 2000, Baghdiguian *et al*, 2001, Shen *et al*, 2001).

The calpain system is thought to have a prominent role in muscle protein turnover, through its involvement in basal protein degradation and cytoskeletal and myofibrillar cleavage (Huang and Forsberg, 1998, Goll *et al*, 2003). They may act as the rate-limiting factor in myofibrillar degradation and disassembly. They are thought to be unable to directly degrade actin and myosin but able to cleave troponin T, desmin, vinculin, talin, spectrin, nebulin and titin; and cleave at a slower rate, troponin I, filamin, C-protein, dystrophin, tropomyosin, α-actinin, and M protein (Taylor *et al*, 1995, Huang and Forsberg, 1998, Goll *et al*, 2003). Integrins (Pfaff *et al*, 1999), other costameric proteins and transmembrane plaques may also be cleaved by calpains (Taylor *et al*,1995, Perrin and Huttenlocher, 2002). They may also associate with some of these target proteins in their resting state. For example, *μ*-calpain has been reported to interact with α-actinin in a resting state (Raynaud *et al*, 2003). These potential substrates are involved in myofibrillar structure and stability, Z-disk integrity, costameric function and cytoskeletal integrity. Their cleavage inevitably leads to a loss of muscle cell structure, integrity and function. This may lead to a lack of ability for cellular mechano-transduction and myofibrillar contraction.

μ- and *m*- calpains and calpastatin are thought to be involved in myoblast fusion (Barnoy *et al*, 1997, Barnoy *et al*, 1998). Integrin B1 subunit, talin, and B-tropomyosin (specific proteins responsible for stability of the membrane-cytoskeletal organisation, and interaction of the cell with the extracellular matrix) are degraded specifically in a process thought to involve *μ*- and *m*- calpains (Barnoy *et al*, 1997, Barnoy *et al*, 1998). These specific cleavage events allows destabilisation of the membrane and the creation of membrane fusion-potent regions.

Calpain 3 is believed to have different functional activities in skeletal muscle compared to *μ*- and *m*- calpains. Calpain-3 mRNA is expressed at levels ~10 times greater than *μ*- and *m*- calpains, although 'free' p94 protein is rapidly degraded within the cell (Ono *et al*, 1999, Goll *et al*, 2003). Its precise functional role is unknown, but it has been observed to exhibit various regulatory functions. It is unlike other calpains in that it doesn't appear to participate in whole-cell cytoskeletal/myofibrillar cleavage and degradation (Ono *et al*, 1999, Goll *et al*, 2003). Although a recent study reported that cells expressing active autolysed p94 were able to cleave talin, filamin A, vinexin, ezrin, along with possibly titin and filamin C

(Taveau *et al*, 2003). The proteolytic cleavage lead to disruption of the actin cytoskeleton and disorganisation of focal adhesions. p94 is known to have a specific binding affinity to titin and is located along the N2 and Z-line in vivo, in immunostained myofibrils. A proposed function for p94 binding to titin may be that titin acts as a negative regulator preventing rapid autolytic cleavage of other p94 molecules, and/or to prevent other calpains (i.e. μ- and *m*-) from binding and initiating cleavage of myofibrillar proteins (Ono *et al*, 1999). p94 may also be involved in regulation of turnover or activity of transcription factors as it posesses a nuclear translocation sequence (NTS) (Ono *et al*, 1999, Goll *et al*, 2003).

2.8.3 Metabolic Role in Skeletal Muscle

Calpains are thought to play a role in hypertrophy, remodelling and atrophy under catabolic conditions, incl. muscular dystrophy states (Goll *et al*, 1998, Hasselgren and Fischer, 2001, Goll *et al*, 2003). Recent work has indicated that they are also play a role in insulin-mediated glucose disposal, fat and carbohydrate metabolism (Baier *et al*, 2000, Walder *et al*, 2002, Otani *et al*, 2004).

Remodelling of the cytoskeletal and myofibrillar apparatus is necessary during periods of rapid myofiber growth, fiber type transitions in response to various stimuli and possibly in regenerating cells. The calpain protease system may function as a rate-limiting step in many of these 'cleavage-dependent' processes. This ties in with the principle that proteolytic cleavage is a valuable means of controlling cellular processes, that doesn't have to be reversible.

Mechanical stimulation/loading and resistance 'training' are thought to affect the calpain-calpastatin system. Chronic low frequency stimulation (CFLS) studies in rat skeletal muscle (Sultan *et al*, 2000) and rabbit (Sultan *et al*, 2001) have showed an exchange of myofibrillar protein isoforms from fast-to-slow, MHCIIb-to MHCIId(x) and MHCIIa. The 'chronic' nature of CLFS cannot be compared to resistance training bouts in humans however as CLFS leads to formation of necrotic fibers and possible mononuclear infiltration. CLFS upregulates $[Ca^{2+}]i$ and free calpain activity, with no change in calpastatin activity. *m*-Calpain is prominent in mainly necrotic fibers and μ-calpain is elevated in intact fibers. In addition μ-calpain and to a lesser

extent *m*-calpain were shown to translocate from the cytosol to the myofibrillar and microsomal structures. CLFS caused a temporary reduction in the expression levels of calpain 3 in rabbit muscle possibly suggesting that it has a regulatory role in fiber type transformations. Féasson *et al*, 2002, showed that an eccentric exercise (muscle lengthening contractions) bout in humans decreased the mRNA levels of μ-calpain and calpain-3 by 25% and 40%, respectively, on day 1 post exercise, whereas *m*-calpain was dramatically increased (220%). Jones *et al*, 2002 found that calpastatin gene expression was increased by 300% following 8 weeks of resistance training in healthy female subjects; and remained increased 4 weeks after the cessation of training ($P < 0.05$). m-Calpain was also increased following training (154%, $P < 0.01$) and remained elevated after cessation ($P < 0.01$).

Calpain activity is important for remodelling, but overactivity has been associated with muscle atrophy (Thompson and Palmer, 1998, Williams *et al*, 1999, Busquets *et al*, 2000). Calpain inhibition has been suggested as a strategy for inducing hypertrophy in a number of settings. β-adrenergic stimulation (discussed at length in Section 2.3.4) increases lean muscle mass (Goll *et al*, 1998, Grant *et al*, 1998), induces a fast-twitch fiber transition (Rajab *et al*, 2000, Depreux *et al*, 2002, Pellegrino *et al*, 2003); and is known to increase calpastatin mRNA and activity, and down-regulate calpain activity (Parr *et al*, 1992, Bardsley *et al*, 1992, Speck *et al*, 1993, Sensky *et al*, 1996, Goll *et al*, 1998, Mc Donagh *et al*, 1999, Navegantes *et al*, 2002). Callipyge lambs with 30-40% greater muscle mass (than in half-siblings), deposited in the pelvic limbs and back, have associated 68-126% higher calpastatin activities. Muscle groups with no increase in mass in callipyge lambs had no change in calpastatin activities (Goll *et al*, 1998). Transgenic mice overexpressing calpastatin have been reported to have higher muscle weight (Otani *et al*, 2004).

Calpain -3 and -10 have been suggested to have a relationship with fat-carbohydrate metabolism/oxidation, insulin signalling, diabetes and obesity progression (Baier *et al*, 2000, Walder *et al*, 2002). There was reduced calpain 3 gene expression in human skeletal muscle from a group of 27 non-diabetic subjects and in *psammomys obesus* (a polygenic animal model of obesity and diabetes) (Walder *et al*, 2002). This correlated with reduced carbohydrate oxidation, elevated blood glucose, insulin, increased body fat and abdominal fat. Genetic variation in the gene encoding calpain 10 has

been linked to reduced skeletal muscle calpain 10 mRNA and insulin resistance (Baier *et al*, 2000), type 2 diabetes (Horikawa *et al*, 2000, Permutt *et al*, 2000) and increased serum cholesterol (Daimon *et al*, 2002) in different sub-populations. Calpain 10 gene polymorphism has also been associated with reduced β_3-adrenoceptor function in human fat cells (Hoffstedt *et al*, 2002), which may reduce fat cell lipolysis and regulate thermogenesis. Otani *et al*, in 2004, using transgenic mice that over-expressed calpastatin found that GLUT4 was increased 3-fold at protein level, whilst decreased at mRNA level (relative to wild type controls). They also showed *m*-calpain can degrade GLUT4 and suggest that the ubiquitously expressed calpain system is involved in the regulation of insulin-stimulated glucose disposal.

The calpain system may play a role in accelerated proteolysis and pathogenesis in skeletal muscle during catabolic conditions including cachexia (Hasselgren and Fischer, 2001). A summary of various studies looking at the effects of different conditions/states on changes in the calpain system is presented in Table, 2.8.3-1. One point of interest not noted in Table 2.8.3-1 is that Mosoni et al, 1999 found that in a fasting study, older rats had higher baseline *m*-calpain mRNA.

Table 2.8.3-1. Reported effects of conditions and states on calpains in skeletal muscle.

Condition or state	Effect on Calpain-Calpastatin system	Reference
Fasting	↑ mRNA for Calpains. ↓ Calpain-3 mRNA.	Mosoni *et al*, 1999, Jagoe *et al*, 2002
Hindlimb unloading	↓ mRNA for Calpain-3, NO CHANGE for *m*-Calpain, ↑ in Calpastatin.	Stevenson *et al* 2003.
Hindlimb unloading in transgenic mice over-expressing Calpastatin.	↓ muscle atrophy by 30% in transgenic mice, compared to normal non-transgene mice.	Tidball and Spencer, 2002
Head trauma	↑ mRNA for *m*-Calpains-2.	Mansoor *et al* 1996.
Sepsis	↑ mRNA for μ-and *m*-Calpains and Calpain 3	Williams *et al*, 1999.
Cancer cachexia	↓ Calpain-3 mRNA with ↑ *m*-Calpain mRNA.	Busquets *et al*, 2000.
IL-6 transgenic mice.	↓ mRNA for Calpain-3, inhibited by MR 16-1 (IL-6 receptor antibody) treatment.	Tsujinaka *et al*, 1996.
Denervation.	↓ mRNA for Calpain-3.	Stockholm *et al*, 2001.

2.8.4 Muscular Dystrophies

The calpain system has a key role in the progression and pathogenesis of muscular dystrophies (MDs). As this is a complex area under investigation by many research groups it requires a greater description. In duchenne (DMD) and some variations of Limb Girdle Muscular Dystrophies (LGMDs) there is a loss of various specific proteins involved in sarcolemmal stability/integrity, force transduction and transmission, e.g. loss of dystrophin or sarcoglycans (Brown *et al*, 1997, Bushby, 1999, Ehmsen *et al*, 2002). This causes the skeletal muscle cells to become more susceptible to damage and loss of sarcolemmal integrity, which in turn increases the amount of Ca^{2+} entering the cell and cytosolic [Ca^{2+}] (Tidball and Spencer, 2000). Research suggests that the increase in Ca^{2+} may be also due to increased activation of leak or stretch regulated Ca^{2+} channels (Mallouk *et al*, 2000) and growth factor-regulated channels (GRC) (Iwata *et al*, 2003). This may set up Ca^{2+} gradients within the cell, increasing the near-membrane concentration instead of a 'whole-cell' rise in concentration (Mallouk *et al*, 2000). This rise in [Ca^{2+}] may cause an up-regulation in calpain activity (Tidball *et al*, 2000). Calpains specifically bound to phospholipids at the membrane, or near membrane activator proteins may also be preferentially activated (Mallouk *et al*, 2000, Tidball and Spencer, 2000).

Muscular dystrophies tend to cause the development of degenerative, necrotic muscle tissue (Chae *et al*, 2001). The suggested model of the sequence of events that may lead to this pathological state, may involve a chain reaction of positive feedback, involving cytosolic Ca^{2+} ion dysregulation and the calpain system (Ono *et al*, 1999). Intitially, as [Ca^{2+}] near-membrane increases calpain activity may also increase. Calpain-mediated Ca^{2+} leak channel activity may increase (Mallouk *et al*, 2000) along with a calpain-mediated decrease in Ca^{2+} ATPases activity (Mallouk *et al*, 2000). This may further increase cytoplasmic [Ca^{2+}], calpain activity and cell damage. Further cell damage, Ca^{2+} dysregulation and calpain activity will initiate caspase dependent/independent cell death pathways (discussed in Section 2.10).

Further evidence that the calpain system is involved in the pathology of dystrophies has been shown by the specific inhibition of calpastatin. Overexpression of a calpastatin transgene in *mdx* dystrophic mice muscle reduced μ- and *m*-calpain activities,

muscle necrosis and hence dystrophic pathology (Spencer and Mellgren, 2002). 'Booster' gene therapy for calpastatin has been suggested to be used clinically in the future as one target of many, to slow/prevent MD pathogenesis (Engvall and Wewer, 2003).

A more specific association of a particular calpain isoform with muscular dystrophy is the role of calpain-3. Two non-sarcoglycan forms of LGMD, types 2A and 2B are thought to involve calpain 3 (Bushby, 1999, Anderson *et al*, 2000). Secondary reduction in calpain 3 expression has been observed in patients with LGMD2B and also miyoshi myopathy (MM), known as primary dysferlinopathies (Anderson *et al*, 2000). Defects in the human calpain 3 gene are responsible for LGMD2A (Ono *et al*, 1999, Baghdiguian *et al*, 1999, Tidball and Spencer, 2000, Chae *et al*, 2001, Richard *et al*, 2000). There is a characteristic atrophy and weakness of the proximal muscle of the limbs (Bushby, 1999, Chae *et al*, 2001). It is unclear how p94 absence/deficiency causes the dystrophic condition characterised by apoptosis. However, there is a very strong correlation between deficiency of p94, myoapoptosis and a perturbation in the IκBα/NF-κB pathway (Baghdiguian *et al,* 1999, Tidball and Spencer, 2000, Richard *et al*, 2000, Baghdiguian *et al*, 2001). One hypothesis is that low/non-existant levels of p94 prevents proteolytic cleavage of the endogenous inhibitor of NF-κB, IκBα. Other studies confirm a relationship between the whole calpain-calpastatin system and regulation of the IκBα-NFκB pathway (Chen *et al*, 2000, Shen *et al*, 2001). NFκB activation is dependent on IKK (Inducible Kinase)-phosphorylation of IκB (inhibitory protein) (Macdonald *et al*, 2003) and degradation. It has been suggested that IκBα (IκBβ IκBε also exist) proteolysis by calpains is the rate-determining step in NFκB activation (Lin *et al*, 1995). A reduction in calpain-dependent proteolysis would mean less NF-κB would be able to translocate to the nucleus and drive transcription of a number of survival genes (Baghdiguian *et al*, 2001).

Figure 2.8.4-1 illustrates a model adapted from Tidball and Spencer, 2000 and Baghdiguian *et al*, 2001, of the possible function of p94 in relation to myoapoptosis observed in LGMD2A. p94 associates with titin along the N_2-line and M-line of the sarcomere. Activation of cell death pathways may lead to apoptosis in skeletal muscle (see Section 2.10). During normal cell function, cell death can be averted through

the actions of cell survival proteins, including anti-apoptotic proteins within skeletal muscle. The up-regulation of these proteins is dependent on NF-κB-dependent gene transcription. For NF-κB to successfully translocate to the nucleus and increase transcription of cell-survival genes, the NF-κB inhibitor IκBα must be cleaved and degraded. Cleavage may be dependent on p94 and possibly μ- and m- calpains. It is also proposed that as p94 has a nuclear translocation sequence, may be able to translocate to the nucleus and cleave the nuclear located form of the NF-κB-IκBα complex. Absence or mutation of p94 may lead to a perturbation in this pathway and increase apoptosis in skeletal muscle.

Figure 2.8.4-1. A proposed model of the action of p94 in skeletal muscle, in relation to the origin of apototic myonuclei in LGMD2A.

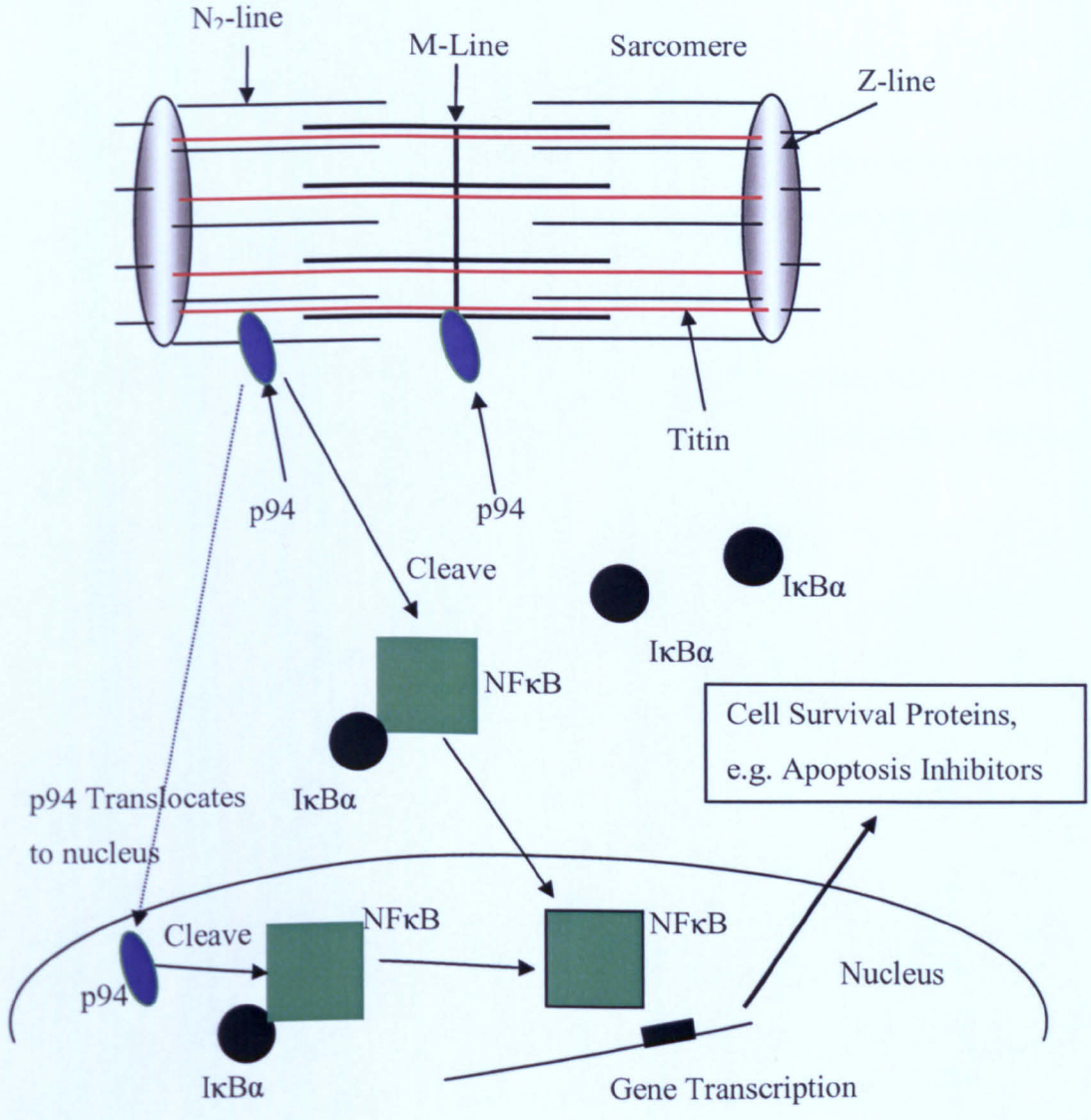

Another hypothesis is that p94 may have an important role in myofibrillar integrity, through its association with titin. Kramerova *et al*, 2004 observed abnormal sarcomere formation in calpain-3 knockout mice. Whether p94 association protects titin from degradation is unknown, but titin which plays a key role in myofibrillar integrity is known to be downregulated in standard DMD (Tkatchenko *et al*, 2001) and may have other unknown regulatory functions; possibly associating with myostatin (Nicholas *et al*, 2002).

2.8.5 Summary

Calpain proteases are calcium-dependent cysteine proteases with many effects globally within cells and tissues. They are involved in the specific cleavage and hence partial degradation of a number of cytoskeletal, myofibrillar and regulatory proteins within skeletal muscle.

A reduction in calpain-mediated proteolysis, mediated by an up-regulation in calpastatin, has been found to coincide with an increase in muscle hypertrophy, during β-adrenergic stimulation, in callipyge lambs and in transgenic mice overexpressing calpastatin.

Calpain-3 and in particular calpain-10 have been linked to alterations in insulin resistance, glucose and fat metabolism. Preliminary studies suggest calpastatin and *m*-calpain may also affect metabolism.

Contraction-induced muscle damage has been shown to increase *m*-calpain and decrease calpain-3 mRNA, possibly indicating part of a remodelling response to allow cytoskeletal and myofibrillar alterations and adaptations.

Components of the calpain system have been found to be differentially altered during a number of catabolic-atrophic states, including fasting, cancer-cachexia, sepsis, hindlimb unloading, denervation, IL-6 transgenic mice and muscular dystrophies. In particular, a rise in *m*-calpain and decrease in calpain-3 activity/mRNA is a common theme. Absence and genetic abnormalities in calpain-3/p94 has been linked to myoapoptosis and a perturbation of the NF-κB pathway during LGMD2A.

Therefore, two distinct roles have now been identified for calpains. Cytoskeletal and myofibrillar proteolysis linked to turnover and remodelling; and proteolysis associated with specific alterations in cellular carbohydrate-fat metabolism and transcription factor regulation.

2.9 THE UBIQUITIN-PROTEASOME SYSTEM

2.9.1 Structure of the Ubiquitin-Proteasome System

The ATP-dependent ubiquitin-proteasome (Ub. Prot.) system is thought to play a major role in basal skeletal muscle protein degradation and myofibrillar degradation under basal and catabolic conditions (Lecker *et al*, 1999, Attaix *et al,* 2001, Jagoe and Goldberg, 2001). The proteins within muscle may undergo complete proteolysis to amino acids through a non-lysosomal, Ca^{2+}-independent, ATP-requiring process.

The Ub. Prot. pathway consists of several components acting in concert. This involves two main processes: the covalent attachment of multiple ubiquitin molecules to the protein substrate and degradation of the targeted protein by the 26S proteasome complex. A number of review articles have been written describing the structural and functional properties of the system (Schwartz and Ciechanover, 1999, Wilkinson, 1999, DeMartino and Slaughter, 1999, Ciechanover *et al*, 2000, Glickman and Ciechanover, 2002, Attaix *et al*, 2001, Attaix *et al*, 2002).

The basic steps are illustrated in Figure 2.9.1-1: Ubiquitin is converted to a high-energy thiolester, by the ubiquitin-activating enzyme, E1. Once activated by E1, one of the several E2 class enzymes (including, ubiquitin-carrier proteins, ubiquitin-conjugating enzymes (UBCs)), transfers ubiquitin from E1 to a member of the E3 ubiquitin-protein ligase family, to which the substrate protein is specifically bound. The E3 enzyme catalyses the conjugation (covalent attachment) of ubiquitin, to the protein substrate. A polyubiquitin chain is synthesised in successive reactions and serves as a recognition 'tag', or 'marker', for the 26S proteasome. The ubiquitin-conjugated protein substrate is then degraded completely by the 26S proteasome complex, with free and reutilisable ubiquitin released.

Figure 2.9.1-1. The ubiquitin-proteasome system pathway. *Ilustrates the basic steps associated with the ubiquitination and subsequent degradation of proteins.*

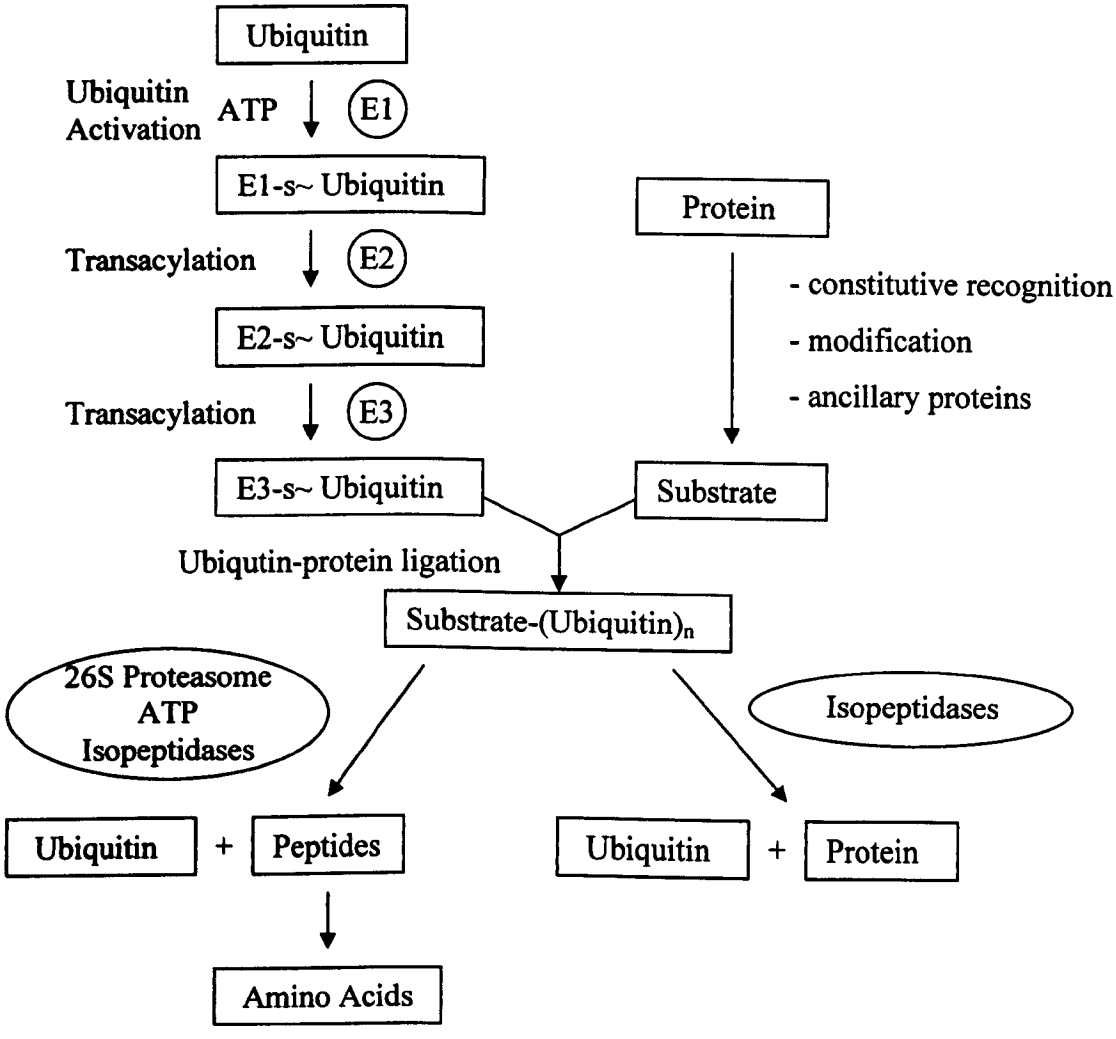

The structure of the proteasome complex is such that it comprises of two 'cap' complexes, PA700 (19S cap) and proteasome activator, PA28 (11 S regulator) that act as regulatory subunits, imparting specificity and control (Figure 2.9.1-2). These are associated with a 20S cylindrical 'core catalytic' structure, which contains 28 subunits forming four rings of seven subunits each. The outer rings (α-subunits) regulate substrate entry, whereas the inner rings (β-subunits) encode the catalytic centers. Association of the 19S and 11S structures generates a 'dumbell-shaped' protein complex (26S proteasome, ~2000kDa). The 26S proteasome is an intricate, structured protease complex with over 30 subunits, ubiquitin and ATP-dependence. It possesses trypsin-like, chymotrypisn-like and post-glutamylpeptidyhydrolytic activities, able to degrade muscle structural proteins (Matsuishi and Okitani, 1997). Of possible significance, a proline-rich endogenous inhibitor of the 20S proteasome, PI31 (Proteasome Inhibitor of 31,000 daltons) was identified, cloned and sequenced from bovine tissue (McCutchen-Maloney *et al*, 2000). It is thought to directly inhibit the 20S and inhibit activation of the proteasome by each of the regulatory proteins, PA700 and PA28.

Associated isopeptidases also play a major role in acting as 'de-ubiquitinating' enzymes. These may have specific regulatory functional roles in stabilising proteins that would be other-wise targeted for degradation, for example.

Although peptide hydrolysis by many proteases does not require energy, the whole protein degradation process is ATP-dependent. ATP hydrolysis is required for ubiquitin activation by E1. ATP is required for assembly of the 26S complex from its components along with ATP probably needed for catalysis of protein un-folding, facilitate entry into the 20S core and proteolytic activities.

Figure 2.9.1-2. Diagram to show representation of A) the proteasome-activator complex and B) the proteasome-inhibitor complex.

A) Proteasome-activator complex

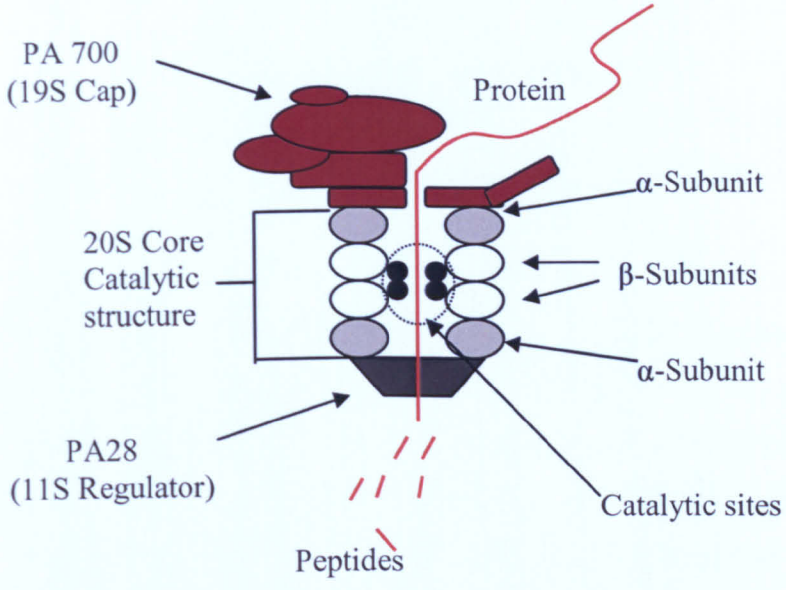

B) Proteasome-inhibitor complex. *A proposed interaction of protein inhibitors with the proteasome, e.g. PI31.*

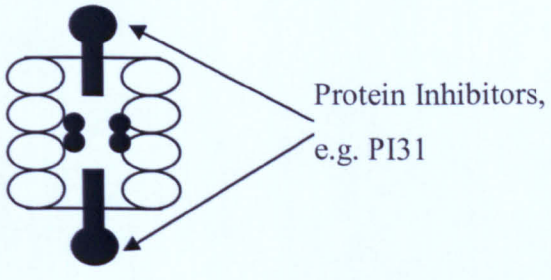

2.9.2 System Function

The Ub. Prot. proteolytic pathway plays a crucial role in the degradation of short-lived and regulatory proteins important in a multitude of cellular processes. Among these are the cell cycle, the cellular response to stress and to extracellular modulators, morphogenesis of neuronal networks, modulation of cell surface receptors, ion channels, the secretory pathway, DNA repair and biogenesis of organelles (Glickman and Ciechanover, 2001). The system plays a critical role in degrading damaged, unfolded and abnormal proteins, including those damaged by free radicals (Merker *et al*, 2001).

The activity of the Ub. Prot. pathway can be regulated and modulated in a number of ways (Thompson and Palmer, 1998, Schwartz and Ciechanover, 1999, Wilkinson, 1999, DeMartino and Slaughter, 1999, Ciechanover *et al*, 2000, Attaix *et al*, 2001, Glickman and Ciechanover, 2002, Attaix *et al*, 2002). Overall activity has been studied by measuring component mRNA, protein levels, proteasome activity, ubiquitin conjugation rates and short-term phosphorylation events. Regulation of system-component gene transcription is unknown at present but may involve a number of factors involved in immuno-inflammatory/stress responses, including glucorticoids/glucocorticoid receptor and cytokines (Thompson and Palmer, 1998, Hasselgren and Fischer, 2001, Penner *et al*, 2002). Binding sites for the transcription factors NF-κB, AP-1, C/EBP-β and -δ in the promoter region of genes for members ubiquitin-proteasome systems have been found (Thompson and Palmer, 1998, Hasselgren and Fischer, 2001, Penner *et al*, 2002).

With regards to proteasome activity, it is recognised that IFN-γ stimulation drastically up-regulates activity (DeMartino and Slaughter, 1999, Glickman and Ciechanover, 2002). Whether this occurs in skeletal muscle and what function it has is unknown. Studies suggest it is activated during antigen processing (DeMartino and Slaughter, 1999, Glickman and Ciechanover, 2002). The proteasome is regulated by at least one endogenous inhibitor as described previously (DeMartino and Slaughter, 1999). Some proteasome subunits have been shown to be subject to phosphorylation and be cGMP-dependent. Poly-ADP-ribose polymerase (PARP) is also thought to

activate the proteasome and may be important in integrating protease and cell death pathways (Thompson and Palmer, 1998, Glickman and Ciechanover, 2002).

2.9.3 Metabolic Role in Skeletal Muscle

The Ub. Prot. pathway within skeletal muscle is thought to play a major role in the complete proteolysis of specific sarcoplasmic and myofibrillar proteins (Lecker *et al*, 1999). Although, there is no evidence to suggest that the pathway can degrade myofibrillar proteins in their intact functional state (i.e. non-cleaved myofilaments linked together by other proteins, in a myofibrillar lattice structure). This system is thought to only degrade myofilaments cleaved and released by the actions of other protease systems (principally the calpains) (Thompson and Palmer, 1998).

Evidence suggests that key components of the system are up-regulated in skeletal muscle in a number of catabolic and stress reaction conditions like cachexia, as reviewed in a number of articles (Mitch and Goldberg, 1996, Lecker *et al*, 1999, Tisdale, 2000, Kotler, 2000, Baracos, 2000, Hasselgren and Fischer, 2001, Jagoe and Goldberg, 2001). Conditions including denervation atrophy, fasting, glucocorticoid treatment, kidney disease, metabolic acidosis, trauma, infection/sepsis, cancer cachexia, MDs, possibly myopathies, burns, hyperthyroidism, diabetes, resistance training and aging exhibit increased system up-regulation/activity (Mitch, 1997, Tisdale, 1999, Llovera *et al*, 1999, Baracos, 2000, Merker *et al*, 2001, Stupka *et al*, 2001, Féasson *et al*, 2002, Lecker et *al*, 2004).

Table 2.9.3-1 summarises observations from various studies relating to the effects of different states and conditions on the Ub.-Prot. system. Most are catabolic states known to induce whole-body and skeletal muscle protein loss due to increased degradation and decreased synthesis. The system may play a key role in the regulation of muscle proteolysis in response to feeding and fasting. This response is probably mediated by glucocorticoids, insulin and amino acids (Thompson and Palmer, 1998, Busquets *et al*, 2000). Interestingly, an increase in Ub.Prot. pathway activity has been observed after eccentric-exercise induced muscle damage (Stupka *et al*, 2001, Féasson *et al*, 2002). This may indicate an up-regulation of the system as part of a

remodelling response to contraction-induced muscle damage, to increase degradation of damaged muscle proteins.

Recent studies have revealed muscle-specific E2 and E3 enzymes that are up-regulated during catabolic, atrophic states (as seen in Table 2.9.3-1). Examples include the $E2_{14k}$, UBC, which functions with E3α (also suggested to be up-regulated in some catabolic conditions) to ubiquitinate muscle proteins in the N-end rule pathway, although recent studies suggest no significant changes in gene expression (Jagoe *et al*, 2002, Lecker *et al*, 2004). Two E3 enzymes have been found to be massively up-regulated during skeletal muscle atrophy under a variety of conditions. They are known as Muscle RING Finger 1 (MuRF1) and Muscle Atrophy F-box (MAFbx)/Atrogin-1, a member of the SCF family of E3s (Bodine *et al*, 2001, Gomes *et al*, 2001). Interestingly, MuRF1 was identified by its interactions with a domain of titin, similar to p94, in a yeast two-hybrid system. MuRF1 and Atrogin-1 have been reported to be up-regulated in rat muscle during immobilisation, denervation, unweighting, treatment with IL-1, treatment with dexamethasone glucocorticoid (Bodine *et al*, 2001). Bodine *et al*, 2001, overexpressed Atrogin-1 in myotubes causing atrophy and mice deficient in either Atrogin-1 or MuRF1 were resistant to atrophy. Gomes *et al*, 2001, reported massive up-regulation in Atrogin-1 gene expression in muscle during fasting (2 days in mice), diabetes (3 day streptozotocin-treated rats), tumor-bearing (yoshida ascites hepatoma for 6 days in rats) and renal failiure (nephrectomised rats).

Another point of interest is that Mosoni *et al*, 1999 found that older rats had higher baseline levels of mRNA for ubiquitin, C2 (proteasome subunit) and $E2_{14k}$ (see Table 2.9.3-1). *m*-Calpain was also found to be increased in the study (listed previously in Table 2.8.3-1). Whether this links to sarcopenia is unknown.

Table 2.9.3-1. Reported effects of conditions and states on Ubiquitin-Proteasome system in skeletal muscle.

Condition or state	Effect on Ubiquitin-Proteasome System	Reference
Fasting	↑ mRNA for Ubiquitin, $E2_{14k}$, subunits of the 20S proteasome and 19S cap including C8 (proteasome unit), Atrogin-1 and MuRF-1.	Mosoni *et al*, 1999. Jagoe *et al*, 2002. Lecker *et al*, 2004
Diabetes with metabolic acidosis and increased glucocorticoid levels.	↑ mRNA for $E2_{14k}$, Ubiquitin and C3 (proteasome subunit), Ubiquitin-fusion proteins, Atrogin-1 and MuRF1	Mitch *et al* 1999. Lecker *et al*, 2004
Obesity.	↑ mRNA of Ubiquitin.	Argilés et al, 1999.
Microgravity-induced atrophy, unloading and immobilised muscle.	↑ mRNA for RC2 and RC9 (proteasome components), polyubiquitin and ubiquitin-conjugating enzyme. ↑ mRNA for E3 enzymes, Atrogin-1, MuRF1	Ikemoto *et al*, 2001, St-Amand *et al*, 2001, Stevenson *et al*, 2003.
Trauma	↑ mRNA of Polyubiquitin and $E2_{14k}$ and proteasome subunits	Mansoor *et al*, 1996, Biolo *et al*, 2000
Sepsis	Proteasome inhibitors ↓ total and myofibrillar breakdown *in vitro* and *in vivo*. ↑ activity of 20S proteasome, inhibited by proteasome inhibitors. ↑ mRNA of subunits RC3, RC9 and RC7, ↑ mRNA for $E2_{14k}$ ↑ mRNA for Ubiquitin in IL-6 knockout mice.	Hobler *et al*, 1998, Williams *et al*, 1998,.Hobler *et al*, 1999a, Hobler *et al*, 1999b, .Fischer *et al*, 2000
-Separate groups of rats with induced sepsis and cancer	Torbafyline (xanthine derivative) inhibited TNF-α production, muscle wasting and ubiqutin-dependent proteolysis.	Lydie *et al*, 2002.
Administration of TNF-α, IFN-γ, IL-1, IL-6 and LIF.	↑ mRNA Ubiquitin with TNF-α, IFN-γ and IL-1. NO CHANGE with IL-6 and LIF.	Llovera *et al* 1998.
Cancer cachexia	↑ Ubiquitin conjugation. ↑ mRNA Ubiquitin and C8 proteasome subunit, subunits of 20S and 19S cap. Atrogin-1 and MuRF-1.	Lazarus *et al*, 1999, Busquets *et al*, 2000, Lecker *et al*, 2004.
Muscular dystrophy, neuromuscular disorders.	↑ expression of proteasomes and staining for ubiquitin.	Kumamoto *et al*, 2000.
Muscle denervation	↑ mRNA Ubiquitin.	Llovera *et al*, 1999.
Eccentric-exercise induced muscle damage.	↑ in proteasome activity. ↑ in Ubiquitin-conjugated proteins	Stupka *et al*, 2001, Féasson *et al*, 2002.

2.9.4 Summary

The ubiquitin-proteasome system is an ATP-dependent system involved in the specific degradation of a wide range of proteins completely to amino acids, including sarcoplasmic and myofibrillar proteins. Specific E2 ubiquitin-carrier, conjugating and E3 ligase enzymes provide substrate targetting specificity to the system.

A number of conditions involve activation of the ubiquitin-proteasome system and many of these result in muscle atrophy. Certain signalling molecules coincide with pathway activity. Alterations in insulin, glucocorticoids and cytokines are implicated in a number of cases (Thompson and Palmer, 1998). Upregulation of the pathway occurs in most types of skeletal muscle damage/trauma, as damaged, mis-folded and abnormal proteins formed are targeted for degradation by the proteasome. For example, mechanical stimulation and contraction-induced damage induces ubiquitin proteasome pathway activation, which may be important during subsequent remodelling of cells, so as to degrade 'old', redundant proteins (Stupka *et al*, 2001, Féasson *et al*, 2002).

Components of interest within skeletal muscle include the specific E2 (e.g. $E2_{14k}$, E2G1), E3 enzymes (e.g. Atrogin-1 and MuRF1), specific proteasome subunits (e.g. C3, C7, C8 C9) and ubiquitin, as all are up-regulated during atrophic-catabolic conditions.

2.10 THE CASPASE PROTEOLYTIC PATHWAY

2.10.1 Structure of the Caspase Proteolytic Pathway

The caspases are highly specific cysteine proteases (cysteine aspartate proteases). Proteolysis by the caspases is restricted and limited. Peptide cleavage occurs only after recognising specific tetrapeptide motifs in target proteins, followed by cleavage of the peptide bond C-terminal to aspartic acid residues, producing disassembly of the protein (Grimm, 2003d). Therefore, they are not involved in gross proteolysis. They do not play a role in basal protein turnover within muscle, but instead are in-

volved in ordered proteolysis having highly specific roles in other cell processes, in particular apoptosis (Israels and Israels, 1999, Budihardjo *et al*, 1999, Slee *et al*, 1999, Strasser *et al*, 2000).

The caspases have many similarities to and inter-relationships with the calpain system. The similarities include specificity of cleavage reactions and similar interactions with protein kinases affecting cell function / regulation; whilst there is a relationship between calpain and caspase interactions during programmed cell death (apoptosis) (Grimm, 2003a, Krebs and Graves, 2000).

The caspases are constitutively expressed zymogens (inactive precursors) present within the cytoplasm. At least 14 mammalian caspases have now been identified (10 human) (Strasser *et al*, 2000, Grimm, 2003d). These proteases are thought to activate themselves and other members of the family in an apoptotic cascade. Caspases are able to activate other procaspases in a sequential cascade, but also are activtated by self-cleavage (Slee *et al*, 1999, Strasser *et al*, 2000, Grimm, 2003d).

The caspase family can be divided into three groups depending on their structure and what is known about their regulation and function (Israels and Israels, 1999, Budihardjo *et al*, 1999, Slee *et al*, 1999, Grimm, 2003d). The first group, known as long prodomain 'initiator' caspases (2,8,9 and 10) are thought to act at a proximal location in the caspase cascade. The second group, the short prodomain terminal 'effectors' (includes 3, 6 and 7) are activated by the initiators. A third group, (including 1, 4, 5, 11, 12, 13, and 14) are believed to play a role in processing the pro-forms of cytokines prior to secretion. Long prodomain caspases contain either a death effector domain (DED), i.e. caspase-8 and -10; or a caspase recruitment domain (CARD) in their prodomain region, i.e. caspase-1, -2, -4, -5, -9, -11, -12 (see Figure 2.10.1-1). The DED and CARD domains mediate recruitment of procaspases to specific signalling complexes, with the aid of specific adaptor molecules. This results in autoactivation/autolysis of the caspase. Short prodomain-effectors are thus unable to be activated this way and rely on activated up-stream initiators.

Regulation of caspase gene transcription is unknown at present (Grimm, 2003d). The caspase system has been suggested to constitutively produce mRNA and regulate ac-

tivation of these inactive zymogens at the level of autolytic cleavage. Recent studies suggest increases in mRNA levels for some caspases (e.g. caspase-3) may coincide with catabolic conditions (see Table 2.10.4-1).

Figure 2.10.1-1. Structure of the caspases. DED, Death Effector Domain. CARD, Caspase Recruitment Domain. L1-L4 loops that form the substrate binding site.

A) Caspases with DEDs (e.g. Caspase-8 and –10)

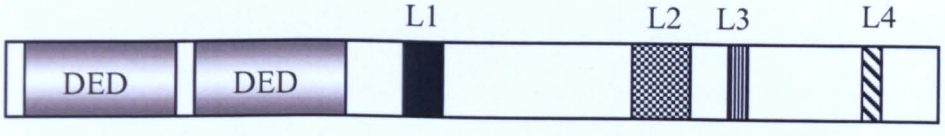

B) Caspases with CARD (Caspase-1, -2, -4, -5, -9, -11 and -12)

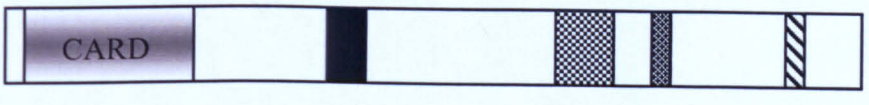

C) Caspases with short prodomain (Caspase-3, -6 and –7)

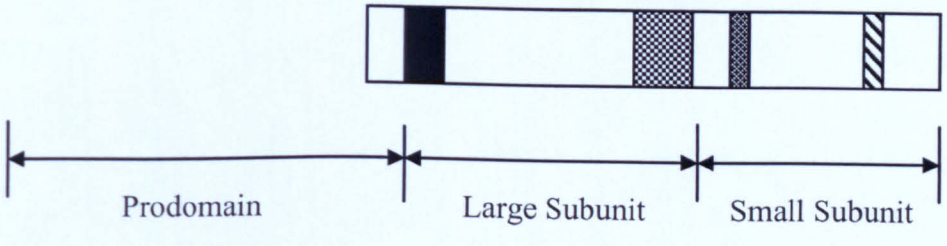

Caspase activity is thought to be increased predominately by caspase-mediated cleavage or autocleavage (Slee *et al*, 1999, Strasser *et al*, 2000, Grimm, 2003d). The calpains may participate in cleavage activation of specific caspases during specific conditions (Nakagawa and Yuan, 2000, Grimm, 2003a, Grimm, 2003c). Some studies have suggested specific protein kinases may have the ability to directly phosphorylate some caspases, inhibiting protease activity, autolytic cleavage and activation (Krebs and Graves, 2000).

2.10.2 Caspase Pathway Function

The caspase proteolytic pathway is intimately involved in the process of controlled cell death, apoptosis (Israels and Israels, 1999, Budihardjo *et al*, 1999, Slee *et al*, 1999, Strasser *et al*, 2000, Grimm, 2003d). Apoptosis is the major physiological mechanism of cell removal, where cells are 'silently' but actively removed under normal conditions, when they reach the end of their life span, are damaged or superfluous (Israels and Israels, 1999). This mechanism of cellular turnover is a general tissue phenomenon necessary for development and homeostasis (Strasser *et al*, 2000). It allows the deletion of excess cells during embryonic development, tissue remodeling and/or regeneration in adult organisms (Sandri and Carraro, 1999, Strasser *et al*, 2000, Grimm, 2003e). Apoptosis keeps cell numbers regulated during excessive cell proliferation (Sandri and Carraro, 1999, Grimm, 2003e). This becomes an important issue during tumor growth (Strasser *et al*, 2000, Grimm, 2003e). Therefore, dysregulation of apoptosis has been implicated in a variety of diseases (Sandri and Carraro, 1999, Israels and Israels, 1999, Strasser *et al*, 2000, Gill *et al*, 2002).

Apoptosis is viewed as a form of programmed cell death (PCD), where the cell eventually after protease action, shrinkage and formation of apoptotic bodies, is rapidly ingested by adjacent macrophages, or other neighbouring phagocytes (Israels and Israels, 1999). As the apoptotic bodies induce no significant cytokine release from the phagocytic cell, there is no concomitant inflammatory response. This therefore, is unlike cell necrosis, in which the release of intracellular proteases and lysozymes induce an inflammatory response (and hence a greater propensity/possibility for wide spread damage) (Israels and Israels, 1999, Grimm, 2003c).

The process of apoptosis and activation of the caspase pathway may be set in motion by the following mechanisms:

1) Genotoxic damage, from cell injury, chemotherapy, radiation etc., initiating activation of the p53 protein (a regulator of DNA transcription), cell-cycle arrest, or apoptosis promotion (Israels and Israels, 1999, Budihardjo *et al*, 1999, Strasser *et al*, 2000). p53 probably regulates ratios of apoptosis-inhibitory proteins (e.g. Bcl-2, and Bcl-X1) and promoters of apoptosis (e.g. Bax, Bad, Bid). A high expression of the Bax group will promote apoptosis by affecting mitochondrial permeability with concomitant release of cytochrome c and apoptosis-inducing factor (AIF). AIF moves to the nucleus to promote nuclear fragmentation. Cytochrome c acts to activate the cytoplasmic protein Apaf-1 (apoptotic protease activating factor), once cytochrome c is bound to Apaf-1, there is subsequent activation of procaspase 9 (i.e. initiator caspases). Caspase-9 activation then acts to activate downstream caspases, including procaspase-3 (effector).

2) Death signals received at the cell surface membrane involves an alternative, non-secretory mechanism of apoptosis. I.e. "death receptors" are expressed on the cell membrane. Fas (CD 95), a cell-surface receptor and a member of the tumour necrosis factor family receptor (TNF-R) family, is a transducer of the apoptotic signal (Israels and Israels, 1999, Strasser *et al*, 2000, Grimm, 2003e). Therefore, the Fas ligand (a member of the TNF family), and TNF produce apoptosis in an analogous fashion-FasL through the Fas receptor protein, and TNF by binding to the TNF receptor (TNFR-1). Binding of ligands, causes "trimerisation" of receptors, activation of death domains (DD), interaction with cytoplasmic proteins, activation of these protein DDs, with eventual recruitment and activation of the caspase cascade, through procaspase-8 activation.

3) Apoptosis may also be stimulated by procaspase activation by granzyme B (the Granzyme system) (Israels and Israels, 1999, Grimm, 2003a). This system allows removal of pathogen infected cells and tumour cells. Perforins and granzymes are proteins contained within the cytoplasmic secretory granules of cytotoxic lymphocytes (CTL's), and natural killer (NK) cells. Upon CTL receptor-mediated binding to

a target cell, perforins and granzyme B, are cosecreted, enter target cell and eventually granzyme B activates caspase cascade.

4) The endoplasmic reticulum (ER), or sarcoplasmic reticulum (SR) in muscle allows the correct folding and modificaton of proteins and acts as a primary Ca^{2+} ion store. Accumulation of misfolded proteins in the ER lumen leads to activation of the 'unfolded protein response' and survival signals. Alterations in ER/SR calcium homeostasis induces SR/ER stress and leads to Ca^{2+} release. These stimuli lead to ER stress which can lead to activation of cell death pathways (Nakagawa and Yuan, 2000, Rao *et al*, 2001, Rao *et al*, 2002, Grimm, 2003c). It has been suggested that ER stress signals activate caspase 12 through a caspase-7-mediated pathway (Rao *et al*, 2001). *m*-Calpain is known to activate caspase 12, in response to an increase in cytosolic near-ER-membrane [Ca^{2+}], due to raised ER Ca^{2+} release (from ER stress); and lead to activation of effector caspases (Nakagawa and Yuan, 2000, Gill *et al*, 2002, Grimm, 2003b). In addition, *m*-calpain may activate pro- and inactivate anti-apoptotic proteins, Bid, and Bcl-xL, respectively. A novel, mitochondrial and Apaf-1-independent apoptotic pathway which may involve cytochrome c and Apaf-1 independent activation of caspase 9 has also been implicated (Rao, 2002). The mitochondria is the major site of oxidative phosphorylation and hence ATP and reactive oxygen species production. It also acts as a secondary store for Ca^{2+} ions and repository for pro- and anti-apoptotic molecules. During ER/SR stress, several other pathways may become activated promoting mitochondrial pro-apoptotic signals. High Ca^{2+} release from the SR and subsequent uptake by the mitochondria (at ER-mitochondrial junctions) can lead to PTP (permeability transition pore) opening and release of apoptogenic factors, Ca^{2+} and cytochrome c.

5) Increased mitochondrial ROS production or exposure to oxidants can lead to cytochrome c release and mitochondrial dysfunction, through a disruption in mitochondrial membrane potential and uncoupling of oxidative phosphorylation, leading to a depletion in [ATP] (Neuss *et al*, 2001, Grimm, 2003b). These occurrences may stimulate caspase-dependent or –independent apoptosis/necrosis-like death pathways.

The above activation mechanisms of apoptosis stimulate effector caspase activity (caspase-3, -6 and –7). This activity is responsible for: Cleavage of cytoskeletal pro-

teins, disruption of the nuclear membrane, disruption of cell-cell contacts and the freeing of the DNA nuclease (CAD, caspase-activated deoxyribonuclease) from its associated protein inhibitor (ICAD) (Strasser *et al*, 2000, Grimm, 2003d). The caspases may in addition act on mitochondrial membranes with further release of cytochrome c and intramitochondrial procaspases (i.e. possible feed forward mechanism) (Grimm, 2003d).

Activation of caspase-mediated restricted proteolysis results not in cellular lysis, but in membrane-bound sealed apoptotic bodies (Israels and Israels, 1999, Strasser *et al*, 2000). Many diverse pro- and anti-apoptotic signals from intra- and extra-cellular origins affect cell death/survival pathways and mediators (Budhardjo *et al*, 1999, Strasser *et al*, 2000, Gill *et al*, 2002, Grimm, 2003a, Grimm, 2003b, Grimm, 2003c). It is the overall balance of these signals that leads to a net effect of cell death progression or survival (Krebs and Graves, 2000, Grimm, 2003e).

It is thought that caspase targets fall into two groups; those that are inactivated upon proteolysis in order to hasten cell death and those that are activated and may contribute to the induction or progression of apoptosis (Krebs and Graves, 2000, Strasser *et al*, 2000). Therefore, the caspases may act within skeletal muscle to aid in deactivation and/or inhibition of various intracellular signalling pathways, involved in cellular growth and proliferation, e.g. caspase-mediated processing of PKC isoforms and members of the MAPK kinase pathways (Smith *et al*, 2000, Krebs and Graves, 2000). Caspase processing of atypical PKC-ζ, activates it and targets it for degradation, by the ubiquitin-proteasome system (Smith *et al*, 2000). Atypical PKC's also regulate the expression of genes that mediate inflammatory responses and cell survival. This is accomplished through NF-kB activation (Smith *et al*, 2000, Grimm, 2003e). Evidence suggests that activated caspases attempt to down-regulate the NF-κB pathway in a number of ways, including the above example (Krebs and Graves, 2000, Grimm, 2003e). Caspase 3 may have a direct effect on the NF-κB pathway, cleaving IκB, creating a truncated, suppressive form of IκB, resistant to degradation (Krebs and Graves, 2000).

2.10.3 Inhibitors of Apoptosis

An important group of regulators of caspase activation and apoptosis is the caspase inhibitors. Termed IAPs (Inhibitors of Apoptosis Proteins), they are are known to directly interact with caspases, inhibit their activity and act as one of the many fail-safe mechanisms within the cell to prevent apoptosis (Budihardjo *et al*, 1999, Gill *et al*, 2002, Grimm, 2003e). Of interest, is the discovery of a skeletal and cardiac muscle specific inhibitor of apoptosis, reported by Koseki *et al*, 1998. ARC, (Apoptosis Repressor with Caspase recruitment domain), was found to selectively inhibit caspase-8 and hence inhibit the extrinsic pathway of death-receptor-induced activation of caspase-8 and subsequent effector activation. ARC was also found to protect heart myogenic cells from hypoxia-induced apoptosis and prevented cytochrome c release (Ekhterae *et al*, 1999). Neuss *et al*, 2001b, found that H_2O_2 exposure in a myogenic cell line lead to dissipation of mitochondrial membrane potential, ATP depletion, mitochondrial dysfunction and loss of plasma membrane integrity leading to cell death, including necrosis-like changes. This was associated with a downregulation of ARC protein levels. Increased expression of ARC prevented H_2O_2-induced cell death, by preservation of mitochondrial integrity.

Figure 2.10.3-1 illustrates a proposed scheme of caspase activation and apoptosis pathways that may function within skeletal muscle. It includes the extracellular death receptor, intracellular mitochondrial and sarcoplasmic reticulum (SR) pathways. The IGF-1 pathway has an anti-apoptotic effect via PI (3) Kinase (PI_3K) and Akt activation, with subsequent inhibition of the pro-apoptotic factor Bax. It was important to include the IGF-1 anti-apoptotic pathway as the GH-IGF axis was discussed in great detail in Section 2.3.3. IGF-1 is one of the most important cell growth regulators affecting protein turnover and satellite cell proliferation and differentiation. β-adrenergic stimulation may also activate PI (3) Kinase (PI_3K) /Akt (Glass, 2003).

Figure 2.10.3-1. A proposed simplified schematic of caspase activation and apoptosis signalling pathways. *Adapted from Gill et al, 2002. Arrows indicate pathway activation. The pro-apoptotic proteins Bax, Bad and Bid are indicated. Possible points of interaction by IAPs (Inhibitors of Apoptosis) and ARC (Apoptosis Repressor with CARD) are in red. SR is sarcoplasmic reticulum.*

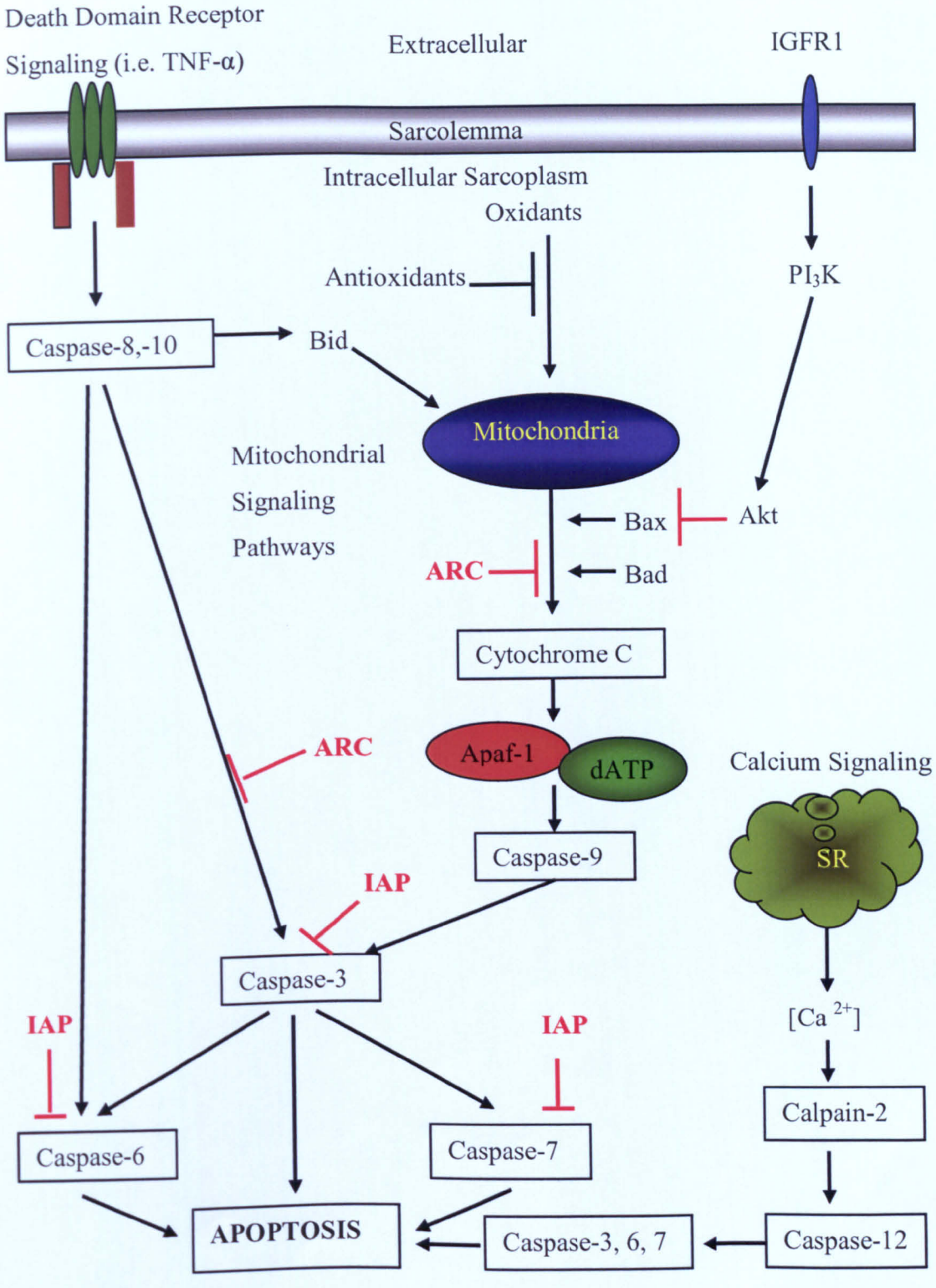

2.10.4 Metabolic Role in Skeletal Muscle

Apoptosis is known to take place in proliferating myoblasts, i.e. an alternative pathway to differentiation and fusion (Sandri and Carraro, 1999). Differentiated and fused myotubes are also known to undergo apoptosis. Excess myoblast and myotube apoptosis may occur during pathogenesis of states like muscular dystrophies, along with adult myofibers. During such catabolic states atrophy eventually takes place, leading to decreases in protein content, cell size and myonuclei. The myonuclei loss during atrophy has been attributed to apoptosis and apopotosis markers have been found (Sandri and Carraro, 1999, Belizário *et al,* 2001, Sandri *et al*, 2001). Examples of states known to affect caspase activation and apoptosis can be found in Table 2.10.4-1.

Table 2.10.4-1. Summary of a number of relevant conditions and states known to affect caspase activation and apoptosis.

Condition or state	Effect on Caspase system and apoptotic markers.	Reference
Inflammatory myopathies	Inflammatory lesions cause expression of cytoplasmic and surface molecules, like Fas, not detected in normal muscle. Muscle fibers may undergo apoptosis via caspase activation.	Li and Dalakas, 2000
Denervation atrophy	IL-1 expression in motor end-plates	Authier *et al,* 1997
Age-related sarcopenia in rats.	50% greater presence of apoptosis markers, including higher cytochrome c and caspase-3.	Dirks and Leeuwenburgh, 2002
LGMD type 2A adult patients	↑ apoptotic myonuclei, perturbation in the NF-κB pathway, loss of functional calpain 3 activity and cytochrome c leakage.	Baghdiguian *et al,* 2001
Duchennne MD (DMD), and facio-scapulo-humeral dystrophy (FSHD) adult patients	Caspase -8, -3, -5, -2, and –7, and granzyme B mRNA detected in DMD muscles but not in normal muscles. FSHD muscles had low levels of caspase-6, -3 and granzyme B. Caspase 3 protein correlated with apoptotic nuclei.	Sandri *et al,* 2001
Cancer cachexia in mice	↑ in Caspase-1, -3, -6, -8, and –9 proteolytic activities. Cytochrome c was present, although no apoptosis present, or DNA fragmentation.	Belizário *et al,* 2001

The last example of a state to be discussed that involves apoptosis and caspase activation is that of the effects of chronic heart failiure (CHF) on skeletal muscle. Gill, *et al*, 2002, and Neuss *et al*, 2001, presented reviews regarding the presence of cardiomyocellular apoptosis and the pathways involved. Many of these pathways are thought to be similar and active in skeletal muscle during CHF (Libera *et al*, 1999, Vescovo *et al*, 2000, Vescovo *et al*, 2002a, Vescovo *et al*, 2002b). The key apoptosis-activating mediators are unknown, but suggested to be through the actions of increased systemic TNF-α and possibly angiotensin II (ANGII) (Libera *et al*, 2001). Studies have detected in rat and human skeletal muscle increased atrophy, fatigability, expression of fast-glycolytic proteins, apoptotic markers and apoptosis during CHF. In particular, elevated levels of caspase-3, and –9, TNF-α (and its second messenger sphingosine) have been detected (Libera *et al*, 1999, Vescovo *et al*, 2000, Vescovo *et al*, 2002a, Vescovo *et al*, 2002b) and Ang II (Libera *et al*, 2001).

As can be observed from Table 2.10.4-1 and in studies related to CHF, caspase-3 is one of the most prominent altering factors in many of the conditions described. Caspase-3 may play a critical role as a key caspase effector protease in many catabolic-atrophic conditions. Other researchers have suggested that caspase-3 may play a role in skeletal muscle differentiation, cell development, regeneration and myofibrillar degradation (Fernando *et al*, 2002, Ruest *et al*, 2002, Du *et al*, 2004a).

2.10.5 Summary

The caspases are specific cysteine proteases involved in selectively cleaving other caspases, regulatory and cytoskeletal proteins. They are constitutively expressed as zymogens within the cell, divided into three groups depending on their structure, regulation and function; and are activated by self-cleavage or by other caspases. Their precise role within skeletal muscle is un-clear, other than there studied function in orchestrating caspase-dependent programmed cell death, apoptosis. Apoptosis has been found to be an important process during tissue development, remodelling, regulation of cell growth and implicated in the pathogenesis of a number of clinical disorders. The caspases themselves are thought to play specific roles in muscle cell development at different stages and induction of pro-apoptotic responses during atrophic, immuno-inflammatory conditions.

The 'initiator' caspases (2, 8, 9 and 10) are activated by diverse intracellular and extracellular pro-apoptotic signals and initiate an intracellular apoptotic caspase cascade. The 'initiator' caspases in turn can activate the down-stream 'effector' caspases (includes 3, 6 and 7), which leads to the 'effector' caspase driven proteolytic cleavage of a number of important cytoskeletal and regulatory proteins. This ultimately leading to membrane blebbing, cell shrinkage, chromosome condensation and fragmentation of DNA and eventual cell death.

In particular caspase-3 has been implicated as the key functioning 'effector' protease in a number of pathological and catabolic-atrophic states. Caspase-3 may have additional roles in muscle cell development and myofibrillar integrity. The muscle-specific caspase inhibitor ARC may play a key functional role in balancing out the pro-apoptotic responses from a number of various stimuli.

2.11 OVERALL SUMMARY OF PROTEOLYTIC SYSTEMS

As described above it is thought that four principle intracellular proteolytic systems operate and function within skeletal muscle, involved in many diverse cellular functions that are just being elucidated. Other proteases may also interact and function within muscle but the work described in this literature review has focused on these four only as they have been reasonably well characterised and known to be under regulatory control. An example of other interacting systems includes the matrix metalloproteases (MMP's), active during cellular catabolic states (Huet *et al*, 2001). The ADAMs, transmembrane zinc metalloproteases and disintegrins are found in skeletal muscle tissue (Seals and Courtneidge, 2003) and expression of ADAM 12 in skeletal muscle reduced pathology in *mdx* mice (Kronqvist *et al*, 2002).

In summary, the lysosomal-cathepsin system may have a minor role in basal skeletal muscle myofibrillar turnover and probably degrades, bulk quantities of sarcoplasmic proteins in to amino acids. However, this system is activated under catabolic conditions, including fasting and those that involve proinflammatory cytokines (Tsujinaka, *et al*, 1996, Deval *et al*, 2001, Jagoe *et al*, 2002). In these conditions it may play a

greater role in myofibrillar degradation and selective proteolysis. Cathepsin L, a main responsive proteolytic enzyme is implicated as playing a key role an all conditions mentioned, along with a possible role in glucose-insulin homeostasis, insulin sensitivity/resistance and glucose oxidation (Huang et al, 2003).

The bulk of skeletal muscle protein degradation may occur through a coordinated response by the calpain and ubiquitin-proteasome systems. The calpains, a highly selective specific cleaving system do not completely degrade proteins to amino acids. They cleave specific sarcoplasmic proteins and many of which are associated with the myofibrillar lattice, initiating Z-disk disintegration and myofilament release. The suggested model is that myofilaments are unable to be degraded by the ubiquitin-proteasome and lysosomal systems whilst in their native functional state within the myofibril. However calpain-mediated processes (other proteases including caspase 3 may be involved) cleave proteins in the myofilaments which then move to the periphery of the myofibril. These myofilaments will then come in to close contact with complete degrading systems. The ubiquitin-proteasome pathway is thought to play a major role in myofibrillar degradation under basal and induced-catabolic conditons and specifically degrades, damaged, denatured and abnormal cell proteins.

Caspase activation does not play a major role in basal protein turnover or bulk proteolysis. Instead it is activated under developmental, catabolic, pathological conditions and cell dysfunction/damage. The calpains and caspases have important functional interactions (through cleavage mediated activation/deactivation) with themselves, each other and other regulatory proteins, like protein kinases and phosphatases within skeletal muscle (Krebs and Graves, 2000). This may affect and alter cell signalling pathways and ultimately regulate cell growth, proliferation, overall protein turnover, cell death and inflammatory responses. The components of greatest interest within muscle include caspase-3 and ARC, a caspase-inhibitor. Caspase-3 is the main effector protease altered during catabolic states and myocellular development; and ARC is a potent muscle tissue-specific caspase inhibitor.

2.12 HYPOTHESIS AND AIM OF WORK UNDERTAKEN

The central hypothesis of this thesis is the assertion that there is a co-ordinated change in the gene expression of key components of intracellular proteolytic pathways under the influence of various physiological and pharmacological stimuli, known to alter skeletal muscle protein turnover and growth. This thesis describes a series of studies designed with the aim of investigating the relationship between altered states of muscle growth and mRNA expression of key components of the proteolytic systems described in this review of the literature.

An initial study involves examining the hypothesis that alterations in the plane of nutritional intake can influence the gene expression of components of the calpain-calpastatin system in rapidly growing cattle. The calpain system was a model system for attempting to assess the gene expression of multiple components using the technique of Quantitative Real-Time RT-PCR.

The thesis then describes the synthesis of cDNA probes for components of the four proteoltytic systems of interest so they could be used to quantitatively measure mRNA gene expression in northern hybridisation's studies, using porcine skeletal muscle RNA.

Having demonstrated that specific probes could be used to detect and quantify northern blot band signals in porcine skeletal muscle, probes were used to investigate the hypothesis that beta-adrenergic agonist administration in pigs would alter mRNA gene expression of components of specific proteolytic systems.

CHAPTER 3 MATERIALS AND METHODS

3.1 MATERIALS

Skeletal muscle tissue samples used both throughout all trial analysis studies and the development of techniques, were obtained from various sources from within the Division of Nutritional Biochemistry; many thanks to all those who made this work possible. Individual acknowledgements are within the appropriate sections. All skeletal muscle samples taken were frozen in liquid nitrogen and stored at −70°C.

All chemicals used were of analytical grade where available and purchased from Fisher Scientific (Leicestershire, UK) unless otherwise stated. Solutions were made in double-distilled deionised water. Molecular biology reagents purchased from Promega (Southampton, UK) were as follows:
Taq Polymerase, 10X Reaction Buffer and 25mM Magnesium Chloride ($MgCl_2$).
M-MLV Reverse Transcriptase and M-MLV Reverse Transcriptase 5X Buffer.
rRNasin® Ribonuclease Inhibitor.
Nucleotides (dNTPS) and random hexamer primers.
Restriction-endonucleases, associated buffers and BSA (Bovine Serum Albumin).
DNA and RNA markers, and DNA loading dye.
Nuclease-free water.
Nucleotides were purchased separately as stocks of 100mM dATP, dTTP, dGTP and dCTP then diluted to 10mM, using nuclease-free water. 10mM dNTP mix was subsequently used for RT (Reverse Transcriptase) and PCR procedures.

Radioisotopes were purchased from Perkin Elmer (USA).

Gel electrophoresis was performed using BioRad (California, USA) electrophoresis tanks and power packs. PCR thermocycler machine used for all PCR and RT reactions was Eppendorf Mastercycler Gradient (Helena Biosciences, Sunderland, UK).

The centrifuges were Heraeus Christ Biofuge A, Beckman J2-21, MSE 18, and Sanyo MSE Hawk 15/05 refrigerated centrifuge.

3.2 GENERAL MOLECULAR BIOLOGY PROCEDURES

All procedures were carried out using sterile pipette tips, autoclaved solutions and wearing latex gloves at all times to prevent nuclease contamination of the samples.

Additional care was taken in cleaning and sterilisation procedures during total RNA extractions and Northern blotting to avoid RNAase contamination, and subsequent RNA degradation. All glassware and plasticware was soaked overnight in 0.1M Sodium Hydroxide and 1mM Ethylene Diamine Tetra-acetic Acid (EDTA), to denature RNAase; then washed with Diethylpyrocarbonate (DEPC (Sigma-aldrich, Dorset, UK))-treated water. DEPC treated water was made by adding 0.5 ml DEPC / 1 l double distilled water, which inactivates RNAase, then left overnight and autoclaved for 3 autoclave cycles. All working solutions and buffers were prepared with DEPC-treated water (except those containing amide groups).

3.3 TOTAL RNA EXTRACTION

Total RNA suitable for use in gene expression experimental procedures was extracted from samples, using an acidified Phenol Guanidine Thiocyanate method adapted from Chomczynski and Sacchi (1987). The reagents required for the procedure can be found within Appendix J.

3.3.1 Extraction Procedure

The Denaturing solution (see Appendix J.) acts as a protein denaturant, thereby inhibiting RNAase activity. To 50 ml of denaturing solution, 0.36 ml β-Mercaptoethanol (β-ME) was added giving a final working concentration of 0.1M (see Appendix J.). As the solution is stable for 1 month at room temperature all extractions were performed in batches within days after solutions were made-up. Frozen muscle tissue stored at -70°C was crushed in liquid nitrogen using a pestle and mortar. Samples were weighed out (1 g ±0.03) into 50 ml sterile screw capped centrifuge tubes (Sarstedt, Numbrecht, Germany). To this was added 10 ml of denaturing solution+β-ME and the sample homogenised (Polytron PT 3000, Kinematica Cincinnati, Ohio, USA) at high speed for approximately 20-30 sec. Once homogenised, a

Phenol Chloroform extraction was performed. The following solutions were added in the order specified, with gentle mixing between each addition of a solution: 1 ml 2M Sodium Acetate pH4,; 10ml water saturated Phenol; 4 ml Chloroform-isoamyl alcohol (49:1). Finally the solution was mixed well by shaking vigorously for 10-20 seconds. Samples were cooled on ice for 15-30 min then centrifuged at 12,000 g (J2-21 Beckmann centrifuge) for 20 min at 4°C. The aqueous phase was removed and transferred to a Corex centrifuge tube. To this 10 ml Isopropanol was added, mixed and samples left to precipitate overnight at -20°C. Samples were centrifuged at 12,000 g (as above) for 20 min at 4°C. Supernatant was removed and discarded and pellet resuspended in 3ml of Denaturing solution+β-ME, 3 ml Isopropanol added, gently mixed and left at -20°C for a minimum of 1 hour. The samples were then centrifuged at 12,000 g for 20 min at 4°C, pelleting the total RNA. Supernatant was removed, pellet washed with 4 ml 75% (v/v) Ethanol, vortexed and centrifuged (as described above). The supernatant had to be completely and carefully removed to avoid disturbing the pellet and redissolved in 2 ml of nuclease-free water. Further precipitation steps were required to remove excess glycogen from the RNA by adding 6 ml 4M Sodium Acetate, mixing, then leaving samples overnight at 0°C. Samples were then centrifuged (as described above), the supernatant removed, then pellet partly air-dried and redissolved in ~100-500 µl (depending on estimated concentration required) nuclease-free water. Samples were stored at –70-80°C.

Total RNA was quantifed using spectrophotometer analysis (Section 3.3.2) and integrity assessed by non-denaturing gel electrophoresis (Section 3.6), using one µg of total RNA/sample. Completely intact and purified total RNA should exhibit two clean sharp bands, corresponding to 28S and 18S ribsomal units. Presence of 'band smearing', particularly at the lower molecular weights, indicates degradation; complete degradation by high intensity low molecular weight banding. DNA contamination was indicated by the presence of band smearing near wells and a large molecular weight band.

3.3.2 Nucleic Acid Quantification and Quality Assessment

RNA and DNA samples in nuclease-free water, had their concentrations measured, along with an estimation of relative impurities by spectrophotometric analysis. Ab-

sorbance at wavelengths, 260 nm (for nucleic acids), 280 nm (for proteins), and for some samples at 320 nm (for contaminants, e.g. guanidinium thiocyanate) were measured using a spectrophotometer (Genequant Pro, Amersham Pharmacia Biotech Buckinghamshire, UK), and ratios 260/280 and 260/320 calculated. 1 µl of stock sample was diluted down at least 50 fold in nuclease-free water, mixed and OD measured (this was repeated in triplicate). For RNA samples a ratio reading of 1.8-2.0 at 260/280 was accepted, for DNA, 1.6-1.8. The RNA concentration was quantified as 40 µg/ml RNA has an absorbance of 1.00 at 260 nm in a 1cm light path.

3.4 QUANTITATIVE REAL-TIME RT-PCR (REVERSE TRANSCRIPTASE-POLYMERASE CHAIN REACTION) ANALYSIS OF GENE TRANSCRIPTS

3.4.1.1 Introduction

Real-time RT-PCR is a means of quantitatively analysing the relative expression of specific mRNA transcripts (Bustin, 2000, Yin *et al*, 2001). The techniques aim is to quantify the relative gene expression of large numbers of samples (using 96-well reaction plate) using very small amounts of starting tissue material or mRNAs with low transcript levels.

The basic methodological concept is that mRNAs within an extracted tissue total RNA pool can be synthesised into a first strand cDNA pool by Reverse Transcription (RT-step). This can then be used as a cDNA template to amplify by PCR specific gene transcripts of interest using specific PCR oligonucleotide primers (and probe). From PCR amplification data relative gene expression can be quantified.

3.4.1.2 RT-PCR (Reverse Transcriptase-Polymerase Chain Reaction)

The Reverse Transcription step (RT-step) involved annealing of short oligonucleotide primers to single stranded RNA. In the studies discussed within this thesis reverse transcription of the entire total RNA pool using random hexamer primers was performed. Once primers were annealed to RNA strands the RNA-dependent DNA polymerase MMLV (Moloney Murine Leukemia Virus) Reverse Transcriptase en-

zyme reverse transcribed RNA strands in the 5′ - 3′ direction using free nucleotides to extend primers (see Figure 3.4.2-1.). The synthesis of a single-stranded (ss) cDNA pool was then used as a suitable template for amplification of specific targets by PCR. The first step involved synthesis of a single, double stranded sequence through forward primer annealing, Taq Polymerase binding and synthesising a complementary strand. A specific template region was amplified using a cyclical process of high temperature (94-95°C) denaturation of ds DNA, annealing of oligonucleotide primers (at a temperature dependant on melting temperature (Tm) of oligonucleotides), and extension of primers in 5′ - 3′ direction (see Figure 3.4.2-1), as Taq Polymerase extends in a 5′ - 3′ direction. A 5′- forward primer anneals to the antisense strand and the 3′- reverse primer anneals to the sense strand. The extension step is performed at a higher temperature (72°C) than the annealing step, as this is the optimum temperature for Taq Polymerase activity (optimum activity is ~60 nucleotides/second). The duration of the extension cycle depends ultimately on the size of the amplicon to be synthesised, such that the larger the amplicon the longer the extension step required. Once the reaction is complete and two ds cDNA strands have been synthesised, the cycle is repeated in the same fashion, yielding twice the number of strands. The number of cycles required depends on the initial level of expression within the sample. Genes of low expression require a greater number of cycles, e.g 35-40 cycles of amplification, to produce a level of detectable PCR product. The maximum number of cycles is 40, as non-specific amplification and amplification errors become more common as the number of cycles increases.

Figure 3.4.1.2-1. Diagram outlining RT-PCR reaction steps, and direction of strand synthesis.

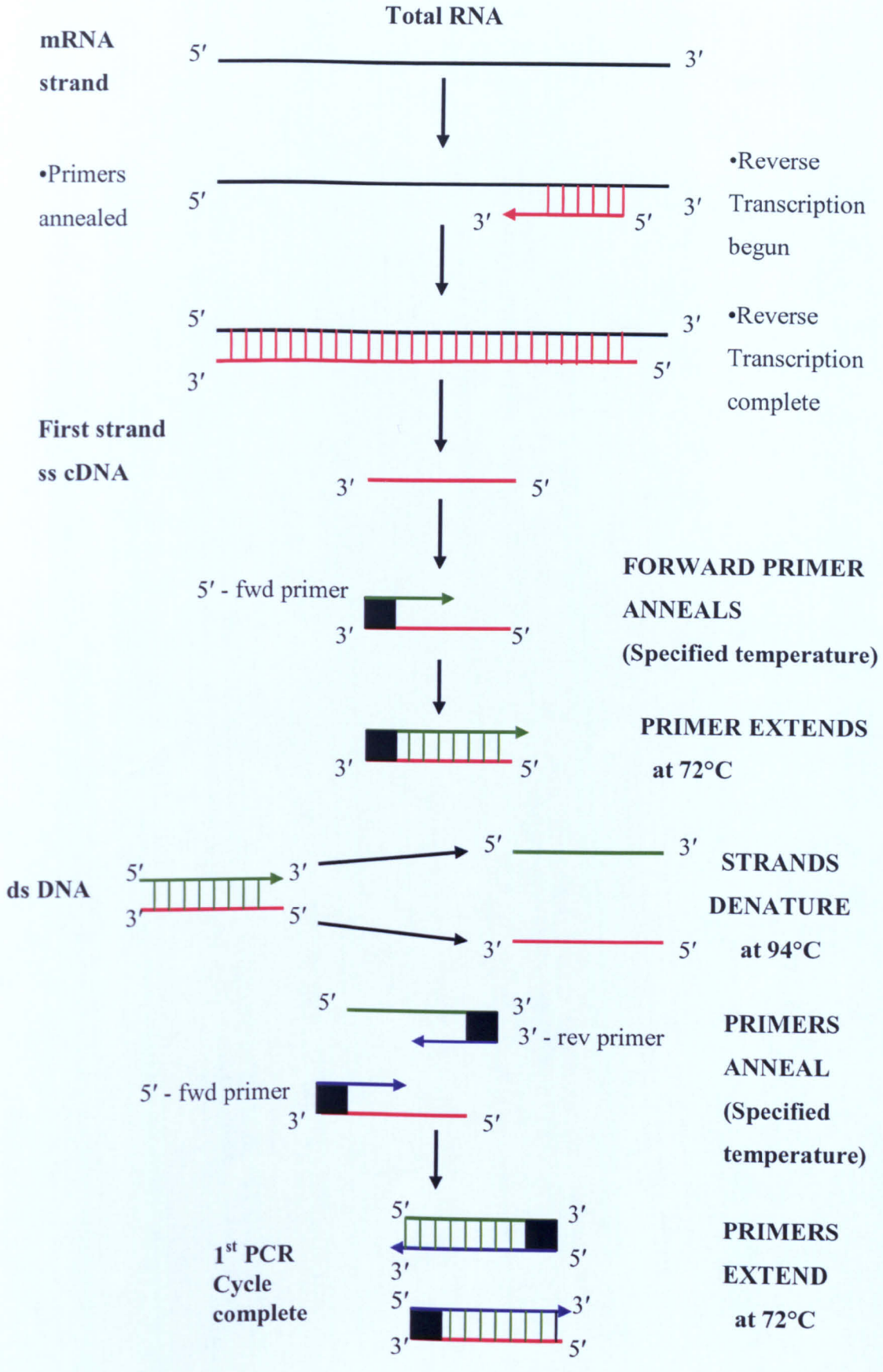

3.4.1.3 Real-time PCR

Specific fluorescent molecules are incorporated into the PCR reaction mix via use of specific oligonucleotide dual-labelled Taqman® probes with end-terminal fluorescent molecules (FAM and TAMRA), or SYBR-Green I dye.

Real-Time PCR differs from PCR performed in a standard thermocycler (as described above) as reactions are performed in a Quantitative Real-Time thermocycler (Perkin Elmer, ABI Applied Biosystems, 7700 thermocycler). This system contains a laser and optical fiber network, causing the excitation of fluorescent molecules and subsequent detection and analysis of light emissions. The continuous collection of DNA template amplification data (as fluorescence intensity data) from each cycle is made.

A) Taqman® Dual Labelled Fluorescence Probe Analysis

Taqman® Probes are 20-25 bp oligonucleotides that anneal to a sequence in the amplicon generated by the forward and reverse primers. The Probe is dual-labelled at the 5′ end with a 'reporter dye' (e.g. FAM) and a 'quencher dye' (e.g. TAMRA), at the 3′ end. The 'Taqman chemistry' reaction involves fluorescence energy transfer (FRET) (Yin *et al*, 2001). The Probe remains in an 'in-active' state when free and bound to DNA strands as the quencher dye prevents the reporter dye fluorescing. Primer extension by the Taq Polymerase (AmpliTaq Gold) allows the 5′ to 3′ exonuclease activity of the Taq Polymerase to degrade the Probe, releasing the reporter dye and produce fluorescence emission (see Figure 3.4.3-1).

Taqman® Probes provide specificity to the PCR reaction. Non-specific amplicon synthesis possible with primer only reactions, are not detected when performing reactions in coordination with a Taqman® Probe. Specificity is also provided as fluorescent signals are only emitted once primer extension of a precise region takes place by Taq Polymerase and Probe subsequently degraded.

Figure 3.4.1.3-1. Quantitative Real-Time PCR using a Taqman® Probe.

Ⓡ= Reporter dye [Q]= Quencher dye.

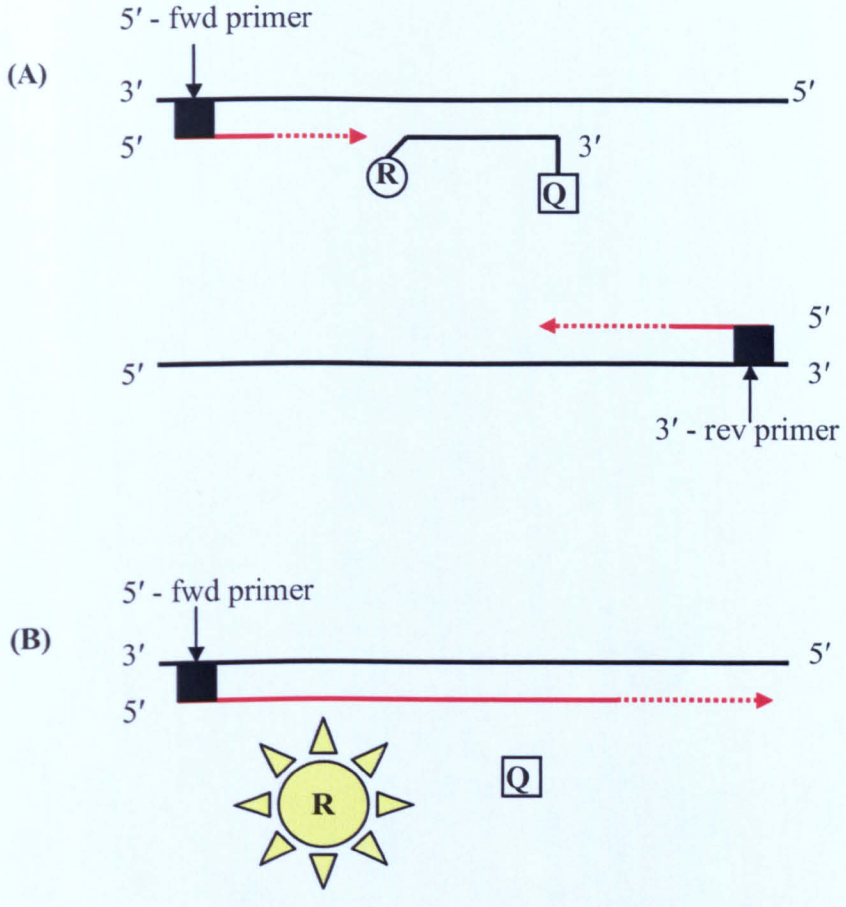

(A) After the ds DNA template is denatured by heating to 95°C, temperature dropped to allow annealing of both specific oligonucleotide primers and Taqman® Probe to amplicon region. Nucleotides are then extended along strands from primers in a 5′ to 3′ direction by Taq Polymerase.

(B) Taq Polymerase degrades annealed Taqman® Probe using 5′ to 3′ nuclease activity. Reporter and quencher dyes are released from strand, Reporter is free from inhibition and emits fluorescence.

Figure 3.4.1.3-2. Quantitative Real-Time PCR using SYBR-Green I.

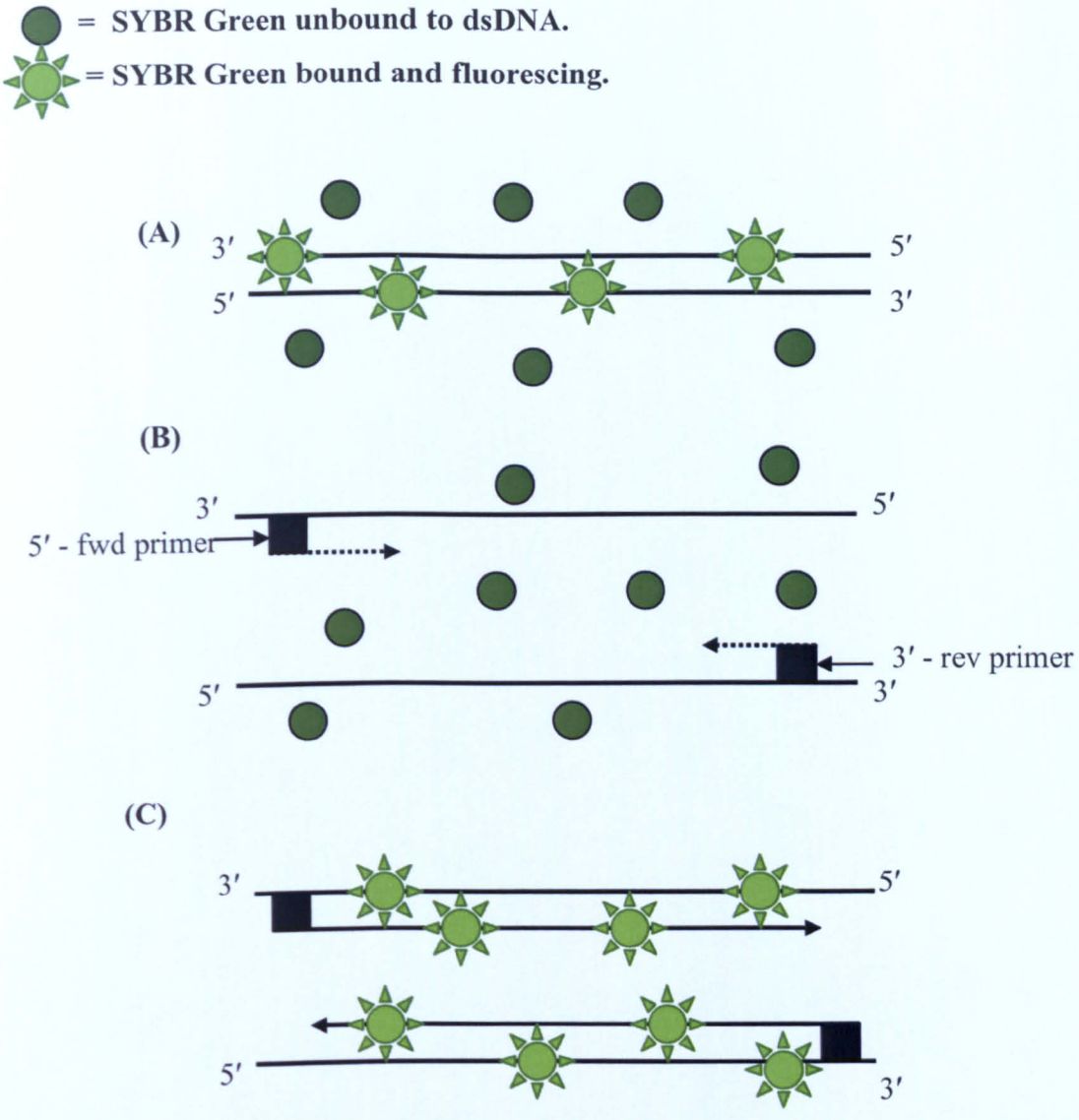

(A) ds DNA has SYBR-Green I bound, emitting fluorescence. (B) The ds DNA template is denatured by heating to 95°C, temperature dropped to allow annealing of specific oligonucleotide primers to amplicon region. As strands are denatured and single-stranded, SYBR-Green I does not emit fluorescence.

(B) Nucleotides are then extended along strands from primers in a 5′ to 3′ direction by Taq Polymerase. SYBR-Green I binds to new ds DNA and emits fluorescence.

B) SYBR-Green I Method

SYBR-Green I is a sensitive dye that emits fluorescence when bound to dsDNA (see figure 3.4.3-2). When using this method fluorescent emissions are detected when SYBR-Green I binds to any dsDNA present during subsequent DNA amplification cycles. Therefore, if dsDNA is of non-specific origin, non-specific fluorescent signals will be detected. Thereby making this method potentially less specific with high noise signals.

Both methods allow quantitative analysis of gene expression through analysis of fluorescence-emission intensity data. Fluorescence data for every step at every cycle is detected, analysed and graphically presented in a data output (Figure 3.4.3-3). Assuming complete PCR reaction efficiency, theoretically fluorescence intensity is directly proportional to [ds DNA] during the linear phase of amplification. Therefore, fluorescence intensity increases exponentially with cycle number as DNA replication is two-fold/cycle. A plateau phase of amplification and fluorescence is reached leading ultimately to reaction end-point. End-point product analysis is a semi-quantitative method which is not accurate, as everything tends towards the same end point quantity.

Figure 3.4.1.3-3. Outline of graphical fluorescence data output of Real-time PCR reactions and relationship between phases of template amplification.

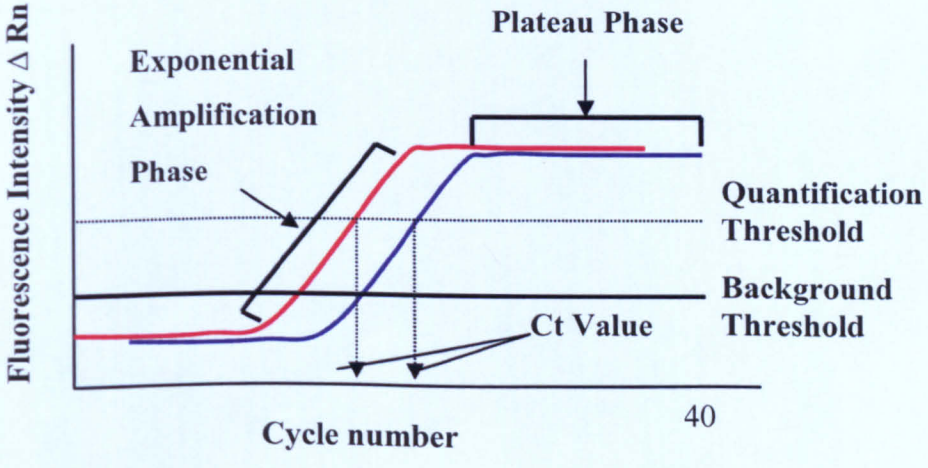

In Figure 3.4.1.3-3 the quantification threshold and background threshold level is indicated. The quantification threshold is the user selected level of intensity of reporter dye emission that is above background emission/noise. This is taken approximately from mid-point of the linear-exponential phase. The cycle number corresponding to the quantification threshold level of fluorescent intensity is known as the cycle threshold (Ct value), which is recorded and can be used to assess relative expression of samples. The greater the initial amount of target template, the lower the cycle value it requires to reach a set level of quantification threshold fluorescence, i.e. lower Ct Value. For example, in Figure 3.4.1.3-3 the sample producing the fluorescence intensity graph in red has a lower Ct value than blue sample, and hence a greater amount of starting template/gene expression.

In summary, the Ct Value data can be used to comparatively assess the original level of [cDNA] target of interest within the total cDNA pool, and hence [mRNA] species of interest within the total RNA pool. This is assuming first strand synthesis is equally efficient between samples. Specific details of method of quantification using Ct values, assessment of reaction efficiencies and examples can be found within Section 3.4.4 and 4.3. The relative gene expression of multiple targets may be quantified from single total RNA extractions, as only small quantities of RNA/cDNA are required per reaction.

3.4.2 Bioinformatics Methods

3.4.2.1 Sequence Retrieval and Multiple Sequence Alignments

For target sequences to be amplified by PCR and Real-Time PCR, specific primers had to be designed based on sequence information of expressed genes of interest. Therefore, relevant complete mRNA sequences for bovine, porcine and human (and other species if necessary) species, were searched for using relevant EBI-EMBL (European Bioinformatics Institute-EMBL)/NCBI (National Center for Biotechnology Information)/DDBJ (DNA DataBank of Japan) nucleotide sequence databases; that can be found within the Hgmp.mrc.ac.uk webpage. Retrieved sequences were saved in appropriate formats (e.g. Fasta) to allow subsequent input into various programs. The mRNA/cDNA sequences were aligned using the CLUSTAL W-multiple

sequence alignment program (EMBL/DDBJ). Sequences in Fasta formats were inputted, aligned with one another and sequence similarity/homology across species analysed. The CLUSTAL W program assigned star symbols (*) underneath alignments at every base which is identical across sequences analysed.

3.4.2.2 BLAST Searches

BLAST searches were routinely used on the NCBI and DDBJ nucleotide databases, to either identify similar sequences in the database, or identify RT-PCR generated products, after DNA sequencing. The sequence of interest (saved in Fasta format) was inserted into the query window within the standard nucleotide BLAST search webpage. Parameters were set for database types to search through (e.g. human, EST, mammals etc.), the number of alignments to be made and how many to be viewed. The BLAST output showed listed sequences aligned to sequence of interest in order of greatest homology, measured by a Score, E Value and % sequence identities (Full explanation of these terms and search examples can be found within Appendix A).

3.4.2.3 Oligonucleotide Primer and Dual-Labelled Fluorescence Probe (Taqman®) Design

Once areas of high sequence homology across species were found, these were used to design Dual-labelled Fluorescence Probes and PCR primers:

Real-Time PCR: an mRNA sequence used in the alignment (preferably same species of interest in Trial sample analysis) was inputted into the Primer Express program (ABI Biosystems), in Fasta format and sequence analysed for optimum specific primer pairs and probes. Areas targetted were of high similarity across species. Using default program parameters an optimum amplicon size of 100 bp was searched for (of optimal 50-150 bp minimum and maximum program parameters), and a large selection of suitable primer pairs and Taqman probes (based on oligonucleotide length, GC base content, and melting temperature, Tm), were listed in an output. When Real-Time RT-PCR was carried out using SYBR-Green method rather than Taqman probes, the program was re-set so as to analyse sequence for optimum primer pairs only. Listed output of primer pairs and probes had to be further carefully manually

analysed to be certain the correct area was targeted for amplification. This was to firstly double-check that primers had been designed to correct parameters. Secondly, slight species variation in sequence data may mean certain primer pairs couldn't be used as they may not be to a very high level of sequence specificity etc. Primers and Taqman probes were manufactured by Sigma-Genosys (Pampisford, UK). Primers were resuspended to 100 pmol/µl then diluted to a working concentration of 10 pmol/µl in nuclease-free water.

Standard PCR: In general, for standard PCR, primers were designed by searching for areas of the highest homology across species. Suggested primer sequences were checked using a primer test program (within Primer Express) for secondary structures etc. Examples of standard PCR primer sequences designed from multiple alignments can be found within Appendix A.

3.4.3 Real-Time Reverse Transcriptase PCR Method

3.4.3.1 Reverse Transcription (RT-Step)

Extracted total RNA samples were quantified and checked for quality and purity, using analysis by spectrophotometer and non-denaturing gel electrophoresis methods (see section 3.32 and 3.6 respectively).

The reverse transcription of total RNA to first strand complimentary DNA involved a 2-step method. The first step required annealing of oligonucleotide primers to the total RNA sample. Random hexamer primers were annealed to total RNA pool. The second step involved reverse transcribing the entire total RNA pool, producing a first strand complimentary DNA pool. The reaction, was set up in 200 µl reaction tubes (Perkin Elmer), in following order:

Reaction Constituents	Volume
Total RNA (0.1 µg/µl)	5.0 µl
Random hexamer primers (0.5 µg/µl)	1.0 µl
Nuclease free water	9.0 µl

Reactions were mixed by pipetting and incubated at 70°C for 5 min to denature secondary structure. Tubes were then immediately placed on ice to prevent secondary structure reforming, but allowing the oligonucleotides to anneal.

The second RT reaction-step was set-up using the following constituents whilst reaction tubes were on ice after previous step:

Reaction Constituent	**Volume**	**Final Conc.**
MMLV Reverse Transcriptase 5X Reaction Buffer *	5.0 µl	
Nucleotides (dNTPs) 10mM	1.25 µl	0.5mM
rRNasin Ribonuclease Inhibitor	0.5 µl	25U
M-MLV Reverse Transcriptase*	1.0 µl	200U
Nuclease-free water	8.0 µl	

*MMLV, Moloney Murine Leukemia Virus Reverse Transcriptase. 5X Reaction Buffer: 50 mM Tris-HCl (pH 8.3 @ 25°C), 75 mM KCl, 3 mM $MgCl_2$ and 10 mM DTT.

The reactions were mixed by pipetting then incubated at room temperature for 10 min to allow random primer extension, followed by 42°C for 60 min.

Samples were diluted four-fold after RT-step with nuclease-free water and stored at -20°C. These samples acted as substrates for subsequent PCR.

3.4.3.2 Real-Time PCR Protocol

Samples were set-up and analysed in triplicate on a 96-well plate. PCR mastermix was prepared on ice in a sterile 1.5 ml microcentrifuge tube, in the following order (see over page) for Taqman® Probe reactions:

The volumes were increased to allow for pipetting errors, i.e. increase mastermix volume by ~$^1/_3$ /reaction; extra 24 µl, equivalent to one extra reaction for each 96 µl triplicate sample.

Reaction Constituents	Volume *
2 X Taqman® mastermix†	12.5 µl
Forward primer (10 µM)	0.75 µl
Reverse primer (10 µM)	0.75 µl
Taqman® Probe (5µM)	0.625 µl
Nuclease-free water	9.375 µl
Total Volume	24 µl

* Volume for a single reaction (multiples of this were always made).

† Reagent acquired from ABI Biosystems. Contains Ampitaq Gold Polymerase and UNG (Uracil Glycosylase).

Mastermix was vortexed, spun down briefly in a centrifuge, and 96 µl taken and pipetted into into tube containing 4 µl bovine 1st strand cDNA pool sample (total RNA equivalent: 4µl = approximately 0.020 µg), or NTC (Non Template Control of 4 µl nuclease-free water) giving a final volume of 25 µl / reaction, effectively 4 reactions for each sampleand an excess of one reaction.

The SYBR-Green I method required a similar reaction set-up, in that 100 µl PCR mastermix + cDNA template reaction mixes were prepared, i.e. 4 x 25 µl reactions (3 +1 extra to account for errors). The difference between methods was that SYBR-Green I required a greater amount of template for reactions (5 µl), due to lower sensitivities, therefore as can be seen below the mastermix volume is 20 µl.

Reaction Constituents	Volume*
2X Taqman® mastermix†	12.5 µl
Forward primer (10pmol/µl)	0.75 µl
Reverse primer (10pmol/µl)	0.75 µl
SYBR Green I ‡ (1 in 50 dilution from 10,000X stock solution)	0.25 µl
Nuclease-free water	5.75 µl
Total Volume	20 µl

* Volume for a single reaction (multiples of this were always made).

† Reagent acquired from ABI Biosystems.

‡ Reagent acquired from Sigma-Aldrich.

Similar to previous Taqman Probe Reaction mix, samples were vortexed, briefly spun down in a centrifuge, placed on ice, and 4 x reaction volume (80 µl using SYBR-Green I) pipetted into tube containing 20 µl bovine 1st strand cDNA pool sample (4 x reaction) or NTC (20 µl nuclease-free water).

Sample tubes from both methods were vortexed, spun down briefly in centrifuge, and pipetted on to a 96-well reaction plate kept on ice. Lid on reaction plate was then sealed.

For all experiments computer program was set-up, and well-loading pattern entered into the Sequence Detection Software program (ABI Biosystems) file. The 96-well reaction plate was taken off ice, loaded into machine and reaction begun using the following thermocycle conditions:

Reaction Phase	Temperature	Time	Cycles
Uracil Glycosylase step	50°C	2 min	1
Amplitaq-Gold Activation step	95°C	10 min	1
Denature	95°C	15 sec	40
Anneal/Extend	60°C	1min	

3.4.4 Data Collection and Analysis

The first experimental procedure undertaken before assaying trial samples was to perform preliminary standard curve experiments for all expressed genes of interest. This was used to check that a linear pattern of expression exists. Known serial dilutions of stock cDNA template (with mastermix and primers) were prepared and loaded on reaction plate as described in procedure above.

Fluorescence emission signals were collected automatically from reaction plate during reaction cycles and plotted onto fluorescent intensity (ΔR_n value) amplification curves (as of figure 3.4.1.3-3). ROX dye contained within the Taqman® mastermix acted as an internal-control dye. Errors in pipetting and hence volume of Taqman® mastermix loaded (and ROX dye), adjusts the fluorescence value for each well. This allowed triplicate sample Ct Values to be validated, by ROX fluorescence quantification.

The NTC triplicate samples containing nuclease-free water allowed for sample contamination and PCR artifacts contributing to a signal to be validated. NTC samples with fluorescent amplification signals present signified template/DNA contamination, therefore indicating nonspecific amplification.

Post-PCR, triplicate reactions were pooled together for each sample and run on a 1.8% non-denaturing agarose gel (see Section 3.6) to check for a single PCR product of correct band size. This indicated specific amplification of the template.

The relationship between Ct value and initial concentration of the template was determined from a graph of Ct value against log RNA equivalent (example in Appendix D.). Theoretically, assuming reaction efficiencies are 100% there is a doubling in [DNA] per cycle. Therefore, 10-fold dilutions in [cDNA] template would produce a slope of –3.3 on a graph of Ct vs $\log_{10}$ [cDNA].

Once experimental procedures were validated for individual expressed genes of interest using method above, trial samples were analysed using protocol described (Section 3.4.3.2). By examining NTC, ROX dye and post PCR products by gel electrophoresis anomalities could be spotted and data accepted or rejected.

3.5.1 Standard PCR Protocols

Standard PCR was performed to produce PCR products of interest to be used as cDNA probes in subsequent gene expression studies (see Section 5 and Appendix A.). In general, AmpliTaq-Gold was used as the enzyme of first choice due to its high efficiency and ease of use (as no manual hot-start was required). Those reac-

tions producing negative results after repeated attempts yielded positive results when using either Taq (Promega) or the Expand Taq (Roche). Expand system is highly efficient and possesses inherent 3'-5' exonuclease proof-reading activity increasing DNA synthesis fidelity. According to the manufacturer, for 200-300 bp fragments Taq has an error rate of 2.6×10^{-5}, whereas Expand 8.5×10^{-6}. Expand was therefore used in problematic reactions.

First-strand cDNA pool was synthesised from 0.5 µg porcine *Longissmus Dorsi* Poly-A$^+$-enriched RNA (T.Parr), using RT-step described. Post-RT-step, cDNA was diluted to 500 µl. 2 to 5 µl dilute first-strand cDNA pool was used as a PCR template (~0.001 µg/µl RNA equivalent), using specific oligonucleotide primers. All reactions were performed in 200 µl thin-walled, PCR reaction tubes (Perkin Elmer). Three different Taq polymerase systems were used in attempts to generate a PCR product:

A) **Taq system (Promega)**: a 39.5 µl mastermix/sample was set up in the following order in a sterile 1.5 ml microcentrifuge tube:

Reaction Constituent	**Volume***
10mM Nucleotide mix (dNTPs)	1.0 µl
Forward primer (10pmol/µl)	1.25 µl
Reverse primer (10pmol/µl)	1.25 µl
10X PCR Buffer†	5.0 µl
$MgCl_2$ (25mM)	2.0 µl
Nuclease-free water	28 µl
Total Volume	40 µl

* Volume for a single reaction (multiples of this were always made).

† 10X PCR reaction buffer contains following constituents: 10mM Tris-HCl (pH 9.0 at 25°C), 50mM KCl, and 0.1% Triton® X-100.

Mastermix was vortexed, spun down briefly in a centrifuge, 39.5 µl taken out and added to each individual 200 µl PCR reaction tube (Perkin Elmer) containing 10 µl dilute template (2 to 5 µl dilute cDNA template, as above and 5 to 8 µl nuclease-free

water-as above). Samples were mixed by pipetting. 0.5 µl Taq enzyme (Promega) (5U/µl) was added to individual reactions after a 'hot start'. Amplification starts at an elevated temperature to try to control mispriming events and increase reaction specificity and sensititvity. Reactions were then mixed by gently 'swirling' with pipette.

Reaction conditions were as follows:

Reaction Phase	Temperature	Time	Cycles
Denature	94°C	3 min	1
Hot Start - 0.5 µl Taq Polymerase/sample addition			
Denature	94°C	30 sec	
Primer Annealing	*°C	30 sec	35
Primer Extension	72°C	60 sec	
Primer Extension/polishing	72°C	5 min	1

*Variable temperature primer annealing step, dependent on primer base pair composition.

B) Amplitaq Gold® Taq System (ABI Biosystems): a similar master mix was prepared as above containing 0.25 µl Perkin Elmer heat-activated AmpliTaq Gold® (5U/µl) Taq Polymerase, PCR buffer and 25mM $MgCl_2$ reagents (Applied Biosystems, Roche). Reagents were prepared in a 40 µl mastermix (using same concentration of constituents as above). Mastermix was added to 10 µl dilute template (as above). Reaction conditions were similar as above except first step was 10 min long at 95°C to activate Amplitaq Gold®, as is a heat-activated enzyme. The last primer extension polishing step was 10 min long.

C) Expand High Fidelity PCR System (Roche): Two separate mastermixes were set up. In one tube, 10mM nucleotides, 10 pmol/µl primers and nuclease-free water was added and mixed. In the second tube, Expand PCR Buffer (+15mM $MgCl_2$), Expand High Fidelity PCR System-enzyme mix (2.6U) (Roche Molecular Biochemicals, Mannheim, Germany) and nuclease-free water was added and mixed. Mastermix concentrations and volumes were similar as above; when mixed with dilute tem-

plate sample (as above), producing a final volume of 50 µl. Reaction conditions were the same as used for the Promega system (a hot start was not required).

All PCR products were viewed by non-denaturing gel electrophoresis (using method described in 3.6) on a 1.8% agarose gel, as expected size of products were in the range of ~200-300bp.

3.5.2 Annealing Temperatures

The primer annealing temperatures for PCR were selected based upon oligonucleotide primer melting temperatures (T_m). T_m's of primer pairs were within 2°C of each other. In general, annealing temperatures were calculated by 5°C below oligonucleotide T_m. However, most PCR reactions were empirically optimised using annealing temperature gradient reactions (using same Eppendorf thermocycler), to assess the optimal temperature producing the highest specific yield of correct PCR product.

3.6 NON-DENATURING GEL ELECTROPHERESIS

Examination of DNA and RNA samples throughout experimental procedures was undertaken by separating samples by electrophoresis using a non-denaturing agarose gel. The percentage of agarose required depended on the size of fragments to be run:

Size of Fragments (bp)	% Agarose (w/v)
> 1 kb	1%
< 1 kb	1.5%
≤ 350 bp	1.8-2.0%

Agarose (Amersham Pharmacia Biotech, Buckinghamshire, UK) was made up to the appropriate % (w/v) with 1xTAE (0.04M Tris, 0.01M glacial acetic acid, 0.7mM EDTA), heated to boiling point, stirred and left to cool down to hand hot temperature. The molten gel was then poured into appropriate gel former with corresponding gel comb and left to set at 4°C. Once the gel was set it was placed in gel tank electrophoresis apparatus which was filled with 1xTAE buffer. Samples were loaded into

wells with all samples having a final volume of 10 µl (unless stated otherwise), and 2 µl loading dye (15% Ficoll® 400, 0.03% bromophenol blue, 0.03% xylene cyanol FF, 0.4% orange G, 10mM Tris-HCL (pH 7.5) and 50mM EDTA) was added giving a ratio of 1 µl dye : 5 µl DNA. Types of markers to be loaded in to separate wells was dependent on the size of sample fragments to be analysed. 100 bp markers with a fragment range of 100-1,500 bp. 1 kb markers with a fragment range of 250-10,000 bp and Lambda DNA/*Hin*dIII markers with a fragment range of 125-23,130 bp.

Gels were run for 45-60 min at 100V or until the loading dye reached 2/3-3/4 length of gel. Gels were subsequently stained in a 1 µg/ml solution of Ethidium Bromide (Sigma-Aldrich, Dorset, UK) for 20-30 min, destained briefly in water and viewed using a UV transilluminator (BioRad, California, USA). Ethidium bromide binds to nucleic acid and fluoresces a red-orange colour under UV light; the greater the fluorescence intensity, the greater amount of DNA/RNA present. The gel image was captured using the MultiAnalyst (BioRad, California, USA) computer software.

3.7.1 GEL EXTRACTION AND PURIFICATION OF PCR PRODUCTS

Generated PCR products subjected to non-denaturing gel electrophoresis were gel-purified. PCR products were pooled together and separated by non-denaturing agarose gel electrophoresis (Section 3.6), with SYBR-Green I (Sigma-Aldrich, Dorset, UK) mixed into samples with loading dye; which binds dsDNA and fluoresces when illuminated with UV. For this procedure 1 µl of SYBR-Green I : 9 µl of PCR product was added at a 1 in 100 dilution (from 10,000X stock solution), standard DNA loading dye added (at appropriate 1 µl : 5 µl DNA), and tube vortexed and spun down. Samples were subjected to non-denaturing electrophoresis. Gel was illuminated on a Dark Reader Transilluminator (Genetic Research Instrumentation Limited, Braintree, UK). Bands were cut out with a new sterile scalpel blade and gel slice weight determined. DNA was extracted from gel slices using the QIAquick Gel Extraction Kit Protocol (Qiagen, Hilden, Germany).

3.7.2 PCR Product Purification

The QIAquick PCR Purification Kit (Qiagen, Hilden, Germany) was used, following the suggested protocol. The method is an affinity column based procedure similar to that described above and in the purification of plasmid from minipreps. PCR products were added to a membrane on a spin column and subjected to a series of centrifugal spin-steps and addition of buffers and wash solutions. DNA was eluted in a volume of 50 µl nuclease-free water.

3.8 LIGATION OF PCR PRODUCTS INTO PLASMID VECTOR

A number of generated PCR products to be used as probes, were ligated into a pGEM®-T Easy Vector (Promega, Southampton, UK). The appropriate molar concentration of DNA to be used for ligations was determined using the following calculation:

$$\frac{\text{ng of vector x kb size of insert}}{\text{kb size of vector}} \times \text{insert : vector molar ratio} = \text{ng of insert}$$

As all PCR products were ~200-300 bp in size and 50 ng of 3.0 kb vector was used in a ratio of 3:1 (insert:vector), the amount of insert was calculated to be ~12.5 ng.

The following reactions were set up in a sterile microcentrifuge tube as follows:

Reagents	**Standard Reaction**	**Background Control**
2X Rapid Ligation Buffer†, T4 DNA Ligase	5 µl	5 µl
pGEM®-T Easy Vector (50 ng)	1 µl	1µl
PCR product	3µl*	-
T4 DNA Ligase (3 Weiss units/µl)	1µl	1µl
Nuclease free water to a final volume of:	10µl	10µl

† 2X Rapid Ligation Buffer, T4 DNA Ligase contains: 60mM Tris-HCl, pH 7.8, 20mM $MgCl_2$, 10mM DTT, 2mM ATP 10% PEG.

* 3µl volume of all PCR products at ~4ng/ µl was used to make up 12.0 ng.

Rapid Ligation Buffer was well thawed and vortexed before use; complete reactions were mixed by pipetting, and incubated at room temperature for 2 hr. Background controls were used during all cloning experiments- to determine the ligation efficiency of the vector alone.

3.9 TRANSFORMATIONS AND CLONING

pGEM®-T Easy Vector-ligation reactions were the transfected into high efficiency competent JM109 cells (Promega, Southampton, UK). Ligation reactions were vortexed, centrifuged down briefly and 2 µl of each reaction (~2.4 ng DNA) added to a sterile microcentrifuge tube placed on ice to which 50 µl of JM109 cells previously slowly thawed on ice (stock cells stored at –70°C) were added. After a 20 min incubation on ice, cells were heat-shocked for 45-50 sec in a 42°C water bath and then put back on ice for 2 min. 950 µl of thawed SOC medium (see Appendix L) was added and tubes incubated at 37°C for 1.5 hr with shaking (Lab Therm, Kohmer, Switzerland). Tubes were centrifuged at ~9,000 g for 5-7 min, 700 µl supernatant removed and pellet resuspended in 200 µl of supernatant. Resuspended cells were pipetted onto duplicate LB-agar plates with 100 µg/ml ampicillin (see Appendix L), i.e. 100 µl resuspended cells /plate; and spread evenly using a sterile glass rod. Plates were incubated overnight (~18 hr) at 37°C.

Using sterile pipette tips single colonies were picked from plates and placed in to a 30 ml universal sterilin tube containing ~3 ml LB media plus ampicillin (100 µg/ml). Sterilins were incubated overnight for ~18 hr at 37°C with shaking.

The bacterial culture was subject to plasmid DNA purification procedure using Wizard® *Plus* SV Minipreps DNA Purification System (Promega, Southampton, UK).

3.10 PLASMID DNA PURIFICATION

The Promega Wizard miniprep kit supplied all necessary reagents and equipment (columns, barrels etc.) and protocol was followed as suggested by the manufacturer. Appropriate solutions volumes, incubation and mixing conditions can be found

within protocol. For preparation of plasmid DNA 1-1.5 ml bacterial culture/cells was routinely used.

3.11 RESTRICTION ENDONUCLEASE DIGEST OF DNA

Purified plasmid+inserts were linearised and insert excised by performing a routine restriction enzyme (RE) digest procedure as suggested by manufacturer (Promega, Southampton, UK).

In a sterile 1.5 ml microcentrifuge tube the following reaction was prepared in order:

Constituent	Volume
Purified plasmid DNA	10 µl
Buffer H * (10X)	2 µl
BSA (1 in 10 dilution of 10 mg/ml stock)	2 µl
Nuclease-free water	5 µl
EcoR I † (12 U/ µl)	1 µl
Final Volume	20 µl

* Buffer H constituents: 900 mM Tris-HCl (pH 7.5), 500 mM NaCl and 100 mM $MgCl_2$.

† EcoR I was RE of choice for pGEM®-T Easy Vector. Same procedure using different RE was used for other inserts/vectors etc.

Digest mix was set-up and incubated for 1 hr at 37°C. 5-10 µl of digest was checked by running on a non-denaturing 1.5% agarose in 1X TAE gel using procedure described.

3.12. ETHANOL PRECIPITATIONS OF DNA

Ethanol precipitations were carried out either to concentrate nucleic acid solutions, or remove contaminating enzymes or reagents. It was used as a routine procedure throughout studies for 'cleaning-up' DNA and RNA samples (as described in RNA extraction procedure). 2.5 volumes of ice-cold 100% ethanol was pipetted into a 1.5

ml microcentrifuge tube containing sample and 0.1 volumes 3 M sodium acetate pH 5.5 added. Sample was mixed by vortexing, briefly centrifuged down and left overnight at –20°C. Samples were centrifuged at 13,000 g (Hawk 15/05 refrigerated centrifuge) for 20 min at 4°C, ethanol layer pipetted off carefully and 1 volume 75% ethanol (ice-cold) added. Sample was mixed by vortexing and centrifuged (as above). Ethanol layer was pipetted off carefully, precipitate air-dried for 5 min and redissolved into a minimal volume of nuclease-free water (20-50 µl).

3.13 DNA SEQUENCING

Purified PCR products and purified plasmids with inserts were sequenced by MWG-Biotech (Germany) to positively confirm the identification of the sequences generated by PCR, using quantities of DNA as directed by supplier.

3.14 NORTHERN BLOTTING

3.14.1 Introduction

Northern Blotting involves the transfer of RNA sequences separated on a denaturing agarose gel to a solid membrane support. The RNA is fixed to the blot (using UV crosslinking) and probe hybridisation experiments may be performed to allow the assessment of the size of full mRNA sequences and quantification of relative expression of transcripts. Hybridised radio-labelled cDNA probes produce quantifiable band signals that can be detected using phosphoimaging technique.

3.14.2 Denaturing Gel Electrophoresis Procedure

Denaturing gels had a maximum of 25 µg RNA loaded per lane. Total RNA was checked for integrity and quality before being subjected to northern blotting, by non-dentauring gel electrophoresis. A full list of chemicals used in procedure can be found in Appendix K.

The agarose gel was prepared using the following constituents:

Constituent	Amount
100mM Sodium Phosphate Buffer, pH6.5	25 ml
Agarose	dependent on % required
H_20	to 250 ml

Molten gel was poured carefully into a large gel former (20 cm x 21 cm).

RNA samples at appropriate concentration and RNA markers (see Appendix K) were denatured by adding the following in order, in sterile 1.5 ml microcentrifuge tubes:

Constituent	Volume	Final Conc.
Total RNA sample/RNA marker	10.0 µl	
Deioinised Glyoxal	8.0 µl	1M
80mM Sodium Phosphate Buffer pH6.5	6.0 µl	10mM
DMSO (Dimethylsulphoxide)	24.0 µl	50%

Samples were mixed, incubated at 50°C for 1 hr, placed on ice then 7.5 µl loading buffer added, which was mixed by pipetting. Gel was run at 120 V for 45 min to allow RNA to run in to gel, then voltage set at 100 V. The running buffer (10 mM Sodium Phosphate, pH6.5) was continuously re-circulated using magnetic stirrers and a peristaltic pump, to prevent the pH of the buffer changing. Gel was run for ~4 hr at 100 V, or until blue bromophenol blue dye had run $^2/_3$-$^3/_4$ down gel. The markers were then cut off using a sterile scalpel blade and soaked in 0.1 M ammonium acetate for 30 min, then subsequently stained in ethidium bromide for 45 min and viewed on UV transilluminator alongside a ruler, to allow marker band measurement.

3.14.3 Blotting Procedure

The gel electrophoresis tank was briefly washed with double-distilled DEPC-treated autoclaved water and tank half-filled with 20X SSC transfer buffer. 2 x 3MM blot paper wicks were wetted with 20X SSC, placed on top of gel in gel former allowing wick ends to dip into 20X SSC. The gel was placed on top of the wicks (see Figure 3.14.3-1).

Figure. 3.14.3-1 Northern blotting apparatus and set-up.

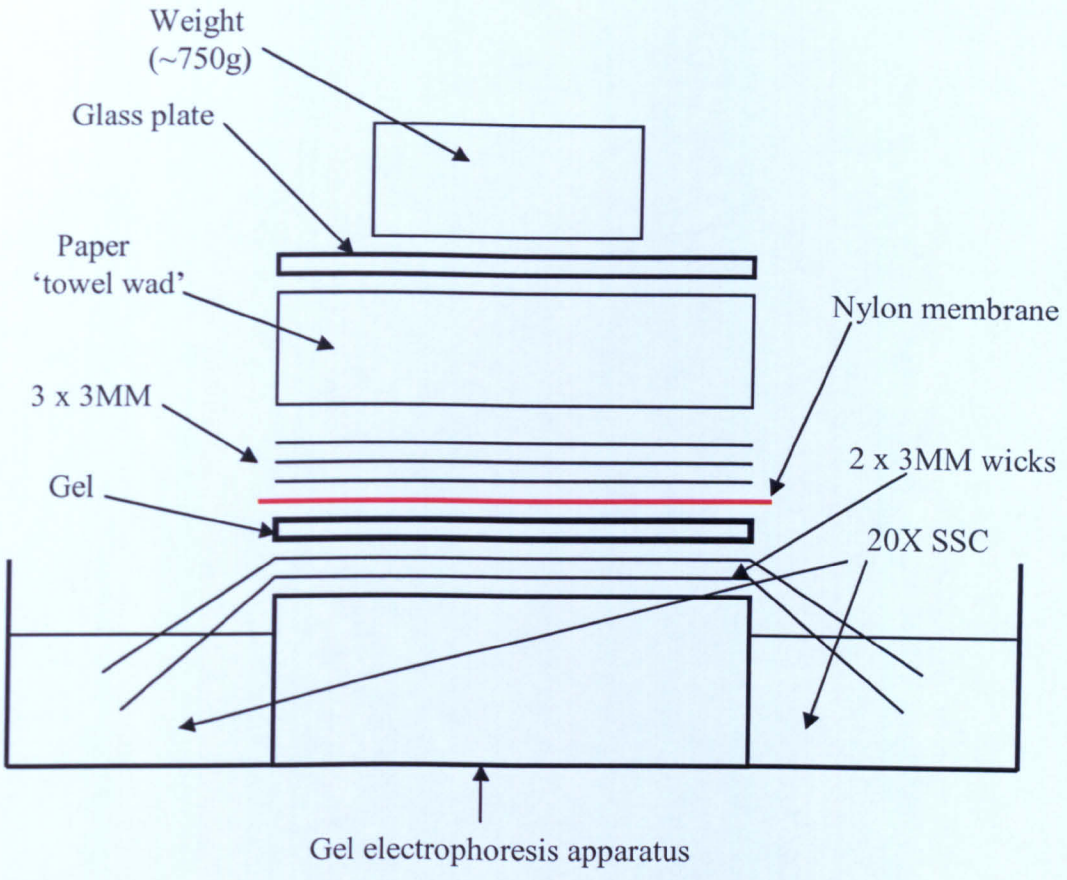

Hybond-N (Amersham Pharmacia Biotech, Buckinghamshire, UK) was placed on top of gel and air bubbles rolled out. 3 x 3MM blot paper was wetted with 20X SSC and placed on top of gel, followed by a paper towel wad, then a ~750 g weight placed on top.

After blotting overnight Hybond N membrane blot was removed, dried between two pieces of 3MM blotting paper and RNA UV crosslinked (UV Stratalinker 1800, Stratagene, California, USA) to the membrane. After crosslinking, 200 ml boiling hot 20mM Tris-HCl pH 8.0 was poured over membrane to remove Glyoxal. Blot was washed with 2 x SSC and stored at 4°C in fresh 2 x SSC.

3.15 RADIOLABELLED PROBE HYBRIDISATION

3.15.1.1 Strip-EZ™ DNA Probe synthesis and Removal Kit

The Strip-EZ™ DNA *Random Primed StripAble™ DNA Probe Synthesis and Removal Kit* (Ambion, Huntingdon, UK), was the kit of choice for radioactively probing trial northern blots. The kit generates a high specific activity probe that is stable during hybridisation and washsteps, but could be cleaved during incubation of blot with Probe Degradation Buffer at 68°C. These 'Milder' probe-removal ('stripping') conditions equated to less blot damage and greater preservation of blot integrity.

3.15.1.2 Protocol

25 ng of linearised DNA template made up to a volume of 9 µl with nuclease-free water, was denatured by heating at 95-100°C for 3-5 min. The probe was then snap-frozen in liquid nitrogen, thawed, microfuged and stored on ice. The following reaction mix was assembled in order, on ice, and mixed by gently pipetting:

Component	Amount/volume
Denatured DNA	9.0 µl
10X Decamer Solution*	2.5 µl
5X Buffer –dATP/–dCTP*	5.0 µl
10X dCTP*	2.5 µl
[α-^{32}P]dATP (3000 Ci/mmol, 10 mCi/ml)	5.0 µl
Exonuclease-free Klenow*	1.0 µl
Nuclease-free Water	made up to 25 µl

*Reagents supplied with kit.

The Probe Reaction mix was subsequently incubated at 37°C for 10-30min, to allow for radiolabelled nucleotide incorporation, the reaction terminated by addition of 1 µl of 0.5M EDTA (supplied with kit).

Radiolabelled cDNA probe was purified using a NICK™ Column (Amersham Pharmacia Biotech, Buckinghamshire, UK), which are prepacked disposable G-50 Sephadex columns. Procedure was as described by manufacturer. The probe was eluted in 600 µl equilibration buffer, whilst a further 400 µl equilibration buffer was added to column, to collect un-incorporated nucleotides. An approximate level of incorporation could be used by comparing the ratio of incorporated vs unincorporated nucleotides using a handheld Geiger counter. Only probes which had incorporated greater than 50% of the isotope into the generated cDNAs were used.

Purified diluted probe was heated to 90°C for 10 min, to denature strands, then diluted in pre-warmed hybridisation buffer and placed into a hybridisation bottle containing a prehybridised northern blot.

3.15.2 Rediprime

The Rediprime II probe-labelling kit (Amersham Pharmacia Biotech, Buckinghamshire, UK) was originally used in preliminary probe hybridisation experiments, in combination with Rapid-hyb buffer. Standard blotting procedures were followed and Rediprime protocol followed as described by manufacturer. A 54 µl reaction was prepared in a sterile 1.5 ml microcentrifuge tube, containing: 10-20 ng cDNA probe, 5.4 µl 10X TE (100 mM Tris-HCl, pH 8, and 10mM EDTA) pH 8 and made up to 54 µl with nuclease-free water. 45 µl of 54 µl mix was denatured by boiling at 100°C for 5 min, snap cooled by placing tube on ice for 5 min and centrifuged down briefly. 45 µl denatured DNA was added to a single Rediprime reaction tube, 5 µl [α-^{32}P] dCTP (3000 Ci/mmol, 10 mCi/ml) was added and tube mixed carefully by pipetting. Reaction was incubated at 37°C for 10 min then purified using NICK™ column method to remove un-incorporated nucleotides.

Purified diluted probe was heated at 100°C for 5 min to denature strands and treated the same as described above.

3.15.3 Probe Hybridisation

3.15.3.1 Rapid-hyb Hybridisation Buffer

Rapid-hyb buffer (Amersham Pharmacia Biotech, Buckinghamshire, UK) was the buffer of choice for all test and trial northern blots, due to its rapid rate of probe hybridisation to northern blots, and hence dramatically decreasing detection time. Most probe hybridisation's required 1-2 hr.

For prehybridisation and hybridisation 0.125 ml/cm^2 was used. Northern blots placed in rotating hybridisation bottles were prehybridised in the buffer at 65°C for 30 min. Labelled probe was diluted into pre-warmed hybridisation buffer, pre-hybridisation buffer poured away and hybridisation buffer plus probe added. Care had to be taken to not directly add buffer to blot, otherwise localised background developed. Hybridisation bottles were continuously rotated, and incubated at 65°C for 1-2 hr. The hybridisation temperature and time was varied to optimise signals depending on individual probe specificity's and expression level of mRNA species. However, lower temperatures produced less specificity, with greater probability of non-specific/multiple band detection. Full optimisation conditions for individual probes used in specific trial analysis can be found in relevant sections in Section 6.

Washsteps were undertaken (see Washstep section), and standard detection methods used (Detection section).

3.15.3.2 ULTRAhyb^{TM} Hybridisation Buffer

ULTRAhyb^{TM} Ultrasensitive Hybridisation Buffer (Ambion, Huntingdon, UK), is reported to drastically increase hybridisation signal, without increasing background, by maximising sensitivity of blot hybridisation. Therefore it is ideal for genes with low expression. Although the product is effective and can be used for short 2 hr procedures, maximum signals are produced using overnight hybridisation's (14-24 hr). ULTRAhyb^{TM} was therefore tested on low signal producing probes/low expressed mRNA species, including ARC, Caspase-3 and Calpain-10. The procedure was followed as described by manufacturer.

3.15.4 Wash Step Procedure

Wash steps were critical for removing excess radiolabelled probe and non-specific hybridisation signals thereby decreasing background signals.

Hybridisation buffer was discarded and the blot washed for 3 x 5 min in 2X SSC, 0.1% SDS (w/v) at room temperature, then for 2 x 10-15 min in 0.1X SSC, 0.1% SDS (w/v) at 60-65°C. Washstep conditions were optimised for individual probes, such that low intensity band signals/low expressed mRNA were washed at a lower temperature (60°C), for 2 x 10 min max. Higher expressed mRNA species producing very high band intensity signals, were washed at 65°C for full 2 x 15 min providing a higher stringency wash. Wash-step conditions optimised for individual probes during trial analysis can be found in relevant sections within Section 6.

3.15.5 Stripping Procedure of Probed Membranes

3.15.5.1 Strip-EZ^{TM}: After probe detection (subsequent section) blots were stripped of hybridised probe using the following freshly prepared Probe Degradation and Probe Reconstitution solutions:

Probe Degradation Solution Component	**Volume**	**Final Conc.**
200X Probe Degradation Buffer	50 µl	1X
100X Degradation Dilution Buffer	100 µl	1X
Nuclease-free water	10 ml	

Probe Reconstitution Solution Component	**Volume**	**Final Conc.**
100X Probe Reconstitution Buffer	100 µl	1X
20% SDS	50 µl	0.1%
Nuclease-free water	10 ml	

N.b. All reagents, apart from nuclease-free water were part of Strip-EZ^{TM} kit.

The 10 ml volume of both buffers was sufficient for treating a 100 cm^2 membrane. The blot was incubated with Probe Degradation Buffer at room temperature for 2 min in a hybridisation bottle. Blot was transferred to a 68°C hybridisation oven, incubated for 10-30 min to degrade the labelled probes and then Probe Degradation Buffer discarded, Blot Reconstitution buffer was then added and incubated in oven for 10-30 min at 68°C. 30 min incubations were required for both steps to adequately strip very intense signals (for example, actin probes). An additional 10 min wash in 0.1% (w/v) SDS at 68°C was used to remove residual signal, using 10 ml / 100 cm^2 blot. Membrane was checked before further use by monitoring blot using a Geiger-counter to ensure proper stripping. If probes were not adequately stripped, (Geiger counts of more than 5 cpm), stripping process was re-done and/or radioactive blot left to decay for an appropriate period.

3.15.5.2 Rediprime: After probe detection, blots were stripped using harsher conditions. The membrane was placed into a bag, ~200-250 ml boiling 0.1% (w/v) SDS poured into bag, the bag sealed and left to cool to room temperature. Procedure was repeated to ensure adequate membrane stripping and blot checked using Geiger-counter, or by exposing to an autoradiograph.

3.16 DETECTION METHOD OF RADIOISOTOPES

Probe-hybridised membranes wrapped in Clingfilm and kept wet (to prevent permanent probe-fixing), were placed in a phosphoscreen (Kodak, Rochester, NY, US) developing cassette. Membranes were left for at least 24 hr before scanning the phosphoscreen in a phosphoimager (BioRad, California, US). Scans were captured, visualised and then analysed using the Quantity One program (BioRad California, US). Detected bands were sized using stained RNA markers.

3.17 BAND INTENSITY ANALYSIS

Using the Quantity One program (BioRad) band signals of interest were quantified using the pixel analysis function of the program. The Quantity One software allows the analysis of band intensity whilst adjusting for background, using pixel volume values (see Figure 2.17-1).

Figure 3.17-1. An example of pixel analysis of detectable bands.

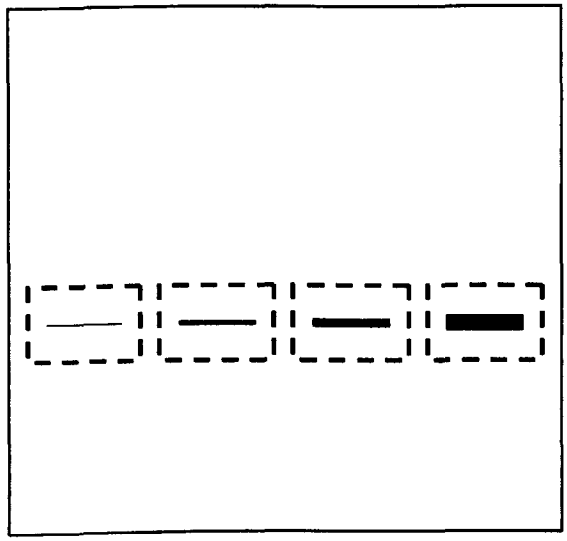

An example of a Northern blot hybridised with radiolabelled probe, scanned, bands detected, picture captured and analysed using Quantity One pixel analysis. Equal sized rectangular boxes were drawn around bands and pixel volume measured within boxes relative to local background signals. As can be seen there is an increasing band signal intensity level across samples, possibly suggesting an increase in expression, only proven once an internal standard is analysed.

3.18 DATA AND STATISTICAL ANALYSIS

For trial sample analysis, adjusted volume measurements were inputted into Microsoft Excel and treatment group mean values, SD (Standard Deviation) and SEM (Standard Error of the Mean) calculated. Individual values for an expressed gene of interest were normalised to an internal standard (e.g. Actin), i.e. adjusted value divided through by internal standard adjusted value. Again, treatment group mean, SD and SEM values were calculated. Bar graphs of mean values + SEM for groups was presented (as seen in Results section).

Statistical analysis of normalised values depended on the type of trial that was undertaken and number of groups to be analysed. For two treatment groups and one individual time point a student t-test analysis was performed. An F-test analysis of data

was performed to assess whether there was significant variance of values within treatment groups. A significance level of < 0.05 was used (*). Greater significance was at < 0.01 (**) and highly significant < 0.001 (***) value.

Where three treatment groups and one time point was used, One-Way ANOVA (Microsoft Excel) analysis of data was applied, using same significance levels as above. Those experiments that required greater evaluation of data between treatment groups were inputted into the SPSS statistical package. A One-Way ANOVA and Bonferroni post-hoc test to examine pair wise significance was applied and interactions between all groups analysed. Trials involving greater than 2 interactions, for example treatment and time, were analysed by Two-Way ANOVA analysis of data using GENSTAT computer program. GENSTAT allowed analysis of all time point and treatment interactions, and incorporated SED (Standard Error of the Difference) values. A comparison of means was performed between individual group pairs within the whole trial groups. This was performed using least significant difference (LSD) values. Care had to be used when using these values as it is only an indication of a potential difference as is any post-hoc test. The LSD value uses the SED value plus a factor for the significance using t values.

LSD = SED x the t value for the level of significance.

The t value was obtained using a students t distribution table (Altman, 1991). The t value depends on the level of significance followed and the degrees of freedom. A 5% level of significance was followed for all LSD value calculations. If the value for LSD is less than the difference between the two means being examined then the values are potentially significantly different.

CHAPTER 4 THE EFFECT OF LEVEL OF NUTRITIONAL INTAKE ON THE CALPAIN SYSTEM

4.1 BOVINE PLANE OF NUTRITION TRIAL

4.1.1 Trial Outline

Gene expression studies, investigating the effects of altered planes of nutritional intake in cattle on components of the calpain system, was undertaken using recently acquired (at that time) Quantitative Real-Time RT-PCR technology. The aim of the investigation was to determine whether restricted nutritional intake and realimentation (refeeding) would affect calpain system component gene expression in skeletal muscle. A secondary component of the study was to determine whether the Real-Time RT-PCR system was a sensitive, reproducible technique for the analysis of calpain system transcript expression; with a view to use this technique to examine the expression of multiple components of the proteolytic systems discussed previously within the literature review.

Dramatic alterations in the level of nutritional intake (i.e. metabolisable energy, macro- and micro-nutrients), so called 'plane of nutrition', in young rapidly-growing farm animals (including cattle), is likely to profoundly influence whole animal and tissue growth rates, and skeletal muscle protein accretion (Kristensen *et al*, 2002, Kristensen *et al*, 2004). It is yet to be established the precise effects feeding and alterations in level of nutritional intake has on skeletal muscle proteolytic system expression, activation and regulation; and, in turn how this is related to muscle protein turnover. Components of the calpain system, as discussed within the review of the literature (Section 2.8.3), are thought to play a role in skeletal muscle growth (Goll *et al*, 1998, Goll *et al*, 2003). There is however a lack of studies investigating the effects of nutritional intake and the regulation of calpain-calpastatin system. Mc Donagh *et al*, 1999 observed a decrease in calpastatin activity in *M. biceps femoris* in lambs after a feed restriction, with no effects on μ- and *m*- calpains. Whereas Kristensen *et al*, 2002 found a positive correlation between growth rates and *m*-calpain activities, with no change in calpastatin, with different feeding level treatments (high, restricted-low and refed-after a restriction), in pigs.

Our hypothesis was that as components of the calpain system are involved in muscle growth and remodelling, dramatic alterations in nutritional intake in growing calves would affect the expression of components of the calpain system. This was supported by the fact that calpastatin and muscle-specific calpain-3 have been implicated in a number of conditions known to affect muscle protein turnover (Goll *et al*, 1998, Baghdiguian *et al*, 2001, Navegantes *et al*, 2002, Tidball and Spencer, 2002).

4.1.2 Trial Details

Bovine Plane of Nutrition trial was carried out by Dr G. Lee and Professor Buttery (Dr G. Lee, Doctorate Thesis: *Nutrient control of the growth hormone and insulin-like growth factor axis in cattle*). Many thanks to them for use of *Longissmus Dorsi* (LD) samples from this trial.

Twenty four weaned Friesian castrated calves at 61 days old (± 9 days) were obtained and initially group housed on straw for the first five days. They were fed 0.5 kg of calf post weaner concentrate (WQC Quality Calves) per animal twice a day, *ad libitum* hay and free access to water. All calves were weighed and randomly allocated to one of three dietary treatment groups (three groups of eight). Calves were individually housed on wood shavings, with free access to a water drinker in each pen. Pens were arranged such that there were six pairs on either side of the barn, with four treatment-animals each side. Each pen-pair had the same treatment group to reduce animal disturbance (i.e. two pen-pairs/side of four animals of same treatment). There then followed a three week acclimitisation period, where calves were introduced to a high plane of nutrition to encourage rapid growth. The animals were fed at 2.5 x the recommended ME for maintenance (based upon ME (joules per day) intake of 5.67 + 0.061 liveweight (kg)/ 0.72 (Ministry of Agriculture, Food and Fisheries (MAFF)/Agricultural Development and Advisory Service (ADAS), 1984)), consisting of 30 g of BOCM Pauls Beef Super Grade diet (see Appendix G) per kg of live weight (70% intake), and 30% hay, which satisfied their nutritional demand.

Day 1 of the trial was was the first day after the three week acclimitisation period. All calves were continued to be fed on the same diet (as above) for a further 16 days. On day 17, the 'LOW' and 'REFED' dietary treatment groups were restricted to 90%

of the recommended ME for maintenance without any adaptation period. The diet constituents remained at 70% intake from concentrates and 30% from hay. The 'HIGH' dietary treatment group remained on 30g of concentrate/ kg live weight, and 30% hay for the remainder of the trial, meeting all dietary needs.

On day 47, the HIGH group continued to receive the same diet, as did the LOW group. The REFED group however, was immediately fed to the same level and diet as the HIGH group. On day 49, four animals from each group were slaughtered. Two weeks later on day 62, the remainder of the animals were slaughtered 15 days post re-feeding. A time-line diagram of the feeding regime is shown in Figure 4.1.2-1.

Samples of *Longissmus Dorsi* (LD) muscle were removed from the carcass immediately after slaughter, weighed briefly and snap frozen in liquid nitrogen for subsequent storage at – 70°C.

Figure 4.1.2-1 Schematic outline of bovine plane of nutrition trial. *The HIGH plane of nutrition group (——) remained at a high level of dietary intake for the entire length of the trial. The LOW plane group (——) began at a high level of dietary intake, then reduced drastically on day 17 for the remainder of the trial. The REFED group (——) began at high level of intake, was reduced on day 17 and then realimented back to a high level of dietary intake on day 47; remaining at that level to slaughter. There were eight animals per group (n=8), with four animals per group slaughtered on day 49 (S1) (n=12), and again at day 62 (S2) (n=12).*

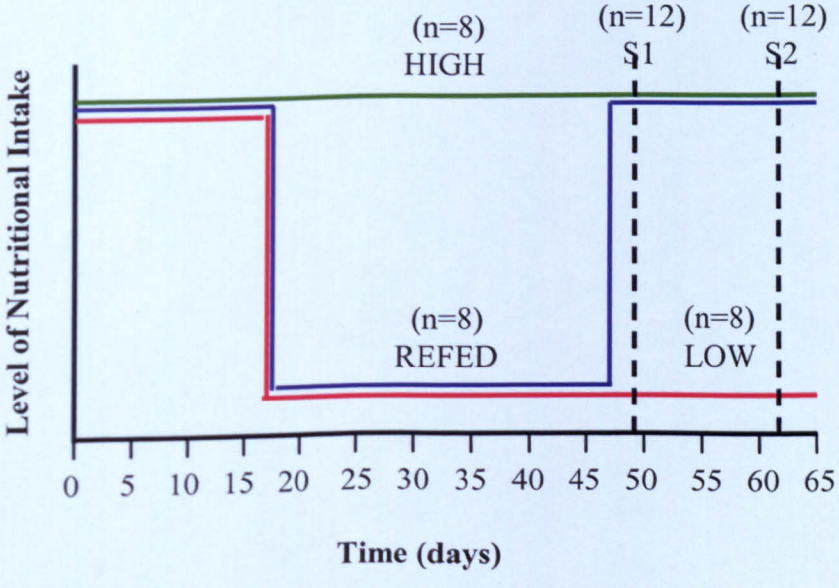

4.2 TOTAL RNA EXTRACTION AND ANALYSIS

From *Longissmus Dorsi* (LD) samples total RNA was extracted procedures as described in Section 3.3. Sample numbers and their respective treatment groups can be found within Appendix H. Extracted total RNA was checked for integrity and quality by standard spectrophotometer analysis and gel electrophoresis techniques (described within Sections 3.3.2 and 3.6, respectively). Total RNA for all twenty three samples showed little signs of qualitative degradation indicated by the lack of ribosomal/low molecular weight smearing and lack of DNA contamination indicated by lack of smeared large molecular weight band near wells (see Figure 4.2-1.)

Figure 4.2-1. The effect of plane of nutrition on bovine LD total RNA quality and integrity. *Non-denaturing gel electrophoresis of LD total RNA (1μg loaded/ sample) on a 1% agarose gel. H = HIGH, L = LOW and R = REFED. 1kb markers (M) were loaded with main fragments noted (bp). Ribosomal RNA (rRNA) is indicated.*

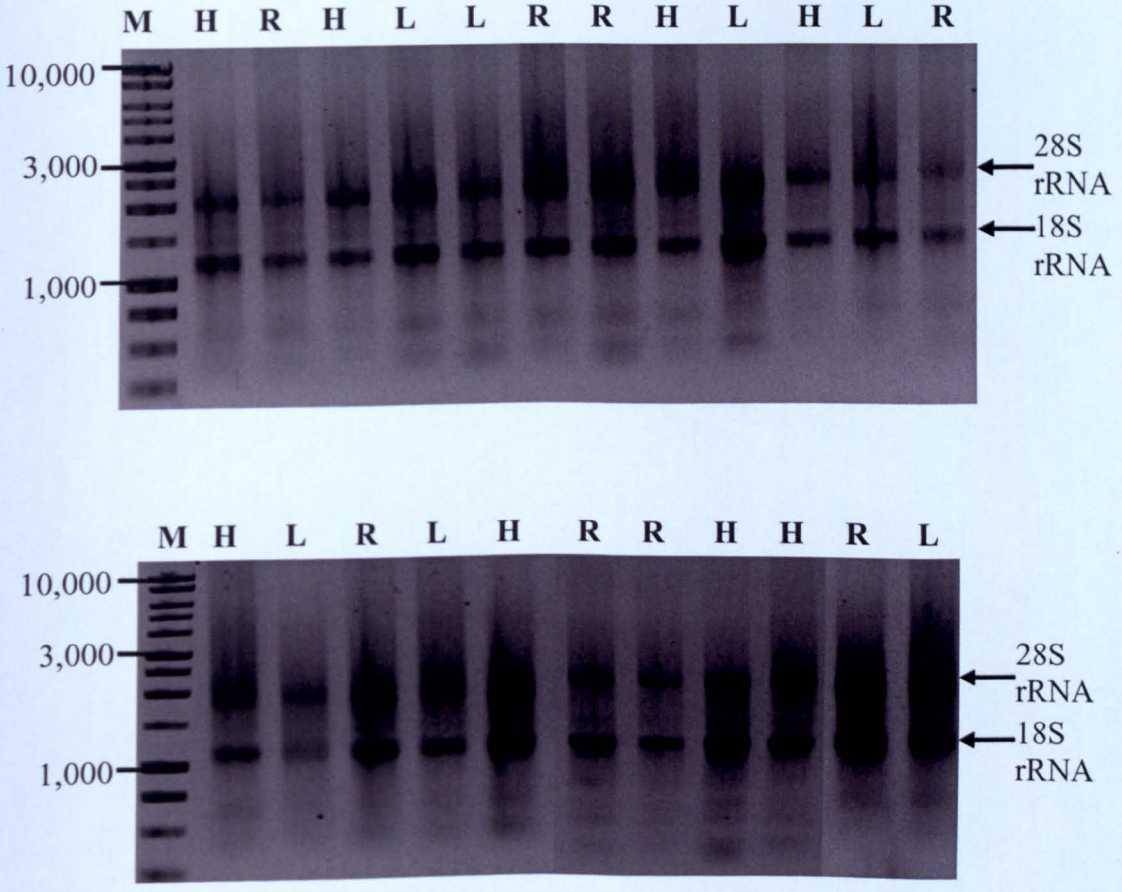

Extractable total RNA yields were determined. A Two-Way ANOVA analysis of data across slaughter date time points was made to assess if treatment or slaughter date had an effect on total RNA yield (Table 4.2-1). There was no significant effect of treatment on yield of total RNA (Table 4.2-1). However, it is noticeable that there was a larger numerical yield value for the REFED group that nears towards significance at both slaughters dates. There was a signifcant effect of slaughter date on yields, the yield of total RNA was greater across all groups for the second slaughter date ($P < 0.05$). Note that samples were randomly extracted suggesting a true effect.

Table 4.2-1. The effect of plane of nutrition on extractable total RNA from LD.
Two-way ANOVA analysis of extractable RNA yields (μg RNA/g tissue). Slaughter date (SL.), number of animals (n=) and group mean yield ± SEM (Standard Error of Mean) for each value is indicated. Significant effect of treatment, time and treatment x time interaction is indicated, using SED (standard error of the difference) and P significance values.

SL.	Treatment Groups			Treatment		Time		Treatment X Time	
	HIGH	LOW	REFED						
	Total RNA (μg / g tissue)			SED	P	SED	P	SED	P
1st	(n=4)	(n=4)	(n=4)						
	151.8	129.8	283.5						
	±19.3	±48.7	±37.7	92.3	0.144	75.4	< 0.05	130.5	0.913
2nd	(n=4)	(n=3)	(n=4)						
	296.0	330.7	504.0						
	±68.0	±127.2	±173.6						

4.3 QUANTITATIVE REAL-TIME RT-PCR ANALYSIS OF GENE TRANSCRIPTS

4.3.1 Experimental Procedure

A total first strand cDNA pool was synthesised for all total RNA samples using Reverse Transcriptase (RT-step) and random hexamer primers (see Section 3.4.3.1). Real-time PCR analysis was subsequently performed on all bovine first strand cDNA pool samples (see Section 3.4.3.2). It must be appreciated that this was the first time Real-Time PCR analysis had been undertaken within the Division of Nutritional Sciences. Part of the work in this thesis was establishing methodologies for analysis by Quantitative Real-Time PCR. Several components of the calpain system and internal standards, actin and rRNA 18S were analysed. Actin and rRNA 18S were chosen as internal standards as they had been used successfully as internal controls for a number of years by many research groups. It was believed that the mRNA levels of these two expressed genes would not significantly change because of treatment. Primers and probes were designed for sequences of interest using procedure described within materials and methods (Section 3.4.2.3). Primers and probes for the ubiquitously expressed μ- and *m*- calpains, muscle-specific calpain-3 and specific endogenous inhibitor calpastatin were specifically designed using available bovine sequence data. Bovine sequence accession numbers as follows: μ-calpain: AF 221129, *m*-calpain: U07850, calpain-3: AF 087569, calpastatin: L 14450. Oligonucleotide sequences and region of amplification within the various mRNA sequences is summarised within Appendix C. At the time, database sequence for bovine actin was not available, therefore primers for actin were selected from regions of high similarity across species, using a multiple alignment of alpha and beta isoform cDNA sequences. This was possible as alpha and beta isoforms sequences are highly similar (an example of an actin sequence alignment across species and isoforms can be viewed in Appendix A). Human alpha-actin was used as sequence to design primers as it was highly similar to other isoforms / species, in area to be amplified (using BLAST search of amplicon, human alpha-actin had 96% sequence identity to porcine alpha actin gene, 94% to porcine beta-actin mRNA and 95% to rabbit alpha-actin mRNA). 18S was designed using human sequence which was highly similar to rat species (using BLAST search of amplicon, human 18S had 100% sequence identity to porcine 18S

gene and bovine mitochondrial RNA and 99% to rat sequence), thus suggesting the sequence is highly conserved across species. Real-Time PCR reactions were performed for ubiquitously expressed μ- and *m*- calpains, calpastatin and actin using the SYBR-green procedure (see Section 3.4.3.2). For muscle-specific calpain-3 and 18S Taqman Quantitative PCR was done using primers and a dual labelled fluorescence probe. Reaction conditions are described within Section 3.4.3.2.

4.3.2 Results

Using the ABI 7700 Prism Quantitative Real-Time thermocycler (ABI Biosystems) the fluorescence data for the PCR amplification of the target cDNAs was collected. This data was analysed using the SDS software package (ABI Biosystems). Graphical representations of changes in fluorescence intensity (ΔRn) values at successive PCR cycles for every reaction in the 96-well plate throughout the time course of the incubation were produced (examples can be seen in Figure 4.3.2-1).

Preliminary evaluation of reaction efficiencies and specificities was performed before trial sample analysis using standard curve analysis (as recommended by ABI Biosystems) to determine linear and quantitative amplification of the target cDNA and post-PCR product gel electrophoresis analysis to determine the specificity of the PCR (as described within Section 3.4.4)

Standard curves were prepared for μ- and *m*- calpains, calpain-3, calpastatin, actin and 18S, using known serial dilutions of a pooled cDNA template. For every cycle of PCR it would be expected that there would be a doubling in the quantity of DNA present if the reaction was 100% efficient. Therefore, the relationship between the factorial change in the concentration of target amplicon DNA present (the dilution factor) from any one concentration to another, ΔD, and the difference between Ct values determined at each of these concentrations, ΔCt, is given by the equation:

$$\Delta D = 2^{-(\Delta Ct)}$$

as long as the Ct values are determined in the exponential amplification phase of the PCR. Therefore it would be expected that a dilution factor of 10 would result in a

corresponding increase in Ct value of 3.322. In addition Ct data obtained from a known serial dilution of template plotted on a graph of $\log_{10}$ [total RNA] (or total RNA equivalents) against Ct value would be expected to have a gradient of approximately –3.3. Such a relationship between template concentration and Ct value would indicate that the reaction was 100% efficient. The standard curve data and graphs plotted for all expressed genes of interest are presented in Appendix D.

Determination of *μ*- and *m*- calpain expression using the SYBR Green method produced standard curves with slopes of –0.1012 and –2.5887, respectively, suggesting it would take 0.1 and 2.6 cycles to amplify a target sequence so that there was a 10 fold increase in DNA copy number. These results suggested a higher than theoretical amplification efficency. This was likely due to non-specific template amplification during each PCR cycle using SYBR green instead of Taqman probe. *μ*-Calpain had a high level of contamination in the Non Template Control (NTC) reaction (NTC Ct value analysis), with NTC data curve very close to serial dilutions curves suggesting amplifcation of non-specific components. As the standard curve and amplification data did not fit the expected theoretical data, *μ*- and *m*- calpains mRNA expression in bovine trial samples could not be analysed. Analysis of calpastatin template amplification using SYBR Green produced a standard curve slope of –3.1455 (see Appendix D), a level closer to the theoretical –3.3 value. This gave a theoretical reaction efficiency of 104%, a slope of 3.3 would be equivalent to a 100% efficiency, which was considered to be an acceptable level (opposed to 122% for *m*- calpain); suggesting a lower level of non-specific amplification and primer-dimer formation. Analysis of calpain-3 using a dual-labelled fluorescence (Taqman) probe produced a slope of –4.1955 (see Appendix D), suggesting a lowered amplification efficiency (85%). Likewise analysis of 18S, also using a dual labelled fluorescence (Taqman) probe, produced a slope of –3.4888 (see Appendix D). However, amplification of actin using SYBR Green produced a slope of –2.8118 (see Appendix D). An interesting point to note was that samples with good efficiencies of PCR amplification produced single specific bands after gel electrophoresis analysis of post-PCR products. In general, a greater amount of primer-dimer formation was detected (low molecular weight smeared bands on the gel) on those that used SYBR Green as opposed to dual labelled fluorescence (Taqman) probes. This may account for reduced/abnormal efficiencies.

As the standard curve gradient values for calpastatin, calpain-3 and 18S were accepted as being in a suitable range from the expected –3.3 slope value, therefore trial sample analysis could be performed. This was performed even though calpastatin did have a level of non-specific amplification and calpain-3 and 18S had lowered efficiencies. Importantly, 18S was a more suitable internal standard to actin as dual labelled fluorescence (Taqman) probe conferred greater reaction specificity and slope value was closest to to –3.3. Amplification of actin templates gave a high level of non-specific primer-dimer amplification. Calpain-3 had lowered reaction efficiency in each round of PCR. Importantly, the primers and dual labelled fluorescence (Taqman) probe did not exhibit non-specific amplification as determined from gel electrophoresis analysis of the products. In addition, the relationships between Ct and $\log_{10}$ [template] was linear. Therefore, calpain-3 probe was used in further trial analysis.

Trial sample Real-Time PCR reactions were performed and analysed for calpain-3, calpastatin and 18S. Template amplification data outputs can be viewed in Figure 4.3.2-1 (A)-(C).

Figure 4.3.2-1. Real-Time RT-PCR template amplification fluorescence data outputs for trial samples. *All bovine trial samples and NTC are shown for (A) Calpain-3, (B) Calpastatin and (C) 18S (internal standard). ΔRn, fluorescence intensity and cycle number are shown. Background threshold and amplification threshold levels are indicated.*

(A)

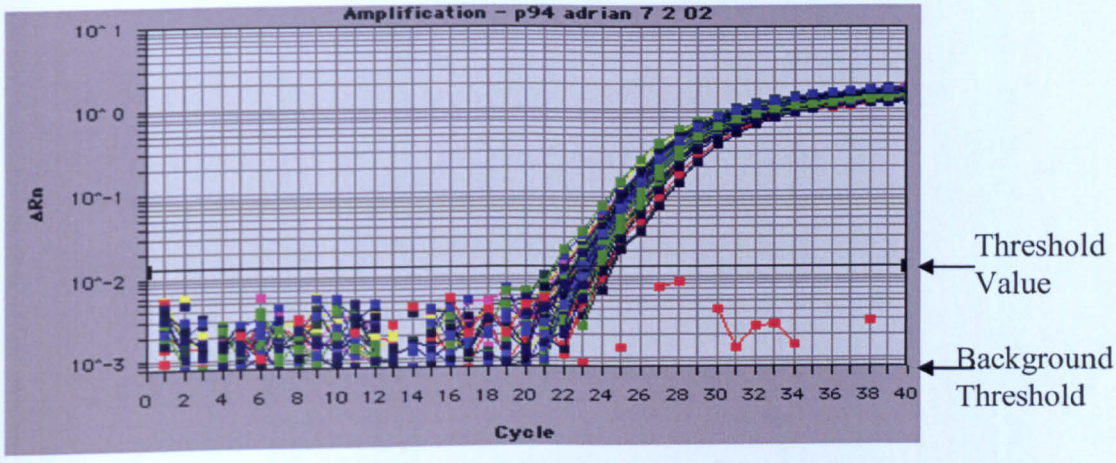

(B)

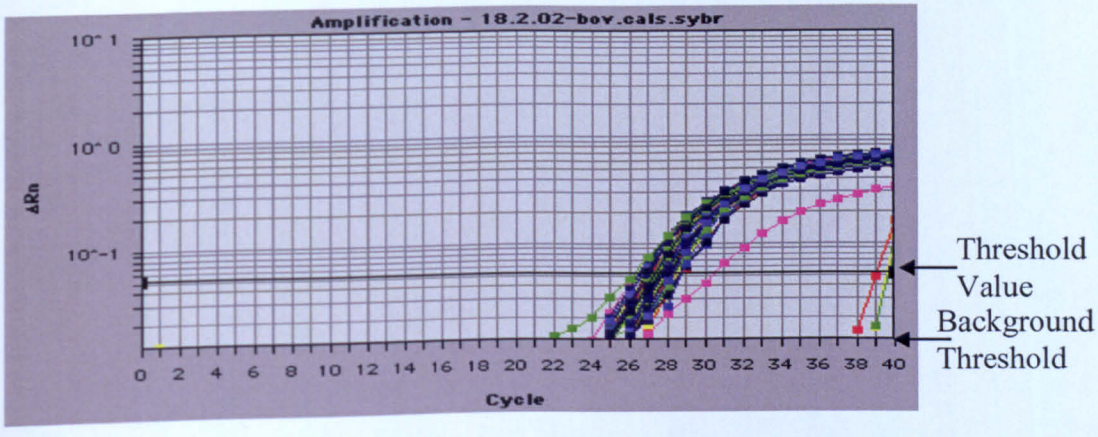

(C)

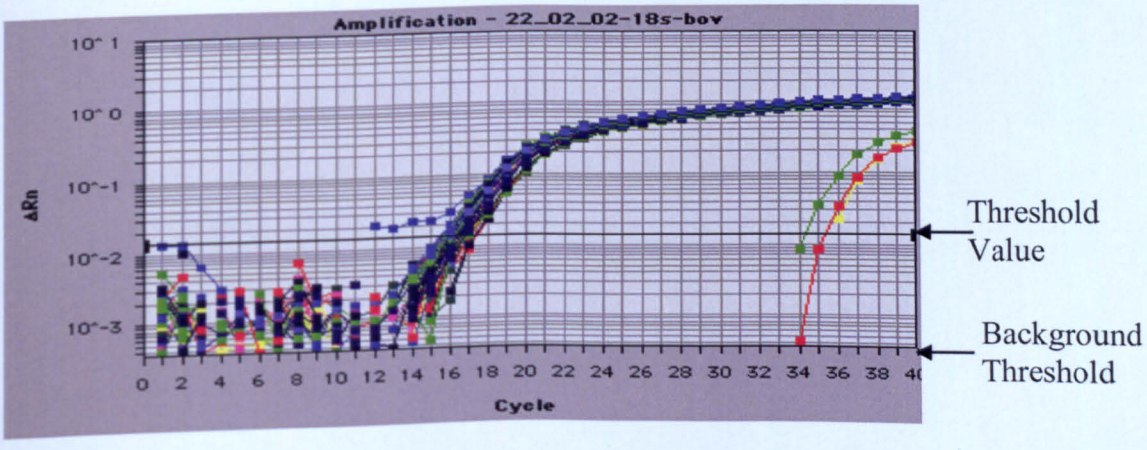

4.3.3 Fluorescence Data Analysis

Average Ct values of trial triplicate samples were taken at a quantification threshold where the amplification curves of all samples were linear, parallel to one another during the exponential amplification phase. The average Ct values were converted into relative amounts of total RNA, using standard curves (log total RNA vs Ct) and antilog of log RNA (see Section 3.44). Values for calpastatin and calpain-3 were normalised to 18S, giving a ratio of gene of interest relative to this internal standard. Mean treatment group values were calculated (Data presented in Tables 4.3.3-1, 4.3.3-2 and Figures 4.3.3-1, 4.3.3-2). A Two-Way ANOVA analysis was performed on all treatment groups comparing time and treatment interactions across all groups.

From Table 4.3.3-1 it can be seen that there was no significant effect overall of dietary treatment on calpain-3 mRNA expression. The LOW group values were numerically lower than the HIGH and REFED groups at the 1st slaughter date. The LSD value indicated that this was potentially significant at a 5% level. The REFED group expression values were also numerically higher than the LOW group at the 2nd slaughter date, but this was not significant.

There was also a definate trend towards significance for the expression of calpain-3 mRNA between the 1st and 2nd slaughter date groups (Time, $P = 0.073$). The values for both the LOW and REFED groups increased from the 1st to 2nd slaughter, whilst the HIGH group decreased slightly suggesting a differential effect of treatment and time. The LSD value indicated that this was potentially significant at a 5% level.

From Table 4.3.3-2 it can be seen that dietary treatment had no significant effect overall on calpastatin mRNA expression. However, in the 1st slaughter group calpastatin mRNA increased in the LOW group compared to the HIGH and REFED groups, numerically in the opposite direction to calpain-3. There was however a trend towards significance overall across slaughter date time points ($P = 0.085$), with all groups having increased calpastatin mRNA values from 1st to 2nd slaughter dates. There was a larger increase in the REFED group across slaughter dates than for other groups. The LSD value indicated that this was potentially significant at a 5% level.

Table 4.3.3-1. The effect of plane of nutrition on relative expression of calpain-3. *Two-way ANOVA analysis of quantified calpain-3 mRNA values normalised to 18S. Slaughter date (SL.), number of animals (n=) and group mean ± SEM (Standard Error of Mean) for each value is indicated. Significant effect of treatment, time and treatment x time is included using SED (standard error of the difference) and P significance values.*

SL.	Treatment Groups			Effect of:					
				Treatment		Time		Treatment X Time	
	HIGH	LOW	REFED	SED	*P*	SED	*P*	SED	*P*
1st	(n=4)	(n=4)	(n=4)						
	1.441	1.009	1.423						
	±0.078	±0.154	±0.139	0.173	0.127	0.141	0.073	0.244	0.312
2nd	(n=4)	(n=3)	(n=4)						
	1.399	1.474	1.807						
	±0.227	±0.199	±0.203						

Figure 4.3.3-1. The effect of plane of nutrition on relative expression of calpain-3 for 1st and 2nd slaughter dates. *Mean quantified values, normalised to 18S, + SEM are presented.*

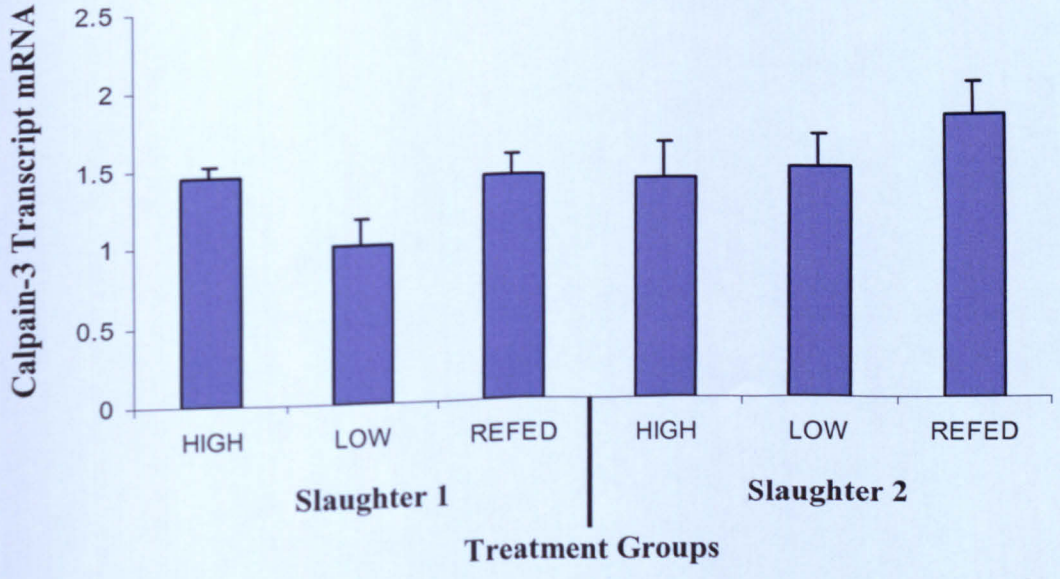

Table 4.3.3-2. The effect of plane of nutrition on relative expression of calpastatin. *Two-way ANOVA analysis of quantified calpastatin mRNA values normalised to 18S. Slaughter date (SL.), number of animals (n=) and group mean ± SEM (Standard Error of Mean) for each value are indicated. Significant effect of treatment, time and treatment x time is included using SED (standard error of the difference) and P significance values.*

SL.	Treatment Groups			Treatment		Time		Treatment X Time	
	HIGH	LOW	REFED	SED	*P*	SED	*P*	SED	*P*
1st	(n=4)	(n=4)	(n=4)						
	0.0363	0.0455	0.0343						
	±0.005	±0.007	±0.007	0.010	0.874	0.008	0.085	0.014	0.649
2nd	(n=4)	(n=3)	(n=4)						
	0.0503	0.0512	0.0584						
	±0.012	±0.020	±0.003						

Figure 4.3.3-2. The effect of plane of nutrition on relative expression of calpastatin for 1st and 2nd slaughters dates. *Mean quantified values, normalised to 18S, +SEM are presented.*

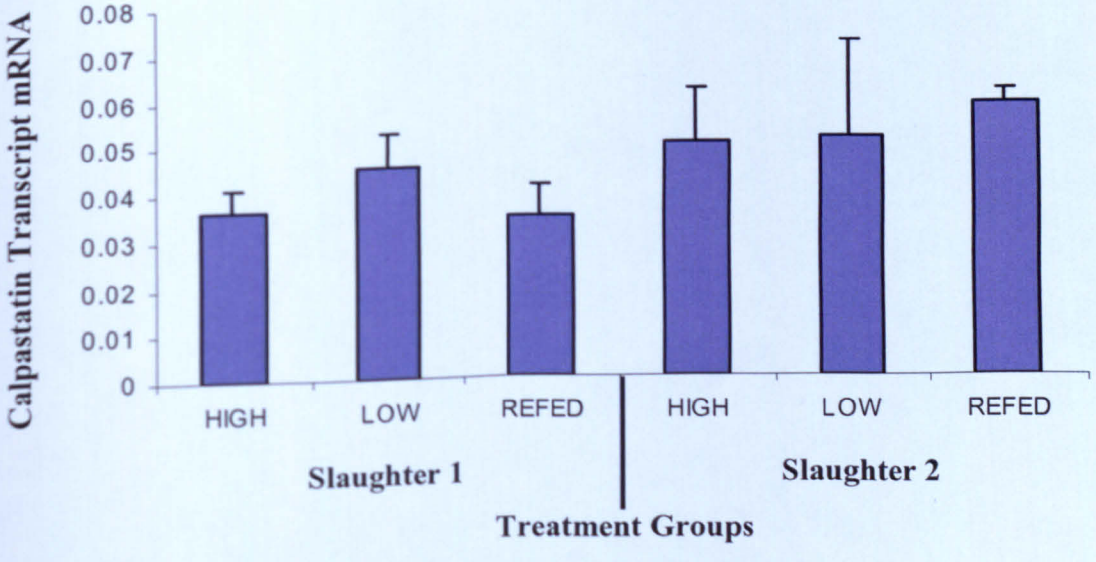

4.4 SUMMARY

A trial was performed in which 24 cattle were placed into different feeding treatment groups. These consisted of a LOW and HIGH plane of nutrition group, along with a REFED group that was realimented back to a HIGH plane from an initial LOW plane, 2 days prior to the 1st slaughter date. Half the animals from each group were slaughtered on the the 1st slaughter date, and the rest of the calves 2 weeks later.

Analysis of extractable total RNA yields from bovine LD showed that there was a significant effect of slaughter date on yields ($P < 0.05$), with second slaughter date groups having greater numerical values. There was no significant effect of treatment, although the REFED group had greater numerical values than the LOW and REFED groups at both time points.

Real-time analysis of the calpain-system and internal standards revealed that the technique can be problematic and requires extensive optimisation and testing. For example, when using SYBR-Green there is a much greater chance of non-specific amplification and primer-dimer formation, potentially invalidating experiments (as was seen for μ- and m- calpains and actin). Also, Taqman Probes may be a preferential technique to SYBR-Green offering a higher level of reaction specificity, confirmed by post-PCR product analysis by gel electrophoresis and standard curve analysis.

Standard curves were generated for all expressed genes of interest. Calpastatin (using SYBR-Green), muscle-specific calpain-3 (using Taqman Probe) and 18S (using Taqman Probe) were the only valid reactions that could be used in trial analysis. When analysing bovine trial samples, Ct values were taken at a suitable quantification threshold level, for each replicate. Values were averaged and quantified into ng equivalent amounts of total RNA using standard curves. There was no significant effect or trend of treatment on 18S values across groups, making 18S a valid internal standard. Quantified data for calpain-3 and calpastatin was normalised to 18S.

Analysis of normalised calpain-3 mRNA data suggested that although there was no overall significant effect of dietary treatment ($P = 0.127$), during the 1st slaughter

only, the LOW group had lower calpain-3 mRNA compared to both the HIGH and REFED (30% lower from HIGH and 29% lower from REFED) groups. The LSD value indicated that this was potentially significant at a 5% level. The REFED group expression values were also numerically higher than the LOW group at the 2nd slaughter date (23% higher), but not significant.

There was a trend towards significance for the effect of slaughter date on calpain-3 mRNA expression ($P = 0.073$). Both the LOW (46% increase) and REFED (27% increase) groups increased by the 2nd slaughter date. The LSD value indicated that this was potentially significant at a 5% level.

There was no observed significant effect of dietary treatment on calpastatin ($P = 0.874$), although in the 1st slaughter mRNA increased in the LOW group compared to the HIGH and REFED groups (25% increase relative to HIGH and 33% relative to REFED).

Calpastatin mRNA expression also increased across all treatment groups from the 1st to the 2nd slaughter with a trend towards significance ($P = 0.085$), with the REFED group having a larger numerical increase across slaughter time. The LSD value indicated that this was potentially significant at a 5% level.

CHAPTER 5 cDNA PROBE DEVELOPMENT

5.1.1 Outline

The hypothesis that proteolytic system components are co-ordinately regulated simultaneously in skeletal muscle, during various stimuli, required a means of investigation. Therefore, the aim was to generate cDNA probe sequences ~200-300 bp in length, by PCR suitable for experimentation on predominantly porcine, but also bovine and possibly human muscle tissues. These were to be used to determine changes in mRNA levels, using northern blot probing, or macroarray experimental procedures. These system components have been reported to be expressed in skeletal muscle, and, up/down-regulated during different physiological and pharmacological conditions, which are known to alter muscle atrophy/hypertrophy state, were focused on.

It became clear that there were many time, financial, and experimental constraints; therefore, the most appropriate strategy would be to aim to synthesise, four-to-five main components for each system, and three-to-four internal standards. The main limitation was the requirement for porcine specific cDNA sequences, when many proteolytic system components had no porcine sequence available in databases. The result, after many months, was the generation of twenty positively identified PCR products, many of which were cloned into a plasmid-vector. Four components each from the caspase, cathepsin and ubiquitin-proteasome systems; five from the calpain system, and three internal standards were selected based on the review of the literature. These included: Caspases- 3, 6 and 7- (all 'effector' caspases), and ARC (Apoptosis Repressor with CARD domain). Cathepsins B, D, L, and H; E2G1- an E2-ubiquitin conjugating enzyme, highly expressed in skeletal muscle, C8- a proteasome subunit, ubiquitin, and atrogin-1- an E3-ubiquitin Ligase, previously mentioned. μ- and m-calpains, calpain-3, calpastatin, and calpain-10. Internal standards- actin, alpha-Tubulin, and TFIID (Transcription Factor II D)/TATA box binding protein.

5.1.2 Scheme of Work

The developmental sequence of events in generation of the twenty cDNA probes are described as follows:

Related mRNA and cDNA sequences for components of interest, across multiple species, were searched for, using SRS (Sequence Retrieval System), and BLAST programs, found on the NCBI, DDBJ and HGMP homepages (as described in Section 3.4.2). Emphasis was placed on available porcine, bovine and human sequences. Retrieved sequences were aligned using the Clustal W sequence alignment program found within the above homepages (see Section 3.4.2). Areas of high sequence homology across species were searched for as a suitable PCR target and used to direct searches for PCR primer pairs. Specific PCR primers were then designed using personal preference based on primer and sequence analysis (including using programs such as Primer Express (ABI Biosystems).

PCR testing and optimisation procedures were then undertaken to synthesise DNA sequences of the correct size and sequence. Porcine skeletal muscle Poly-A^+ enriched RNA was used as a PCR template after an RT-step (see Section 3.4.3.1) to produce first strand cDNA. Basic PCR procedures were then used (see Section 3.5.1). The number of cycles used in all reactions was 35; as it was believed that many of the genes of interest are expressed at low levels.

All PCR reactions, including controls, e.g. NTC (Non Template Control), were tested by standard gel electrophoresis and staining techniques. Once positive results were obtained, i.e. detection of a single band of the correct size (see examples, Figure. D in Appendices A1-20), with no band present in NTC; positive PCR reactions were pooled together, separated by gel electrophoresis, and gel purified using standard technique. Once purified, samples were separated by gel electrophoresis and stained, to check the size and quality of the DNA recovered.

Many of the cDNA sequences (Appendices A 1-5, 7-10, and 12), were suitable to be cloned into a pGem-T Easy Vector (see Section 3.8-3.9). This was an important step as many of the sequences are novel, were problematic to synthesise by PCR, and meant, if cloned successfully, large quantities of DNA could be synthesised.

Problematic PCR targets, with an inability to produce a single band of the correct size, after gel electrophoresis and staining, underwent rigorous investigatory steps including (in this progressive sequence): varying a) annealing temperatures, b) template concentration, c) Taq polymerase type, d) DMSO addition (to denature any secondary structure formation) and e) change in primer location/size-composition.

Examples of problematic PCR reactions included Ubiquitin (Appendix A-11), which required a change in primer pair sequence, temperature gradient experiments and Expand Taq system (Roche Molecular Biochemicals, Mannheim, Germany) to achieve a PCR product of the correct size and sequence; it was also found impossible to clone after numerous attempts. Cathepsin B PCR product (Appendix A-5) was found after DNA sequencing to have a good sequence alignment, yet the cloned insert had a poor sequence alignment similarity to Cathepsin B.

Cathepsin D (Appendix A-6) and Calpain-10 (Appendix A-17) proved to be impossible PCR targets; at present there is no porcine or bovine sequence data available for these two in all relevant databases. Calpain-10 has proved difficult to clone in farm species (unpublished observations). Therefore, human EST (Expressed Sequence Tag) "IMAGE" clones, with 100% sequence alignment to retrieved human sequences- PCR target regions, were ordered from the IMAGE (Integrated Molecular Analysis of Genomes and their Expression) Consortium (see Appendix E). Standard bacterial-plasmid growth and purification procedures were used, yielding purified plasmid DNA (see Section 3.9, 3.10 and Appendix E). Plasmid DNA was linearised (as described in Appendix E, using protocol in Section 3.11) and used as a PCR template. Finally, original primers designed previously, were used to successfully synthesise a cDNA sequence of correct size and sequence. Note; calpain-10 still required a long series of optimisation steps (change of primer pairs, temperature-gradient PCR and taq enzyme variation), to yield a positive result.

The final step involved analysis of all twenty synthesised PCR products and cloned inserts, by DNA sequencing (see Section 3.13). Returned sequences were recorded as shown in relevant box (Figure E) in Appendices A1-20.

Sequence identification was validated by performing BLAST searches, using the relevant database homepages (e.g. NCBI) (see Section 3.4.2.2); all twenty cDNA sequences were positively confirmed to be closest matched to mRNA/cDNA sequence identities of interest. From the BLAST program sequence list output, the three sequences most similar, or those from species of interest (i.e. Porcine, bovine and human), have been recorded in in Appendices A1-20 (Figure F); if no species of interest sequence data is available, ovine, murine, rat and related species have been listed. A score (in bits), sequence identity (value and %), and E Value has been recorded for each sequence noted (an explanation of the Score and E value can be found in Appendix A); for purposes of easy-viewing and comparison, the sequence identity only, has been noted within two summary tables in this section. The sequence identity value relates to the exact number of nucleotide bases matched from the specific cDNA probe sequence, and the sequence it is aligned with. For example, Cathepsin-D, is a 204 bp long PCR product, of which 134 bp were successfully sequenced; exactly matching base-for-base with a 134 bp region of 2038 bp, M11233: human cathepsin-D. A 134/134 nucleotide identity value (100%), is therefore given.

5.2 PCR PRODUCT/cDNA PROBE SUMMARY

Figures 5.2-1 and 5.2-2 show agarose gel electrophoresis pictures of all twenty cDNA probes generated and purified. The first two pictures (Figure 5.2-1) show all PCR products, except Caspase-3 and Cathepsin-L as limited PCR products were left in stock and therefore omitted from gel picture. The gel picture in Figure 5.2-2 is of selected cloned cDNA plasmid inserts, excised and purified. These system components were problematic to PCR in sufficient quantities for experimentation. Therefore, large quantities of cDNA was generated for each cDNA probe by performing large culture experiments, midi-prep plasmid purification methods and scaled-up bulk RE digests (see Appendix F).

Table 5.2-1 summarises all 20 probes generated, including amplicon probe sizes and sequence identity scores for closest porcine, bovine and human sequences of interest (after previous BLAST searches).

Figure 5.2-1 Nondenaturing 1.8% agarose gel electrophoresis of purified PCR products. *PCR products at different concentrations, with 100 bp markers (M), either side of gel. Three main bands of 100 bp markers (in bp), are noted either side (see list bottom of page for corresponding probe no.s and names).*

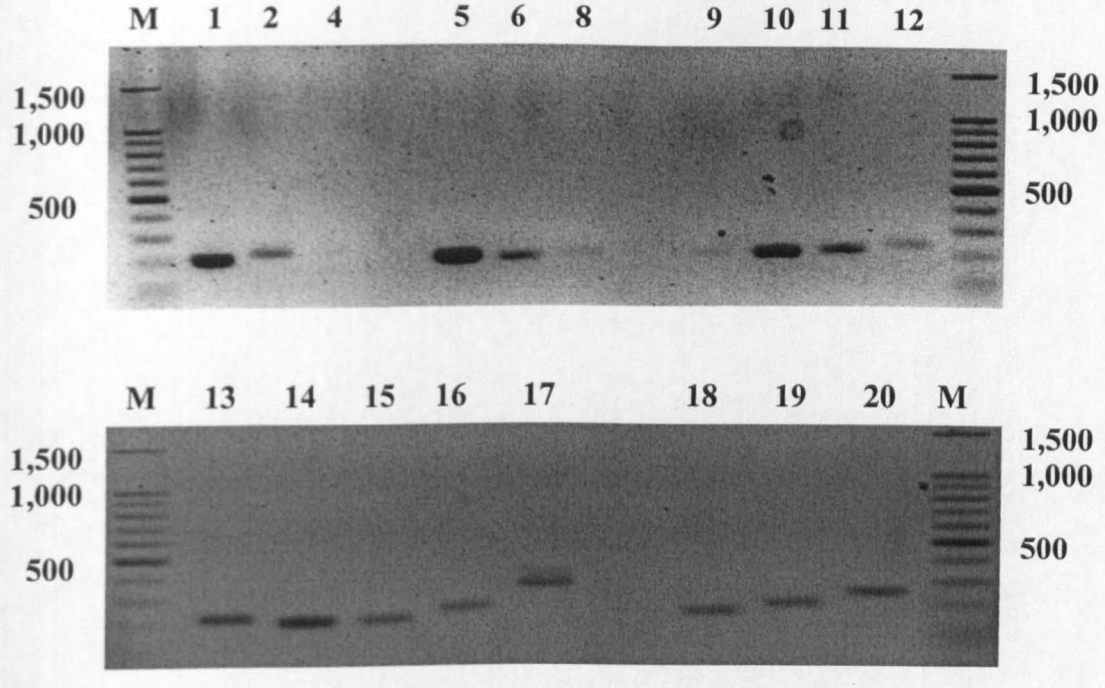

Figure 5.2-2. Nondenaturing 1.8% agarose gel electrophoresis of purified cDNA plasmid inserts. *Probes 3, 4, 7, 8, 12 and 9 are loaded, with 100 bp markers (M), either side of gel. Three main bands of 100 bp markers (in bp), are noted either side.*

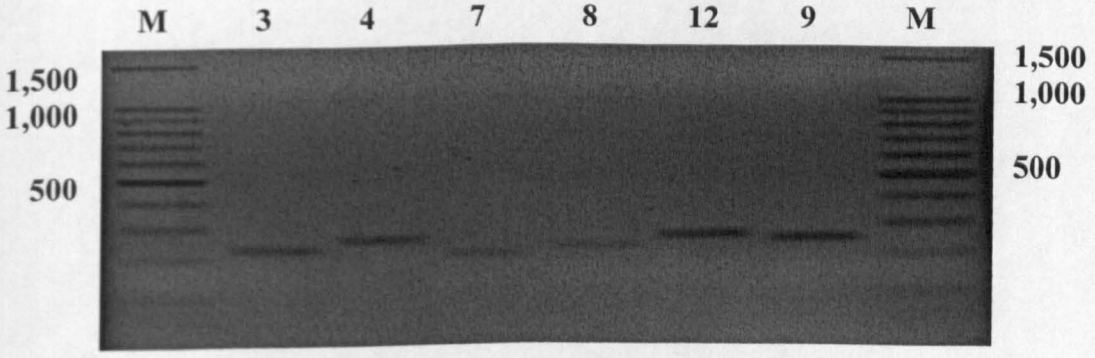

Key for Figure 5.2-1 and 5.2-2: 1: Caspase-7, 2: ARC, 3: Caspase-3, 4: Caspase-6, 5: Cathepsin-B, 6: Cathepsin-D, 7: Cathepsin-L, 8: Cathepsin-H, 9:E2G1, 10: C8, 11: Ubiquitin, 12: Atrogin-1, 13: μ- Calpain, 14: *m*-Calpain, 15: Calpain-3, 16: Calpastatin, 17: Calpain-10, 18: Actin, 19: Alpha-tubulin, 20: TFIID

Table 5.2-1. Summary of generated cDNA probes. *Table to summarise in order 1-20 (numbers correspond to those indicated in Figures 5.2-1 and 5.2-2), the number, name, and amplicon probe size in bp of individual cDNA probes, and their sequence identity scores (as %) for closest porcine, bovine and human species sequences. NSD = No Sequence Data available in nucleotide databases. The corresponding appendix section is noted for each probe.*

No	Probe Name	Size (bp)	Sequence identity (%) of probe to closest species of interest sequence.			Appendix
			Porcine	Human	Bovine	
1	**Caspase-7**	207	NSD	91%	NSD	A-1
2	**ARC**	240	NSD	84%	NSD	A-2
3	**Caspase-3**	209	99%	90%	89%	A-3
4	**Caspase-6**	242	NSD	91%	NSD	A-4
5	**Cathepsin-B**	206	NSD	91%	91%	A-5
6	*** Cathepsin-D**	204	NSD	100%	85%	A-6
7	**Cathepsin-L**	220	99%	89%	88%	A-7
8	**Cathepsin-H**	213	99%	90%	NSD	A-8
9	**E2G1**	213	NSD	93%	NSD	A-9
10	**C8**	217	NSD	94%	NSD	A-10
11	**Ubiquitin**	229	99%	91%	94%	A-11
12	**Atrogin-1**	247	NSD	93%	NSD	A-12
13	**μ-Calpain**	201	99%	88%	93%	A-13
14	***m*-Calpain**	201	99%	88%	88%	A-14
15	**Calpain-3**	201	100%	90%	94%	A-15
16	**Calpastatin**	236	100%	87%	86%	A-16
17	*** Calpain-10**	333	NSD	100%	NSD	A-17
18	**Actin**	201	100%	97%	95%	A-18
19	**Alpha-Tubulin**	218	NSD	96%	97%	A-19
20	**TFIID**	251	NSD	93%	NSD	A-20

*Cathepsin-D and Calpain-10 were sequences amplified from human IMAGE clones, hence have high identity to human species.

5.3 NORTHERN BLOT RADIOACTIVE PROBE TESTING

The next course of action was to determine if the cDNA probes could detect their complementary sequence by probing Northern blots of porcine skeletal muscle total and poly A^+-enriched RNA with radioactively labelled cDNA probes. A selection of probes were chosen and tested based on: probable level of expression in skeletal muscle, probable change in mRNA level with treatments, sequence alignment score with porcine, bovine and human tissue specific mRNA sequences and possible novel role in skeletal muscle (i.e. Calpain-10 and ARC). Probes tested included: ARC, Caspase-3, Cathepsin-L, E2G1, Ubiquitin, Atrogin-1, Calpain-3, Calpain-10 and Actin.

Probes were tested on Northern blots of porcine total RNA and Poly-A^+-enriched RNA. This RNA was separated on a denaturing agarose gel, and blotted onto hybond N, using technique described in Section 3.14.

Probe testing and evaluation was critical as many sequences like E2G1 and Atrogin-1, have no porcine sequence data available. PCR products were generated from porcine skeletal muscle, Poly-A^+-enriched RNA template (after RT step), but PCR primers were designed from human sequence data. BLAST searches after DNA sequencing confirmed 93% identities to human sequence for both system components. Therefore, it was assumed that porcine skeletal muscle expresses near identical sequences for E2G1 and Atrogin-1 with identical functions, although further studies would need to unequivocally confirm this.

A comparison of all available mRNA sequences held in databases (including those previously used in Clustal W multiple sequence alignments and BLAST searches (see Appendices 1-20) was made (see Table 5.3-1.), to estimate the probable size of the Northern blot probe signal band. This was complicated, as many of the proteolytic system components of interest had little, or no porcine sequence data (as described) and species available may not have had complete sequences, or they were alternatively spliced, giving a range of sizes for their appropriate mRNA species.

Many of the sequences in the database may have the potential to be alternatively spliced, or the sequence within the databse may have been for the open-reading frame (ORF) only or part of the ORF. A full mRNA with associated untranslated regions may be much longer.

An extended period of probe hybridisation testing and optimisation was undertaken (see Section 3.15) to attempt to produce detectable, specific quantifiable band signals for each probe as described within the Laboratory Methods. Radioactive probe-labelling protocols: [α- ^{32}P] dCTP Rediprime system, and [α- ^{32}P] dATP Strip-EZ system; and hybridisation buffers: Rapid-Hyb and Ultrahyb, were used for these procedures (Section 3.15.3.1 and 3.15.3.2, respectively). The Strip-EZ system combined with Rapid-Hyb buffer was preferred, and utilised for the remainder of all experiments; due to greater preservation of Northern blot membranes from damage, an ability to probe membranes a greater number of times, and speed of hybridisation. All data and pictures presented are Northern blots probed using this technique only, unless stated otherwise. Figure. 5.3-1 shows phosphoimages of all probes tested.

The cDNA probes produced specific detectable and quantifiable bands on porcine Northern blots (see Figure 5.3-1); however, some probes produced slight discrepancies in size and/or multiple band signals. Unknown band signals may be due to transcript variants, similar sequence cross hybridisation, or unknown porcine sequences/variations. Therefore, attempts at ascertaining band signal sequence identities were made; using previously described BLAST searches of nucleotide databases, for high scoring (bit score), similar related-sequences aligned to cDNA probes used in Northern probing. A full summary table of related mRNA sequences for Caspase-3, E2G1, Ubiquitin, Atrogin-1 and Calpain-3, is presented in Appendix B.

Figure 5.3-1. Phosphoimages of porcine skeletal muscle RNA Northern test blots. *Northern blots hybridised with [α- ^{32}P] dATP-labelled cDNA probes; using Strip E-Z probe-labelling kit and Rapid Hyb hybridisation buffer, unless stated otherwise (in brackets). Main representatives of each proteolytic system and internal standards have been presented. P A = Poly A RNA, T = Total RNA, and numbers indicate amount of RNA in weight (μg), loaded on Northern blot.*

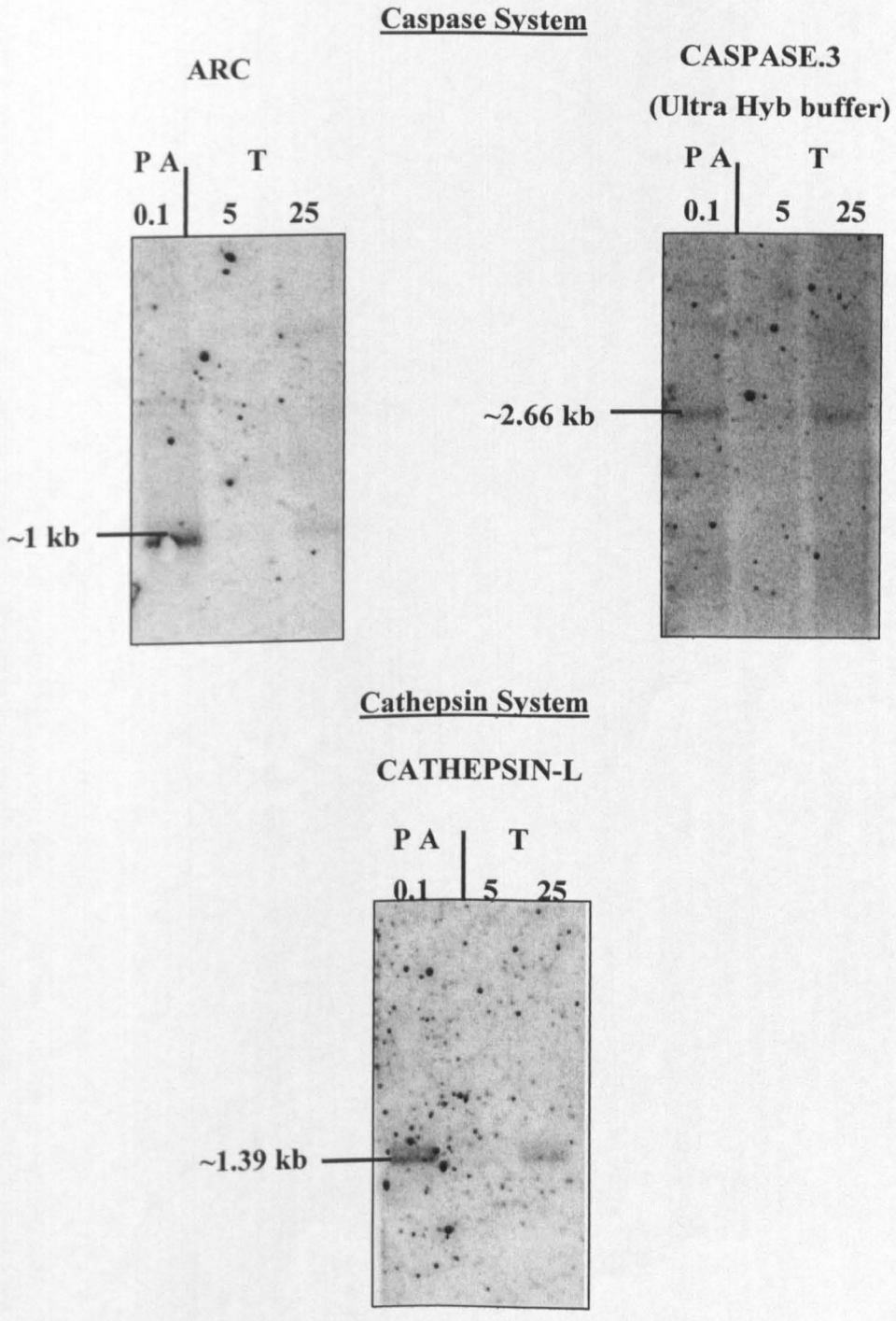

Ubiquitin-Proteasome System

E2G1

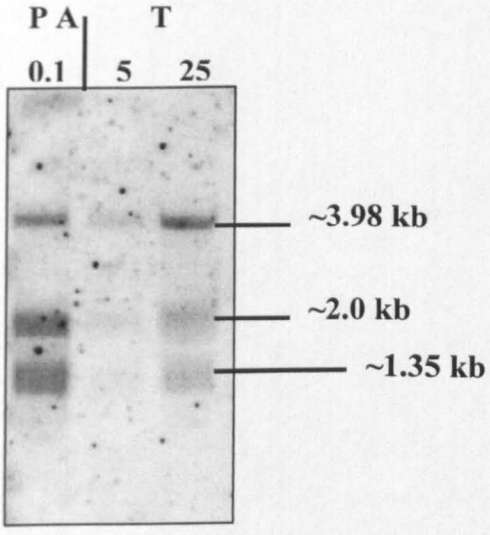

E2G1 (Rediprime probe-labelling kit)

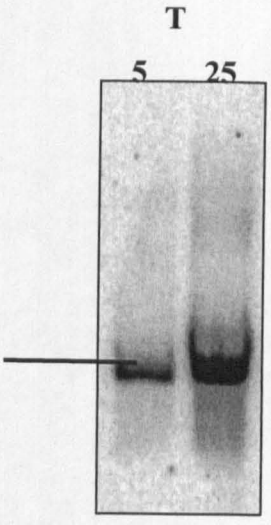

(C) (11) UBIQUITIN

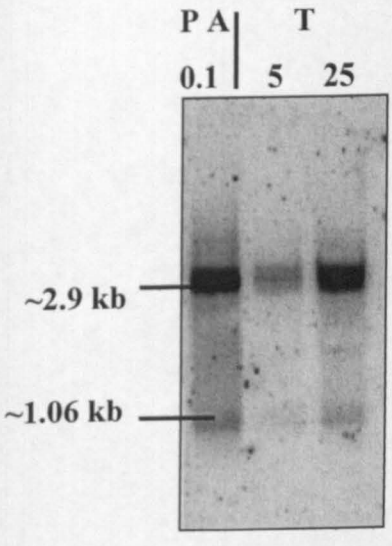

(C) (12) ATROGIN-1

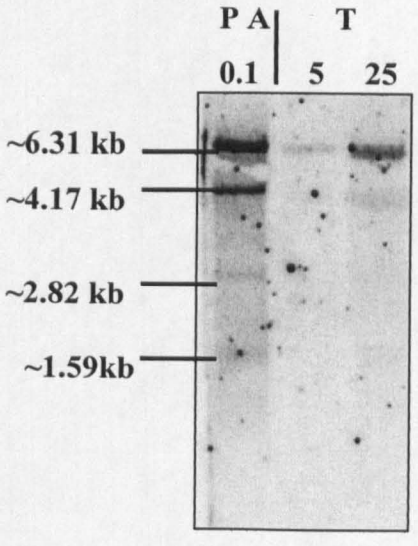

Calpain System

CALPAIN-3

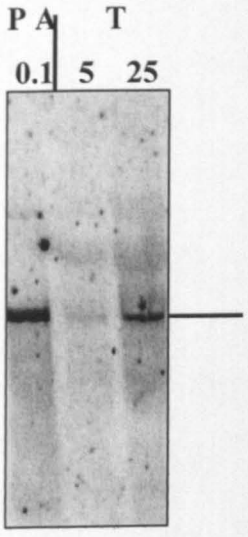

~3.2 kb

CALPAIN-3 (Long probe-see appendix A15)

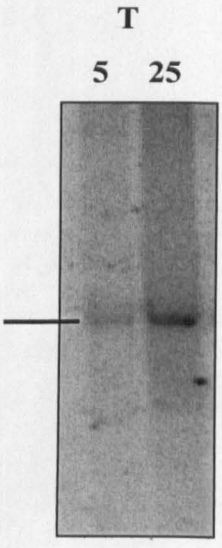

Internal Standard

CALPAIN-10

~2.6 kb

ACTIN

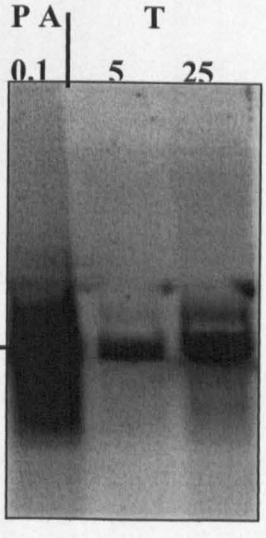

~1.49 kb

Table 5.3-1. Comparison of sizes of available mRNA sequence of interest. *Sequence accession number, species, and size is included (taken from Appendix A : Sequence retrieval/multiple sequence alignments, and BLAST search). A summary of detected Northern blot signal band sizes is included; taken from phosphoimages in Figure 5.3-1.*

cDNA Probe	Sequence Acc. No. and Species	Size (bp) in Database	N-Blot band sizes (bp)
(2) ARC	AF043244 – Human AY459322 – Murine	900 983	~1000
(3) Caspase-3	AB029345 – Porcine	834	~2660
(7) Cathepsin-L	D37917 – Porcine	1378	~1390
(9) E2G1	D78514 – Human AF099093 – Rat AK013902 – Murine	617 931 1543	~3981, ~1995, ~1350
(11) Ubiquitin	M26880 – Human	2309	~2900, ~1060
(12) Atrogin-1	AY059629 – Human AF441120 – Murine AY059628 – Rat	1068 2064 1053	~6310, ~4170, ~2820, ~1585
(15) Calpain-3	AF043295 – Porcine	2512	~3200
(17) Calpain-10	AF089088 – Human	2620	~2600
(18) Actin	J00068 – Human NM 174225 – Bovine	1374 1485	~1490

Northern testing showed that the probes for Cathepsin-L, and Actin were able to produce single, specific reproducible band signals at ~1.39 and ~1.49 kb, respectively; that corresponded to the correct complete mRNA sequence sizes (see Table 5.3-1). The Actin signal had a very strong band intensity, and 'vertical-spread' across blot; corresponding to the very high expression level of actin within skeletal muscle, and a degree of cross-hybridisation with other similar-sized actin isoforms (other than alpha-actin), e.g. beta (~1.8-2.2 kb), and gamma (~1.9 kb).

Calpain-3 and the long-Calpain 3 probe were able to produce a strong, reproducible, signal single specific band at ~3.2 kb; although long-Calpain 3 was shown to be more specific than the shorter probe. The porcine sequence, AF043295, available within the database is 2512 bp long. This is for calpain-3 mRNA sequence but does not contain the untranslated regions, which if included gives a size of ~3.2 kb. In addition, The three complete calpain-3 sequences from Bovine, Ovine and Human species, are 2955, 3165 and 3243 bp respectively, which also indicates that the expected size of calpain-3 mRNA would be in this range (see Appendix B).

ARC, Caspase-3, and Calpain-10 were difficult to detect. Band signals detected were from porcine Poly-A^+-enriched RNA samples, indicating low tissue expression levels. Single, specific bands detected are thought to be the correct size based on what evidence is available (comparing available sequences from Table 5.3-1 and Appendix B), however no porcine sequence data is available for ARC or Calpain-10. Calpain-10 was generated from a human IMAGE clone; therefore, any specific band signal would represent a human cDNA probe cross-hybridising with a porcine mRNA sequence. Caspase-3 had a specific band signal size of ~2.6 kb, which is believed to correspond to a porcine skeletal muscle transcript variant/isoform. Human caspase-3 transcript variant alpha is 2646 bp, and human isoform alpha, 2635 (Appendix B). UltraHyb hybridisation buffer was used to produce a result for Caspase-3, as the buffer system allows greater sensitivity by detecting low expression levels.

E2G1, Ubiquitin and Atrogin-1 produced multiple band signals with porcine Poly-A^+-enriched and total RNA Northern blots, even with higher stringency hybridisation conditions. E2G1 probing produced three relatively strong, reproducible bands, at

~3.98, ~2.0 and ~1.35 kb. Noting the size of other sequences found (Appendix B), i.e. the human transcript variants, it is possible porcine E2G1 may be alternatively spliced. The ~1.35 kb band is believed to be the correct band to focus attention on, as using the Rediprime probe-labelling protocol, produced a single specific band at that size. Ubiquitin probing produced two bands, ~2.9 and ~1.01 kb. From the available sequences for Ubiquitin B and C (found in Appendix B), it would seem likely that the ~2.9 and ~1.01 kb bands correspond to porcine Ubiquitin B and C, respectively; considering also that the probe sequence produced a 99% sequence identity match with what porcine sequence was available (Appendix A:11, Figure. F [acc.no. M18159]). Atrogin-1 probing produced four bands, ~6.31, ~4.17, ~2.82 and ~1.59 kb. It is most probable the band to focus on is the ~1.59 kb signal, based on what sequence evidence is available (Table 5.3-1. and Appendix B). As all bands from E2G1, Ubiquitin and Atrogin-1 probing were to be found within the Poly A^+-enriched sample of Northern blots, ribosomal RNA signals can be discounted as ribosomal RNA should not be present within the Poly A^+-enriched RNA. It is possible that multiple band signals are due to unknown porcine skeletal muscle transcript variants, or, non-specific hybridisation with other mRNA sequence targets; as PCR primers were based on human sequence, and no porcine sequence exists for E2G1 and Atrogin-1.

Therefore, the following probes were selected for further experimentation based on there strength of signal, specificity, reproducibility, and interest: Cathepsin-L, long-Calpain-3, Actin, and possibly E2G1 and Atrogin-1.

5.4 SUMMARY

As has been presented within this section and in detail within Appendix A; twenty cDNA probes were generated by PCR, and confirmed by DNA sequencing and subsequent BLAST search analysis, to be closest matched with the mRNA sequence identities of interest.

The selection of probes tested on Northern blots was based on their possible functional importance within skeletal muscle (based on current literature), in addition to insufficient time and resources to test and optimise all twenty. It was theorised that

many of the sequences of interest are expressed within porcine skeletal muscle, play a role in specific states affecting muscle protein turnover, and could be detected and quantified using Northern blot hybridisation experiments. After testing, the choice of probes that produced the most specific and reproducable signals on porcine RNA Northern blots, and were most likely of porcine origin (based on fact that PCR primers designed using porcine sequence and generated using porcine skeletal muscle) were Cathepsin-L, long-Calpain-3 and Actin. This was essential as further trial studies were to use pigs as treatment subjects.

CHAPTER 6 THE EFFECTS OF A BETA-ADRENERGIC AGONIST ON PROTEASE EXPRESSION IN PIGS

6.1 INTRODUCTION

Previous studies (as described previously in Section 2.3.4) have shown that chronic administration of the synthetic β_2-adrenoceptor agonist clenbuterol has a potent nutrient repartitioning effect in farm animals (Bell *et al*, 1998, Mersmann, 1998). Clenbuterol induced increases in skeletal muscle hypertrophy and protein accretion are thought to be through alterations in muscle protein turnover, specifically by decreasing protein breakdown (Mersmann, 1998, Navegantes *et al*, 2002). A proteolytic system which is known to have alterations in activity and mRNA levels with β-adrenoceptor agonist treatment, are components of the calpain system, specifically the endogenous inhibitor calpastatin (Parr *et al*, 1992, Bardsley *et al*, 1992, Speck *et al*, 1993, Sensky *et al*, 1996, Goll *et al*, 1998, Mc Donagh *et al*, 1999, Navegantes *et al*, 2002). It is thought that these alterations in specific components are thought to induce, or be involved in the processes of cell remodelling, hypertrophy and possibly fiber transformation (Goll *et al*, 1998, Navegantes *et al*, 2002, Goll *et al*, 2003).

However, the precise effects of chronic and acute β-adrenoceptor stimulation- through endogenous and exogenous β-receptor agonists, such as adrenaline and clenbuterol respectively, on the expression of muscle proteolytic systems is unknown.

Three separate studies had been performed within the Department of Nutritional Sciences. These studies investigated the effects of variable dose, chronic and acute β-adrenergic agonist administration in pigs. Pig *Longissmus Dorsi* (LD) total RNA samples from all three trials were available for gene expression analysis. Therefore, northern blots were run and hybridised with specific protease system component cDNA probes. It was hypothesised that β-adrenoceptor agonist treatment through clenbuterol administration and adrenaline infusion would alter the gene expression of components of the calpain-calpastatin system, and other protease system components.

6.2 THE EFFECT OF 24 HOUR AND 7 DAY CLENBUTEROL TREATMENT IN PIGS

6.2.1 Trial Details

Samples were obtained from a trial that had been carried out by Dr. Paul Sensky, the details of which are briefly outlined below:

Thirty six Large White pigs were individually penned, housed approximately 2 weeks prior to treatment and fed a standard finisher diet (see Appendix I), which satisfied the nutritional requirement, up to the day before slaughter. The pigs were trained to eat their diet within a 60-min period by offering them 2 kg feed and withdrawing it 1 h later, as the clenbuterol was to be fed in the animals diet. Animals were randomly divided into three treatment groups of twelve animals: Group (A): controls, (B): 7 day treatment of a 5 parts per million (ppm) dose of clenbuterol (Sigma)/day and (C): 24 h treatment of 5 ppm daily dose of clenbuterol. The start of the treatment groups were staggered to allow for three consecutive slaughter dates; start dates were: day 19, 20 and 21, and slaughter dates: day 26, 27 and 28. Therefore, four animals from each group (i.e. 12 animals total) started treatments, and were slaughtered together on the same dates. The 24 h group (C) started clenbuterol treatment on day 25, 26 and 27 of the trial. Figure 6.2.1-1 illustrates the plan for individual treatment groups over the time course of the trial.

Animals were slaughtered by electrical stunning and severance of the carotid arteries. Samples of LD muscle were removed from the carcass immediately after slaughter and snap frozen in liquid nitrogen for subsequent storage at – 70°C.

Figure 6.2.1-1. Schematic outline of clenbuterol trial. *Control group A (—), remained on the same diet for the whole time of the trial. Group B (—) was treated with a dietary supplemental dose of 5 ppm clenbuterol daily for 7 days before slaughter. Group C (—) was treated with a dietary supplemental dose of 5 ppm clenbuterol for 24 h before slaughter. As can be observed above, treatment start-dates and slaughter-dates were staggered.*

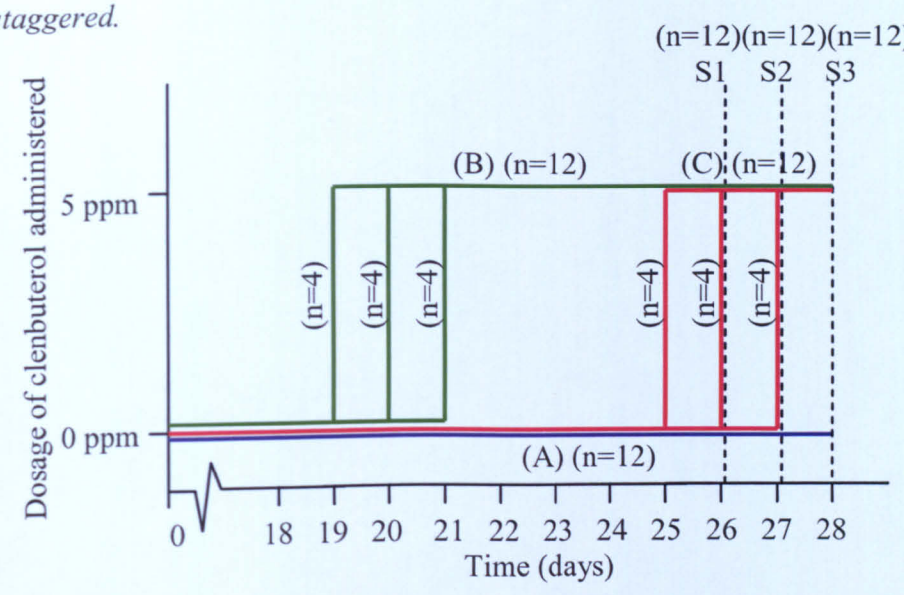

6.2.2 Total RNA Extraction and Analysis

Due to constraints of total RNA northern blot analysis (i.e. number of wells on a gel) LD samples of eight animals from each group were analysed. LD samples were randomly selected, 0.1 g weighed out and subject to total RNA extraction, using the RNAgents® Total RNA Isolation System kit (Promega, Southampton, UK). The procedure was followed as described by the manufacturer and uses a similar method described previously (Section 3.3.1). Total RNA was extracted and checked for integrity and quality by spectrophotometer analysis (see Section 3.3.2) and gel electrophoresis (see Section 3.6). As can be seen in Figure 6.2.2-1 the gel pictures suggest that total RNA samples show some signs of degradation due to presence of low molecular weight banding and some 'smearing' of the rRNA bands. However, the 18S band appeared intact and therefore total RNA was used for further analysis. Subsequent northern blot analysis showed that bands were indeed intact. There was no distinct DNA contamination present.

Figure 6.2.2-1. The effect of clenbuterol on porcine LD total RNA quality and integrity. *Non-denaturing gel electrophoresis of skeletal muscle (LD) total RNA samples (1µg loaded/ sample) on a 1% agarose gel. Samples were loaded in order of groups (A) Control, (B) 7-Day, to (C) 24-Hour, with eight samples/group. 1kb markers (M) were loaded on the left hand side of gel, and used to separate treatment groups, with main fragment lengths noted (bp). Ribosomal RNA (rRNA) is indicated.*

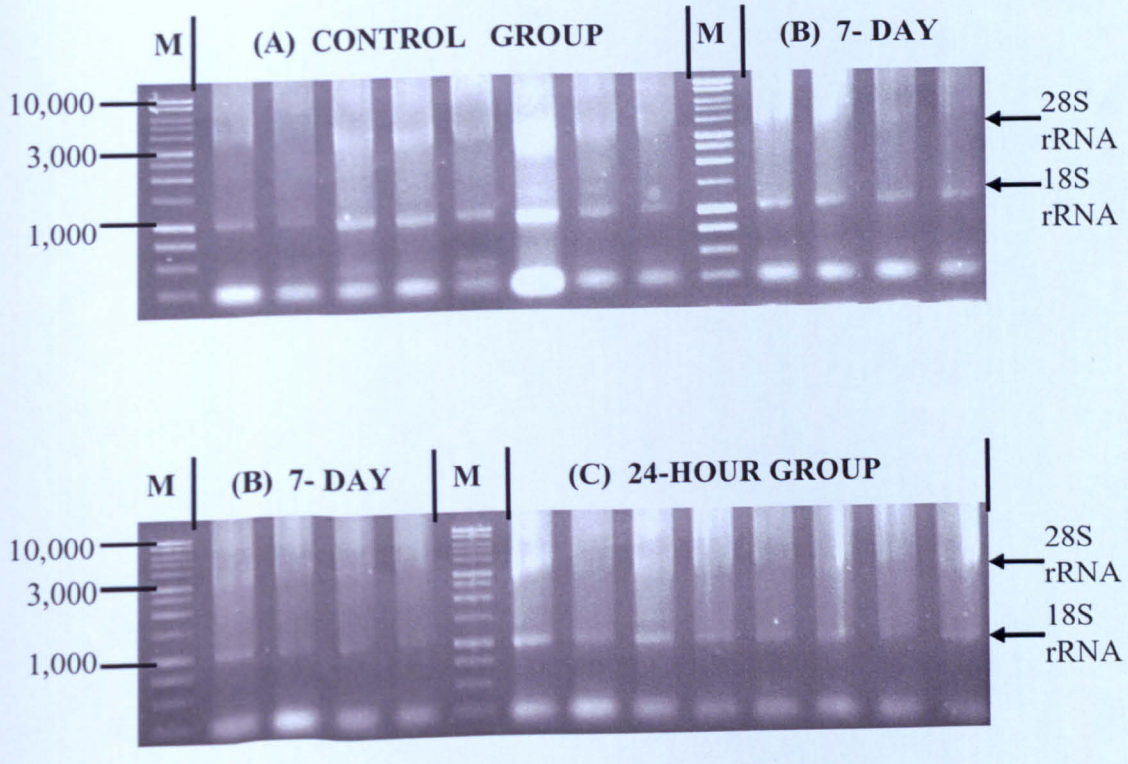

Total RNA extraction yields were calculated and analysed to determine if group yields were affected by treatments. A One-way ANOVA was performed. As can be seen in Table 6.2.2-1 there was no significant effect of treatment on total RNA yields.

Table 6.2.2-1. The effect of clenbuterol on porcine LD total RNA extraction yield. *Mean total RNA yields (μg RNA / 0.1 g tissue) ± SEM for all treatment groups. Number of samples analysed (n) is indicated. P value for One-Way ANOVA analysis of data.*

Treatment Groups Total RNA μg / 0.1 g muscle			*P*
A: Control (n=8)	**C: 24-Hour Clenbuterol (n=8)**	**B: 7-Day Clenbuterol (n=8)**	
49.4 ±5.0	**33.4 ±9.6**	**42.6 ±6.6**	**0.278**

6.2.3 Glycogen Assay

A glycogen assay was performed on 30 LD samples (10 samples per group) to assess whether clenbuterol treatment affected muscle glycogen metabolism (many thanks to Ms G. Carter). As described in detail in Section 2.3.4, it would be expected that clenbuterol and beta-agonist treatment would mobilise and therefore deplete muscle glycogen stores. Glycogen levels were calculated as mg per g tissue. As can be seen from Table 6.2.3-1. there was a highly significant effect of treatment on muscle glycogen levels ($P < 0.001$), which indicates that clenbuterol treatment had depleted muscle glycogen stores. These results give a direct indication that the dose of clenbuterol administered had caused an effect in the animals. It is interesting to note that the effect on the animals treated for 24 hours was more marked than that for those treated for 7 days.

Table 6.2.3-1. The effect of clenbuterol on porcine LD glycogen stores. *Mean Glycogen (mg / g tissue) ± SEM for all treatment groups. Number of samples analysed (n) is indicated. P value from One-Way ANOVA analysis of data.*

Treatment Groups Glycogen mg / g			*P*
A: Control (n=10)	**C: 24-Hour Clenbuterol (n=10)**	**B: 7-Day Clenbuterol (n=10)**	
9.489 ±0.492	**1.392 ±0.114**	**4.246 ±0.480**	**< 0.001**

6.2.4 Northern Blot Analysis

Total RNA (25 μg) extracted from eight animals from each treatment group were loaded onto a denaturing agarose gel (those on gel in Figure 6.2.2-1), run by electrophoresis and blotted overnight onto a Hybond N membrane, described previously (see Section 3.14).

The northern blot was subsequently probed with cDNAs for cathepsin-L, E2G1, long-calpain-3 and actin, in that order (cDNA probes are described in Chapter 5 and Appendix A). Probes were labelled with [α- ^{32}P]dATP using the Strip-EZ procedure (see Section 3.15.1.1), hybridised using Rapid-Hyb buffer (see Section 3.15.3.1) and stripped from membrane using Strip-EZ (see Section 3.15.5.1). This combined procedure allowed blot integrity to be maintained during a number of probe-hybridisations, preventing membrane damage and the resulting high background signals.

Table 6.2.4-1 shows the probe-hybridisation conditions developed to optimise band signals.

Table 6.2.4-1. Optimised probe hybridisation, northern blot washstep and signal detection conditions. *Hybridisation temperature (Hyb. Temp.), hybridisation time (Hyb. Time), final high stringency washstep conditions and time to develop signal (Dev. Time) are included.*

Probe	Hyb. Temp.	Hyb. Time	High Stringency Wash step	Dev. Time
Cathepsin-L	58°C	2 hr	0.1 x SSC + 0.1% SDS for 30 min/65°C	3 day
E2G1	60°C	2 hr	0.5 x SSC + 0.1% SDS for 30 min /60°C	2 day
Long-Calpain-3	65°C	2.25 hr	0.1 x SSC + 0.1% SDS, 20 min / 65°C	3 days
Actin	65°C	1 hr	0.1 x SSC + 0.1% SDS, 30 min / 65°C	~18 hr

Detected band-signal sizes (kb) were determined to correctly identify band identities (see Section 5.3). Band signal intensities for each sample were analysed as described within Section 3.17.

Cathespin-L, long-calpain-3 and actin probing produced single specific bands at correct sizes, i.e. 1.38, 3.2 and 1.49 kb, respectively (see Figure 6.4.3-1). E2G1 produced four bands, 6.0, 3.8, 2.0 and 1.4 kb. The 1.4 kb band had previously been identified as the band of interest (as discussed in Section 5.3).

Figure 6.2.4-1. The effect of clenbuterol on the mRNA expression of proteolytic system components in porcine LD (1). *Phosphoimages of northern blot (25 µg total RNA loaded onto gel/sample), probed as described previously using following probes: (A): Cathepsin-L, (B): E2G1, (C): long-Calpain-3 and (D): Actin. Control, 7 day and 24 hour Clenbuterol treatments are indicated.*

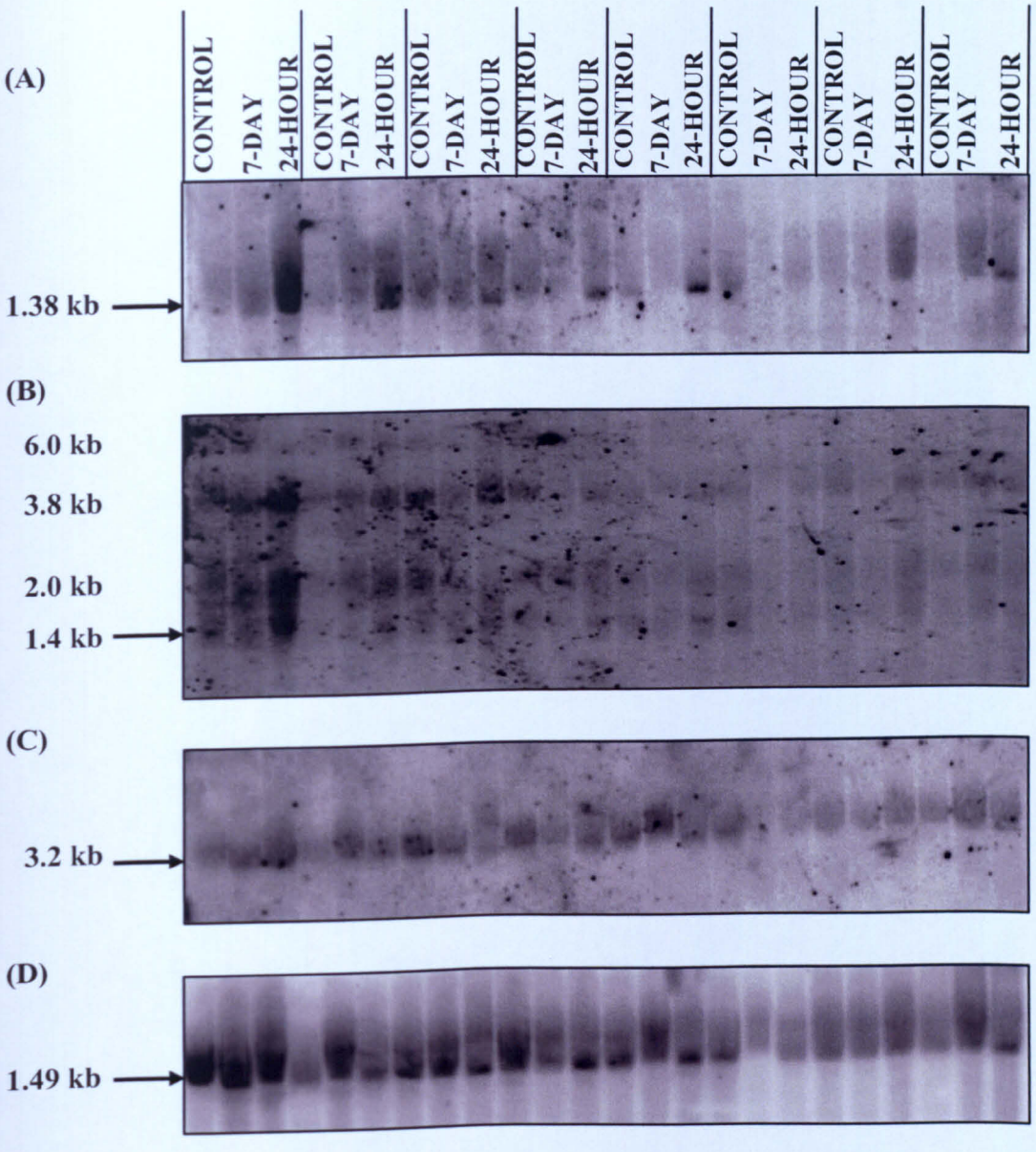

The gels were loaded with equal quantities of total RNA as determined by the methodology described previously (Section 3.3.2). Assuming that total RNA loaded was the same across the gel, as can be seen in Table 6.2.4-2, clenbuterol treatment did not significantly affect actin mRNA expression. Band intensity values for actin were analysed across treatment groups to ensure treatment had not affected the mRNA expression of this internal standard (see Table 6.2.4-2).

Therefore, detected band signal intensities for Cathepsin-L, E2G1 and Calpain-3 were normalised to Actin and treatment group mean ratio values and SEM calculated (Table 6.2.4-3 and Figure 6.2.4-2).

Table 6.2.4-2. The effect of clenbuterol on the mRNA expression of actin. *Table to show comparison of group mean northern band intensity values in counts per mm2 (CNT/mm2) for Actin +/- SEM. Number of samples analysed (n) is indicated. P value from One-Way ANOVA.*

Treatment groups Actin Band intensity CNT/mm^2 / 25 µg total RNA			***P***
Control Group (n=8)	**24-hour Group (n=8)**	**7-Day Group (n=8)**	
194045.2 ±21124.7	178695.1 ±12009.9	168461.9 ±27992.9	0.701

A One-way ANOVA of E2G1 and Calpain-3 ratio values showed no significant change with clenbuterol treatment, whereas Cathepsin-L showed a highly significant ($P < 0.001$) result (see Table 6.2.4-3).

Table 6.2.4-3. The effect of clenbuterol on the mRNA expression of proteolytic system components in porcine LD. *Table to show comparison of treatment group mean Northern blot band intensity ratio values normalised to Actin, +/- SEM for northern blots probed with Cathepsin-L (Cath.L), E2G1 and long-Calpain-3 (Calp.3) cDNA's. Number of samples analysed (n) is indicated. Note that some band signals were undetectable. P value from One-Way ANOVA test.*

Probe	Treatment groups Band intensity ratio to actin						*P*
	n	Control Group	n	24-hour Group	n	7-Day Group	
Cath.-L	8	0.000549 ±0.00012	8	0.002408 ±0.00033	5	0.000819 ±0.00017	< 0.001
E2G1	8	0.002882 ±0.00046	8	0.004533 ±0.00052	6	0.003727 ±0.00122	0.260
Calp.3	8	0.031517 ±0.00516	8	0.037879 ±0.00762	8	0.041745 ±0.00967	0.644

Bonferroni Post-Hoc test after One-way ANOVA for Calpain-3 and E2G1 showed there was no significant difference between group interactions. However, the minimal increase in Calpain-3 was 32% after 1 week of treatment, relative to controls (see Figure 6.2.4-2 (C)). E2G1 increased by 57% relative to controls after 24 hour of treatment, although not significant ($P = 0.316$) (see Figure 6.2.4-2 (B)). Cathepsin-L analysis indicated that the 24 hour treatment group was significantly greater than Control group ($P < 0.001$), a 339% increase relative to controls (see Figure 6.2.4-2 (A)). The 7-Day group was numerically greater than the control group (49% increase, relative to controls), although not significant. The 24 hour group was found to be also significantly greater than 7-Day group ($P < 0.01$), with a 194% increase.

Figure 6.2.4-2. The effect of clenbuterol treatment on mRNA expression of proteolytic system components in porcine LD (2). *Mean relative northern band intensity ratio values normalised to actin, + SEM are presented, for (A) Cathepsin-L, (B) E2G1 and (C) Calpain-3.* ***a = p <0.001, b = b < 0.01.***

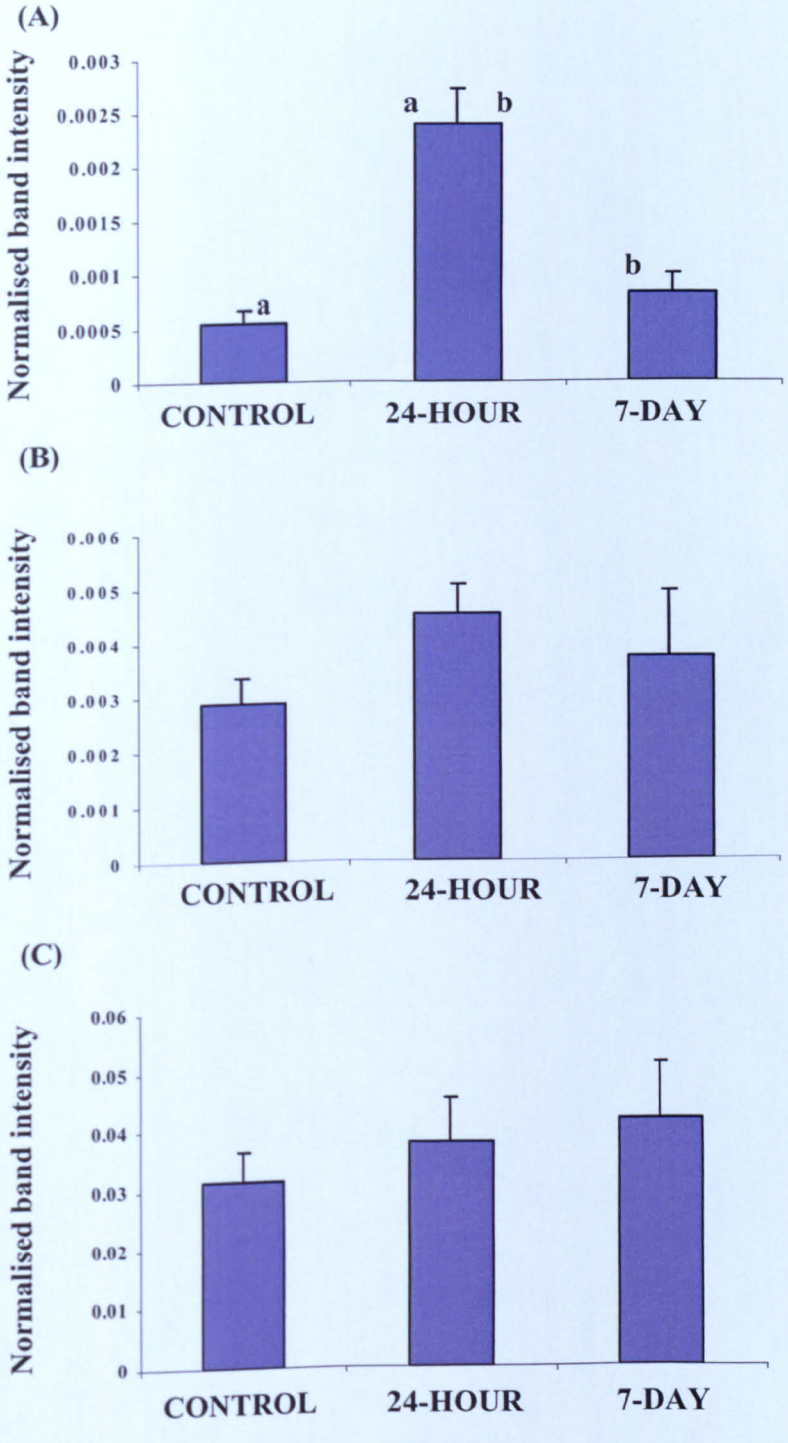

6.2.5 Summary

A trial was performed in which chronic and acute doses of the specific β_2-adrenergic agonist clenbuterol was administered to pigs.

LD total RNA extraction yield analysis for group samples showed that there was no significant effect of clenbuterol treatment on extractable total RNA yields ($P = 0.278$).

Glycogen assay analysis of trial samples (10 samples per treatment group) revealed that treatment had a highly significant effect on glycogen levels ($P < 0.001$). 24-hour clenbuterol treatment decreased average glycogen levels (mg per g tissue) by 85%, relative to Controls. The 7-Day group glycogen levels rose back up, compared to 24-hour treatment group, with a 55% decrease relative to Controls.

Northern blot probe-hybridisation studies revealed no significant difference between treatments for E2G1 and muscle-specific calpain-3 expression, although both increased numerically. E2G1 had increased by 57% relative to Controls after 24 hour of treatment and calpain-3 increased by 32% relative to Controls after 1 week of treatment. Cathepsin-L after 24 hour clenbuterol treatment increased by 339% relative to Controls. This value was highly significant ($P < 0.001$). Cathepsin-L was numerically greater in the 7-day group relative to Control group with a 49% increase. This was found not to be significant. The 24-hour treatment was also significantly greater ($P < 0.01$) to the 7-day treatment (a 194% increase). Therefore, cathepsin-L mRNA expression was observed to increase rapidly to a highly significant value, then decrease after 7-day of treatment.

6.3 THE EFFECT OF ACUTE BETA-ADRENERGIC AGONIST ADMINISTRATION IN PIGS

6.3.1 Introduction

There is great interest as to at what time point after administration of a beta-adrenergic agonist does mRNA expression change for various proteases. This would help to indicate whether transcriptional activating pathways are having significant effects in certain time frames after stimulation. As was observed in the previously described study in Section 6.2, there was a highly significant change in cathepsin-L mRNA after 24-hour 5 ppm clenbuterol treatment. Calpain-3 and E2G1 showed no significant change with treatment. However the numerical change was: E2G1 increased by 57% for the 24-hour group and calpain-3 by 32% after 7-day treatment. Therefore, it was of interest to see whether an acute, 16-hour large dose (20 ppm) of clenbuterol would alter mRNA expression of cathepsin-L and calpain-3, as it is known that at this dose level there is a significant effect on the expression of ubiquitous calpains and calpastatin.

6.3.2 Trial Details

Trial was carried out by Dr Paul Sensky and is described in Parr *et al* 2001. Briefly the details of the trial were:

Twelve Large White x Landrace gilts comprising six pairs of full siblings were individually penned 4 weeks prior to treatment and fed a standard finisher diet (similar to that described within Appendix I, : 52.3% wheat, 20.1% barley, 23.7% soya, 1.3% Betamix, 1.3% limestone, 1.1% phosphate, 0.2% salt, plus 575 mg/kg synthetic lysine) up to the day before slaughter. The pigs were trained to eat their diet within a 1 hr period by offering them 2 kg feed and withdrawing it 1 hr later as the diet would contain the oral dose of clenbuterol. All pigs were trained within 3 days. On the evening prior to slaughter (16 hrs pre-slaughter) six pigs received the standard diet as normal (control group), while their respective siblings received the same diet supplemented with 20 ppm clenbuterol (Sigma-Aldrich). With the exception of one animal in the clenbuterol group, all animals ate their diet within 1 h, and the animal that

did not eat its diet was excluded from further analysis. Sixteen hours after treatment the animals were slaughtered by electrical stunning and severance of the carotid arteries. Samples of LD muscle were removed from the carcass within 5 min of slaughter and snap frozen in liquid nitrogen then stored at – 70°C.

6.3.3 Total RNA Extraction and Analysis

Total RNA was extracted from trial LD muscle samples for six control animals and five clenbuterol-treated animals by Dr T.Parr, using the methodology as described in Section 3.3. Total RNA extraction yields were calculated for all samples as μg total RNA per g tissue (see Table 6.3.3-1). As can be seen in Table 6.3.3-1 there was no significant effect of treatment on yields of total RNA.

Table 6.3.3.-1. Effect of clenbuterol on quantity of total RNA extracted in porcine LD. *Mean total RNA extraction yields (μg RNA / g tissue) ± SEM for both groups. Number of samples analysed (n) is indicated. P value from t-test analysis of data.*

Treatment Groups Total RNA (μg /g muscle)		***P***
Control (n=6)	**Clenbuterol (n=5)**	
1124 ±147.4	**1021.6 ±84.3**	**0.58**

6.3.4 Northern Blot Analysis

A northern blot was run using method described previously (see Section 3.14), with 20 μg total RNA loaded for each sample. The blot had been previously been probed twice.

The northern blot was probed with Cathepsin-L and long-Calpain-3 cDNA probes, in that order. As blot had been previously probed using different cDNA probes other than Cathepsin-L and long-Calpain-3, blot integrity and RNA quality was compromised. This was apparent as band signals were more difficult to detect and quantify (see Figure 6.3.4-1). Therefore due to its low expression, analysis of E2G1 was not possible. Probes were labelled with [α- ^{32}P]dATP using the Strip-EZ procedure (see Section 3.15.1.1), hybridised using Rapid-Hyb buffer (see Section 3.15.3.1) and stripped using Strip-EZ kit (see Section 3.15.5.1). This allowed reprobing of the membrane with less membrane damage.

Band signals were optimised for all probe-hybridisations using the following conditions discussed in Table 6.3.4-1:

Table 6.3.4-1. Optimised probe hybridisation, northern blot washstep and signal detection conditions. *Hybridisation temperature (Hyb. Temp.), hybridisation time (Hyb. Time), final high stringency washstep conditions and time to develop signal (Dev. Time) are included.*

Probe	Hyb. Temp.	Hyb. Time	High Stringency Wash step	Dev. Time
Cathepsin-L	60°C	2.5 hr	0.1X SSC + 0.1% SDS for 30 min / 60°C	2 days
Long-Calpain-3	65°C	2.25 hr	0.1X SSC + 0.1% SDS for 30 min / 60°C	2 day

Detected band-signal sizes (kb) were determined to correctly identify band identities (see Section 5.3). Band intensity analysis was performed as described in Section 3.17.

Cathespin-L and long-Calpain-3 probing produced single specific bands at correct sizes, i.e. 1.38 and 3.2 respectively (see Figure 6.3.4-1) Cathepsin-L produced a less

clear and sharp signal than Calpain-3 despite attempts at optimising signal (see Table 6.3.4-1). Actin expression data had been determined from probing the membrane with a specific actin probe previously. Although phosphoimage is not shown, band intensity absorption data is included in Table 6.3.4-2.

Figure 6.3.4-1. The effect of an acute clenbuterol dose on the mRNA expression of proteolytic enzymes in porcine LD. *Phosphoimages of northern blot (20 μg total RNA loaded on to gel/sample) probed as described above using following probes: (A): Cathepsin-L, and (B): long-Calpain-3. Cont. = Control, Clen. = Clenbuterol.*

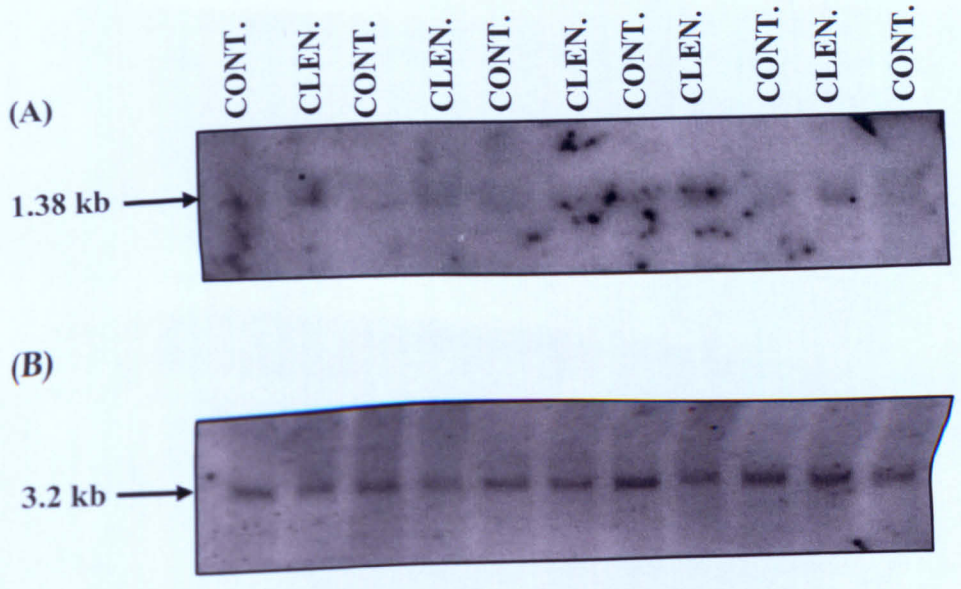

Band intensity values for actin were analysed across treatment groups to ensure treatment had not affected the mRNA expression of this internal standard (see Table 6.3.4-1). As can be seen in Table 6.3.4-2, clenbuterol treatment did not significantly affect actin mRNA expression, based on the assumption that equal quantities of total RNA were loaded on the blot.

Table 6.3.4-2. The effect of clenbuterol on the mRNA expression of actin. *Northern blot band intensity values (absorption units) ± SEM values. Number of samples analysed (n) is indicated. P value from t-test.*

Treatment groups Actin Band intensity (absorption units) / 20μg total RNA		***P***
Control Group (n=6)	**Clenbuterol Group (n=5)**	
46.167 ±2.696	42.109 ±6.604	0.558

Band signal intensities for cathepsin-L and calpain-3 were normalised to actin. Group means and SEM values were calculated (see Table 6.3.4-3 and Figure 6.3.4-2). T-test analysis of data was performed showing no significant change due to treatment for the expression of both cathepsin-L and calpain-3 mRNA (see Table 6.3.4-3). Examination of the numerical values showed that the Cathepsin-L group mean ratio value increased by 53% after treatment, relative to actin. Calpain-3 decreased by 9% with treatment.

Table 6.3.4-3. The effect of an acute clenbuterol dose on the mRNA expression of proteolytic enzymes in porcine LD. Table to show comparison of group mean northern band intensity ratio values, normalised to Actin +/- SEM, using Cathepsin-L (Cath.L), and long-Calpain-3 (Calp.3) probes. Number of samples analysed (n) is indicated. P value from t-test.

Probe	**Treatment groups** Band Intensity Ratio Values				***P***
	n	**Control Group**	n	**Clenbuterol Group**	
Cath.L	6	76.203 ±21.862	5	116.379 ±27.807	0.279
Calp.3	6	13.208 ±0.904	5	11.978 ±1.205	0.427

Fig 6.3.4-2. The effect of an acute clenbuterol dose on relative expression of proteolytic enzymes in porcine LD. *Group mean relative northern blot band intensity ratio values normalised to actin + SEM are presented, for (A) Cathepsin-L and (B) Calpain-3.*

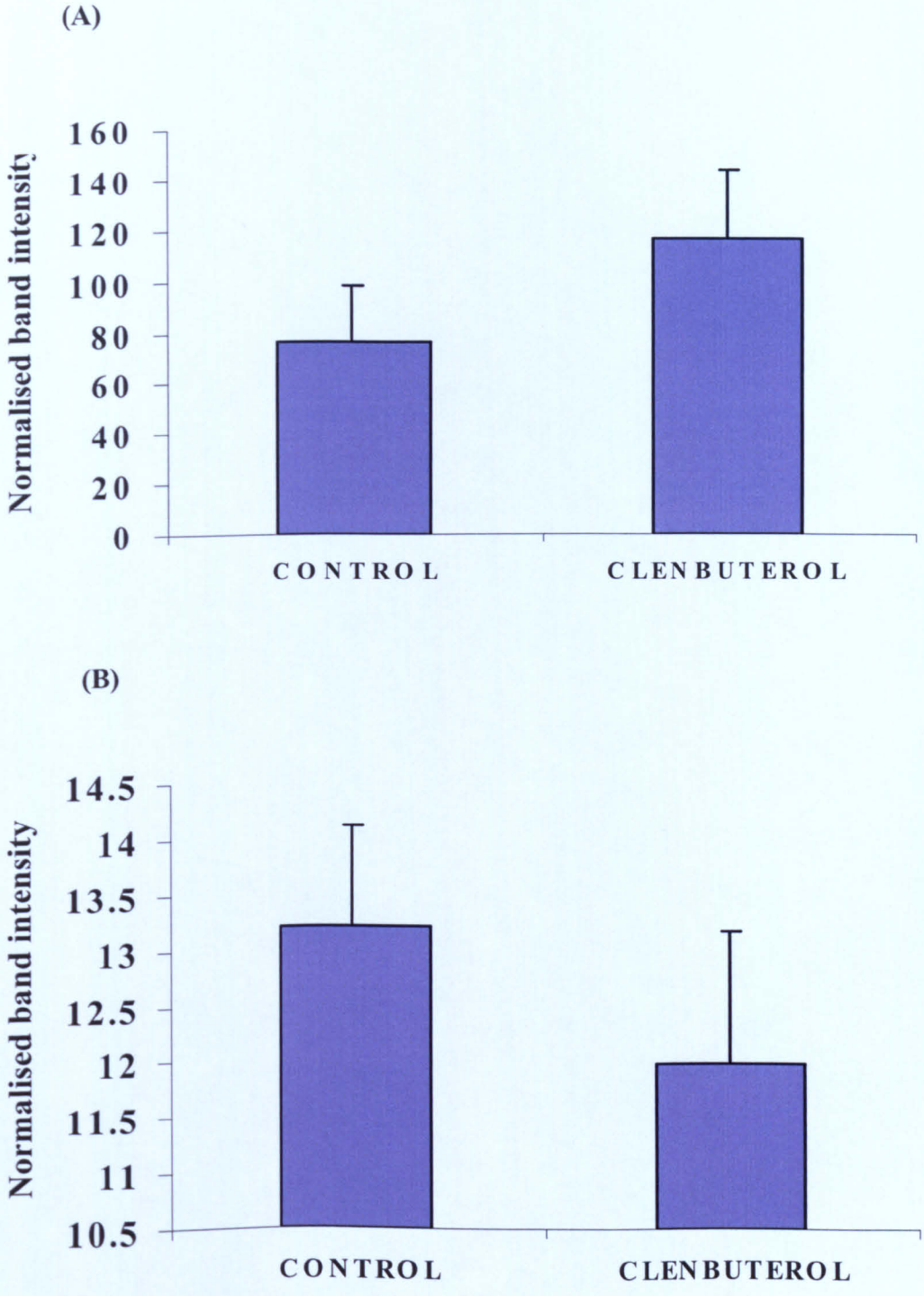

6.3.5 Summary

The trial involved administering an acute high dose (20 ppm) of clenbuterol to pigs for 16 hr, before slaughter.

Analysis of LD total RNA extraction yields found that there was no significant effect of treatment on group total RNA yields.

Northern blot probing using Cathepsin-L and long-Calpain-3 produced detectable band signals of the correct sizes, i.e. 1.38 and 3.2 kb. Detected band intensities were normalised to Actin generating normalised ratio values. Analysis of treatment group normalised band intensity ratio values showed there was no significant change in cathepsin-L and calpain-3 relative expression with clenbuterol treatment. However, cathepsin-L increased by 53% relative to Controls with treatment, which is in the same direction as observed previously in the trial described in Section 6.2. Calpain-3 decreased by 9% relative to Controls with treatment, which is unlike the numerical change observed in trial in Section 6.2. However, this increase is small and probably reflects that there was no significant difference in calpain-3 expression between treatments.

6.4 THE EFFECTS OF CHRONIC ADMINISTRATION OF ADRENALINE ON PROTEASE mRNA EXPRESSION IN PIGS

6.4.1 Introduction

The trials discussed in Section 6.2.and 6.3 involved acute and chronic administration of the specific β_2-adrenergic agonist clenbuterol. Another study performed within the Division of Nutritional Sciences involved chronic adrenaline administration in pigs. It was an important study so as to analyse the effects of chronic administration of an endogenous β-adrenergic agonist on the mRNA expression of specific proteases in skeletal muscle.

It has been documented that the endogenous catecholamines adrenaline and noradrenaline are known to have positive effects on skeletal muscle protein turnover, possibly increasing protein synthesis and decreasing protein degradation (Navegantes *et al*, 2002) (discussed in Section 2.3.4). Adrenaline is a non-specific β-adrenergic agonist, known to have binding affinities for the β_1, β_2 and β_3 receptor subtypes. Therefore, the effects of adrenaline may be different compared to a selective β_2-adrenergic agonist, such as clenbuterol. Another point of the study is to assess the effects of chronic administration as this is an 'unnatural' pattern of endogenous adrenaline release and stimulation of β-adrenergic receptors .

6.4.2 Trial Details

Samples were obtained from a trial carried out previously (Sensky *et al*, 1996, Parr *et al*, 2000). Brief details are discussed below:

Twenty female Landrace x Large White pigs consisting of ten pairs of full siblings were used in the trial in which an individual of each pair was intravenously infused with adrenaline (treated group) at a continuous rate of 0.15 μg/kg/min while the sibling received placebo (control group) at the same rate, using an osmotic minipump inserted into the cephalic vein. After the 7-day infusion period the pigs were slaughtered by electrical stunning and severance of the carotid arteries. Samples of LD

muscle were removed from the carcass within 5 min of slaughter and snap frozen in liquid nitrogen for subsequent storage at –70°C. Unfortunately, only six out of the ten adrenaline treated animals survived. Therefore, six adrenaline treated and ten placebo animals were used in subsequent analysis.

6.4.3 Total RNA Extraction and Analysis

LD samples were subject to total RNA extraction procedures, using the methodology as described previously (Section 3.3.1), by Dr Mike Arnold. Total RNA was checked for integrity and quality by spectrophotometer analysis (see Section 3.3.2) and gel electrophoresis (see Section 3.6). Figure 6.4.3-1 shows total RNA ribsomal bands have similar intensities indicating that the determined RNA concentration was correct and equal quantities of total RNA were loaded on the gel. Figure 6.4.3-1 also indicated that 18S and 28S rRNA were intact with little degradation, ideal for further northern blot analysis.

Figure 6.4.3-1. The effects of adrenaline on quality and integrity of porcine LD total RNA. *Non-denaturing gel electrophoresis of skeletal muscle (LD) total RNA (1μg loaded/ sample) on a 1% agarose gel. Samples are loaded in P= Placebo and A= Adrenaline treatment pairing. 1kb markers (M) are loaded with selected fragment lengths noted (bp). Ribosomal RNA (rRNA) is indicated.*

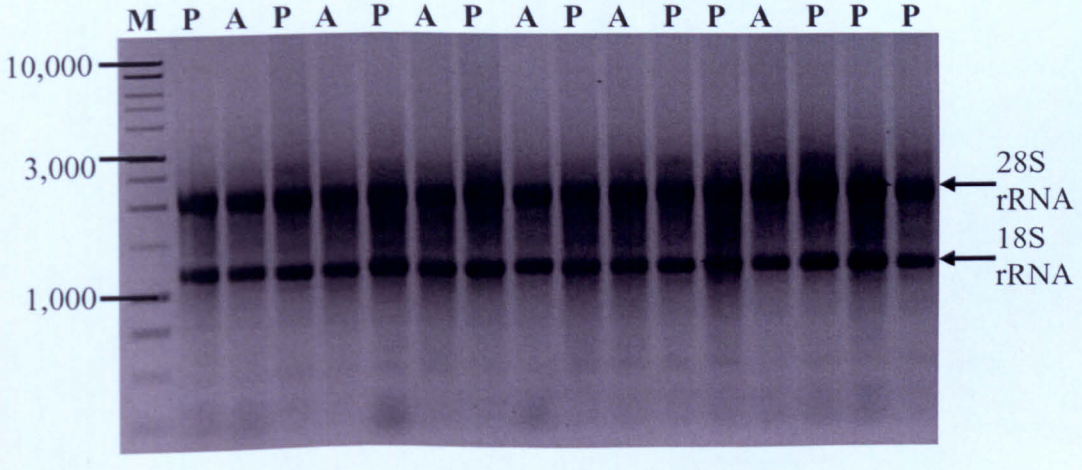

Total RNA extraction yields were calculated for six sibling pair samples as μg RNA per g tissue (see Table 6.4.3-1). A t-test analysis of data was performed to assess whether treatment significantly affected extractable total RNA yields (see Table 6.4.3-1). As can be seen in Table 6.4.3-1 there was no significant effect of treatment on yields, although the values for the adrenaline treated samples were numerically higher.

Table 6.4.3-1. Effect of adrenaline treatment on quantity of total RNA extracted from porcine LD. *Mean total RNA extraction yields (μg RNA / g tissue) ± SEM for both groups. P value from t-test analysis of data.*

Treatment Groups Total RNA (μg /g muscle)		***P***
Placebo (n=6)	**Adrenaline (n=6)**	
795.3 ±147.8	1058.7 ±125.0	0.204

6.4.4 Northern Blot Analysis

Total RNA (15 μg) from all samples from each treatment group was loaded onto a denaturing agarose gel, following Placebo-Adrenaline sample pairing loading pattern (as used in gel in Figure 6.4.3-1). Samples were run by denaturing gel electrophoresis and gel blotted overnight onto a Hybond N membrane using northern blotting procedures described previously (see Section 3.14).

The northern blot was subsequently probed with Cathepsin-L, long-Calpain-3 and Actin cDNA probes, in that order. E2G1 did not produce a clear quantifiable signal as was probed last in experimental order. Probes were labelled with [α- ^{32}P]dATP using the Strip-EZ procedure (see Section 3.15.1.1), hybridised using Rapid-Hyb

buffer (see Section 3.15.3.1) and stripped using Strip-EZ (see Section 3.15.5.1). This helped maintain membrane integrity and allow re-probing.

Band signals were optimised for all probe-hybridisations using the conditions described in Table 6.4.4-1.

Table 6.4.4-1. Optimised hybridisation conditions. *Hybridisation temperature (Hyb. Temp.), hybridisation time (Hyb. Time), final high stringency washstep conditions and time to develop signal (Dev. Time) are included.*

Probe	Hyb. Temp.	Hyb. Time	High Stringency Wash step	Dev. Time
Cathepsin-L	58°C	2.5 hr	2X SSC + 0.1% SDS for 30 min / 60°C	4 days
Long-Calpain-3	65°C	2 hr	0.1X SSC + 0.1% SDS for 20 min / 65°C	~18 hr
Actin	65°C	1.25 hr	0.1X SSC + 0.1% SDS for 30 min / 65°C	~18 hr

Detected band-signal sizes (kb) were determined to correctly identify band identities (see Section 5.3). Band intensity analysis was performed as described in Section 3.17.

Cathepsin-L, long-Calpain-3 and Actin probing produced single specific bands at correct sizes, i.e. 1.38, 3.2 and 1.49 kb, respectively (see Figure 6.4.4-1). Cathepsin-L produced a less clear and sharp signal than Calpain-3 and Actin despite numerous attempts at optimising signal.

Band intensity values for actin were analysed across treatment groups to ensure treatment had not affected the mRNA expression of this internal standard (see Table 6.4.4-2). As can be seen in Table 6.4.4-2 adrenaline administration did not significantly affect actin mRNA expression.

Figure 6.4.4-1. The effects of chronic adrenaline administration on the mRNA expression of proteolytic enzymes in porcine LD. *Phosphoimages of northern blot (15 µg total RNA loaded onto gel/sample), probed as described previously, using following probes: (A): Cathepsin-L, (B): long-Calpain-3 and (C): Actin. Cont. = Control, Adren. = Adrenaline.*

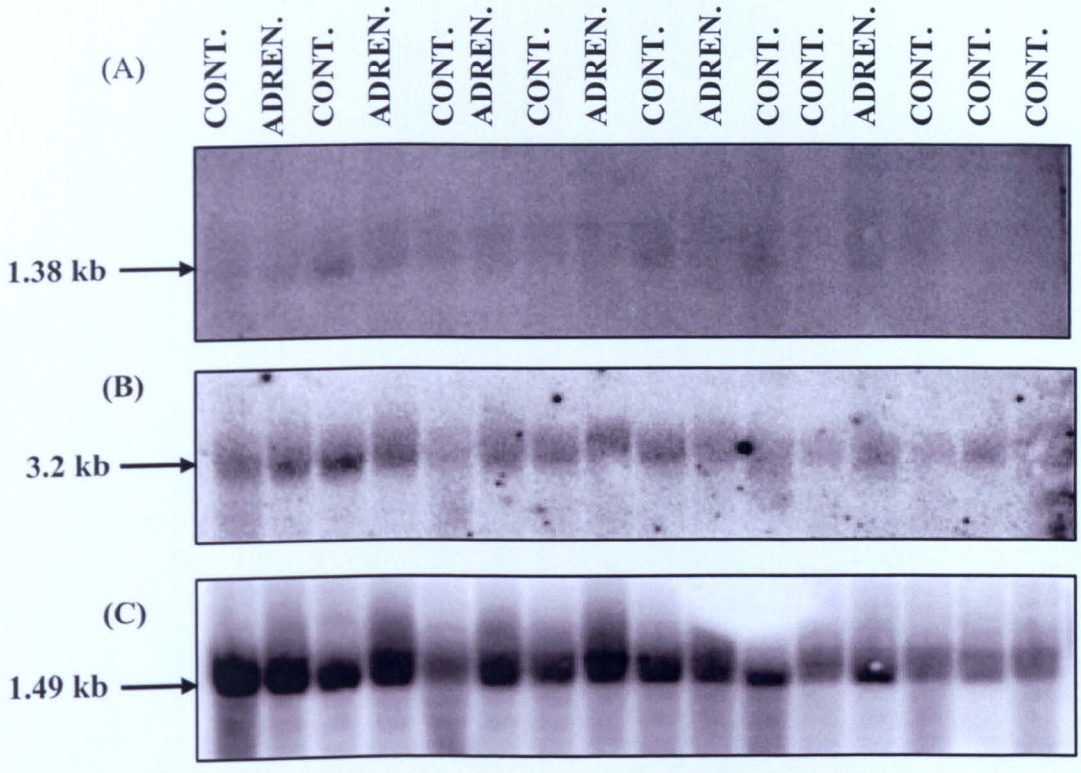

Table 6.4.4-2. The effect of adrenaline administration on the mRNA expression of actin. *Northern blot band intensity values (CNT/mm^2) ± SEM values. Number of samples analysed (n) is indicated. P value from t-test.*

Treatment groups Actin Band Intensity (CNT/mm^2)		***P***
Control/Placebo Group (n=10)	**Adrenaline Group (n=6)**	
1241.839 ± 158.526	1505.377 ± 168.480	0.297

Band signal intensities for Cathepsin-L and Calpain-3 were normalised to Actin. Group means and SEM were calculated (see Table 6.4.4-3 and Figure 6.4.4-2). The numerical change was that Cathepsin-L decreased by 23.9%. Calpain-3 increased by 39.9%. However, T-test analysis of data showed no significant change in values with treatment for either Cathepsin-L or Calpain-3 mRNA expression (see Table 6.4.4-3).

Table 6.4.4-3 Effects of chronic adrenaline administration on mRNA expression of proteolytic enzymes in porcine LD. *Table to show comparison of group mean northern band intensity ratio values normalised to Actin +/- SEM, for Cathepsin-L (Cath.L) and Calpain-3 (Calp.3). Number of samples analysed (n) is indicated. P value from t-test.*

Probe	n	Placebo Group	n	Adrenaline Group	*P*
Cath-L	9	0.380 ±0.051	6	0.289 ±0.053	0.258
Calp-3	9	1.028 ±0.173	5	1.438 ±0.205	0.159

Figure 6.4.4-2. The effects of chronic adrenaline administration on relative mRNA expression of proteolytic enzymes in porcine LD. *Mean, relative northern band intensity ratio values normalised to Actin, + SEM are presented for (A) Cathepsin-L and (B) Calpain-3.*

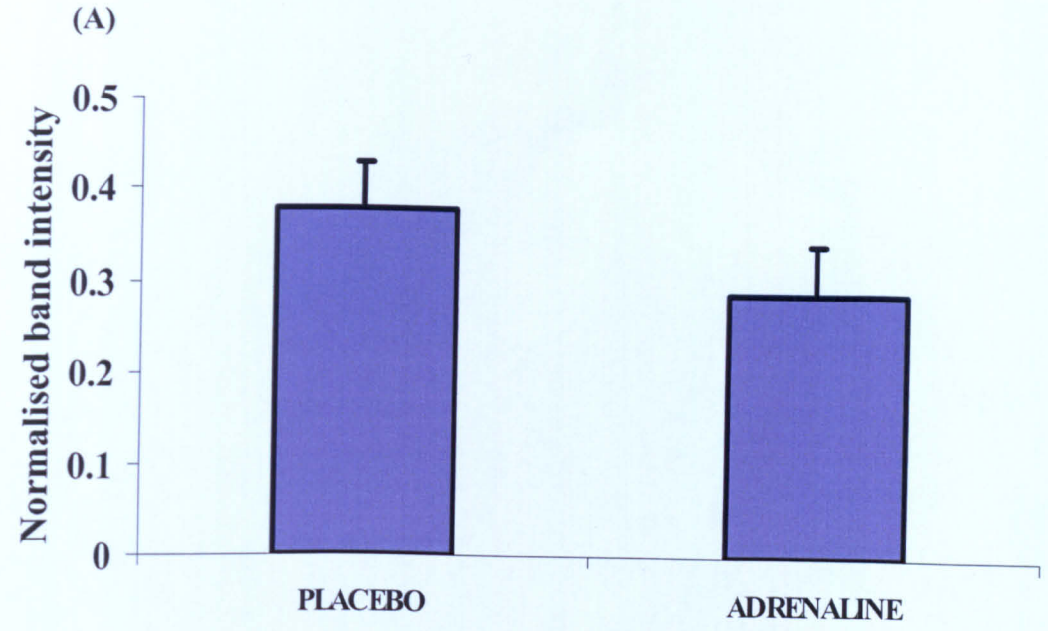

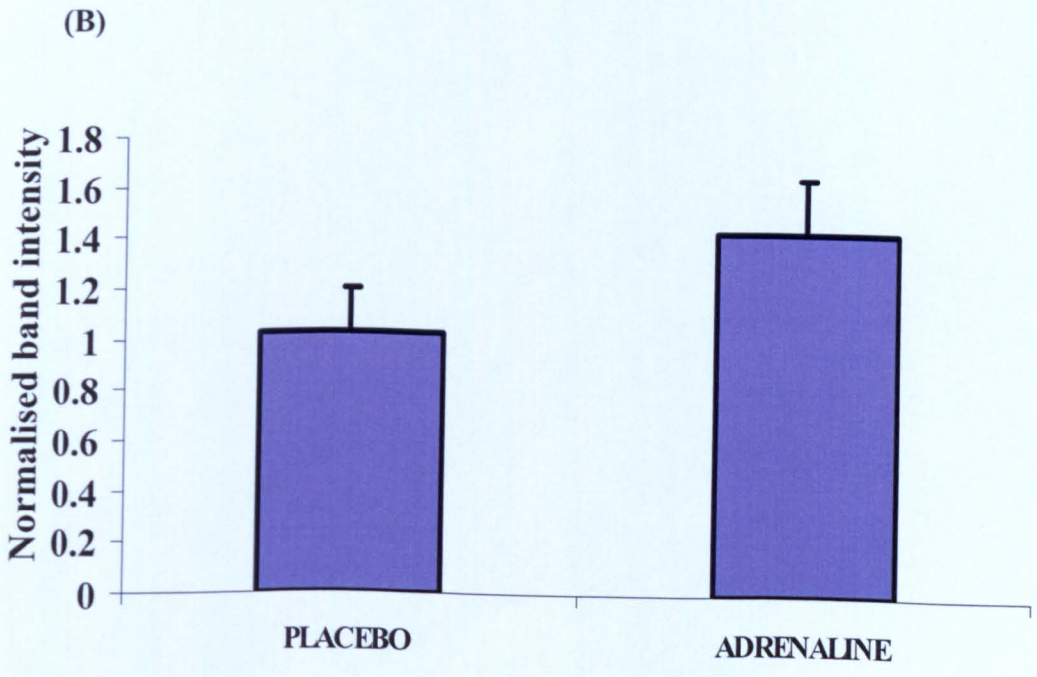

6.4.5 Summary

The trial described above was performed where the endogenous β-adrenergic agonist adrenaline was infused at a continuous rate for seven days in pigs. Four out of the ten adrenaline-treated pigs died or were unable to be used further in the trial.

LD total RNA extraction yields were calculated for both placebo and adrenaline groups. T-test analysis of data showed no significant effect of treatment on extractable yields, although adrenaline treated animals had a numerically higher value.

RNA samples were analysed by northern blot probe-hybridisation. Cathepsin-L, long-Calpain-3 and Actin produced detectable band signals of the correct sizes, i.e. 1.38, 3.2 and 1.49 kb, respectively. Actin band intensities were not found to significantly alter with treatment. Band signal intensities for Cathepsin-L and Calpain-3 were analysed and normalised to Actin, generating ratio values. T-test showed there was no significant change in mRNA expression with adrenaline treatment for both Cathepsin-L and Calpain-3. Numercially Cathepsin-L decreased by 24% and Calpain-3 increased by 40%.

CHAPTER 7 DISCUSSION

7.1 BOVINE PLANE OF NUTRITION TRIAL

7.1.1 Introduction

This study investigated the effects of different planes of nutrition and refeeding after a feed restriction, on the mRNA expression of components of the calpain system within skeletal muscle of calves. During periods of rapid muscle tissue growth, which takes place in young fast growing calves, there is a relatively high level of hypertrophy and remodelling taking place within myofibers (Lee, 2001, Kristensen *et al*, 2002, Sazili, 2003, Kristensen *et al*, 2004) These processes and general muscle protein turnover are thought to be sensitive to the plane of nutrition (see Section 2.3.5). Well fed young animals are thought to exhibit higher rates of protein turnover, protein accretion and growth (Kristensen *et al*, 2002, Kristensen *et al*, 2004). It has been suggested that during feed restriction there is a decrease in both growth rate and protein turnover rates. If the restriction becomes extended and severe to the extent that the animals are in negative nutritional balance, muscle atrophy will eventually manifest due to a rise in net proteolysis.

It has been previously shown that during re-alimentation after a feed restriction there is a greater than normal rise in growth rates and protein turnover, leading to so called 'compensatory growth' (Kristensen *et al*, 2002, Kristensen *et al*, 2004). The level of compensatory growth and associated change in protein turnover rate depends on the length and intensity/severity of the previous feed restriction, the length of the refeeding period and whether it is an unrestricted feed intake period or not.

It has been proposed that the calpain protease system and endogenous inhibitor calpastatin plays a role in the processes of myofibrillar protein degradation and thereby the processes of myofiber hypertrophy/atrophy, remodelling and transformation (Goll et al, 1998, Thompson and Palmer, 1998, Goll *et al*, 2003). Only a small number of studies have been performed measuring calpain system changes at mRNA and protein level in response to altered planes of nutrition in farm animals. Mc Donagh *et*

al, 1999, reported a significant decrease in calpastatin activity ($P < 0.01$) in *M. biceps femoris* of lambs during a restricted feed intake (low plane of nutrition-60% maintenance feed intake, 7 days prior to slaughter), after an initial two weeks fed at twice maintenance (200%), with no effect on μ- and *m*- calpains. Du *et al*, 2004b, observed a significantly greater calpastatin content/immunoreactivity ($P < 0.05$) in *Longissmus* muscle from control group cows compared to nutrient-restricted cows, with no change in the activities of μ- and *m*- calpains.

In comparison to Mc Donagh *et al*, 1999, Kristensen *et al*, 2002 found that there was a positive correlation between growth rates and *m*-calpain activities in pigs fed different planes of nutrition. Calpastatin activity was also found to be unchanged with dietary treatments. In re-fed pigs (after a 60% of ad libitum feed restriction) increased growth rate (compensatory growth) was followed by an increase in the μ-calpain-calpastatin ratio. In a later study by Kristensen *et al*, 2004, it was found that there was no significant effect of plane of nutrition in pigs, on the activities of μ-calpain, *m*-calpain or calpastatin at slaughter. However, growth rates did correlate with increased *m*-calpain, cathepsins B and B+L activities. Therefore, in summary, a minimal number of studies have been performed with contradictory results, with regards to the effects of plane of nutrition on the calpain-calpastatin system.

It is important to emphasise that many of the studies, including the bovine plane of nutrition discussed here, focus upon calpastatin mRNA, protein and activity measurements, as *in vivo* the calpain:calpastatin activity ratio is thought to be of greatest importance. This ratio gives an indication of the overall 'proteolytic potential'.

Within the present study 24 calves were initially fed a high plane of nutrition (2.5 x the ME for maintenance) and placed into different feeding treatment groups (see Section 4.1). 8 calves were placed on a low plane of nutrition (LOW group) and feed-restricted to 90% ME for maintenance, with the aim of inducing growth arrest, but not muscle atrophy. A group of 8 calves were re-alimented back up to a high plane of nutrition (REFED group) after a 90% ME feed restriction, with the aim of re-establishing growth and inducing compensatory growth. A third group of 8 calves were fed a high plane of nutrition (HIGH group) throughout the entire trial to encourage rapid growth. Four animals from each group were slaughtered 2 days after

the REFED group began re-alimentation and the remaining animals 13 days later. Animal growth rates were initially 1.02±0.04 kg/day on the high plane of nutrition before dietary treatments began (Lee, 2001). In the LOW plane and REFED groups growth was successfully stopped by restricted feeding (growth rates: -0.01 ±0.02 kg/d and –0.04±0.03 kg/day, respectively). Re-alimentation in the REFED group over 15 days significantly increased growth rates ($P < 0.001$) to 1.14±0.19 kg/day, which did not differ from that of the HIGH group. This suggested that as although growth was successfully re-initiated, compensatory growth was not induced. The HIGH group animals were significantly heavier ($P < 0.05$) at slaughter than the other two groups.

Quantitative mRNA expression of calpain-3, calpastatin, and 18S was analysed from bovine *Longissmus Dorsi* (LD) samples by Quantitative Real-Time RT-PCR, using Taqman Probe and SYBR-Green methods. The ubiquitous μ- and *m*- calpains were unable to be measured due to non-specific template amplification problems, described in Section 4.3.

7.1.2 The Effect of Plane of Nutrition on Extractable Total RNA Yield from Bovine *Longissmus Dorsi* Samples

In the present study the amount of total RNA extracted per g of bovine LD was found to significantly increase ($P < 0.05$) across all treatment groups from the 1st to 2nd slaughter dates (13 days later) (see Table 4.2-1). As samples were randomly selected during the total RNA extraction procedure, this is unlikely to represent an artifact of sample selection. This increase in total RNA is coincident with the period where these young farm animals would be expected to undergo changes in muscle growth and remodelling (which was observed in this study) (G.Lee, 2001). Therefore, although total protein levels may not alter to an extent that can be accurately measured at a significant level in a short time period (13 days-associated with this trial), it would be expected that total mRNA is likely to increase to prepare the myofibers for further adaptations. There was no significant effect of dietary treatment on total RNA, although the REFED group yield was greater numerically than both the HIGH and LOW groups at both slaughter dates. This suggests that there may be a minor effect of refeeding and re-initiation/compensatory growth on total RNA levels.

7.1.3 The Effect of Plane of Nutrition on Relative Expression of Calpain-3

Muscle-specific calpain-3 was an important component to analyse as no previous studies have investigated the effect of altered planes of nutrition and growth rates on calpain-3 gene expression. The precise function of calpain-3 within skeletal muscle is unknown and debatable. Calpain-3 may play a role in transcription factor, myofibrillar structure and metabolic regulation (Baghdiguian *et al*, 2001, Walder *et al*, 2002, Goll *et al*, 2003, Kramerova *et al*, 2004). Therefore calpain-3 is thought to act as a protease with specific regulatory functions and not participate in gross, non-specific proteolysis. Calpain-3 gene expression has been reported to decrease in skeletal muscle during atrophic states including hindlimb unloading in rats (Stevenson *et al*, 2003), denervation in mice (Stockholm *et al*, 2002), cachexia in rats (Busquets *et al*, 2000) and in IL-6 transgenic mice (Tsujinaka *et al*, 1996). A deficiency in calpain 3 leads to LGMD type 2 A and myoapoptosis in humans (Ono *et al*, 1999, Baghdiguian *et al*, 1999, Richard *et al*, 2000, Tidball *et al*, 2000, Chae *et al*, 2001) (as discussed in detail in Section 2.8.4). In all of the states described above there is an associated characteristic protein-catabolic response, leading to an atrophic condition, that may involve the formation of apopotic nuclei.

Within this study it was found that there was no statistically significant effect overall of plane of nutrition on calpain-3 mRNA expression ($P = 0.127$) in LD samples (see Table 4.3.3-1). The LOW plane group in 1st slaughter had lower levels of calpain-3 mRNA compared to both HIGH plane and REFED groups (30% lower relative to HIGH and 29% lower relative to REFED). The LSD value indicated that this was potentially significant at a 5% level. The REFED group had higher calpain-3 values than the LOW plane group (23% higher) at the 2nd slaughter date.

Considering the low numbers of animals per group used in this trial these trends in mRNA expression suggest that calpain-3 mRNA may decrease during restricted feeding. A significant reduction in calpain-3 mRNA has been observed after a 2 day fast in mice (Jagoe *et al*, 2002), although fasting is obviously a far more severe level of nutrient restriction. The potential effects of restricted feeding on lowering calpain-3 gene expression fits in with the observations and hypothesis that calpain-3 mRNA is reduced during catabolic-atrophic states (Tsujinaka *et al*, 1996, Busquets *et al*,

2000, Baghdiguian *et al*, 2001, Stevenson *et al*, 2003). However as will be later discussed, the level of feed restriction was believed not to be severe enough to initiate significant muscle proteolysis and atrophy. This was assumed based on the effects of the feed restriction on growth rates and low level of lean tissue loss. It is probable that if the dietary restriction was more severe leading to muscle atrophy, a greater decrease in calpain-3 gene expression may be observed. The results in this thesis also indicate that calpain-3 mRNA may also be sensitive to the effects of refeeding as mRNA values for the REFED group in 1st slaughter were up to the HIGH plane group value range within the 2 day refeeding period.

There was a trend towards significance for the effect of slaughter date on calpain-3 mRNA expression ($P = 0.073$) (see Table 4.3.3-1). There was an increase in calpain-3 mRNA in both the LOW (46% increase) and REFED (27% increase) groups from the 1st to 2nd slaughter dates. The LSD value indicated that this was potentially significant at a 5% level. The HIGH plane group effectively remained unchanged. As these mRNA expression values were corrected to 18S and do not merely reflect a change in total RNA levels, as reported in Section 7.1.2.

Assuming changes in calpain-3 mRNA results in an increase in the levels of their respective protein the trend in increase in calpain-3 mRNA expression for the LOW and REFED groups (but not HIGH) between slaughter time points, may suggest possible compensatory mechanisms taking place within the myofiber to either avoid atrophy (in LOW plane group) and/or initiate 'catch-up' growth (in REFED group). This is obviously assuming that calpain-3 has a role in the regulation of hypertrophy/atrophy, metabolic and regulatory pathways, as has been suggested by researchers; acting as a highly specific protease not participating in basal proteolysis.

This model for calpain-3 action is supported to some degree by the following observations: p94 protein is localised to titin along the N2 line and Z-disk, and has been been suggested to possibly play a role in the regulation of myofibrillar turnover (Ono *et al*, 1999, Goll *et al*, 2003) (see Section 2.8.2). In calpain-3 deficient (knockout) mice, abnormal sarcomere formation has been reported, suggesting a role of calpain-3 in myofibrillogenesis and sarcomere remodelling (Kramerova *et al*, 2004). Calpain-3 mRNA is expressed at levels ~10 times greater than μ- and *m*- calpains, but

p94 protein is rapidly autolysed when dis-associated from titin suggesting it may have an important cellular function (Ono *et al*, 1999, Goll *et al*, 2003). An absence in p94 leads to a dystrophic condition in the regions of the psoas, soleus and deltoid muscles (LGMD2A), associated with weakness, atrophy and apoptosis. This evidence alone suggests that the muscle-specific calpain-3 protease has important regulatory roles and doesn't act as a 'traditionally-viewed' protease involved in basal protein turnover. Why a deficiency in a protease would lead to a dystrophic state was contrary to previous views on the actions of proteases, and contrary to the Duchenne dystrophic state characterised by raised μ- and *m*- calpain activities. Another perplexing question is why only the muscles of the proximal limbs are affected, when all skeletal muscles are affected in other dystrophic states (e.g. Duchenne). The LGMD2A dystrophic state has found to correlate with a disturbance in the normal functioning of the IκBα/NF-κB pathway within affected skeletal muscle (Baghdiguian *et al,* 1999, Tidball *et al*, 2000, Richard *et al*, 2000, Baghdiguian *et al*, 2001). As calpain-3 has a potential nuclear translocation signal region in its sequence, it has been suggested to potentially alter transcription factor pathways (Ono *et al*, 1999, Goll *et al*, 2003). It has been proposed that calpain-3 may potentially cleave the IκBα inhibitor allowing free NF-κB to increase transcription of a number of cell survival proteins, including anti-apoptotic proteins (Tidball and Spencer, 2000 and Baghdiguian *et al*, 2001). Interestingly, a recent study by Combaret *et al*, 2003 showed that in calpain-3 deficient mice although protein turnover rates, ubiquitination and cathepsins B and B+L activities were not significantly different from controls, cathepsin-L, the 14-kDa ubiquitin-conjugating enzyme and the C2 subunit of the 20S proteasome significantly decreased in mRNA levels by ~47% ($P < 0.005$) in *gastrocnemius* muscle. This may suggest calpain-3 plays a role in the regulation of transcription of proteases. In addition, studies also suggest that a reduction in calpain-3 may also be involved in the response to contraction-mediated cell damage in skeletal muscle (Sultan *et al*, 2001, Féasson *et al* 2002). In the eccentric contraction induced damage study in humans (Féasson *et al* 2002) mRNA expression of calpain-3 was rapidly reduced after exercise whilst there was simultaneously an increase in *m*-calpain mRNA, cathepsins-B+L and proteasome activity. This may suggest that calpain-3 plays a role in the remodelling response to training/contraction-induced damage.

Although speculative it would be interesting to suggest that calpain-3 may have some functional inter-relationships with the caspase system, considering the relationship and similarity between the ubiquitous calpain and caspase system, and their involvement in cell death and the NF-κB pathway (Krebs and Graves, 2001).

Another important observation is that reduced calpain-3 mRNA has shown to be correlated with insulin resistance in humans (Walder *et al*, 2002). It would be interesting to suggest that if calpain-3 does have a potential correlative relationship and role in glucose metabolism and/or insulin function/resistance as suggested by Walder *et al*, 2002, calpain-3 has a bifunctional role related to metabolism and signalling rather than a gross proteolytic role.

The increase in calpain-3 gene expression associated with refeeding is rapid and dramatic in that levels rise to similar levels to that of the HIGH plane group within 2 days of refeeding. Taking the above obsevations and theories in to account this is a potentially important observation that may suggest that calpain-3 mRNA is sensitive to nutritional intake and may be involved in triggering the compensatory growth response associated with refeeding.

Therefore in summary, a reduction or loss in calpain-3 mRNA as observed during the conditions described (including fasting) may potentially aid in inducing or be associated with a loss in myofibrillar integrity and/or an increased susceptibility for atrophy and apoptosis. The rapid rise in calpain-3 mRNA with refeeding may potentially suggest calpain-3 has a signalling role that may aid in the induction of the compensatory growth response.

7.1.4 The Effect of Plane of Nutrition on Relative Expression of Calpastatin

The mRNA expression of the endogenous calpain inhibitor calpastatin did not significantly alter with plane of nutrition ($P = 0.874$) in bovine LD samples (see Table 4.3.3-2). However, the LOW plane group in the 1st slaughter had higher levels numerically compared to the HIGH plane (25% greater relative to HIGH group) and REFED group (33% higher relative to REFED group).

Kristensen *et al*, 2002 hypothesised that during a feed restriction calpain-dependent proteolysis is down-regulated and net protein turnover rates are reduced. A potential mechanism by which this may occur is through a rise in calpain-inhibitory calpastatin activity. Stevenson *et al*, 2003 investigated the effects of hindlimb unloading in rat *Soleus* muscle for 1, 4, 7 and 14 days, on the expression of numerous genes using Affymetrix Gene Chip technology. Interestingly, calpastatin was significantly upregulated, calpain-2 did not change and calpain-3 significantly downregulated, along with a calpain activator (diazepam-binding inhibitor). This may suggest that in some atrophic-catabolic states calpastatin is differentially regulated and may be up-regulated initially to avoid excessive calpain-dependent proteolysis. Considering the low numbers of animals per group used in this trial, although not a significant change, the numerical difference in the LOW group fits with the hypothesis that an increase in calpastatin during a feed restriction may act as a compensatory mechanism to protect the muscle from excessive calpain proteolysis, subsequent myofibrillar degradation and myofiber atrophy.

However, observations within our laboratories showed that immunoreactivity 135 kDa calpastatin estimated at 0 hr post-slaughter was not significantly affected ($P > 0.05$) by feeding level in LD muscle from calves in this present trial (Sazili, 2003, Sazili *et al*, 2003). Immunoreactivity of μ- calpain, m- calpain was also unchanged.

There was also an increase in calpastatin mRNA expression for all dietary treatment groups with a trend towards significance ($P = 0.085$) from the 1st to the 2nd slaughter dates (see Table 4.3.3-2). The REFED group increased over the 13 day period between slaughter dates and the LSD value indicated that this was potentially significant at a 5% level. These mRNA expression values were corrected to 18S and don't merely reflect a change in total RNA levels, as reported in Section 7.1.2.

Interestingly, the numerical values for 135 kDa calpastatin immunoreactivity at 0 hr post-mortem increased numerically in all dietary treatment groups across slaughter dates (Sazili, 2003, Sazili *et al*, 2003).

The potential trend of an increase in calpastatin gene expression in a short time period of 13 days (between slaughter dates) may be part of the cellular growth program

within skeletal muscle, i.e. as an animal goes through rapid growth an increase in calpastatin would act as one mechanism of many to initiate skeletal muscle growth.

As described within Section 2.8.3, increased calpastatin activities have been reported in the pelvic limbs and back muscles of callipyge lambs, which have 30-40% more muscle mass (Goll *et al* 1998). Mice with overexpression of a calpastatin transgene were observed to have greater muscle mass (Otani *et al*, 2004). Overexpression has also been shown to reduce hindlimb unloading atrophy by 30% (Tidball and Spencer, 2002) and reduce calpain activity, necrosis and dystrophic pathology in *mdx* dystrophic mice (Spencer *et al* 2002). β-adrenergic stimulation increases lean mass deposition (Goll *et al*, 1998, Grant *et al*, 1998) thought to be due in part to an induced reduction in calpain proteolysis, through increased calpastatin inhibitory activity (Parr *et al*, 1992, Speck *et al*, 1993, Sensky *et al*, 1996, McDonagh *et al*, 1999, Navegantes *et al*, 2002). Therefore, these overall observations may suggest that for a significant change in calpastatin to be induced, there needs to be a more drastic or 'unnatural' stimulatory effect on hypertrophy/atrophy signalling pathways within skeletal muscle.

7.1.5 Summary of Plane of Nutrition Discussion

In summary, there was a significant increase (P <0.05) in total RNA extraction yield per g of bovine LD across all dietary treatment groups over the 13 day period between slaughter dates. This suggests that in young, fast-growing calves, the total cellular RNA pool increases in LD over a short time period, irrespective of plane of nutrition; possibly in preparation for further cell growth and remodelling events. Interestingly, according to data from G.Lee thesis (Lee, 2003) there was an increase in GH receptor mRNA in LD of calves from this trial from the 1st to the 2nd slaughter dates. It would be interesting to speculate whether a significant increase in GH receptor expression would lead to a greater amount of GH stimulatory effects on skeletal muscle and subsequent rise in protein synthesis (and total RNA pool).

Although not significant the REFED group total RNA yield was numerically greater than both the HIGH and LOW groups (at both slaughter dates). This trend may fit with the hypothesis that refeeding after a feed restriction induces a compensatory

growth response. Therefore once the animal is re-fed, a further up-regulation in the cellular total RNA pool may take place. Although noting that heightened compensatory growth didn't take place in the REFED group within this trial (confirmed by growth rates). Kristensen *et al*, 2002, found that total RNA concentrations in *Semitendinosus* in pigs were significantly greater in highly fed and refed pigs and correlated with growth rates. Interestingly, the group also found that total RNA concentrations in LD significantly correlated with growth rates and *m*-calpain activities.

The trend for calpain-3 and calpastatin gene expression to increase numerically in treatment groups across slaughter dates (as discussed in 7.1.3 and 7.1.4), may also be as the young calves (slaughtered at 5 month old) were still undergoing changes in muscle size (hypertrophy), metabolic and contractile properties (remodelling). This may be confirmed in part by the change in total RNA discussed above. An essential part of these processes during rapid growth and development would hence involve cytoskeletal remodelling and myofibrillar hypertrophy, which may constitutively require an increase in calpastatin and specific functions of calpain-3. Note that Sazili, 2003 found that calpastatin immunoreactivity at 0 hr post-slaughter was numerically higher in all treatment groups in the 2nd slaughter date, compared to 1st slaughter date.

It was important to take into account that a 90% of maintenance ME feed restriction (LOW group) was not severe enough to induce atrophy in young, fast-growing calves. At 90% of maintenance ME a reduction in growth rate to conserve nutrients, an increase in fat mobilisation and oxidation is the theoretical observation unless the animal develops an illness or infection. Atrophy only develops when the length and severity of the feed restriction is increased. According to data from G.Lee thesis, during the LOW plane feed restriction there was a group decrease in body weight, growth rates and increase in fat mobilisation, which was altered after re-alimentation, indicating a significant metabolic effect on the animals.

G.Lee also found that LD GH receptor mRNA and IGF-1 mRNA did not significantly change with dietary treatment, suggesting that the feed restriction wasn't severe; even though hepatic IGF-1 mRNA was significantly reduced and insulin levels reduced. Therefore, the anti-proteolytic effects of local IGF-1 may have been main-

tained. According to A.Sazili thesis (Sazili, 2003), calpain protein levels were not significantly raised during the feed restriction. This suggests that the LOW plane diet induced growth arrest, but not myofiber atrophy and probably didn't significantly increase calpain-dependent degradation; as there was no change in calpain or calpastatin protein at slaughter in either groups. However, activity was not measured.

Potentially important observations seen with dietary treatment included lower calpain-3 levels in the LOW plane group and the rapid rise in calpain-3 in REFED group, within the 1st slaughter date groups. These potentially significant results indicate that calpain-3 gene expression may alter rapidly with change in nutritional intake in a pattern which fits with current hypothetical functions for calpain-3.

With regards to transcriptional control of calpain-3, little is known at present. As calpain-3 is reduced in so many diverse atrophic-catabolic states it is probable there is a common regulator/s of transcription that alters rapidly after the onset of various states. Féasson *et al*, 2002 found that calpain-3 mRNA was decreased immediately post-eccentric exercise, suggesting that transcription is rapidly regulated. Calpain-3 mRNA has been found to be reduced during cachexia (Busquets *et al*, 2000) which may suggest involvement of immuno-inflammatory mediators. IL-6 transgenic mice have been found to have lowered calpain-3 mRNA which was inhibited when an IL-6 receptor antibody was administered (Tsujinaka *et al*, 1996), suggesting proinflammatory cytokines are involved. Other obvious targets would include endocrine mediators including glucocorticoids, a reduction/resistance to insulin /IGF-1 and possibly GH.

Binding sites have been found within the large and small calpain subunits for transcription factors AP-1 and CCAAT/enhancer binding protein (C/EBP) (Penner *et al*, 2001, Hasselgren and Fischer, 2001), whereas analysis of the calpain-3 sequence has found binding sites for NF-kB in the promoter region of the gene, but not AP-1 or C/EBP (Sorimachi *et al*, 1996). AP-1, C/EBP and NF-kB are associated with immuno-inflammatory responses and all have been found to be up-regulated during sepsis (Macdonald *et al*, 2003), and specifically within muscle during sepsis (Penner *et al*, 2001, Hasselgren and Fischer, 2001). AP-1, C/EBP and NF-kB have therefore been suggested to be involved in the induction of the proteolytic response in muscle,

providing the trigger for an increase in transcription of protease system components (Penner *et al*, 2001, Hasselgren and Fischer, 2001). It is possible calpain-3 and the ubiquitous calpains may be differentially regulated in some way by these transcriptional regulators. This is likely considering that during many of the catabolic-atrophic states mentioned there is an associated decrease in calpain-3, but increase in ubiquitous calpain mRNA/activity (see Section 2.8.3) and rise in other proteolytic system components, e.g. lysosomal-cathepsins and ubiquitin-proteasome components (see Sections 2.7.2 and 2.9.3). Considering also the potential relationship between p94 and the IκBα/NFκB pathway, it would be interesting to suggest that NFκB may in some way play a regulatory role in calpain-3 transcription.

Calpastatin has been proposed to be regulated by the cAMP responsive element binding protein (CREBP) activated through a β_2-adrenergic pathway involving PKA (Navegantes *et al*, 2002). It is known that during fasting and many stressful catabolic states endogenous catecholamine (noradrenaline and adrenaline) levels rise above normal baseline levels (Biolo *et al*, 1997, Ingenbleek and Bernstein, 1999). Obviously the level depends on the intensity of the stressful stimuli (Ingenbleek and Bernstein, 1999). Speculative questions of interest therefore include whether a repeated trial with a larger number of animals and a more severe feed restriction would initiate significant rises in plasma noradrenaline and adrenaline. Would these raised levels of endogenous catecholamines in turn significantly increase calpastatin mRNA, protein and activity levels. This would be interesting so as to understand whether calpastatin mRNA rises in certain catabolic-atrophic conditions, as has been observed in hindlimb un-loading by Stevenson et al, 2003, and the non-significant numerical increase in mRNA expression observed within this trial in the low plane group of the 1st slaughter.

Overall, feeding affects multiple signalling pathways in skeletal muscle, through the effects of nutrients and endocrine mediators. Therefore, in reality calpain-3 transcription may be regulated by the net effect of a number of different stimulatory and inhibitory pathways. For example, the effects of feeding on the ubiquitous calpains and calpastatin has been found to be very variable across animal studies, leading to the development of opposing hypotheses of system regulation by researchers as described in 7.4.1. This suggests that as no true consensus has been found, feeding and

planes of nutrition alters a myriad of complex signalling pathways that may lead to variable effects. Therefore, transcriptional regulators may be speculated on but until extensive studies on gene transcription and promoter studies provide conclusive evidence, little can be known for definate.

Another important point to note is that the bovine *Longissmus Dorsi* (LD) samples are predominantly fast-twitch fibers (Totland and Kryvi, 1991). Fast-twitch fibers, as described in Section 2.2.3 are thought to be have dynamic characteristics, greater plasticity for necessary metabolic and contractile adaptations and most susceptible to atrophy and hypertrophy (Pette and Staron, 2000, Maltin *et al*, 2001, Spangenburg and Booth, 2003). Expression levels of calpastatin is known to vary between fiber types, with predominantly slow twitch muscles having greater levels compared to predominantly fast twitch muscles (unpublished observations). One question of interest during the rapid growth and development phase in calves, is whether fiber type characteristics alter in LD, would this in turn affect/be dependent on calpain-3 and calpastatin and would feeding level have an additional effect.

It is important to re-iterate that the low number of animals per treatment group may have contributed to many of the trends observed in the mRNA expression of calpain-3 and calpastatin being non-significant. As many of the trends are logical changes as the fact they did not reach significance may be down to a lack of treatment group numbers. For example, a future trial may involve up to 8-12 animals per treatment group to observe an improved statistical significance.

In addition the studies carried out in this thesis using Real-Time PCR were some of the first carried out within the Division of Nutritional Sciences and therefore indicated some of the potential problems associated with this technique.

7.2 cDNA PROBE DEVELOPMENT

7.2.1 Introduction

As described within Section 5, twenty cDNA probes were successfully generated by RT-PCR for components of the four proteolytic systems discussed within this thesis. They were designed to be used in further probe-hybridisation experiments such as Northern blotting and possibly cDNA macroarray experimentation. The cDNA macroarray experimental methods considered were based on Clontech, custom self-made arrays (BD Biosciences Clontech, 2002). The approach being similar to microarray technology except a small select number (~20) of cDNA probes of ~200-300 bp are required. Microarrays have been used previously (Nguyen *et al*, 1995, Lee *et al*, 1999, Feng *et al*, 2000, Lockhart and Winzeler, 2000). The macroarray was considered as a method of investigating 'global' protease gene expression in a single experiment, whereas methods such as Quantitiative Real-Time PCR, Northern blotting and RPA's (Ribonuclease Protection Assays) are specific to a single expressed gene of interest at a time. Testing of the cDNAs before their application to an array indicated that not all the probes had sufficient specificity to be used to identify specific mRNA species. Due to time constraints, Northern blotting was performed instead of the macroarray approach, using a specific selection of cDNA probes tested on porcine RNA. Those expressed genes of interest of components of proteolytic systems that are known to have important regulatory functions and/or key roles during atrophy and hypertrophy were used.

Only a small number of the PCR products/cDNA probes were generated first time experimentally. Many required a long testing and optimisation period, using different reaction conditions, PCR primers and Taq enzymes to attain a specific PCR product (as described in Section 5.1).

7.2.2 Probe Development and Testing

Of the caspase system, only caspase-3 had porcine sequence data available. Caspase-3 cDNA was successfully generated and found to have a 99% sequence identity match to the porcine caspase-3 sequence (after DNA sequencing). This made it an

ideal candidate probe for porcine RNA Northern blot probing; especially considering caspase-3 is an effector protease with a possible key role in myofiber development, cell death/survival and degradation of specific proteins during muscle hypertrophy/atrophy (see Section 2.10.5). Caspase-3 is also used in other experiments by researchers to indicate a generic change in the caspase system.

Caspase -6, -7 and ARC (Apoptosis Repressor with CARD domain) had no porcine sequence data available, therefore DNA sequenced PCR products were assumed to be the porcine expressed genes of interest (based on sequence similarity with other species sequences). ARC was also tested on porcine Northern blots as it was believed to play an important role in muscle-specific caspase inhibition. Specific band signals detected for both caspase-3 and ARC were determined as being the correct size based on database sequence analysis (Appendix B). However, data for ARC was unclear as there was only human sequence available in the database. Unfortunately caspase-3 and ARC were unable to produce reproducable and quantifiable band signals on Northen blots. This probably reflects low tissue expression levels in normal, basal cell conditions. This was reflected in the difficulties in trying to RT-PCR these cDNAs which produced low levels of cDNA even after extended cycles. As described in Section 2.10, the caspases are constitutively expressed zymogens, which are activated on autolysis. As they are involved in apoptosis induction, it may be a dangerous cellular situation to have high levels of mRNA and protein of caspases in normal, functional cells. However, after specific stimuli, e.g. chronic cytokines (TNF) the cell may then require an up-regulation of caspase mRNA. Detecting these changes would probably require a more sensitive method like Quantitative Real-Time PCR. However, subsequent experiments in our laboratories have also indicated that caspase-3 is difficult to quantify using Real-Time PCR due to its low levels of expression and resulting high Ct values obtained close to the limits of sensitivity.

Cathepsin L and H both had available porcine sequence data available and specific PCR products were generated, both with 99% sequence identity with the porcine database sequences. Cathepsins B and D had no porcine sequence data available and PCR was problematic, although a specific band of the correct size and identity was generated. The cathepsin D probe had to be generated from a human EST IMAGE clone and therefore the PCR product was human tissue specific.

Cathepsin L was used in subsequent porcine RNA Northern blot testing procedures as firstly; the PCR product of the correct identity was easily generated and porcine specific. Secondly, Cathepsin L is thought to play a major role in the response to catabolic stimuli within skeletal muscle (see Section 2.7.2). Cathepsin L produced a highly reproducable and quantifiable signal of the correct size with testing. (see Section 5.3).

Ubiquitin was the only ubiquitin-proteasome system component to have porcine sequence data available. Subsequent PCR produced a specific band of the correct size and sequence identity (99% identity to porcine database sequence). For E2G1, C8 and atrogin-1, specific PCR products of the correct sizes were generated and from DNA sequencing their sequence identities were believed to be correct, by comparing them to those already present within the database. E2G1, atrogin-1 and ubiquitin were then tested on Northern blots as they may all play important roles in skeletal muscle protein degradation during atrophic-catabolic states (see Section 2.9.3). E2G1 was chosen as very little information regarding this ubiquitin-conjugating enzyme is available, except that it is highly expressed in skeletal muscle and therefore may play a role in the degradation of muscle-specific proteins (e.g. myofibrillar proteins). It may play a similar role to $E2_{14K}$, ubiquitin-conjugating enzyme, known to be up-regulated during catabolic conditions (Wing and Banville, 1994, Solomon *et al*, 1998). E2G1 and ubiquitin produced reproducable and quantifiable bands with Northern blots. After extensive sequence database analysis (as described in Appendix B) it was found that E2G1 has transcript variants that may be expressed in porcine skeletal muscle (although based on deduction). Ubiquitin is known to produce two specific band signals on a Northern blot (Llovera *et al*, 1999, Busquets *et al*, 2000), although the band sizes depend on the species. Atrogin-1 produced multiple bands of unknown identity on Northern blots. Database analysis showed that Atrogin-1 may have transcript variants in human tissue (see Appendix B). However, as other bands were unidentifiable and no porcine sequence data is available, atrogin-1 was not used in further experiments.

Although porcine sequence data for μ- and *m*- calpains, calpain-3 and calpastatin was available and used in designing PCR primers, PCR was problematic. To produce a

specific PCR product of the correct identity, PCR was performed using porcine clones (previously made by colleagues within the department) as DNA template. Calpain-10 was unable to be successfully generated from porcine tissue, using primers based on human sequence, as no porcine sequence is available at present. Subsequent studies have had difficulty isolating this cDNA. Therefore, a cDNA probe was successfully generated by PCR using a human calpain-10 EST IMAGE clone as template. Calpain -3 and -10 were the only components of the Calpain system to be tested on porcine Northern blots. Calpain-3 produced a specific, reproducable and quantifiable signal at the correct size (based on evaluation of transcripts in Appendix B). Calpain-10 produced a single specific band signal which was believed to be the correct mRNA species (based on human sequence data). However, the non-reproducability of the signal may be due to low expression levels or simply that the porcine sequence differs somewhat in sequence identity to human calpain-10.

Of the internal standard probes generated, actin and alpha-tubulin had porcine sequence data available, where as TFIID had only human and murine available. However, PCR products of the correct identity were produced and actin was later used for Northern blot testing as it has been used as a reliable and suitable internal standard in a number of settings. Actin probing produced a single reproducable and quantifiable band of the correct size.

7.2.3 Summary

Twenty cDNA probes were generated by PCR with varying difficulty with the aim of hybridising specifically to transcripts in porcine skeletal muscle tissue RNA samples. Northern blotting techniques were used to determine whether the cDNA probes would specifically hybridise to their corresponding expressed target gene of interest within porcine RNA samples. Therefore, if the technique would not work for specific probes then it would be unlikely to work on a macroarray, which essentially relies on the same experimental technology. As no pig nucleotide sequence was available for many of the expressed genes of interest, PCR and subsequent probe testing on porcine RNA Northern blots became diffcult and time consuming. Many of the band signals produced on Northern blots had to have their mRNA identities deduced based on literature and further database searches for transcript variants and species variabil-

ity. As non-specific cross-hybridisation with other similar mRNA species is possible this process had to be rigorous. Understanding that all cDNA probes were DNA sequenced and their identities were thought to be closest matched to the expressed genes of interest obviously strengthened any questions on band identities.

7.3 COMPARISON OF GENE EXPRESSION TECHNIQUES

The use of cDNA probes in Northern blotting experiments has many benefits over other methods and has been considered to be a reliable and reproducable technique in quantifying gene expression. If enough experimental sample numbers, strict RNA extraction and quantification procedures are followed and probes optimised correctly, Northern blotting may produce specific reproducable band signals of a measurable size in kb and intensity. One problem with Northern blotting however, is the physical inability to be able to run a large number of RNA samples (>30) by gel electrophoresis and blot them. This is due to obvious size limits of the gel former, of the number of samples which can be loaded onto a single gel.

Quantitative Real-Time PCR has found to be a very sensitive method, allowing a large number of samples to be analysed with quick throughput. However, there are many problems associated with reaction optimisation and reproducability as contamination issues, non-specific amplification and incorrect reaction efficiencies can easily invalidate results. As described within Section 4.3, it was not possible to successfully quantify μ- and *m*- calpain due to problems with reduced reaction efficiency and non-specific template amplification, making subsequent experiments invalid. The use of a Taqman probe offers a higher level of specificity due to binding of probe instead of primers alone. However, the main problems associated with Taqman probes is the financial cost and time required to optimise the experimental conditions to ensure specific detection of mRNAs. Therefore, I was unable to repeat experiments for μ- and *m*- calpain using Taqman probes.

Microrarrays have 1000s of cDNAs of expressed genes of interest dotted onto a solid support (usually glass). This allows an overview of the global picture of gene expression in a particular tissue sample. The issues with this method include its great financial expense, difficulty with sensitivity and significance of results. Macroarrays are

not as expensive as microarrays and can be custom made. However, little studies have been performed using custom made, non-commercial arrays. Specificity of probes is a major consideration with this technique as the probes have to be designed for optimised specificity. Macroarray development has never been attempted before in out department and therefore is a part of future work. Considering all 20 cDNA probes were successfully generated, it would be interesting to have them dotted onto a nylon support and used in array test experiments.

Although not described in this thesis, ribonuclease protection assays (RPA's), can also be a very sensitive and accurate method of quantifying gene expression, once method has been optimised. This is another technique to be developed as part of future work.

7.4 THE EFFECTS OF A BETA-ADRENERGIC AGONIST ON PROTEASE EXPRESSION IN PIGS

7.4.1 Introduction

The following studies to be discussed are concerned with the effects of beta-adrenergic stimulation on the mRNA expression of muscle-specific calpain-3, cathepsin-L and E2G1 (a ubiquitin-conjugating enzyme), in pig *Longissmus Dorsi* (LD) skeletal muscle.

Following the development studies described above, Northern blotting was used as the technique of choice as it has been used previously to successfully quantify the mRNA expression of multiple proteolytic system components during various catabolic-atrophic states (Mansoor *et al*, 1996, Rallière *et al*, 1997, Mosoni *et al*, 1999, Deval *et al*, 2001, Farges *et al*, 2002).

The selection of expressed genes analysed were chosen based on their functional roles within skeletal muscle, relevance to hypertrophy/atrophic states. In addition, the specificity, quantifiability and reproducability of the cDNA probes previously generated, with porcine RNA Northern blots was an important concern.

From studies examining proteolytic enzyme expression in atrophy studies cathepsin-L is thought to play a key role during the early stages of atrophic and catabolic states, with increases observed at mRNA and protein level (Deval *et al*, 2001). For example, cathepsin-L mRNA increased in mice *Gastrocnemius* within 24 hour of fasting, when 11 other lysosomal proteases did not change (Jagoe *et al*, 2002). Cathespins L mRNA expression increased two- to three fold in rat *Gastrocnemius* during fasting, cancer cachexia, uremic and diabetic states when other lysosomal proteases did not change (Lecker *et al*, 2004).

E2G1 is a specific E2 ubiquitin-conjugating enzyme, found in abundance within skeletal muscle and therefore may play a role in the degradation of muscle-specific proteins by the ubiquitin-proteasome system within skeletal muscle. E2 enzymes have been previously observed to increase in mRNA expression in muscle during a number of atrophic-catabolic states (Wing and Banville, 1994, Solomon *et al*, 1998, Hasselgren and Fischer, 2001).

Calpain-3 function has been discussed a number of times throughout this thesis. It is of great interest as it is thought not to act as a protease involved in gross protein turnover, but may have important regulatory roles within skeletal muscle. It has been hypothesised to play a role in myofibrillar integrity, glucose-fatty acid metabolism and cell survival (Ono *et al*, 1999, Tidball and Spencer, 2000, Baghdiguian *et al*, 2001, Walder *et al*, 2002, Goll *et al*, 2003, Kramerova *et al*, 2004) and known to decrease at mRNA level in response to catabolic states like cachexia (Busquets *et al*, 2000) and denervation (Stockholm *et al*, 2002). It was important to focus attention towards calpain-3 as little is known about the effects of β-adrenergic stimulation on calpain-3, where as there is a wealth of confirmed information and observations known with regards to the effects of β-adrenergic stimulation on the ubiquitous calpains and calpastatin.

The first two studies involved the effects of chronic and acute administration of the selective β_2-adrenergic agonist clenbuterol, a known nutrient-repartitioning agent. As previously described, clenbuterol is known to induce fat mobilisation and muscle hypertrophy in farm animals when chronically administered (Mersman, 1998, Bell *et al*, 1998). Clenbuterol and other selective β_2-adrenergic agonists are thought to in-

duce protein accretion and muscle hypertrophy through decreasing protein degradation and possibly by increasing synthesis (Mersman, 1998, Bell *et al*, 1998, McDonagh *et al*, 1999). The calpain-calpastatin system is thought to be the principal protease system that is affected by β_2-adrenergic agonists (Bardsley *et al*, 1992, Mersman, 1998, Goll *et al*, 1998, Navegantes *et al*, 2002). A decrease in mRNA and activity of μ-calpain, along with increases in calpastatin mRNA and activity, with variable effects on *m*-calpain has been reported with β_2-adrenergic agonist administration (Parr *et al*, 1992, Bardsley *et al*, 1992, Speck *et al*, 1993, McDonagh *et al*, 1999, Navegantes *et al*, 2002). Little is known regarding the effects of clenbuterol and β-adrenergic agonists on calpain-3 gene expresson. An incomplete report by Ji *et al*, 1993 (abstract) found that administration of 20 ppm ractopamine (a β-adrenergic agonist) for 24 days in pigs decreased calpain-3 gene expression by 30% ($P < 0.02$) in LD muscle. The effects of clenbuterol on other proteolytic system components remains largely unknown.

The third study to be discussed involves the effects of chronic adrenaline administration on calpain-3 and cathepsin-L mRNA expression. Adrenaline is an endogenous non-specific β-adrenergic receptor agonist known to have a catabolic effect on lipid and glucose metabolism, but a positive anabolic effect on protein metabolism in skeletal muscle (Rooyackers and Nair, 1997, Mersman, 1998, Navegantes *et al*, 2002). Adrenaline has been reported to decrease proteolysis within skeletal muscle through a β_2-adrenoceptor mediated pathway, however little is known about the precise effects of adrenaline on proteolytic system regulation (Rooyackers and Nair, 1997, Navegantes *et al*, 2001, Navegantes *et al*, 2002). Samples from this present study were previously analysed by colleagues from the department of Nutritional Sciences. It was found that adrenaline infusion had no effect on μ- and *m*- calpain activities, but increased calpastatin mRNA and activity ($P < 0.01$) in porcine LD muscle, leading to a reduced calpain:calpastatin activity ratio ($P < 0.01$) (Sensky *et al*, 1996, Parr *et al*, 2000).

The β-adrenergic stimulation studies differ greatly from the plane of nutrition trial as previous studies suggest conclusively that the specific nutrient repartitioning agents, β-adrenergic agonists, increase muscle protein accretion significantly, coinciding with consistently observed significant alterations in the ubiquitous calpain system

and calpastatin. The consistant observed alterations in activity and gene transcription of calpastatin and the ubiquitous calpains has been suggested to be linked to activation of specific β-adrenergic stimulatory pathways, leading to cAMP formation, PKA activation and phosphorylation of a number of target proteins (see Section 2.3.4.3) (Navegantes *et al*, 2002). Target proteins suggested include those involved in glycogen metabolism, cAMP response element binding protein (CREBP), calpains and calpastatin (as phosphorylation sites have been identified within sequences) (Frayn, 1997d, Goll *et al*, 2003). It is believed CREBP may regulate the transcription of calpastatin as CREBP binding sites have been identified within the bovine calpastatin sequence (Cong *et al*, 1998).

Therefore, specific β-adrenergic stimulatory pathways have been confirmed to affect the ubiquitous calpains and calpastatin, however, this is in direct contrast to the highly variable effect feeding and plane of nutrition has on the ubiquitous calpains and calpastatin. As multiple signalling pathways are altered globally by the response to feeding due to alterations in nutrients and hormones, this may lead to unpredictable effects on the calpain proteolytic system. Calpain-3 however, was shown from data in this thesis to be potentially responsive to plane of nutrition, but regulators of transcription are unknown. Calpain-3 as yet, has not been studied extensively in relation to β-adrenergic stimulation.

Lastly, it was important to take in to account when analysing changes in data that pigs are not as responsive to β-adrenergic agonists as other farm animals, such as cattle and sheep (Mersmann, 1998). From numerous studies performed it has been found that on average there is a 4% increase in muscle mass with β-adrenergic agonists in pigs, 10% in cattle and 25% in sheep. (Mersmann, 1998).

7.4.2 The Effect of 24 Hour and 7 day Clenbuterol Treatment in Pigs

The present study investigated the effects of an acute (24 hour) and chronic (7 day) 5 ppm daily dose of clenbuterol on glycogen store depletion and the mRNA expression of muscle-specific calpain-3, cathepsin-L and E2G1 within porcine LD samples, using Northern blot hybrisation experimental techniques.

To ascertain whether the 5ppm clenbuterol treatment dose was adequate, effective and produced the desired characteristic effects on metabolism, glycogen levels were measured in porcine LD samples. Glycogen assay experiments indicated there was a highly significant effect ($P < 0.001$) of clenbuterol on glycogen store depletion (see Table 6.2.3-1). Glycogen levels (mg / g tissue) were depleted by 85% (relative to controls) within 24 hours of treatment indicating that the expected effect on glycogen breakdown and depletion was observed. This finding is in agreement with the observation that β_2-adrenergic stimulation has a catabolic effect within muscle and fat tissue with regards to carbohydrate and fat metabolism (Frayn, 1997d, Mersmann, 1998). Within skeletal muscle these processes are believed to be activated through β_2-adrenergic pathways described within Section 2.3.4.3 (see Figure 2.3.4.3-1), involving cAMP formation and PKA activation (Frayn, 1997d, Mersmann, 1998). Therefore, results from this study confirmed that the intracellular β_2-adrenergic pathways believed to alter calpain-calpastatin system components are being activated at this lower dose of β_2-adrenergic agonist (5 ppm). Of interest however was the observation that levels began to rise back up after 7 days of treatment, i.e. a 55% decrease, relative to controls. The subsequent rise in glycogen stores after 7 days of treatment may be attributed to the down-regulatory, de-sensitisation effect of chronic stimulation of β_2-adrenergic pathways within skeletal muscle (Mersmann, 1998).

Total RNA was hence extracted from bovine LD muscle tissue. Analysis of extraction yields per 0.1 g LD tissue showed there was no significant effect of clenbuterol treatment on total RNA yield ($P = 0.278$) (see Figure 6.2.2-1).

A northern blot was prepared and hybridised with radio-labelled cDNA probes for the proteolytic system components and the internal standard actin (described in Section 6.2.4). Analysis of northern blot band signals for actin showed there was no significant effect of clenbuterol treatment on actin mRNA expression ($P = 0.701$) (see Table 6.2.4-2). Assuming equal amounts of total RNA was loaded onto the northern blot, the analysis above of total RNA yield and actin expression indicates that any measurable changes in gene expression for other proteolytic system components are not the result of experimental errors or artifacts.

Muscle-specific calpain-3 mRNA expression was found to not significantly change with clenbuterol treatment, although levels did increase numerically by 32%, relative to Control group, after 1 week of treatment. Previous observations had reported that calpain-3 mRNA significantly decreased by 30% with 20 ppm ractopamine treatment in pigs (Ji *et al*, 1993).

There was no significant effect of clenbuterol on E2G1 mRNA expression, although values increased numerically by 57%, relative to Control group after 24 hour clenbuterol treatment. If this is a trend it may signify a rapid response to an acute dose of clenbuterol. At present however, there is no literature that has studied the effects of β_2-adrenergic agonists on the expression or regulation of E2 enzymes.

The greatest effect in terms of mRNA expression was the change in cathepsin-L mRNA levels which increased by 339%, relative to Control group, after 24 hour clenbuterol treatment (P <0.001). In the 7 day clenbuterol group cathepsin-L mRNA was 49% greater, relative to Control group, therefore decreased to a level found to be significantly lower than the 24 hour group (P <0.01). The pattern of mRNA expression suggests that there is a rapid, acute response to clenbuterol treatment, which decreases in intensity over time, after 7 days of chronic stimulation. This is a similar pattern of response to the effects of clenbuterol on glycogen stores. Data is of a similar relative magnitude but in the opposite direction, i.e. glycogen stores are depleted as cathepsin-L mRNA expression is increased. The trends of a decline in response over time may be due in part to the effects of chronic stimulation on the desenstisation and downregulation of β-adrenergic pathways.

The response and pattern of expression of cathepsin-L mRNA has not been reported before and it may signify an acute response to β-adrenergic stimulation. As has been described throughout this thesis the catecholamine and β-adrenergic agonist compounds are known as counterregulatory and catabolic hormones. Their positive effects on hypertrophy and lean body mass deposition are only observed after the chronic moderate-high dose administration of selective β_2-adrenergic agonists (Mersmann, 1998). Therefore, it may be that the initial effects of these compounds are to signal an acute stress response, similar to that produced by endogenous catecholamines and activate specific degradatory systems differentially. If the non-

significant trend of E2G1 to increase within 24 hours of administration is a reflection of a general change in this proteolytic system then it strengthens the argument discussed here. Interestingly, many studies have shown variable results with regards to the effects of stimulation on protein degradation. However, there is conclusive evidence that β-adrenergic treatment lowers calcium-dependent, calpain-mediated proteolysis (Navegantes *et al*, 2002).

Although highly speculative one explanation may be that sarcoplasmic proteins are differentially regulated to myofibrillar proteins. Clenbuterol treatment may decrease myofibrillar degradation (through calpain-calpastatin system alterations), yet simultaneously increase sarcoplasmic protein degradation via specific lysosomal cathepsin activation. McDonagh *et al*, 1999 reported that 7 day treatment with clenbuterol increased protein synthesis ($p < 0.01$) but had no effect on degradation, even though μ-calpain activity ($P < 0.01$) was reduced and calpastatin activity ($P < 0.1$) increased. He suggested also that the discrepancy may be due to a differential regulation of myofibrillar and sarcoplasmic protein degradation. E2G1 is involved in the degradation of specific cellular proteins, including sarcoplasmic proteins, via ubiquitin tagging and subsequent targetting to the proteasome.

Another speculative theory may be that the dramatic rise in cathepsin-L and numerical increase in E2G1 may be part of a rapid response in a muscle remodelling-growth program, induced by β_2-adrenergic agonists. As has been suggested throughout this thesis, during periods of muscle remodelling and catch-up/compensatory muscle growth there is a tendency for protein degradation to increase, or for specific proteolytic system components to be upregulated. As mentioned previously in bovine plane of nutrition discussion, Kristensen et al, 2002 found that growth rates correlated with *m*-calpain activities in pigs and an increase in the μ-calpain-calpastatin ratio was observed in refed pigs (after a feed restriction). Kristensen *et al*, 2004 found growth rates correlated with increased *m*-calpain, cathepsins B and B+L activities in pigs fed different planes of nutrition.

Interestingly, mRNA levels for the 14kDa-ubiquitin conjugating enzyme E2 were found to decrease in response to muscle reloading (18 hr post-reloading), after unloading-induced atrophy, in addition to other ubiquitin-proteasome system compo-

nents (ubiquitin and 20S proteasome subunits C8, C9) and *m*-calpain increasing in mRNA expression (Taillandier *et al*, 2003). It was suggested by the author that this response may play an important role in the potential remodelling response to reloading-induced 'catch-up' growth and recovery. Féasson *et al*, 2002 found that the rapid response to eccentric exercise included an increase in *m*-calpain (1 day post-exercise) and eventually over time (7-14 day post-exercise) increases in cathespins B+L and proteasome activities. Along this line of thought β-adrenergic agonist administration has been obseved to increase *m*-calpain activity in some studies (Parr *et al*, 1992, Bardsley *et al*, 1992).

Further work is needed to clarify if the increase in cathepsin-L mRNA is a result of an increase in transcription due to stimulation of β_2-adrenergic pathways, cAMP formation and PKA activation. The logical steps to take would be to analyse the cathepsin-L sequence data and attempt to identify CREBP binding sites within the promoter region. Transcription run-off experiments could be performed to ascertain whether the increase in mRNA is a result of transcription or due to changes in mRNA turnover/stability. As described previously, the effects of clenbuterol on glycogen breakdown are of a similar pattern to cathepsin-L mRNA expression, suggesting the rise in expression may be due to activation of specific β_2-adrenergic stimulatory pathways and not an unknown mechanism. Later experiments are then required to confirm if there is a subsequent up-regulation of cathespin-L protein levels and activity.

7.4.3 The Effect of Acute Beta-Adrenergic Agonist Administration in Pigs

The present study investigated the effects of administration of an acute 16 hour, 20 ppm dose of clenbuterol on the mRNA expression of muscle-specific calpain-3 and cathepsin-L in porcine LD samples, using northern blot hybridisation experimental techniques.

Total RNA was extracted from porcine LD samples and yields per g tissue analysed. There was no significant effect of treatment on extractable total RNA yields. (P = 0.58) (see Table 6.3.3-1). This therefore indicated that any experimental changes observed were not due to extraction artifacts.

A northern blot was prepared from porcine LD total RNA and hybridised with radio-labelled cDNA probes for calpain-3, cathepsin-L and actin (internal standard). Analysis of actin band intensity data showed there was no significant effect of clenbuterol treatment on actin mRNA expression ($P = 0.558$) (Table 6.3.4-2). This meant band intensity data for calpain-3 and cathepsin-L could be normalised to actin, producing valid results.

There was no significant effect of the acute dose of clenbuterol on calpain-3 and cathepsin-L mRNA relative expression. Calpain-3 decreased by 9% ($P = 0.427$) with treatment, which is unlike the result observed in the 5 ppm clenbuterol trial in discussed in Section 7.4.2. Cathepsin-L increased by 53% with treatment ($P = 0.279$). The rise in cathepsin-L is the same direction observed previously in the 5 ppm clenbuterol trial described Section 7.4.2. However, cathepsin-L didn't produce the clearest of band signals which may have contributed to lower rises in mRNA expression (see Figure 6.3.4-1). Unfortunately, the low number of samples involved in the acute dose trial (Control, n = 6 and Clenbuterol, n = 5) may be a limiting factor with assessing true significant changes.

The numerical increase in cathepsin-L mRNA after a 16 hour 20 ppm dose of clenbuterol mirrors the results from the previous study and further suggests that cathepsin-L mRNA increases as a possible rapid stress response. Although the effect was not statistically significant as opposed to the highly significant effect observed previously, this may be due to various reasons. Firsly, there were less sample numbers in this trial which may have had an impact on the level of statistical significance not being reached. Further studies would need to be performed with a larger number of animals to confirm whether the rise in cathepsin-L mRNA is consistantly. Secondly, the strength and quality of the northern blot band signals were relatively poor as can be viewed in Figure 6.3.4-1, which may have led to insignificant results.

7.4.4 The Effects of Chronic Administration of Adrenaline on Protease mRNA Expression in Pigs

This study investigated the effects of chronic-7 day adrenaline administration on the mRNA expression of muscle-specific calpain-3 and cathepsin-L in porcine *Longissmus Dorsi* samples, using northern blot hybridisation techniques.

Total RNA was extracted and analysed to see if adrenaline treatment affected extractable yield. There was no significant effect of treatment on total RNA yield per g LD porcine muscle tissue (P = 0.204) (see Table 6.4.3-1). This indicated that any changes observed in gene expression studies were not the result of extraction artifacts.

A northern blot was prepared from porcine total RNA samples and hybridised with radiolabelled cDNA probes for calpain-3, cathepsin-L and actin. Adrenaline administration did not significantly affect actin mRNA expression (P = 0.297) (see Table 6.4.4-2). This indicated that actin could be used to adequately normalise band intensity values for calpain-3 and cathepsin-L.

There was no significant change in calpain-3 mRNA expression values with 7-day adrenaline treatment (P = 0.159). Calpain-3 increased numerically by 40%, relative to controls, a similar trend to that seen in trial discussed in Section 7.4.2, after 1 week of 5 ppm clenbuterol administration (i.e. a 33% increase).

There was no significant effect of 7-day adrenaline treatment on cathepsin-L mRNA expression values (P = 0.258). Cathepsin-L decreased numerically by 24% which is a different response to the trials discussed in Section 7.4.2 and 7.4.3.

The different trend in response of cathepsin-L mRNA expression may be as adrenaline is a non-selective β-adrenergic agonist. Adrenaline is known to activate β_1- β_2- and β_3- adrenoceptors, although β_2 is the predominant receptor in skeletal muscle (Mersmann, 1998). As described previously in Section 7.4.2, the response of cathepsin-L mRNA to clenbuterol is thought to be due to stimulation of specific β_2-adrenergic pathways within skeletal muscle. Therefore, activation of multiple β-

adrenergic signalling pathways by adrenaline administration may lead to an alternative transcriptional response, or no change in cathepsin-L mRNA expression (as change was not statistically significant). Further studies would need to confirm whether theories are valid using a larger number of animals, adrenaline treatment at variable doses and time patterns.

7.4.5 Beta-Adrenergic Stimulation Discussion

In summary, a 5 ppm dose of clenbuterol acted as predicted on glycogen stores in porcine LD by significantly depleting them within 24 hour of administration. This indicated that specific β_2-adrenergic signalling pathways were being activated within skeletal muscle leading to increased glycogen breakdown, presumably through increased cAMP formation and PKA activation.

Cathespin-L mRNA was dramatically increased through an acute 5 ppm dose of clenbuterol, which decreased in intensity after 7 day chronic adminstration. E2G1 mRNA values increased numerically with a similar trend to cathepsin-L, although not significant. This may indicate that the initial stages of β_2-adrenergic stimulation (acute) may be seen as a stressor. Catecholamines are traditionally viewed as catabolic, counterregulatory stress hormones (described in Section 2.3.4). Another likely view may be that the coordinate rise may indicate an induction of a remodelling-growth response to β_2-adrenergic stimulation. This theory is consistant with the increase in *m*-calpain activity observed with β-adrenergic treatment and other conditions that involve compensatory/ 'catch-up' growth and remodelling.

After 1 week of chronic administration of 5 ppm clenbuterol glycogen stores began to rise, but were still lower than controls and cathepsin-L mRNA fell. This similar pattern of response may suggest the down-regulation and/or desensitisation of β_2-adrenergic signalling pathways. Studies have suggested that chronic administration of specific β_2-adrenergic agonists causes down-regulation and/or desensitisation of β_2-adrenergic receptor pathways leading to a down-regulation of cellular β_2-adrenergic agonist responses within skeletal muscle (Mersmann, 1998, Kearns *et al*, 2001, Depreux *et al*, 2002, Pellegrino *et al*, 2003, Ryall *et al*, 2003, Shumay *et al*, 2003).

Whether the rapid rise in cathepsin-L and possibly E2G1 is coordinately up-regulated with other components of the lysosomal-cathepsin and ubiquitin-proteasome systems is unknown and requires further investigation. Analysis of the promoter region of sequences for components of the ubiquitin-proteasome system has found that there are binding sites for the transcription factors NF-κB, AP-1, C/EBP-β and δ (Hasselgen and Fischer, 2001, Penner *et al*, 2002). As has been previously mentioned all these transcription factors are associated with immuno-inflammatory responses and may be regulated by cytokines, glucocorticoids and other endocrine mediators, including insulin (Thompson and Palmer, 1998, Bertrand *et al*, 1998, Bertrand *et al*, 1999, Hasselgen and Fischer, 2001, Penner *et al*, 2002, Macdonald *et al*, 2003). Therefore, further studies are required to see whether other protease components are altered by clenbuterol treatment and whether the up-regulation involves CREBP or other regulators described above.

During clenbuterol administration calpain-dependent proteolysis is known to be altered and reduced, which is associated with muscle hypertrophy during long term β-adrenergic agonist treatment. Therefore, the results described in this thesis go some way to suggest that overall clenbuterol may differentially affect multiple proteolytic systems. Whether this in turn initiates a remodelling response or differentially affects intracellular protein pools (i.e. myofibrillar and sarcoplasmic) is unknown.

Calpain-3 mRNA expression was not significantly altered by clenbuterol treatment, either acute at 5 ppm or 20 ppm, or chronic dose at 5 ppm. This was not in accordance with the only previous incomplete study performed investigating the effects of β-adrenergic agonist administration on calpain-3 mRNA (Ji *et al*, 1993); which observed a decrease in calpain-3 mRNA with ractopamine administration. Chronic adrenaline administration also failed to produce a significant treatment effect. The lack of treatment effect may suggest that calpain-3 is not affected by β_2-adrenergic signalling pathways (PKA and CREBP) and doesn't play an extensive role in initiating the changes in myofiber hypertrophy associated with β-adrenergic stimulation. Taking in to account these observations, other studies and the effects of plane of nutrition in calves, it is probable calpain-3 plays a more important regulatory role in muscle-specific signalling pathways (e.g. IκBα:NF-κB pathway) and metabolism.

In conclusion, it is of great importance to study the effects of clenbuterol and β-adrenergic agonists on muscle protein metabolism, proteolytic system regulation and associated signalling pathways, as β-adrenergic agonists have been extensively proven to increase muscle mass and protein accretion. It is this property of these agents that makes them potentially useful tools in livestock production and in clinical settings such as reducing muscle atrophy and weakness in muscular dystrophies, cachectic and sarcopenic states.

7.6 CONCLUSIONS

Proteolysis within skeletal muscle as described within the literature review is a complex co-ordinated process involving multiple protease systems and requires further investigation.

In young fast growing calves, there was a significant increase in the cellular total RNA pool in fast twitch muscle fibers (LD), over a short time period of 13 days (between slaughter dates). The group of animals refed back up to a high plane of nutrition after a feed restriction, were found to have higher numerical levels of total RNA compared to low and high plane groups, at both slaughter dates, although not significant.

Calpain-3 mRNA increased numerically between the two slaughter dates time period of two weeks, in the low plane of nutrition and refed animal groups, with a trend towards significance. Calpastatin gene expression also increased numerically across all treatment groups during the two slaughter date time period, with a trend towards significance. This suggested that in young fast growing calves, heightened levels of growth and remodelling takes place within fast twitch muscle fibers; which may involve alterations in components of the calpain-calpastatin system.

Overall there was no signficant effect of plane of nutrition on calpain-3 gene expression. However, calpain-3 was lower during the 1st slaughter date in the low plane of nutrition group, compared to the high plane and refed animal groups. The refed ani-

mals in the 1st slaughter date had levels similar to the high plane group suggesting calpain-3 gene expression is sensitive to nutritional intake. The data in this thesis suggests that calpain-3 gene transcription may be regulated by nutritional intake, possibly involving multiple signalling pathways. The pathways that affect calpain-3 may be unlike those that affect ubiquitous calpain and calpastatin gene transcription, as the effects of feeding and nutritional intake on ubiquitous μ- and m- calpain and calpastatin has been reported to be highly variable.

Calpastatin gene expression did not significantly alter overall with plane of nutrition. Although not significant, higher levels numerically were found in the low plane group in the 1st slaughter, compared to both high plane and refed groups.

Administration of the selective β_2-adrenergic agonist, clenbuterol (5 ppm) induced a rapid depletion of muscle glycogen stores, a classical catabolic response involving stimulation of β_2-adrenergic signalling pathways, which decreased in intensity with chronic 7 day administration. Acute 24 hour administration dramatically increased cathepsin-L mRNA, a response which also decreased with chronic administration, suggesting similar β_2-adrenergic signalling pathways may be utilised to alter cathepsin-L transcription. The precise significance of this response on cathepsin-L is unclear at this present time and requires further investigation. E2G1 increased numerically with the same pattern as cathepsin-L, although not significant. This suggested a rapid up-regulatory response by specific proteolytic systems to an acute clenbuterol dose. Chronic administration may however downregulate these β_2-selective pathways within muscle, as glycogen levels and cathepsin-L began to move towards control levels with chronic clenbuterol administration. A 16 hour 20 ppm does of clenbuterol failed to increase cathepsin-L mRNA significantly, although there was a numerically increase. Chronic 7 day adrenaline infusion failed to increase cathepsin-L mRNA. It was hypothesised that this may be due to the non-specific effects of adrenaline, activating other β-adrenergic receptor pathways and/or not maximally stimulating β_2-adrenergic receptors. The effects of β-adrenergic stimulation on calpain-3 is unclear at this present time and requires further work, as no significant trends were apparent in any of the β-adrenergic stimulation studies. This may suggest that calpain-3 gene transcription is regulated by alternative regulators/signalling pathways, compared to the ubiquitous calpains and calpastatin.

7.5 FUTURE WORK

7.5.1 Plane of Nutrition

To clarify the effects of plane of nutrition on proteolytic systems, a future trial would firstly ensure a greater number of animals per treatment group would be used. As changes in expression are small, a larger number of animals is required to overcome experimental variation. Different feeding patterns and levels of feed restriction could also be set up. A feeding restriction that induces atrophy would be of great interest as many of the protease systems are known to be up-regulated during catabolic/atrophic states. Another interesting trial component would be to use an older animal group in comparison. It is possible that older animals lose some of the compensatory muscle-protective/growth mechanisms discussed within this thesis, that may be active during altered planes of nutrition in young, growing animals. As described within the Introduction, age-associated sarcopenia is associated with loss of muscle mass, through alterations in endogenous endocrine and neural pathways.

In terms of laboratory work, it would be interesting to have protein turnover and proteolysis rate measurements. It is would be advantageous to be able to re do μ- and *m*-calpain Quantitiative Real-Time PCR studies using a Taqman probe. It is important to have data for the entire calpain system, as the calpain:calpastatin ratio is thought to give an indication of the overall calpain proteolytic potential, over seperate calpain or calpastatin measurements. Key components from other proteolytic systems including: Cathepsin L, E2G1, atrogin-1 and caspase-3 could also be measured using Real-Time PCR, to have a view of coordinate changes within other systems. Any future work would ideally be validated by performing Northern blot experiments in coordination.

7.5.2 β-Adrenergic Stimulation

For the β-adrenergic stimulation trials a greater number of animals per treatment group is also important in future trials for similar reasons, as described above. For example, the 5 ppm clenbuterol trial showed greater significant changes in measurements compared to the other β-adrenergic trials, which had lower sample numbers.

Once optimised other cDNA probes may be tested on northern blots. Other components of the lysosomal, ubiquitin-proteasome and caspase systems would be interesting to evaluate. Other methods of detection could be incorporated including Quantitative Real-Time PCR, especially for those mRNA species with low expression levels (e.g. caspase-3).

7.5.3 Detection Methods

The main aim of future work would be to move towards developing and optimising a cDNA macroarray, with proteolytic system components specific to porcine tissue and human and bovine if possible. However, one issue with the array technique is the inability to detect relatively small changes consistantly and effectively. For example, with the plane of nutrition trial there were only small, subtle changes in mRNA expression observed to be taking place, that may not be identified in array studies. In terms of cDNA probes, porcine nucleotide sequence for many of the expressed genes of interest should be available in the near future. This could then be used in hybridisation experiments for a number of animal trials and possibly human trials, to investigate global cellular gene expression.

Another aspect that could be investigated to strengthen the work with gene expression studies, is performing protein level and protease activity studies. This obviously would aid in understanding the relationship between mRNA levels and subsequent changes in protein and activity levels.

BIBLIOGRAPHY

ADAMS GR, CAIOZZO VJ and BALDWIN KM. (2003) Skeletal muscle unweighting: spaceflight and ground-based models. *Journal Applied Physiology* 95: 2185-2201.

ADAMS GR. (2002) *Exercise effects on muscle insulin signaling and action.* Invited review: Autocrine/paracrine IGF-1 and skeletal muscle adaptation. *Journal Applied Physiology* 93: 1159-1167.

ALLEN DL and LEINWARD LA. (2002) Intracellular calcium and myosin isoform transitions. *The Journal of Biological Chemistry* vol. 277, no.47: 45323-45330.

ALTMAN DG. (1991) The t distribution. In: *Practical Statistics for Medical Research,* pp. 521-522. Chapman and Hall, London.

ALVAREZ B, QUINN L S, BUSQUETS S, QUILES MT, LÓPEZ-SORIANO FJ and ARGILÉS JM. (2002) Tumor necrosis factor-α exerts interleukin-6-dependent and –independent effects on cultured skeletal muscle cells. *Biochimica et Biophysica Acta* 1542: 66-72.

ANDERSON LVB, HARRISON RM, POGUE R, VAFIADAKI E, POLLITT C, DAVISON K, MOSS JA, KEERS S, PYLE A, SHAW PJ, MAHJNEH I, ARGOV Z, GREENBERG CR, WROGEMANN K, BERTORINI T, GOEBEL HH, BECKMANN JS, BASHIR R and BUSHBY KMD. (2000) Secondary reduction in calpain 3 expression in patients with limb girdle muscular dystrophy type 2B and miyoshi myopathy (primary dysferlinopathies). *Neuromuscular Disorders* 10: 553-559.

AOKI K, IMAJOH S, OHNO S, EMORI Y, KOIKE M, KOSAKI G, SUZUKI K. (1986) Complete amino acid sequence of the large subunit of the low-Ca^{2+}-requiring form of human Ca^{2+}-activated neutral protease (μCANP) deduced from its cDNA sequence. *FEBS* vol. 205, no. 2, pp. 313-317.

ARGILÉS JM, BUSQUETS S, ALVAREZ B and LÓPEZ-SORIANO FJ. (1999) Mechanism for the increased skeletal muscle protein degradation in the obese zucker rat. *Journal Nutrition. Biochemistry* 10:244-248.

ATTAIX D, COMBARET L, POUCH M-N and TAILLANDIER D. (2001) Regulation of proteolysis. *Current Opinion Clinical Nutrition Metabolism Care* 4:45-49.

ATTAIX D, COMBARET L, POUCH M-N and TAILLANDIER D. (2002) Cellular control of ubiquitin-proteasome-dependent proteolysis. *Journal Animal Science* 80(E. Suppl. 2):E56-E63.

AUTHIER F-J, CHAZAUD B, MHIRI C, ELIEZER-VANEROT M-C, PORON F, BARLOVATZ-MEIMON G and GHERARDI RK. (1997) Interleukin-1 expression in normal motor endplates and muscle fibers showing neurogenic changes. *Acta Neuropathol* 94:272-279.

AUERSWALD EA, NAGLER DK, GROSS S, ASSFALG-MACHLEIDT I, STUBSS MT, ECKERSKORN C, MACHLEIDT W and FRITZ H. (1996) Hybrids of chicken cystatin with human kininogen domain 2 sequences exhibit novel inhibition of calpains, improved inhibition of actinidin and impaired inhibition of papain, cathepsin L and cathepsin B. *European Journal of Biochemistry*, Vol 235, 534-542.

AWEDE BL, THISSEN J-P and LEBACQ J. (2002) Role of IGF-1 and IGFBPs in the changes of mass and phenotype induced in rat soleus by clenbuterol. *American Journal Physiology Endocrinology Metabolism* 282: E31-E37.

BAGHDIGUIAN S, RICHARD I, MARTIN M, COOPMAN P, BECKMANN JS, MANGEAT P and LEFRANC G. (2001) Pathophysiology of limb girdle muscular dystrophy type 2A: hypothesis and new insights into the IκBα/NF-κB survival pathway in skeletal muscle. *Journal Molecular Medicine* 79:254-261.

BAGHDIGUIAN SM, MARTIN M, RICHARD I, PONS F, ASTIER C, BOURG N, HAY RT, CHEMALY R, HALABY G, LOISELET J, ANDERSON LVB, LOPEZ DE MUNAIN A, FARDEAU M, MANGEAT P, BECKMANN JS and LEFRANC G. (1999) Calpain 3 deficiency is associated with myonuclear apoptosis and profound perturbation of the IκBα /NF-κB pathway in limb-girdle muscular dystrophy type 2A. *Nature Medicine* vol. 5, 5: 503-511.

BAIER LJ, PERMANA PA, YANG X, PRATLEY RE, HANSON RL, SHEN G-Q, MOTT D, KNOWLER WC, COX NJ, HORIKAWA Y, ODA N, BELL GI and BOGARDUS C. (2000) A calpain-10 gene polymorphism is associated with reduced muscle mRNA levels and insulin resistance. *Journal Clinical Investigations* 106:R69-R73.

BALAGE M, SINAUD S, PROD'HOMME M, DARDEVET D, VARY TC, KIMBALL SR, JEFFERSON LS and GRIZARD J. (2001) Amino acids and insulin are both required to regulate assembly of the eIF4E·eIF4G complex in rat skeletal muscle. *American Journal of Physiology Endocrinology Metabolism* 281: E565-E574.

BARACOS VE. (2000) Regulation of skeletal-muscle-protein turnover in cancer-associated cachexia. *Nutrition* 16:1015-1018.

BARDSLEY RG, ALLCOCK SMJ, DAWSON NW, DUMELOW JA, HIGGINS YV, LASSLETT AK, LOCKLEY AK, PARR T and BUTTERY PJ. (1992) Effect of β–agonists on expression of calpain and calpastatin activity in skeletal muscle. Biochimie vol.74, pp. 267-273.

BARNOY S, GLASER T and KOSOWER NS. (1997) Calpain and calpastatin in myoblast differentiation and fusion: effects of inhibitors. *Biochimica et Biophysica Acta* 1358:181-188.

BARNOY S, GLASER T and KOSOWER NS. (1998) The calpain-calpastatin system and protein degradation in fusing myoblasts. *Biochimica et Biophysica Acta* 1402:52-60.

BASS J, OLDHAM J, SHARMA M and KAMBADUR R. (1999) Growth factors controlling muscle development. *Domestic Animal Endocrinology* 17: 191-197.

BAUD L, FOUQUERAY B and BELLOCQ A. (2001) Cytokines and hormones with anti-inflammatory effects: new tools for therapeutic intervention. *Current Opinion Nephrology Hypertension* 10:49-54.

BD BIOSCIENCES CLONTECH. (2002) BD Atlas™ cDNA expression arrays user manual.

BEITZEL F, GREGOREVIC P, RYALL JG, PLANT DR, SILLENCE MN and LYNCH GS. (2004) β_2-Adrenoceptor agonist fenoterol enhances functional repair of regenerating rat skeletal muscle after injury. *Journal of Applied Physiology* 96: 1385-1392.

BELIZARIO JE, LORITE MJ and TISDALE MJ. (2001) Cleavage of caspases -1, -3, -6, -8 and –9 substrates by proteases in skeletal muscles from mice undergoing cancer cachexia. *British Journal of Cancer* vol. 84, no. 8, 1135-1140.

BELL AW, BAUMAN DE, BEERMANN DH and HARRELL RJ. (1998) Nutrition, development and efficacy of growth modifiers in livestock species. *Journal Nutrition* 128: 360S-363S.

BERTRAND F, ATFI A, CADORET A, L'ALLEMAI G, ROBIN H, LASCOLS O, CAPEAU J and CHERQUI G. (1998) A role for nuclear factor κB in the antiapoptotic function of insulin. *The Journal of Biological Chemistry* vol. 273, no. 5, pp. 2931-2938.

BERTRAND F, DESBOIS-MOUTHON C, CADORET A, PRUNIER C, ROBIN H, CAPEAU J, ATFI A and CHERQUI G. (1999) Insulin antiapoptotic signaling involves insulin activation of thenuclear factor κB-dependent survival genes encoding tumour necrosis factor receptor-associated factor 2 and manganese-superoxide dismutase. *The Journal of Biological Chemistry* vol. 274, no. 43, pp. 30596-30602.

BHASIN S, WOODHOUSE L and STORER TW. (2001) Proof of the effect of testosterone on skeletal muscle. *Journal of Endocrinology* 170:27-38.

BIOLO G, TOIGO G, CIOCCHI B, SITULIN R, ISCRA F, GULLO A and GUARNIERI G. (1997) Metabolic response to injury and sepsis: changes in protein metabolism. *Nutrition* vol. 13, no. 9(suppl).

BIRAI D, JAKUBIEC-PUKA A, CIECHOMSKA I, SANDRI M, ROSSINI K, CARRARO U and BETTO R. (2000) Loss of dystrophin and some dystrophin-associated proteins with concomitant signs of apoptosis in rat leg muscle overworked in extension. *Acta Neuropathol* 100:618-626.

BISTRIAN BR. (1999) Dietary treatment in secondary wasting and cachexia. *Journal Nutrition.* 129: 290S-294S.

BODINE SC, LATRES E, BAUMHUETER S, LAI V H-K, NUNEZ L, CLARKE BA, POUEYMIROU WT, PANARO FJ, NA E, DHARMARAJAN K, PAN Z-Q, VALENZUELA DM, DECHIARA TM, STITT TN, YANCOPOULOS GD and GLASS DJ. (2001) Identification of ubiquitin ligases required for skeletal muscle atrophy. *SCIENCE* vol 294, 1704-1708

BREIER BH. (1999) Regulation of protein and energy metabolism by the somatotropic axis. *Domestic Animal Endocrinology* 17: 209-218.

BROWN RH. (1997) Dystrophin-associated proteins and the muscular dystrophies. *Annual Review Medicine.* 48:457-66.

BUDIHARDJO I, OLIVER H, LUTTER M, LUO X and WANG X. (1999) Biochemical pathways of caspase activation during apoptosis. *Annual Review Cell Developmental Biology* 15:269-90.

BUSHBY KMD. (1999) Making sense of the limb-girdle muscular dystrophies. *Brain* 122: 1403-1420.

BUSQUETS S, ALVAREZ B, LLOVERA M, AGELL N, LOPEZ-SORIANO FJ and ARGILES JM. (2000) Branched-chain amino acids inhibit proteolysis in rat skeletal muscle: Mechanisms involved. *Journal of Cellular Physiology* 184(3): 380-384.

BUSQUETS S, GARCIA-MARTINEZ C, ALVAREZ B, CARBÓ N, LÓPEZ-SORIANO FJ and ARGILÉS. (2000) Calpain-3 gene expression is decreased during experimental cancer cachexia. *Biochimica et Biophysica Acta* 1475:5-9.

BUSTIN SA. (2000) Absolute quantification of mRNA using real-time reverse transcription polymerase chain reaction assays. *Journal of Molecular Endocrinology* 25, 169-193.

CAMPBELL WG, GORDON SE, CARLSON CJ, PATTISON JS, HAMILTON MT and BOOTH FW. (2001) Differential global gene expression in red and white skeletal muscle. *American Journal of Physiology Cell Physiology* 280: C763-C768.

CARDOSO LA and STOCK MJ. (1998) Effect of clenbuterol on endocrine status and nitrogen and energy balance in food-restricted rats. *Journal Animal Science* 76:1012-1018.

CARSON JA and WEI L. (2000) Integrin signaling's potential for mediating gene expression in hypertrophying skeletal muscle. *Journal Applied Physiology* 88: 337-343.

CASSE AH, DESPLANCHES D, MAYET-SORNAY MH, RACCURT M, JEGOU S and MOREL G. (2003) Growth hormone receptor expression in atrophying muscle fibers of rats. *Endocrinology* 144(8):3692-3697.

CHAE J, MINAMI N, JIN Y, NAGAGAWA M, MURAYAMA K, IGARASHI F and NONAKA I. (2001) Calpain 3 gene mutations: genetic and clinico-pathologic findings in limb-girdle muscular dystrophy. *Neuromuscular Disorders* 11, 547-555.

CHEN F, DEMERS LM, VALLYATHAN V, LU Y, CASTRANOVA V and SHI X. (2000) Impairment of NF-κB activation and modulation of gene expression by calpastatin. *American Journal Physiology Cell Physiology* 279: C709-C716.

CIECHANOVER A, ORIAN A and SCHWARTZ AL. (2000) Ubiquitin-mediated proteolysis: biological regulation via destruction. *BioEssays* 22:442-451.

CLAEYSSENS S, BOUTELOUP-DEMANGE C, GACHON P, HECKETSWEILER B, LEREBOURS E, LAVOINNE A and DÉCHELOTTE P. (2000) Effect of enteral glutamine on leucine, phenylalanine and glutamine metabolism in hypercortisolemic subjects. *American Journal of Physiology Endocrinology Metabolism* 278: E817-E824.

COMBARET L, BÉCHET D, CLAUSTRE A, TAILLANDIER D, RICHARD I and ATTAIX D. (2003) Down-regulation of genes in the lysosomal and ubiquitin-proteasome proteolytic pathways in calpain-3-deficient muscle. *The International Journal of Biochemistry and Cell Biology* 35: 676-684

CONG M, THOMPSON VF, GOLL DE and ANTIN PB. (1998) The bovine calpastatin gene promoter and a new N-terminal region of the protein are targets for cAMP-dependent protein kinase activity. *The Journal of Biological Chemistry.* Vol.273, no.1: 660-666.

COSTA ND, MCGILLIVRAY C, BAI Q, WOOD JD, EVANS G, CHANG KC. (2004) Restriction of dietary energy and protein induces molecular changes in young porcine skeletal muscles. *Journal of Nutrition*, 134:2191-2199.

DAIMON M, OIZUMI T, SAITOH T, KAMEDA W, YAMAGUCHI H, OHNUMA H, IGARASHI M, MANAKA H and KATO T. (2002) Calpain 10 gene polymorphisms are related, not to type 2 diabetes, but to increased serum cholesterol in japanese. *Diabetes Research and Clinical Practice* 56: 147-152.

DAWSON RT. (2001) HORMONES AND SPORT, Drugs in sport-the role of the physician. *Journal of Endocrinology*, **170**, 55-61.

DE FEO P. (1998) Fed state protein metabolism in diabetes mellitus. *Journal of Nutrition* 128: 328S-332S.

DEMARTINO GN and SLAUGHTER CA. (1999) The proteasome, a novel protease regulated by multiple mechanisms. *The Journal of Biological Chemistry* vol. 274, no. 32, pp. 22123-22126.

DEPREUX FFS, GRANT AL, ANDERSON DB and GERRARD DE. (2002) Paylean alters myosin heavy chain isoform content in pig muscle. *Journal Animal Science*. 80:1888-1894.

DEVAL C, MORDIER S, OBLED C, BECHET D, COMBARET L, ATTAIX D and FERRARA M. (2001) Identification of cathepsin L as a differentiallly expressed message associated with skeletal muscle wasting. *The Biochemical Journal* Vol. 360, part 1, pp: 143-150.

DIFFEE GM, KALFAS K, AL-MAJID S and MCCARTHY DO. (2002) Altered expression of skeletal myosin isoforms in cancer cachexia. *American Journal Physiology Cell Physiology* 283: C1376-C1382.

DIRKS A and LEEUWENBURGH. (2002) Apoptosis in skeletal muscle with aging. *American Journal Physiology Regulatory Comparative Physiology* 282: R519-R527.

DOHERTY FJ and MAYER RJ. (1992) The protein turnover 'cycle'. In: *Intracellular Protein Degradation,* pp. 1-8. Oxford University Press, Oxford.

DOHERTY FJ and MAYER RJ. (1992) Methods used to study intracellular proteolysis. In: *Intracellular Protein Degradation,* pp. 9-14. Oxford University Press, Oxford.

DOHERTY FJ and MAYER RJ. (1992) The mechanisms- pathways of intracellular proteolysis. In: *Intracellular Protein Degradation,* pp. 15-32. Oxford University Press, Oxford.

DOHERTY FJ and MAYER RJ. (1992) Molecular recognition and intracellular proteolysis. In: *Intracellular Protein Degradation,* pp. 33-42. Oxford University Press, Oxford.

DOHERTY FJ and MAYER RJ. (1992) Regulation of intracellular protein turnover. In: *Intracellular Protein Degradation,* pp. 43-49. Oxford University Press, Oxford.

DU J, WANG X, MIERELES C, BAILEY JL, DEBIGARE R, ZHENG B, PRICE R and MITCH WE. (2004) Activation of caspase-3 is an initial step triggering accelerated muscle proteolysis in catabolic conditons. *Journal Clinical Investigations* 113:115-123.

DU M, ZHU MJ, MEANS WJ, HESS BW and FORD SP. (2004) Effect of nutrient restriction on calpain and calpastatin content of skeletal muscle from cows and fetuses. *J. Anim. Sci.* 82:2541-2547.

DUCHAINE D. (1995) Thermogenic agents and body temperature. In: *Underground Bodyopus*, pp. 163-174. XIPE Press, Nevada, US.

EHMSEN J, POON E and DAVIES K. (2002) The dystrophin-associated protein complex: *Journal of Cell Science* 115, 2801-2803.

EICKHOFF B, KORN B, SCHICK M, POUSTKA A and BOSCH J. (1999) Normalization of array hybridization experiments in differential gene expression analysis. *Nucleic Acids Research* 27, no.22, *e33*.

EKHTERAE D, LIN Z, LUNDBERG MS, CROW MT, BROSIUS III FC and NÚNEZ G. (1999) ARC inhibits cytochrome *c* release from mitochondria and protects against hypoxia-induced apoptosis in heart-derived H9c2 cells. *Circulation Research.* 85:e70-e77.

ENGVALL E and WEWER UM. (2003) The new frontier in muscular dystrophy research: booster genes. *FASEB Journal* 17, 1579-1584.

ERVASTI JM. (2003) Costameres: the achilles heel of herculean muscle. *The Journal of Biological Chemistry* vol. 278, no. 16, pp. 13591-13594.

FARGES M-C, BALCERZAK D, FISHER BD, ATTAIX D, BÉCHET D, FERRARA M and BARACOS VE. (2002) Increased muscle proteolysis after local trauma mainly reflects macrophage-associated lysosomal proteolysis. *American Journal Physiology Endocrinology Metabolism* 282: E326-E335.

FÉASSON L, STOCKHOLM D, FREYSSENET D, RICHARD I, DUGUEZ S, BECKMANN JS and DENIS C. (2002) Molecular adaptations of neuromuscular disease-associated proteins in response to eccentric exercise in human skeletal muscle. *Journal of Physiology* 543.1, pp. 297-306.

FENG X, JIANG Y, MELTZER P and YEN PM. (2000) Thyroid hormone regulation of hepatic genes *in vivo* detected by complementary DNA microarray. *Molecular Endocrinology* 14(7): 947-955.

FERNANDO P, KELLY JF, BALAZSI K, SLACK RS and MEGENEY LA. (2002) Caspase 3 activity is required for skeletal muscle differentiation. *PNAS* vol. 99, no. 17, pp. 11025-11030.

FISCHER D, GANG G, PRITTS T and HASSELGREN P-O. (2000) Sepsis-induced muscle proteolysis is prevented by a proteasome inhibitor *in Vivo. Biochemical and Biophysical Research Communications* 270, 215-221 (2000)

FITTS RH, RILEY DR and WIDRICK JJ. (2000) *Physiology of a microgravity environment*, invited review: microgravity and skeletal muscle. *Journal Applied Physiology* 89: 823-839.

FORHEAD AJ, LI J, GILMOUR RS, DAUNCEY MJ and FOWDEN AL. (2002) Thyroid hormones and the mRNA of the GH receptor and IGFs in skeletal muscle of fetal sheep. *American Journal of Physiology Endocrinology Metabolism* 282: E80-E86.

FOWLER EG, GRAVES MC, WETZEL GT and SPENCER MJ. (2004) Pilot trial of albuterol in Duchenne and Becker muscular dystrophy. *Neurology* 62:1006-1008.

FRAYN KN. (1997) Metabolic characteristics of the organs and tissues. In: *Metabolic Regulation, A Human Perspective*, pp. 49-87. Portland Press Ltd, London.

FRAYN KN. (1997) Some inportant endocrine organs and hormones. In: *Metabolic Regulation, A Human Perspective*, pp. 87-102. Portland Press Ltd, London.

FRAYN KN. (1997) Integration of carbohydrate, fat and protein metabolism in the whole body. In: *Metabolic Regulation, A Human Perspective*, pp. 103-141. Portland Press Ltd, London.

FRAYN KN. (1997) Coping with some extreme conditions. In: *Metabolic Regulation, A Human Perspective*, pp. 163-196. Portland Press Ltd, London.

FRAYN KN. (1997) Diabetes mellitus. In: *Metabolic Regulation, A Human Perspective*, pp. 219-232. Portland Press Ltd, London.

FRAYN KN. (1997) Energy balance and body weight regulation. In: *Metabolic Regulation, A Human Perspective*, pp. 233-251. Portland Press Ltd, London.

FRAYN KN. (1997) The nervous system and metabolism. In: *Metabolic Regulation, A Human Perspective*, pp. 143-162. Portland Press Ltd, London.

GARLICK PJ, MCNURLAN MA, BARK T, LANG CH and GELATO MC. (1998) Hormonal regulation of protein metabolism in relation to nutrition and disease. *Journal Nutrition.* 128: 356S-359S.

GARROW JS, JAMES WPT and RALPH A. (2000) Composition of the body. In: *Human Nutrition and Dietetics,* pp. 13-23. Churchill Livingstone, London.

GARROW JS, JAMES WPT and RALPH A. (2000) Fuels of the tissues. In: *Human Nutrition and Dietetics,* pp. 37-59. Churchill Livingstone, London.

GARROW JS, JAMES WPT and RALPH A. (2000) Nutrition and ageing. In: *Human Nutrition and Dietetics,* pp. 465-470. Churchill Livingstone, London.

GARROW JS, JAMES WPT and RALPH A. (2000) Nutritional support in sepsis, trauma and other clinical conditions. In: *Human Nutrition and Dietetics,* pp. 483-499. Churchill Livingstone, London.

GARROW JS, JAMES WPT and RALPH A. (2000) Proteins. In: *Human Nutrition and Dietetics,* pp. 77-96. Churchill Livingstone, London.

GILL C, MESTRIL R and SAMALI A. (2002) Losing heart: the role of apoptosis in heart disease—a novel therapeutic target? *FASEB Journal.* 16, 135-146.

GLASS DJ. (2003) Signalling pathways that mediate skeletal muscle hypertrophy and atrophy. *Nature Cell Biology* vol. 5: 87-90.

GLICKMAN MH and CIECHANOVER A. (2002) The ubiquitin-proteasome proteolytic pathway: destruction for the sake of construction. *Physiology Rev* 82: 373-428.

GOLL DE, THOMPSON VF, TAYLOR RG and OUALI A. (1998) The calpain system and skeletal muscle growth. *Canadian Journal Animal Science* 78: 503-512.

GOLL DE, THOMPSON VF, HONGQI L, WEI W and CONG J. (2003) The calpain system.*Physiol.Rev.*,83:731-801.

GOMES MD, LECKER SH, JAGOE RT, NAVON A and GOLDBERG AL. (2001) Atrogin-1, a muscle-specific F-box protein highly expressed during muscle atrophy. *PNAS* vol. 98, no. 25: 14440-14445.

GRANT AL and GERRARD DE. (1998) Cellular and molecular approaches for altering muscle growth and development. *Journal of Animal Science* 78: 493-502.

GREIWE JS, KWON G, MCDANIEL ML and SEMENKOVICH CF. (2001) Leucine and insulin activate p70 S6 kinase through different pathways in human skeletal muscle. *American Journal of Physiology Endocrinology Metabolism* 281: E466-E471.

GRIMBLE RF. (2003) Nutritional therapy for cancer cachexia. *Gut* **52**: 1391-1392.

GRIMM S. (2003) Caspase-independent cell death. In: *Genetics of apoptosis,* pp. 203-223. BIOS Scientific Publishers Ltd, Oxford, UK.

GRIMM S. (2003) Mitochondria in apoptosis induction. In: *Genetics of apoptosis,* 116-133. BIOS Scientific Publishers Ltd, Oxford, UK.

GRIMM S. (2003) The role of the endoplasmic reticulum in apoptosis. In: *Genetics of apoptosis,* pp.93-113. BIOS Scientific Publishers Ltd, Oxford, UK.

GRIMM S. (2003) The role of caspases in apoptosis. In: *Genetics of apoptosis,* pp.31-45. BIOS Scientific Publishers Ltd, Oxford, UK.

GRIMM S. (2003) Death receptors in apoptosis. In: *Genetics of apoptosis,* pp. 1-30. BIOS Scientific Publishers Ltd, Oxford, UK.

GROUNDS MD, WHITE JD, ROSENTHAL N and BOGOYEVITCH MA. (2002) The role of stem cells in skeletal and cardiac muscle repair. *The Journal of Histochemistry & Cytochemistry* vol. 50(5): 589-610.

GROUNDS MD and TORRISI J. (2004) Anti-TNFα (Remicade®) therapy protects dystrophic skeletal muscle from necrosis. *FASEB Journal.* 18, 676-682.

GRUNDIG P and BACHMANN M. (1995) Clenbuterol. In: *World Anabolic Review,* 1996, pp. 48-57. MB Muscle Books, M.bodingbauer, D-Selm.

HASSELGREN P-O and FISCHER JE. (2001) Muscle cachexia: current conceots of intracellular mechanisms and molecular regulation. *ANNALS OF SURGERY* vol. 233, no. 1, 9-17.

HENRICKS DM, JENKINS TC, WARD JR, KRISHNAN CS and GRIMES L. (1994) *Journal of Animal Science*, 72:2289-2297.

HERRINGTON J and CARTER-SU C. (2001) Signaling pathways activated by the growth hormone receptor. *TRENDS in Endocrinology & Metabolism.* Vol. 12, no. 6: 252-257.

HOBLER SC, TIAO G, FISCHER JE, MONACO J and HASSELGREN P-O. (1998) Sepsis-induced increase in muscle proteolysis is blocked by specific proteasome inhibitors. *American Journal Physiology* 274 (*Regulatory Integrative Comparative Physiology* 43): R30-R37.

HOBLER SC, WANG JJ, WILLIAMS AB, MELANDRI F, SUN X, FISCHER JE and HASSELGREN P-O. (1999) Sepsis is associated with increased ubiquitin-conjugating enzyme $E2_{14k}$ mRNA in skeletal muscle. *American Journal Physiology* 276 (*Regulatory Integrative Comparative Physiology* 45): R468-R473.

HOBLER SC, WILLIAMS A, FISCHER D, WANG JJ, SUN X, FISCHER JE, MONACOJJ and HASSELGREN P-O. (1999) Activity and expression of the 20S proteasome are increased in skeletal muscle during sepsis. *American Journal Physiology* 277 (*Regulatory Integrative Comparative Physiology* 46): R434-R440.

HOFFSTEDT J, NÄSLUND E and ARNER P. (2002) Calpain-10 gene polymorphism is associated with reduced β_3-adrenoceptor function in human fat cells. *The Journal of Clinical Endocrinology & Metabolism* 87(7):3362-3367.

HOPKINS DL and THOMPSON JM. (2001) The relationship between tenderness, proteolysis, muscle contraction and dissociation of actomyosin. *Meat Science* 57: 1-12.

HOPKINS DL and THOMPSON JM. (2001) Inhibition of protease activity. Part 1. The effect on tenderness and indicators of proteolysis in ovine muscle. *Meat Science* 59: 175-185.

HOPKINS DL and THOMPSON JM. (2001) Inhibition of protease activity 2. Degradation of myofibrillar proteins, myofibril examination and determination of free calcium levels. *Meat Science* 59: 199-209.

HORIKAWA Y, ODA N, COX NJ, LI X, ORHO-MELANDER M, HARA M, HINOKIO Y, LINDNER TH, MASHIMA H, SCHWARTZ PEH, BOSQUE-PLATA L, HORIKAWA Y, ODA Y, TOSHIUCHI I, COLILLA S, POLONSKY KS, WEI S, CONCANNON P, IWASAKI N, SCHULZE J, BAIER LJ, BOGARDUS C, GROOP L, BOERWINKLE E, HANIS CL and BELL GI. (2000) Genetic variation in the gene encoding calpain-10 is associated with type 2 diabetes mellitus. *Nature Genetics* vol. 26:163-175.

HUANG J and FORSBERG NE. (1998) Role of calpain in skeletal-muscle protein degradation. *Proc. Natl. Acad. Science USA* vol. 95, pp. 12100-12105.

HUANG X, VAAG A, CARLSSON E, HANSSON M, AHRÉN B and GROOP L. (2003) Impaired cathepsin L gene expression in skeletal muscle is associated with type 2 diabetes. *Diabetes* 52:2411-2418.

HUANG Y and WANG KKW. (2001) The calpain family and human disease. *TRENDS in Molecular Medicine* vol.7, no.8.

HUET C, LI Z-F, LIU H-Z, BLACK RA, GALLIANO M-F and ENGVALL E. (2001) Skeletal muscle cell hypertrophy induced by inhibitors of metalloproteases; myostatin as a potential mediator. *American Journal Physiology Cell Physiology* 281: C1624-C1634.

IKEMOTO M, NIKAWA T, TAKEDA S, WATANABE C, KITANO T, BALDWIN KM, IZUMI R, NONAKA I, TOWATARI T, TESHIMA S, ROKUTAN K and KISHI K. (2001) Space shuttle flight (STS-90) enhances degradation of rat myosin heavy chain in association with activation of ubiquitin-proteasome pathway. *The FASEB Journal* express article 10.1096/fj.00-0629fje.

IMAJOH S, AOKI K, OHNO S, EMORI Y, KAWASAKI H, SUGIHARA H and SUZUKI K. (1988) Molecular cloning of the cDNA for the large subunit of the high-Ca^{2+}-requiring form of human Ca^{2+}-activated protease. *Biochemistry* 27: 8122-8128.

INGENBLEEK Y, and BERNSTEIN L. (1999) The stressful condition as a nutritionally dependent adaptive dichotomy. *Nutrition* vol. 15, no. 4.
ISRAELS LG and ISRAELS ED. (1999) Apoptosis. *The Oncologist* 4;332-339.

ISRAELS LG AND ISRAELS ED. (1999) Apoptosis. *The Oncologist*, 4: 332-339.

IWATA Y, KATANOSAKA Y, ARAI Y, KOMAMURA K, MIYATAKE K and SHIGEKAWA M. (2003) A novel mechanism of myocyte degenration involving the Ca^{2+} -permeable growth factor-regluated channel. *The Journal of Cell Biology*, vol.161, no.5, 957-967.

JACKSON NC, CARROLL PV, RUSSELL-JONES DL, SÖNKSEN PH, TREACHER DF and UMPLEBY AM. (1999) The metabolic consequences of critical illness: acute effects on glutamine and protein metabolism. *American Journal of Physiology* 276 (*Endocrinology Metabolism.* 39): E163-E170.

JAGOE RT and GOLDBERG AL. (2001) What do we really know about the ubiquitin-proteasome pathway in muscle atrophy? *Current Opinion Clinical Nutrition Metabolism Care* 4:183-190.

JAGOE RT, LECKER SH, GOMES M and GOLDBERG AL. (2002) Patterns of gene expression in atrophying skeletal muscles: response to food deprivation. *FASEB Journal* 16, 1697-1712.

JI SQ, HANCOCK DL, BIDWELL CA and ANDERSON DB. (1993) Effect of ractopamine on expression of skeletal muscle specific calpain in finishing pigs fed high and low dietary protein. *Abstract for International Workshop on Proteolysis at Clermont Ferrand, 24-28th May 1993,* 149.

JONES SW, STEENAGE GR, SLEE A, SIMPSON EJ, BARDSLEY RG, PARR T and GREENHAFF PL. (2002) Resistance training induces the expression of calpain protease inhibitor calpastatin in human. *The Journal of Physiology* **543P** 86P.

KÄÄRIÄINEN M, LILJAMO T, PELTO-HUIKKO M, HEINO J, JÄRVINEN M, KALIMO H. (2001) Regulation of α7 integrin by mechanical stress during skeletal muscle regeneration. *Neuromuscular Disorders* 11: 360-369.

KATSUMI A, ORR WA, TZIMA E and SCHWARTZ MA. (2004) Integrins in mechanotransduction. *The Journal of Biological Chemistry*, vol. 279, No. 13, pp. 12001-12004.

KEARNS CF, MCKEEVER KH, MALINOWSKI K, STRUCK MB and ABE T. (2001) Chronic administration of therapeutic levels of clenbuterol acts as a repartitioning agent. *Journal Applied Physiology* 91: 2064-2070.

KISSSEL JT, MCDERMOT MP, MENDELL JR, KING WM, PANDYA S, GRIGGS RC and TAWIL R. (2001) Randomized, double-blind, placebo-controlled trial of albuterol in facioscapulohumeral dystrophy. *Neurology* 57: 1434-1440.

KIYMA, Z ALEXANDER BM, VAN KIRK EA, MURDOCH WJ, HALLFORD DM and MOSS GE. (2004) Effects of feed restriction on reproductive and metabolic hormones in ewes. *Journal of American Science*, 82:2548-2557.

KOSEKI T, INOHARA N, CHEN S and NÚNEZ G. (1998) ARC, an inhibitor of apoptosis expressed in skeletal muscle and heart that interacts selectively with caspases. *Proc. Natl. Acad. Science USA* vol. 95, pp. 5156-5160.

KOTLER D and HEYMSFIELD SB. (1998) HIV infection: a model chronic illness for studying wasting diseases. *American Journal Clinical Nutrition* 68:519-20.

KOTLER DP. (2000) Cachexia. *Ann Intern Medicine* 133:622-634.

KREBS EG and GRAVES JD. (2000) Interactions between protein kinases and proteases in cellular signaling and regulation. *Advan. Enzyme Regul.* Vol. 40, pp. 441-470.

KRAMEROVA I, KUDRYASHOVA E, TIDBALL JG and SPENCER MJ. (2004) Null mutation of calpain 3 (p94) in mice causes abnormal sarcomere formation *in vivo* and *in vitro*. *Human Molecular Genetics*, Vol. 13, No. 13, pp. 1373-1388.

KRONQVIST P, KAWAGUCHI N, ALBRECHTSEN R, XU X, SCRODER HD, MOGHADASZADEH B, NIELSEN FC, FROHLICH C, ENGVALL E and WEWER UM. (2002) ADAM12 alleviates the skeletal muscle pathology in *mdx* dystrophic mice. *American Journal of Pathology* 161, 1535-1540.

KRISTENSEN L, THERKILDSEN M, BIIS B, SØRENSEN MT, OKDBJERG N, PURSLOW PP and ERTBJERG P. (2002) Dietary-induced changes of muscle growth rate in pigs: Effects on in vivo and postmortem muscle proteolysis and meat quality. *J. Anim. Sci.* 2002. 80:2862-2871

KRISTENSEN L, THERKILDSEN M, AASLYNG MD, OKDBJERG N, and ERTBJERG P. (2004) Compensatory growth improves meat tenderness in gilts but not in barrows. *J. Anim. Sci.* 82:3617-3624

KUHN KS, SCHUHMANN K, STEHLE P, DARMEUN D and FÜRST P. (1999) Determination of glutamine in muscle protein facilitates accurate assessment of proteolysis and de novo synthesis-derived endogenous glutamine production. *American Journal Clinical Nutrition* 70:484-9.

KUMAMOTO T, FUJIMOTO S, ITO T, HORINOUCHI H, UEYAMA H and TSUDA T. (2000) Proteasome expression in the skeletal muscle of patients with muscular dystrophy. *Acta Neuropathol* 100:595-602.

KUMAR A and BORIEK AM. (2003) Mechanical stress activates the nuclear factor-kappa B pathway in skeletal muscle fibers: a possible role in duchenne muscular dystrophy. *FASEB Journal* 17, 386-396.

KUMAR A, KHANDELWAL N, MALYA R, REID M, BORIEK AM. (2004) Loss of dystrophin causes aberrant mechanotransduction in skeletal muscle fibers. *FASEB Journal*, 18, 102-113.

LACKEY BR, GRAY SL and HENRICKS DM. (1999) The insulin-like growth factor (IGF) system and gonadotropin regulation: actions and interactions. *Cytokine and Growth Factor Reviews* 10: 201-217.

LADNER KJ, CALIGIURI MA and GUTTRIDGE DC. (2003) Tumour necrosis factor-regulated biphasic activation of NF-κB is required for cytokine-induce loss of skeletal muscle gene products. *The Journal of Biological Chemistry.* Vol. 278, No.4, pp. 2294-2303.

LAZARUS DD, DESTREE AT, MAZZOLA LM, MCCORMACK TA, DICK LR, XU B, HUANG JQ, PIERCE JW, READ MA, COGGINS MB, SOLOMON V, GOLDBERG AL, BRAND SJ and ELLIOTT PJ. (1999) A new model of cancer cachexia: contribution of the ubiquitin-proteasome pathway. *American Journal Physiology* 277 (*Endocrinology Metabolism* 40): E332-E341.

LECKER SH, SOLOMON V, MITCH WE and GOLDBERG AL. (1999) Muscle protein breakdown and the critical role of the ubiquitin-proteasome pathway in normal and disease states. *Journal Nutrition.* 129: 227S-237S.

LECKER SH, JAGOE RT, GILBERT A, GOMES M, BARACOS V, BAILEY J, PRICE R, MITCH WE and GOLDBERG AL. (2004) Multiple types of skeletal muscle atrophy involve a common program of changes in gene expression. *FASEB Journal* 18, 39-51.

LEE C-K, KLOPP RG, WEINDRUCH R and PROLLA TA. (1999) Gene expression profile of aging and its retardation by caloric restriction. *Science* 285: 1390-1393.

LEE G. (2001) Nutrient control of the growth hormone and insulin-like growth factor axis in cattle. Thesis submitted to the University of Nottingham for the degree of Doctor of Philosophy.

LI M and DALAKAS MC. (2000) Expression of human IAP-like protein in skeletal muscle: a possible explanation for the rare incidence of muscle fiber apoptosis in T-cell mediated inflammatory myopathies. *Journal of Neuroimmunology* 106: 1-5.

LIBERA LD, ZENNARO R, SANDRI M, AMBROSIO GB and VESCOVO G. (1999) Apoptosis and atrophy in rat slow skeletal muscles in chronic heart failure. *American Journal Physiology* 277 (*Cell Physiology* 46): C982-C986.

LIBERA D L, RAVARA B, ANGELINI A, ROSSINI K, SANDRI M, THIENE G, BATTISTA AMBROSIO G and VESCOVO G. (2001) Beneficial effects on skeletal muscle of the angiotensin II type 1 receptor blocker irbesartan in experimental heart failure. *Circulation* 103(17): 2195-2200.

LIN Y, BROWN K and SIEBENLIST U. (1995) Activation of NF-κB requires proteolysis of the inhibitor IκB-α: signal-induced phosphorylation of IκB-α alone does not release active NF-κB. *Proc. Natl. Acad. Science USA* vol. 92, pp. 552-556.

LIU Z and BARRETT EJ. (2002) Human protein metabolism: its measurement and regulation. *American Journal of Physiology Endocrinology Metabolism* 283: E1105-E1112.

LLOVERA M, CARBÓ N, LÓPEZ-SORIANO J, GARCÍA-MARTÍNEZ, BUSQUETS S, ALVAREZ B, AGELL N, COSTELLI P, LÓPEZ-SORIANO FJ, CELADA A and ARGILÉS JM. (1998) Different cytokines modulate ubiquitin gene expression in rat skeletal muscle. *Cancer Letters* 133: 83-87.

LLOVERA M, GARCÍA-MARTÍNEZ C, AGELL N, LÓPEZ-SORIANO FJ, AUTHIER FJ, GHERARDI RK and ARGILES JM. (1999) Ubiquitin gene expression is increased in human muscle undergoing neurogenic involvement. *Neurochemistry International* 34: 137-140.

LOCKHART DJ and WINZELER EA. (2000) Genomics, gene expression and DNA arrays. *Nature* 405: 827-836.

LORTIE MB and MOON TW. (2003) The rainbow trout skeletal muscle β-adrenergic system: characterization and signaling. *American Journal Physiology Regul Integr Comparative Physiology* 284: R689-R697.

LYDIE C, TILIGNAC T, CLAUSTRE A, VOISIN L, TAILLANDIER D, OBLED, C, TANAKA, K and ATTAIX D. (2002) Torbafylline (HWA 448) inhibits enhanced

skeletal muscle ubiquitin-proteasome-dependent proteolysis in cancer and septic rats. *The Biochemical Journal*, Vol. 361, pp. 185-192.

LYNCH GS, CUFFE SA, PLANT DR and GREGOREVIC P. (2001) IGF-1 treatment improves the functional properties of fast- and slow-twitch skeletal muscles from dystrophic mice. *Neuromuscular Disorders* 11: 260-268.

LYNCH GS, HINKLE RT and FAULKNER JA. (2001) Force and power output of diaphragm muscle strips from *mdx* and control mice after clenbuterol treatment. *Neuromuscular Disorders* 11 192-196.

MA H, FUKIAGE C, KIM YH, DUNCAN MK, REED NA, SHIH M, AZUMA M and SHEARER TR. (2001) Characterization and expression of calpain 10. *The Journal of Biological Chemistry* vol. 276, no. 30. pp. 28525-28531.

MACALLAN DC. (1999) Wasting in HIV infection and AIDS. *Journal Nutrition.* 129: 238S-242S.

MACDONALD J, GALLEY HF and WEBSTER NR. (2003) Oxidative stress and gene expression. *British Journal of Anaesthesia* 90 (2): 221-32.

MALLOUK N, JACQUEMOND V and ALLARD B. (2000) Elevated subsarcolemmal Ca^{2+} in *mdx* mouse skeletal muscle fibers detected with Ca^{2+}-activated K^+ channels. *PNAS* vol. 97, no. 9, 4950-4955.

MALTIN CA, DELDAY MI, SINCLAIR KD, STEVEN J and SNEDDON AA. (2001) Impact of manipulations of myogenesis *in utero* on the performance of adult skeletal muscle. *Reproduction* 122:359-374.

MANN M. (1999) Approved pharmacological interventions for wasting: an overview and lessons learned. *Journal Nutrition.* 129: 303S-305S.

MANSOOR O, BEAUFRERE B, BOIRIE Y, RALLIERE C, TAILLANDIER D, AUROUSSEAU E, SCHOEFFLER P, ARNAL M and ATTAIX D. (1996) Increased mRNA levels for components of the lysosomal, Ca^{2+}-activated, and ATP-ubiquitin-dependent proteolytic pathways in skeletal muscle from head trauma patients. *Proc. Natl. Acad. Science USA* vol. 93, pp. 2714-2718.

MATSUISHI M and OKITANI A. (1997) Proteasome from rabbit skeletal muscle: some properties and effects on muscle proteins. *Meat Science* vol. 45, no. 4, 451-462.

MAYER K, SEEGER W and GRIMMINGER F. (1998) Clinical use of lipids to control inflammatory disease. *Current Opinion Clinical Nutrition Metabolism Care* 1:179-184.

MCCUTCHEN-MALONEY SL, MATSUDA K, SHIMBARA N, BINNS DD, TANAKA K, SLAUGHTER CA and DEMARTINO GN. (2000) cDNA cloning, expression, and functional characterization of PI31, a proline-rich inhibitor of the proteasome. *The Journal of Biological Chemistry* vol. 275, no.24, pp. 18557-18565.

MCDONAUGH MB, FERNANDEZ C and ODDY VH. (1999) Hind-limb protein metabolism and calpain system activity influence post-mortem change in meat quality in lamb. *Meat Science* 52: 9-18.

MERKER K, STOLZING A and GRUNE T. (2001) Proteolysis, caloric restriction and aging. *Mechanisms of Ageing and Development* 122:595-615.

MERSMANN HJ. (1998) Overview of the effects of β-adrenergic agonists on animal growth including mechanisms of action. *Journal Animal Science* 76:160-172.

MITCH WE and GOLDBERG AL. (1996) Mechanisms of muscle wasting; The role of the ubiquitin-proteasome pathway. *The New England Journal of Medicine* vol. 335, no. 25, 1897-1905.

MITCH WE. (1997) Mechanisms causing loss of lean body mass in kidney disease. *American Journal Clinical Nutrition* 67:359-66.

MITCH WE, BAILEY JL, WANG X, JURKOVITZ C, NEWBY D and PRICE SR. (1999) Evaluation of signals activating ubiquitn-proteasome proteolysis in a model of muscle wasting. *American Journal Physiology* 276 (*Cell Physiology* 45): C1132-C1138.

MITCHELL PO and PAVLATH GK. (2001) A muscle precursor cell-dependent pathway contributes to muscle growth after atrophy. *American Journal Physiology Cell Physiology* 281: C1706-C1715.

MITCHELL PO, MILLS ST and PAVLATH GK. (2002) Calcineurin differentiallly regulates maintenance and growth of phenotypically distinct muscles. *American Journal of Physiology Cell Physiology* 282: C984-C992.

MOSONI L, MALMEZAT T, VALLUY MC, HOULIER ML, ATTAIX D and MIRAND PP. (1999) Lower recovery of muscle protein lost during starvation in old rats despite a stimulation of protein synthesis. *American Journal Physiology* 277 (*Endocrinology Metabolism* 40): E608-E616.

NAKAGAWA T and YUAN J. (2000) Cross-talk between two cysteine protease families: activation of caspase-12 by calpain in apoptosis. *The Journal of Cell Biology* vol. 150, no. 4, 887-894.

NAVEGANTES LCC, RESANO NMZ, MIGLIORINI RH and KETTELHUT IC. (1999) Effect of guanethidine-induced adrenergic blockade on the different proteolytic systems in rat skeletal muscle. *American Journal Physiology* 277:E883-E889.

NAVEGANTES LCC, RESANO NMZ, MIGLIORINI RH and KETTELHUT IC. (2001) Role of adrenoceptors and cAMP on the catecholamine-induced inhibition of proteolysis in rat skeletal muscle. *American Journal Physiology Endocrinology Metabolism* 280: E663-E668.

NAVEGANTES LCC, MIGLIORINI RH and KETTELHUT IC. (2002) Adrenergic control of protein metabolism in skeletal muscle. *Current Opinion Clinical Nutrition Metabolism Care* 5:281-286.

NEUSS M, CROW MT, CHESLEY A and LAKATTA EG. (2001) Apoptosis in cardiac disease—what is it—how does it occur. *Cardiovascular Drugs and Therapy* 15: 507-523.

NEUSS M, MONTICONE R, LUNDBERG MS, CHESLEY AT, FLECK E and CROW MT. (2001) The apoptotic regulatory protein ARC (Apoptosis Repressor with Caspase recrutiment domain) prevents oxidant stress-mediated cell death by preserving mitochondrial function. *The Journal of Biological Chemistry* vol. 276, no. 36, pp. 33915-33922.

NGUYEN C, ROCHA D, GRANJEAUD S, BALDIT M, BERNARD K, NAQUET P and JORDAN BR. (1995) Differential gene expression in the murine thymus assayed by quantitative hybridization of arrayed cDNA clones. *Genomics* 29: 207-216.

NICHOLAS G, THOMAS M, LANGLEY B, SOMERS W, PATEL K, KEMP CF, SHARMA M and KAMBADUR R. (2002) Titin-cap associates with, and regulates secretion of, myostatin. *Journal of Cellular Physiology* 193, pp. 120-131.

OHARA N, TASHIRO T, YAMAMORI H, TAKAGI K, NAKAJIMA N and SUNAGA K. (1995) Clinical study of amino acid metabolism of skeletal muscle under surgical stress. *Japanese Journal of Surgical Metabolism and Nutrition* 19: 15-24.

OLSON EN and WILLIAMS RS. (2000) Remodeling muscle with calcineurin. *BioEssays* 22: 510-519.

ONO Y, SORIMACHI H and SUZUKI K. (1999) New aspect of the research on limb-girdle muscular dystrophy 2A: a molecular biologic and biochemical approach to pathology. *Trends Cardiovascular Medicine* vol. 9, no.5.

OTANI K, HAN D-H, FORD EL, GARCIA-ROVES PM, YE H, HORIKAWA Y, BELL GI, HOLLOSZY JO and POLONSKY KS. (2004) Calpain system regulates muscle mass and glucose transporter GLUT4 turnover. *Journal Biological Chemistry* 10.1074/jbc.M400213200.

PARR T, BARDSLEY RG, RS GILMOUR and BUTTERY PJ. (1992) Changes in calpain and calpastatin mRNA induced by beta-adrenergic stimulation of bovine skeletal muscle. *European Journal of Biochemistry*, vol. 208, 333-339.

PARR T, SENSKY PL, SCOTHERN GP, BARDSLEY RG, BUTTERY PJ, WOOD JD and WARKUP C. (1999) Relationship between skeletal muscle-specific calpain and tenderness of conditioned porcine longissmus muscle. *Journal Animal Science* 77:661-668.

PARR T, SENSKY PL, ARNOLD MK, BARDSLEY RG and BUTTERY PJ. (2000) Effects of epinephrine infusion on expression of calpastatin in porcine cardiac and skeletal muscle. *Archives of Biochemistry and Biophysics* vol. 374, no. 2, pp. 299-305.

PARR T, SENSKY PL, BARDSLEY RG and BUTTERY PJ. (2001) Calpastatin expression in porcine cardiac and skeletal muscle and partial gene structure. *Archives of Biochemistry and Biophysics* vol. 395, no. 1, pp. 1-13.

PAUL AC and ROSENTHAL N. (2002) Different modes of hypertrophy in skeletal muscle fibers. *The Journal of Cell Biology* vol. 256, no. 4: 751-760.

PELLEGRINO MA, D'ANTONA G, BORTOLOTTO S, BOSCHI F, PASTORIS O, BOTTINELLI R, POLLA B and REGGIANO C. (2003) Clenbuterol antagonizes glucocorticoid-induced atrophy and fibre type transformation in mice. *Exp Physiology* 89.1 pp 89-100.

PENNER G, GANG G, WRAY C, FISCHER JE and HASSELGREN P-O. (2001) the transcription factors NF-κB and AP-1 are differentially regulated in skeletal muscle during sepsis. *Biochem. Biophys. Res. Commun.* 281: 1331-1336.

PENNER G, GANG G, SUN X, WRAY C and HASSELGREN P-O. (2002) C/EBP DNA-binding activity is upregulated by a glucocorticoid-dependent mechanism in septic muscle. *American Journal Physiology Regulatory Integrative Comparative Physiology* 282: R439-R444.

PERMUTT MA, BERNAL-MIZRACHI E and INOUE H. (2000) Calpain 10: the first positional cloning of a gene for type 2 diabetes? *The Journal of Clinical Investigation* vol. 106, no.7, pp. 819-821.

PERRIN BJ and HUTTENLOCHER A. (2002) Molecules in focus, Calpain. *The International Journal of Biochemistry and Cell Biology* 34: 722-725.

PETTE D and STARON R. (2000) Myosin isoforms, muscle fiber types, and transitions. *Microsc Research Tech* 50:500-509.

PFAFF M, DU X and GINSBERG MH. (1999) Calpain cleavage of integrin β cytoplasmic domains. *Federation of European Biochemical Societies Letters* vol 460, issue 1, pp. 17-22.

PI-SUNYER FX. (2000) Overnutrition and undernutrition as modifiers of metabolic processes in disease states. *American Journal Clinical Nutrition,* 72(suppl):533S-7S.

PRESTON T, SLATER C, MCMILLAN DC, FALCONER JS, SHENKIN A and FEARON KCH. (1998) Fibrinogen synthesis is elevated in fasting cancer patients with an acute phase response. *The Journal of Nutrition* vol. 128, no.8, pp. 1355-1360.

PROCTOR DN, BALAGOPAL P and NAIR KS. (1998) Age-related sarcopenia in humans is associated with reduced synthetic rates of specific muscle proteins. *Journal Nutrition.* 128: 351S-355S.

RAINA N and JEEJEEBHOY KN. (1998) Changes in body composition and dietary intake induced by tumour necrosis factor α and corticosterone-individually and in combination. *American Journal of Clinical Nutrition.* 68: 1284-90.

RALLIÈRE C, TAUVERON I, TAILLANDIER D, GUY L, BOITEUX J-P, GIRAUD B, ATTAIX D and THIÉBLOT P. (1997) Glucocorticoids do not regulate the expression of proteolytic genes in skeletal muscle from cushings syndrome patients. *Journal of Clinical Endocrinology and Metabolism* vol. 82, no.9

RAJAB P, FOX J, RIAZ S, TOMLINSON D, BALL D and GREENHAFF PL. (2000) Skeletal muscle myosin heavy chain isoforms and energy metabolism after clenbuterol treatment in the rat. *American Journal Physiology Regulatory Integrative Comparative Physiology* 279: R1076-R1081.

RAO RV, HERMEL E, CASTRO-OBREGON S, DEL RIO G, ELLERBY LM, ELLERBY HM and BREDESEN DE. (2001) Coupling endoplasmic reticulum stress to the cell death program. *The Journal of Biological Chemistry* vol. 276, no. 36, pp. 33869-33874.

RAO RV, CASTRO-OBREGON S, FRANKOWSKI H, SCHULER M, STOKA V, DEL RIO G, BREDESEN DE and ELLERBY HM. (2002) Coupling endoplasmic reticulum stress to the cell death program. *The Journal of Biological Chemistry* vol. 277, no.24, pp. 21836-21842.

RAYNAUD F, BONNAL C, FERNANDEZ E, BREMAUD L, CERUTTI M, LEBART M-C, ROUSTAN C, OUALI A and BENYAMIN Y. (2003) The calpain 1-α-actinin interaction. *European Journal Biochemistry* 270, 4662-4670.

RENNIE MJ and TIPTON KD. (2000) Protein and amino acid metabolism during and after exercise and the effects of nutrition. *Annual Review of Nutrition.* 20:457-83.

RICHARD I, ROUDAUT C, MARCHAND S, BAGHDIGUIAN S, HERASSE M, STOCKHOLM D, ONO Y, SUEL L, BOURG N, SORIMACHI H, LEFRANC G, FARDEAU M, SÉBILLE A and BECKMANN JS. (2000) Loss of calpain 3 proteolytic activity leads to muscular dystrophy and to apoptosis-associated IκBα/nuclear factor κB pathway perturbation in mice. *The Journal of Cell Biology* volume 151, number 7, 1583-1590.

ROOYACKERS OE and NAIR KS. (1997) Hormonal regulation of human muscle protein metabolism. *Annual Reviewof Nutrition.* 1997. 17:457-85.

ROUBENOFF R. (1997) Inflammation and hormonal mediators of cachexia. *Journal Nutrition.* 127: 1014S-1016S.

ROUBENOFF R. (1999) The pathophysiology of wasting in the elderly. *Journal Nutrition.* 129: 256S-259S.

RUEST L-B, KHALYFA A and WANG E. (2002) Development-dependent disappearance of caspase-3 in skeletal muscle is post-transcriptionally regulated. *Journal of Cellular Biochemistry* 86:21-28.

RYALL JG, GREGOREVIC P, PLANT DR, SILLENCE MN and LYNCH GS. (2002) β_2-Agonist fenoterol has greater effects on contractile function of rat skeletal muscle than clenbuterol. *American Journal Physiology Regul Integrative Comparative Physiology* 283: R1386-R1394

RYALL JG, PLANT DR, GREGOREVIC P, SILLENCE MN and LYNCH GS. (2003) β_2-agonist administration reverses muscle wasting and improves muscle function in aged rats. *Journal Physiology* 555.1 pp 175-188.

SADOSHIMA J and IZUMO S. (1997) The cellular and molecular response of cardiac myocytes to mechanical stress. *Annual Review of Physiology.* 59: 551-71.

SANDRI M and CARRARO U. (1999) Apoptosis of skeletal muscles during development and disease. *The International Journal of Biochemistry & Cell Biology* 31, 1373-1390.

SANDRI M, EL MESLEMANI AH, SANDRI C, SCHJERLING P, VISSING K, ANDERSEN JL, ROSSININ K, CARRARO U and ANGELINI C. (2001) Caspase 3 expression correlates with skeletal muscle apoptosis in duchenne and facioscapulo human muscular dystrophy. A potential target for pharmacological treatment? *Journal of Neuropathology and Experimental Neurology* vol. 60, no.3, 302-312.

SAZILI AQ. (2003) Calpastatin and meat tenderness in sheep and cattle. A thesis submitted to the University of Nottingham for the degree of Doctor of Philosophy.

SAZILI AQ, LEE GK, PARR T, SENSKY PL, BARDSLEY RG and BUTTERY PJ. (2003) The effect of altered growth rates on the calpain proteolytic system and meat tenderness in cattle. *Meat Science* 66, 195-201.

SAZONTOVA TG, MATSKEVRICH AA and ARKHIPENKO YV. (1999) Calpains: physiological and pathophysiological significance. *Pathophysiology* 6: 91-102.

SCHWARTZ AL and CIECHANOVER A. (1999) The ubiquitin-proteasome pathway and pathogenesis of human diseases. *Annual Review Medicine.* 50:57-74

SEALS DF and COURTNEIDGE SA. (2003) The ADAMs family of metalloproteases: multidomain proteins with multiple functions. *GENES & DEVELOPMENT.* 17:7-30.

SENSKY PL, PARR T, BARDSLEY RG, BUTTERY PJ. (1996) The relationship between plasma epinephrine concentration and the activity of the calpain system in porcine longissmus muscle. *Journal of Animal Science* 74: 380-387.

SEMSARIAN C, WU M-J, JU Y-K, MARCINIEC T, YEOH T, ALLEN DG, HARVEY RP and GRAHAM RM. (1999) Skeletal muscle hypertrophy is mediated by a Ca^{2+}-dependent calcineurin pathway. *NATURE* vol. 400: 576-585.

SHEN J, CHANAVAJHALA P, SELDIN DC and SONENSHEIN GE. (2001) Phosphorylation by the protein kinase CK2 promotes calpain-mediated degradation of IκBα. *The Journal of Immunology* 167: 4919-4925.

SHUMAY E, GAVI S, WANG H-Y and MALBON CC. (2004) Trafficking of β2-adrenergic receptors: insulin and β-agonists regulate internalization by distinct cytoskeletal pathways. *Journal of Cell Science* 117, 593-600.

SLEE EA, HARTE MT, KLUCK RM, WOLF BB, CASIANO CA, NEWMEYER DD, WANG H-G, REED JC, NICHOLSON DW, ALNEMRI ES, GREEN DR and MARTIN SJ. (1999) Ordering the cytochrome c-initiated caspase cascade: Hierarchical activation of caspases-2, -3, -6, -7, -8, and −10 in a caspase-9—dependent manner. *The Journal of Cell Biology* vol. 144, no. 2, 281-292.

SMITH L, CHEN L, REYLAND ME, DEVRIES TA, TALANIAN RV, OMURA S and SMITH JB. (2000) Activation of atypical protein kinase C ζ by caspase processing and degradation by the ubiquitin-proteasome system. *The Journal of Biological Chemistry* vol. 275, no.51, pp. 40620-40627.

SNEDDON AA, DELDAY MI and MALTIN CA. (2000) Amelioration of denervation-induced atrophy by clenbuterol is associated with increased PKC-α activity. *American Journal Physiology Endocrinology Metabolism* 279: E188-E195.

SNEDDON AA, DELDAY MI, STEVEN J and MALTIN CA. (2001) Elevated IGF-II mRNA and phosphorylation of 4E-BP1 and $p70^{s6k}$ in muscle showing clenbuterol-induced anabolism. *American Journal Physiology Enodocrinol Metabolism* 281: E676-E682.

SOLOMON V, LECKER SH and GOLDBERG AL. (1998) The N-end rule pathway catalyzes a major fraction of the protein degradation in skeletal muscle. *The Journal of Biological Chemistry.* Vol. 273, No.39, pp.25216-25222.

SONKSEN PH. (2001) Insulin, growth hormone and sport. *Journal of Endocrinology* 170: 13-25.

SORIMACHI H, IMAJOH-OHMI S, EMORI Y, KAWASAKI H, OHNO S, MINAMI Y and SUZUKI K. (1989) Molecular cloning of a novel mammalian calcium-dependent protease distinct from both m- and μ- types. *The Journal of Biological Chemistry* vol. 264, no. 33, pp. 20106-20111.

SORIMACHI H, FORSBERG NE, LEE H-J, JOENG S-Y, RICHARD I, BECKMANN JS, ISHIURA S and SUZUKI K. (1996) Highly conserved structure in the promoter region of the gene for muscle-specific calpain, p94. *Biol. Chem.* Vol. 377, pp. 859-864.

SPANGENBURG EE. (2003) IGF-1 isoforms and ageing skeletal muscle: an 'unresponsive' hypertrophy agent? *Journal of Physiology*, **547.1**, p.2

SPANGENBURG EE and BOOTH FW. (2003) Molecular regulation of individual skeletal muscle fibre types. *Acta Physiology Scand* 2003, 178, 413-424.

SPECK PA, COLLINGWOOD KM, BARDSLEY RG, TUCKER GA, GILMOUR RS and BUTTERY PJ. (1993) Transient changes in growth and in calpain and calpastatin expression in ovine skeletal muscle after short-term dietary inclusion of cimaterol. *Biochimie*, 75 (10): 917-923.

SPENCER MJ and MELLGREN RL. (2002) Overexpression of a calpastatin transgene in *mdx* muscle reduces dystrophic pathology. *Human Molecular Genetics* vol. 11, no.21, pp. 2645-2655.

ST-AMAND J, OKAMURA K, MATSUMOTO K, SHIMIZU S and SOGAWA Y. (2001) Characterization of control and immobilized skeletal muscle: an overview from genetic engineering. *FASEB Journal* 15: 684-692.

STEVENSON EJ, GIRESI PG, KONCAREVIC A and KANDARIAN SC. (2003) Global analysis of gene expression patterns during disuse atrophy in rat skeletal muscle. *Journal Physiology* 551.1, pp33-48.

STOCKHOLM D, HERASSE M, MARCHAND S, PRAUD C, ROUDAUT C, RICHARD I, SEBILLE A and BECKMANN JS. (2001) Calpain 3 mRNA expression in mice after denervation and during muscle regeneration. *American Journal Physiology Cell Physiology* 280: C1561- C1569.

STRASSER A, O'CONNOR L and DIXIT VM. (2000) Apoptosis signaling. *Annual Review Biochemistry* 69:217-45.

STUPKA N, TARNOPOLOSKY MA, YARDLEY NJ and PHILLIPS SM. (2001) Cellular adaptation to repeated eccentric exercise-induced muscle damage. *Journal Applied Physiology* 91: 1669-1678.

SULTAN KR, DITTRICH BT and PETTE D. (2000) Calpain activity in fast, slow, transforming, and regenerating skeletal muscles of rat. *American Journal Physiology Cell Physiology* 279: C639-C647.

SULTAN KR, DITTRICH BT, LEISNER E, PAUL N and PETTE D. (2001) Fiber type-specific expression of major proteolytic systems in fast- to slow-transforming rabbit muscle. *American Journal Physiology Cell Physiology* 280: C239-247.

SWOAP SJ, HUNTER RB, STEVENSON EJ, FELTON HM, KANSAGRA NV, LANG JM, ESSER KA and KANDARIAN SC. (2000) The calcineurin-NFAT pathway and muscle fiber-type gene expression. *American Journal of Physiology Cell Physiology* 279: C915-C924.

SYMONDS ME, ANDREWS DC and JOHNSON P. (1989) the endocrine and metabolic response to feeding in the developing lamb. *Journal of Endocrinology*, **123**, 295-302.

TAILLANDIER D, AUROSSEAU E, COMBARET L, GUEZENNEC C-Y and ATTAIX D. (2003) Regulation of proteolysis during reloading of the unweighted soleus muscle. *The International Journal of Biochemistry and Cell Biology* 35 : 665-675.

TAVEAU M, BOURG N, SILLON G, ROUDAUT C, BARTOLI M and RICHARD I. (2003) Calpain 3 is activated through autolysis within the active site and lyses sarcomeric and sarcolemmal components. *Molecular and Cellular Biology*, vol. 23, no. 24, p. 9127-9135.

TAYLOR RG, GEESINK GH, THOMPSON VF, KOOHMARAIE M and GOLL DE. (1995) Is Z-disk degradation responsible for postmortem tenderization? *Journal Animal Science* 73:1351-1367.

THOMPSON MG and PALMER RM. (1998) Signalling pathways regulating protein turnover in skeletal muscle. *Cell. Signal.* vol. 10, no. 1, pp. 1-11.

TIDBALL JG and SPENCER MJ. (2000) Calpains and muscular dystrophies. *The International Journal of Biochemistry & Cell Biology* 32: 1-5.

TIDBALL JG and SPENCER MJ. (2002) Expression of a calpastatin transgene slows muscle wasting and obviates changes in myosin isoform expression during murine muscle disuse. *Journal of Physiology* 545.3. pp. 819-828.

TISDALE MJ. (1999) Wasting in cancer. *Journal Nutrition.* 129: 243S-246S.

TISDALE MJ. (2000) Metabolic abnormalities in cachexia and anorexia. *Nutrition* 16:1013-1014.

TKATCHENKO AV, PIÉTU G, CROS N, GANNOUN-ZAKI L, AUFFRAY C, LÉGER JJ and DECHESNE CA. (2001) Identification of altered gene expression in skeletal muscle from duchenne muscular dystrophy patients. (2001) *Neuromuscular Disorders* 11: 269-277.

TOTLAND GK and KRYVI H. (1991) Distribution patterns of muscle fibre types in major muscles of the bull (*Bos taurus*). *Anatomy and Embryology.* 184: 441-450.

TOUMI H and BEST TM. (2003) The inflammatory response: friend or enemy for muscle injury? *British Journal Sports Medicine* 2003;37:284-286.

TSUJINAKA T, FUJITA J, EBISUI C, YANO M, KOMINAMI E, SUZUKI K, TANAKA K, KATSUME A, OHSUGI Y, SHIOZAKI H and MONDEN M. (1996) Interleukin 6 receptor antibody inhibits muscle atrophy and modulates proteolytic systems in interleukin 6 transgenic mice. *Journal Clinical Investigations* 97:244-249.

TSUJINAKA T, KISHIBUCHI M, YANO M, MORIMOTO T, EBISUI C, FUJITA J, OGAWA A, SHIOZAKI H, KOMINAMI E and MONDEN M. (1997) Involvement of interleukin-6 in activation of lysosomal cathepsin and atrophy of muscle fibers induced by intramuscular injection of turpentine oli in mice. *Journal Biochemistry* 122: 595-600.

VANN RC, NGUYEN HV, REEDS PJ, BURRIN DG, FIOROTTO ML, STEELE NC, DEAVER DR and DAVIS TA. (2000) Somatotropin increases protein balance by lowering body protein degradation in fed, growing pigs. *American Journal of Physiology Endocrinology Metabolism* 278: E477-E483.

VERRET C, POUSSARD S, TOUYAROT K, DONGER C, SAVART M, COTTIN P and DUCASTAING A. (1999) Degradation of protein kinase Mα by μ-calpain-protein kinase Cα complex. *Biochimica et Biophysica Acta* 1430: 141-148.

VESCOVO G, VOLTERRANI M, SANDRI M, CECONI C, LORUSSO R, FERRARI R, AMBROSIO GB and LIBERA LD. (2000) Apoptosis in the skeletal muscle of patients with heart failure: investigation of clinical and biochemical changes. *Heart* 2000;84:431-437.

VESCOVO G, RAVARA B, ANGELINI A, SANDRI M, CARRARO U, CECONI C and LIBERA LD. (2002) Effect of thalidomide on the skeletal muscle in experimental heart failure. *The European Journal of Heart Failure* (uncorrected proof).

VESCOVO G, RAVARA B, GOBBO V, SANDRI M, ANGELINI A, BARBERA MD, DONA M, PELUSO G, CALVANI M, MOSCONI L and LIBERA LD. (2002) L-Carnitine: a potential treatment for blocking apoptosis and preventing skeletal muscle myopathy in heart failure. *American Journal Physiology Cell Physiology* 283: C802-C810.

VESTERGAARD M, PURUP S, FRYSTYK J, LØVENDAHL P, SØRENSEN MT, RIIS PM, FLINT DJ and SEJRSEN. (2003) Effects of growth hormone and feeding level on endocrine measurements, hormone receptors, muscle growth and performance of prepubertal heifers. *Journal of Animal Science*, 81:2189-2198.

VOET AND VOET. (1995) Motility: muscles, cilia, and flagella. In: *Biochemisty, Second Edition*, pp. 1234-1260. Wiley, Canada.

VOET AND VOET. (1995) Protein degradation. In: *Biochemisty, Second Edition*, pp. 1010-1014. Wiley, Canada.

VOMDAHL S., HAUSSINGER, D. (1996) Nutritional state and the swelling-induced inhibition of proteolysis in perfused rat liver. *Journal of Nutrition*, vol. 126, 395-402.

WALDER K, MCMILLAN J, LAPSYS N, KRIKETOS A, TREVASKIS J, CIVITARESE A, SOUTHON A, ZIMMET P and COLLIER G. (2002) Calpain 3 gene expression in skeletal muscle is associated with body fat content and measures of insulin resistance. *International Journal of Obesity* 26: 442-449.

WEINSTEIN RB, SLENTZ MJ, WEBSTER K, TAKEUCHI JA and TISCHLER ME. (1997) Lysosomal proteolysis in distally or proximally denervated rat soleus muscle. *American Journal Physiology* 273: R1562-R1565.

WILKINSON KD. (1999) Ubiquitin-dependent signaling: The role of ubiquitination in the response of cells to their environment. *Journal Nutrition.* 129: 1933-1936.

WILLIAMS A, WANG JJ, WANG L, SUN X, FISCHER JE and HASSELGREN P-O. (1998) Sepsis in mice stimulates muscle proteolysis in the absence of IL-6. *American Journal Physiology* 275 (*Regulatory Integrative Comparative Physiology* 44):R1983-R1991.

WILLIAMS AB, DECOURTEN-MYERS GM, FISCHER JE, LUO G, SUN X and HASSELGREN P-O. (1999) Sepsis stimulates release of myofilaments in skeletal muscle by a calcium-dependent mechanism. *FASEB Journal* 13, 1435-1443.

WING SS and BANVILLE D. (1994) 14-kDa ubiquitin-conjugating enzyme: structure of the rat gene and regulation upon fasting and insulin. *Am. J. Physiol.* 267 (*Endocrinol. Metab.* 30): E39-E48.

YARASHEKI KE, ZACHWIEJA JJ, GISCHLER J, CROWLEY J, HORGAN MM and POWDERLY WG. (1998) Increased plasma Gln and Leu R_a and inappropriately low muscle protein synthesis rate in AIDS wasting. *Journal Physiology* 275 (*Endocrinology Metabolism* 38): E577-E583.

YEH SS and SCHUSTER MW. (1999) Geriatric cachexia: the role of cytokines. *American Journal Clinical Nutrition* 70:183-97.

YIN JL, SHACKEL NA, ZEKRY A, MCGUINNESS PH, RICHARDS C, VAN DER PUTTEN K, MCCAUGHAN GW, ERIS JM and BISHOP GA. (2001) Real-time reverse transcriptase-polymerase chain reaction (RT-PCR) for measurement of cytokine and growth factor mRNA expression with flurogenic probes or SYBR Green I. *Immunology and Cell Biology* 79, 213-221.

ZHANG X-J, CHINKES DL, WOLF SE and WOLFE RR. (1999) Insulin but not growth hormone stimulates protein anabolism in skin wound and muscle. Am. J. Physiol. 276 (Endocrinol. Metab. 39): E712-E720.

APPENDIX A. cDNA PROBE DEVELOPMENT

This section of the appendix contains information and data, previously summarised within the cDNA Probe Development section (Chapter 5). The following describes in 'probe order' 1-20 (Appendix A1-20), detailed figured and sectioned information regarding:

Fig. A) cDNA/mRNA sequences available in nucleotide database for specified gene of interest. Each related sequence- to be used for a multiple sequence alignment (Fig. B), is numbered, followed by an accession number, and species identification, e.g. for Caspase-7 (appendix A1): 1)- U39613 - Human. It is assumed that sequences are mRNA species unless stated otherwise in brackets, e.g. (cDNA EST clone etc.)

Fig. B) A cDNA/mRNA multiple sequence alignment across species using sequences in Fig. A. Sequences are aligned in a numbered order, as indicated in A).* symbol indicates that a base is conserved across all sequences analysed. The region illustrated includes the specific PCR target region of the sequences. Forward and reverse PCR primer locations are highlighted in red, and by directional arrows.

Fig. C1) PCR conditions: Indicated are the optimal conditions (arrived at experimentally) for yielding a positive PCR result: Primer length, and sequence; start and finish base numbers of one of the sequences indicated in Fig. A., and PCR amplicon size; optimum annealing temperature, number of thermocycles, and Taq polymerase used is indicated and PCR conditions were as indicated in materials and methods.

Fig. C2) Problematic PCR reactions, that involved profound alterations in PCR conditions to yield a positive result, are described in an additional box directly below Figure. B. Alternative PCR template and primers are described.

Fig. D) An example of a positive PCR result, viewed after gel electrophoresis and staining, next to a 100 bp marker.

Fig. E) Sequence of the PCR product/cloned cDNA plasmid insert generated is included; along with note of length in bp.

Fig. F) A summary of a BLAST search on the sequenced PCR product. Three examples are given of mRNA sequences (unless stated otherwise under description) with the closest homology, and if possible, closest human, porcine, bovine, or ovine tissue-specific alignments. The accession number, species and description is listed; along with a sequence 'identities' value and % (previously described in results section), alignment score in 'bits', and an E Value.

Score and E Value: These are based on the statistical analysis of sequence comparisons, described in detail on the NCBI homepage. The Score, in 'bits', is a normalised raw data score, that takes in to account specific statistical parameters. A score value is given to sequence comparisons, such that the higher the bit score, the greater the similarity of sequences. Blast outputs are arranged in a listed manner in order of Score numbers. The E Value describes the number of sequence 'hits' that can be "expected", by chance, when searching a specific database, with a specific sequence of certain length. The lower the E Value, and closer to 0, the more significant the search alignment is, i.e. the lower the probability the sequence is found by pure chance. The E Value takes in to account the raw score value and sequence length, such that smaller sequences will obviously have a higher probability (or expect value) to be found by chance.

APPENDIX A1: CASPASE-7

Figure A. Available Caspase-7 sequences.

No.	Acc.No.	Species
1)	U39613	Human
2)	U67321	Murine
3)	U47332	Hamster (Golden Hamster)

N.B. No Porcine, Bovine or Ovine sequence data available.

Figure B. Multiple alignment of sequences for Caspase-7. PCR target region and primer locations are included.

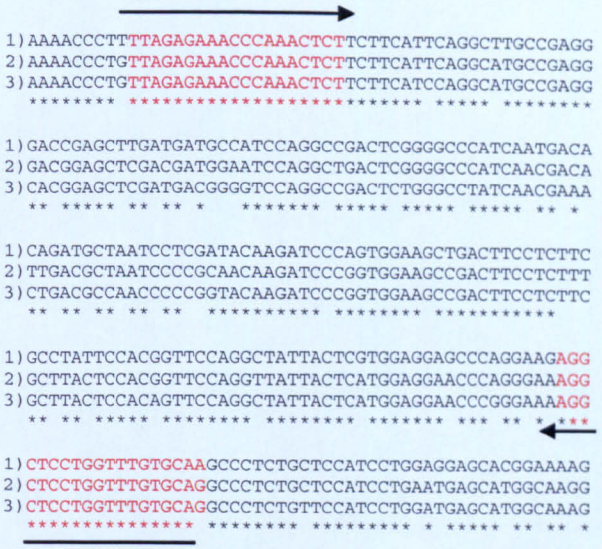

Figure C1. PCR Conditions.

Fwd. primer- 19 bp
(TTAGAGAAACCCAAACTCT)

Start- 1107 of 2006 bp sequence (2).

Rev. primer- 19 bp
(TTGCACAAACCAGGAGCCT)

Finish- 1313 of 2006 bp sequence (2).

Amplicon size- 207 bp

Annealing temp.- 53°C

Cycles- 35

Promega taq polymerase

Figure D. Caspase-7 PCR product run on a 1.5% agarose gel, alongside a 100bp marker.

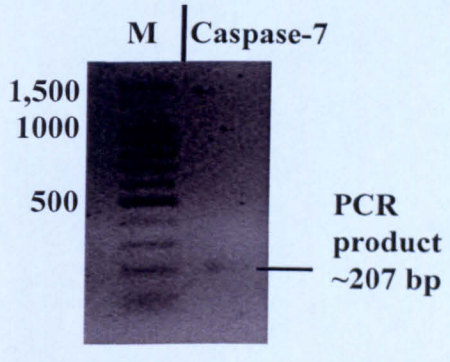

Figure E. DNA sequencing of cloned cDNA insert.

TTAGAGAAACCCAAACTCTTCTTCATTCAGGCTTG
CCGGGGCACGGAGCTCGATGACGGGATCCAGGCA
GACTCGGGGCTTATCAATGACACAGATGCTAATCC
CCGGTATAAGATCCCAGTTGAAGCCGACTTTCTCT
TCGCCTATTCCACAGTTCCAGGCTATTACTCATGGA
GGAGCCCGGGGAGAGGCTCCTGGTTGGGCAA
(206 bp sequenced)

Figure F. Significant sequences from BLAST search of sequence in Fig. E.

Significant sequence alignment to:

Acc.No.	Species	Description	Identities	Score (bits)	E value
U67206	Human	Caspase-7	182/200 (91%)	254	6e-65
U47332	Golden Hamster	Caspase-7	178/200 (89%)	222	2e-55
Y13088	Murine	Caspase-7	174/200 (87%)	190	7e-46

APPENDIX A2: ARC (Apoptosis repressor with CARD domain)

Figure A. Available ARC sequences.

Acc.No.	Species	Description
AF043244	Human	ARC mRNA, 900 bp's, complete cds

N.B. No Porcine, Bovine, Ovine, sequence data available.

Figure C1. PCR Conditions.

Fwd. primer- 20 bp
(AAACGCCTGGTCGAGACGCT)

Start- 168 bp.

Rev. primer- 19 bp
(CACGTGCTGCCAGTCCCAA)

Finish- 407 bp.

Amplicon size- 240 bp

Annealing temp.- 58°C

Cycles- 35

Promega taq polymerase

Figure B. Human ARC mRNA sequence. PCR target region and primer locations are included.

AGCCTGAGGAGGAGACAGGACAGAGCGTCTGGAGAGGCAGGAGGACACCGAGTTCCCCGTGTTGGCCTCC
AGGTCCTGTGCTTGCGGAGCCGTCCGGCGGCTGGGATCGAGCCCCGACAATGGGCAACGCGCAGGAGCGG

CCGTCAGAGACTATCGACCGCGAGCGGAAACGCCTGGTCGAGACGCTGCAGGCGGACTCGGGACTGCTGT
TGGACGCGCTGCTGGCGCGGGGCGTGCTCACCGGGCCAGAGTACGAGGCATTGGATGCACTGCCTGATGC
CGAGCGCAGGGTGCGCCGCCTACTGCTGCTGGTGCAGGGCAAGGGCGAGGCCGCCTGCCAGGAGCTGCTA
CGCTGTGCCCAGCGTACCGCGGGCGCGCCGGACCCCGCTTGGGACTGGCAGCACGTGGGTCCGGGCTACC

GGGACCGCAGCTATGACCCTCCATGCCCAGGCCACTGGACGCCGGAGGCACCCGGCTCGGGGACCACATG
CCCCGGGTTGCCCAGAGCTTCAGACCCTGACGAGGCCGGGGGCCCTGAGGGCTCCGAGGCGGTGCAATCC
GGGACCCCGGAGGAGCCAGAGCCAGAGCTGGAAGCTGAGGCCTCTAAAGAGGCTGAACCGGAGCCGGAGC
CAGAGCCAGAGCTGGAACCCGAGGCTGAAGCAGAACCAGAGCCGGAACTGGAGCCAGAACCGGACCCAGA
GCCCGAGCCCGACTTCGAGGAAAGGGACGAGTCCGAAGATTCCTGAAGGCCAGAGCTCTTGACAGGCGGT
GCCCCGCCCATGCTGGATAGGACCTGGGATGCTGCTGGAGCTGAATCGGATGCCACCAAGGCTCGGTCCA
GCCCAGTACCGCTGGAAGTGAATAAACTCCGGAGGGTCGGACGGGACCTGGGCTCTCTCC

Figure D. ARC PCR product run on a 1.5% agarose gel, alongside a 100bp marker.

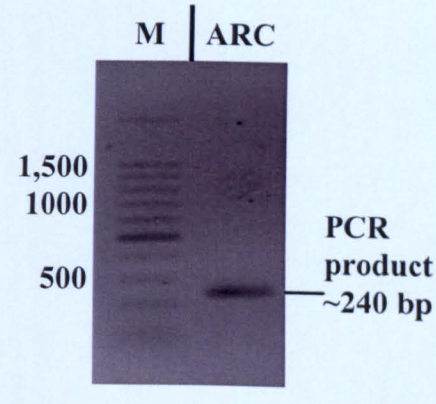

Figure E. DNA sequencing of cloned cDNA insert.

AAACGCCTGCCCGAGACGCTACAGGCAGACTCAGGGC
TGCTGCCGGATGCGCTGCTGGCACGGGGCGTGCTCAGC
CGGACTAGACCACGATGCGTTGGACGCACTGCCTGATG
CCGAGCGCAGGGTACGTCGCCTGCTGCTGCTGGTGCAA
AGCAAGGGCGAGGCCGCCTGCCGTGAACTGTTGAACTG
CGCCCAGCGAACCGTGCACGCACCCGACCCCGCTTGGG
ACTGGCAGCACGTG
(241 bp sequenced)

Figure F. Significant sequences from BLAST search of sequence in Fig. E.

Significant sequence alignment to:

Acc.No.	Species	Description	Identities	Score (bits)	E value
AF043244	Human	ARC	204/241 (84%)	176	1e-41
AY459322	Murine	ARC	127/152 (83%)	95.6	4e-17

APPENDIX A3: CASPASE-3

Figure A. Available Caspase-3 sequences.

No.	Acc.No.	Species
1)	U19522	Murine
2)	U84410	Rat
3)	U27463	Hamster (Chinese Hamster)
4)	U13737	Human
5)	AB029345	Porcine
6)	AF068837	Ovine

Figure C1. PCR Conditions.

Fwd. primer- 21 bp
(CATAGCAAAAGGAGCAGTTTT)

Start- 322 of 834 bp sequence (5).

Rev. primer- 21 bp
(CCACTGTCCGTCTCAATCCCA)

Finish- 530 of 834 bp sequence (5).

Amplicon size- 209 bp

Annealing temp.- 59°C

Cycles- 35

Promega taq polymerase

Figure E. DNA sequencing of cloned cDNA insert.

CATAGCAAAAGGAGCAGTTTTATCTGCGTGCTTCTA
AGCCATGGTGAAGAAGGAAAAATTTTTGGAACAAA
TGGACCTGTTGATCTGAAAAAATTAACAAGTTTCTT
CAGAGGGGACTGTTGTAGAACTCTAACTGGCAAAC
CCAAACTTTTCATAATTCAGGCCTGCCGAGGCACAG
AATTGGACTGTGGGATTGAGACGGACAGTGG
(209 bp sequenced)

Figure B. Multiple alignment of sequences for Caspase-3. PCR target region and primer locations are included.

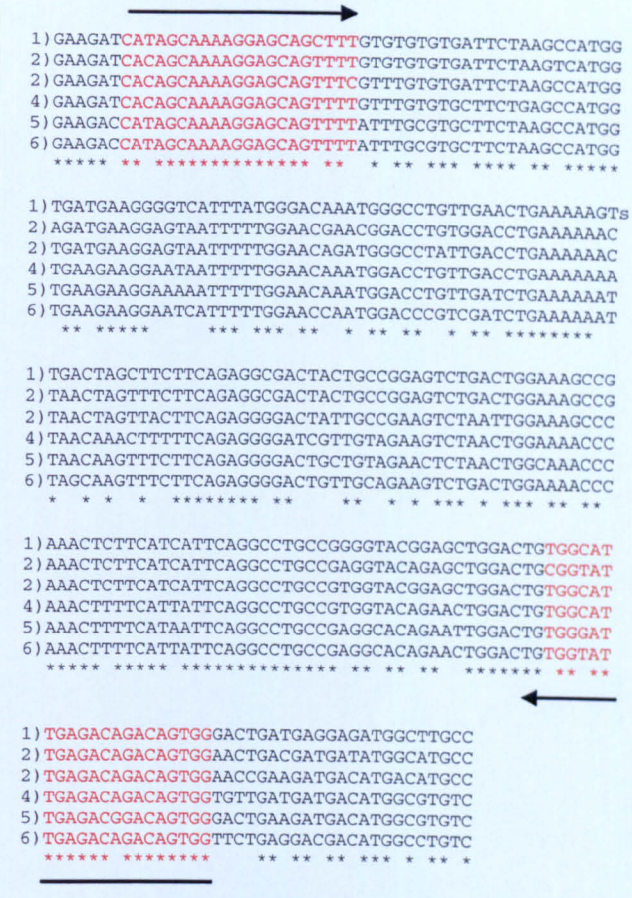

Figure D. Caspase-3 PCR product run on a 1.5% agarose gel, alongside a 100bp marker.

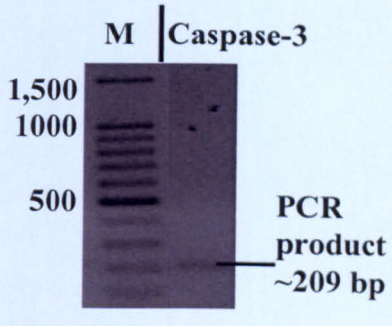

Figure F. Significant sequences from BLAST search of sequence in Fig. E.

Significant sequence alignment to:

Acc.No.	Species	Description	Identities	Score (bits)	E value
AB029345	Porcine	Caspase-3	207/209 (99%)	398	e-108
AY575000	Bovine	Caspase-3	188/209 (89%)	252	2e-64
U13737	Human	Caspase-3	186/206 (90%)	250	9e-64

APPENDIX A4: CASPASE-6

Figure A. Available Caspase-6 sequences.

No.	Acc.No.	Species
1)	U20536	Human
2)	Y13087	Murine

N.B. No Porcine, Bovine or Ovine sequence data available.

Figure B. Multiple alignment of sequences for Caspase-6. PCR target region and primer locations are included.

```
1)CTTACCCGCAGGTTTTCAGATCTAGGATTTGAAGTGAAATGCTTTAATGATCTTAAAGCA
2)CTGACTCGCAGGTTTTCAGATCTAGGATTTGAAGTGAAATGCTTTAACGACCTCAGAGCA
  ** ** ********************************************** ** ** * ****

1)GAAGAACTACTGCTCAAAATTCATGAGGTGTCAACTGTTAGCCACGCAGATGCCGATTGC
2)GAAGAACTCCTGCTCAAAATTCACGAGGTGTCGACTTCAAGCCACATAGATGCCGATTGC
  ******** ********************** ******** *** ******* **************

1)TTTGTGTGTGTCTTCCTGAGCCATGGCGAAGGCAATCACATTTATGCATATGATGCTAAA
2)TTCATCTGTGTCTTCCTGAGCCATGGGGAAGGCAACCACGTTTACGCATACGACGCCAAA
  **  * ********************** ******** *** **** ***** ** ** ***

1)ATCGAAATTCAGACATTAACTGGCTTGTTCAAAGGAGACAAGTGTCACAGCCTGGTTGGA
2)ATTGAAATTCAGACGTTGACTGGCTTGTTCAAAGGAGACAAGTGTCAGAGCCTGGTTGGA
  ** *********** ** ****************************** ************

1)AAACCCAAGATATTTATCATCCAGGCATGTCGGGGAAACCAGCACGATGTGCCAGTCATT
2)AAACCCAAGATATTTATCATCCAGGCCTGTCGGGGTAGCCAGCATGACGTACCCGTGGTT
  ********************** ******** * ****** ** ** ** **  **
```

Figure C1. PCR Conditions.

Fwd. primer- 21 bp (CGCAGGTTTTCAGATCTAGGA)

Start- 303 of 1545 bp sequence (1).

Rev. primer- 20 bp (TTGGGTTTTCCAACCAGGCT)

Finish- 544 of 1545 bp sequence (1).

Amplicon size- 242 bp

Annealing temp.- 62°C

Cycles- 35

Perkin Elmer Amplitaq Gold polymerase/ Promega taq polymerase

Figure D. Caspase-6 PCR product run on a 1.5% agarose gel, alongside a 100bp marker.

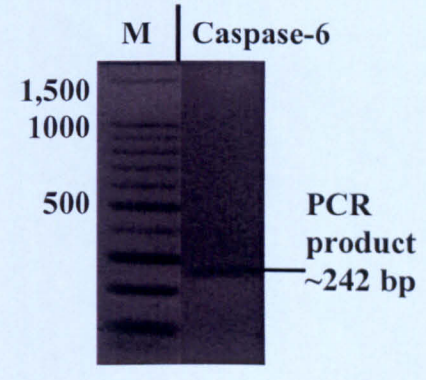

Figure E. DNA sequencing of cloned cDNA insert.

TTGGGTTTTCCAACCAGGCTCTGACACTTGTCTCCTTTGAAC
AAGCCAGTCAGTGTCTGAATTTCAATTTTGGCATCATATGC
GTAGATGTGATTGCCTTCGCCGTGACTCAGGAAAACACACA
AAAAGCAGTCGGCATCTACATGGCTAGCAGTTGATGCCTCA
TGAATTTTGAGCAGTAATTCTTCAGCTCTAAGATCATTAAA
GCATTTCACTTCAAATCCTAGATCTGAA
(234 bp sequenced of antisense strand)

Figure F. Significant sequences from BLAST search of sequence in Fig. E.

Significant sequence alignment to:

Acc.No.	Species	Description	Identities	Score (bits)	E value
U20536	Human	Caspase-6	214/234 (91%)	305	2e-80
AF025670	Rat	Caspase-6	206/233 (88%)	248	4e-63
Y13087	Murine	Caspase-6	205/234 (87%)	234	7e-59

APPENDIX A5: CATHEPSIN-B

Figure A. Available Cathepsin-B sequences.

No.	Acc.No.	Species
1)	X82396	Rat
2)	M14222	Murine
3)	L16510	Human
4)	L06075	Bovine

N.B. No Porcine sequence data available

Figure. Multiple alignment of sequences for Cathepsin-B. PCR target region and primer locations are included.

```
1)ACAGCGAGAAGGAGATCATGGCGGAAATCTACAAAAATGGCCCAGTGGAGGGTGCTTTTA
2)ACAGTGTGAAGGAGATCATGGCAGAAATCTACAAAAATGGCCCAGTGGAGGGTGCCTTCA
3)ATAGCGAGAAGGACATCATGGCCGAGATCTACAAAAACGGCCCCGTGGAGGGAGCTTTCT
4)ACAACGAGAAGGAGATCATGGCAGAGATCTACAAAAATGGCCCAGTCGAGGGGGCCTTCT
  * *  * ****** ******** ** ********** ***** ** ***** ** **

1)CTGTGTTTTCTGACTTCTTGACTTACAAATCAGGCGTATACAAGCATGAAGCCGGTGATG
2)CTGTGTTTTCTGACTTCTTGACTTACAAATCAGGAGTATACAAGCATGAAGCCGGTGATA
3)CTGTGTATTCGGACTTCCTGCTCTACAAGTCAGGAGTGTACCAACACGTCACCGGAGAGA
4)CTGTGTACTCGGACTTCCTGCTATACAAGTCTGGGGTGTACCAGCACGTCTCTGGAGAGA
  ******  ** ****** **   ***** ** ** ** *** * ** *   * ** **

1)TGATGGGAGGCCATGCCATCCGCATTCTGGGCTGGGGAATAGAGAATGGAGTACCCTACT
2)TGATGGGTGGCCACGCCATCCGCATCCTGGTCTGGGGAGTAGAGAATGGAGTTCCCTACT
3)TGATGGGTGGCCATGCCATCCGCATCCTGGGCTGGGGAGTGGAGAATGGCACACCCTACT
4)TTATGGGAGGCCACGCCATCCGCATCCTAGGCTGGGGAGTGGAGAACGGCACCCCCTACT
  * ***** ***** ********** ** * ******* * ***** **    *******

1)GGCTGGTAGCAAACTCCTGGAACGTTGACTGGGGTG
2)GGCTGGCAGCCAACTCTTGGAACCTTGACTGGGGTG
3)GGCTGGTTGCCAACTCCTGGAACACTGACTGGGGTG
4)GGCTGGTCGGCAACTCCTGGAACACTGATTGGGGTG
  ******  *  ***** ******  *** ********
```

Figure C1. PCR Conditions.

Fwd. primer- 20 bp (GAGAAGGACATCATGGCCGA)

Start- 883 of 1996 bp sequence (3).

Rev. primer- 21 bp (CAGTCAGTGTTCCAGGAGTTG)

Finish- 1088 of 1996 bp sequence (3).

Amplicon size- 206 bp

Annealing temp.- 57°C

Cycles- 35

Perkin Elmer Amplitaq Gold polymerase/ Promega taq polymerase

Figure C2.

Target amplification problematic; Accomplished using primers above on a long (~581 bp) Cathepsin-B PCR product made using above Rev.primer, and another 20 bp Fwd.primer(TTCGGGGCTGTGGAAGCCAT), start-508 bp sequence (3).

Figure D. Cathepsin-B PCR product run on a 1.5% agarose gel, alongside a 100bp marker.

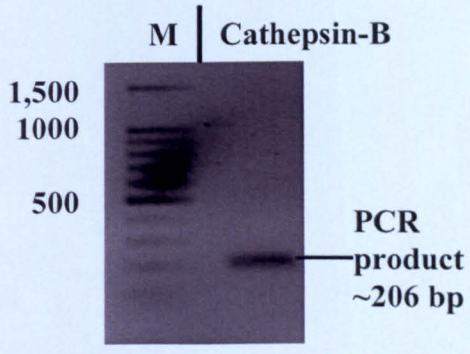

Figure E. DNA sequencing of PCR product.

GGCCCGGTCGAGGGGGCCTTCACTGCTGTACTCGG
ACTTCCTGCAGTATAAGTCTGGAGTGTACCAGCAC
GTCACAGGAGACTTGATGGGAGGCCATGCCATCCG
CATCCTGGGCTGGGGAGTGGAGAATGGCACCCCCT
ACTGGCTGGTCGGCAACTCCTGGAACACTGA
(171 bp sequenced)

Figure F. Significant sequences from BLAST search of sequence in Fig. E.

Significant sequence alignment to:

Acc.No.	Species	Description	Identities	Score (bits)	E value
L06075	Bovine	Cathepsin-B	156/171 (91%)	212	2e-52
L16510	Human	Cathepsin-B	132/145 (91%)	184	4e-44
X82396	Rat	Cathepsin-B	73/83 (87%)	86	3e-14

APPENDIX A6: CATHEPSIN-D

Figure A. Available Cathepsin-D sequences.

No.	Acc.No.	Species
1)	M11233	Human
2)	BM471202	Human
3)	AF164143	Ovine
4)	X53337	Murine
5)	X54467	Rat

N.B. No Porcine sequence data available

Figure B. Multiple alignment of sequences for Cathepsin-D. PCR target region and primer locations are included.

Figure C1. PCR Conditions.

Fwd. primer- 21 bp
(ATCTCCGTCAACAACGTGCTG)

Start- 667 of 2038 bp sequence (1).

Rev. primer- 20 bp
(GTGGACCTGCCAGTAGGCCT)

Finish- 870 of 2038 bp sequence (1).

Amplicon size- 204 bp

Annealing temp.- 57°C

Cycles- 35

Perkin Elmer Amplitaq Gold polymerase

Figure C2.

PCR from porcine template problematic; Human Image Clone:-5563106, acc.no:-BM471202,(983 bp), used as template; target region 100% alignment to (1).

Figure. Cathepsin-D PCR product run on a 1.5% agarose gel, alongside a 100bp marker.

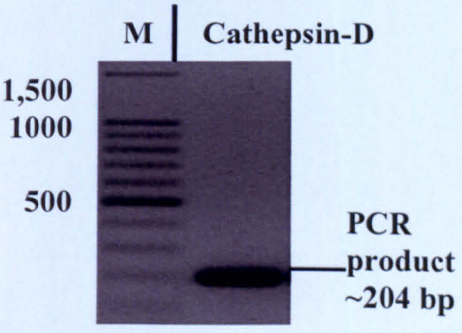

Figure E. DNA sequencing of PCR product.

TCTTCTCCTTCTACCTGAGCAGGGACCC
AGATGCGCAGCCTGGGGGTGAGCTGAT
GCTGGGTGGCACAGACTCCAAGTATTA
CAAGGGTTCTCTGTCCTACCTGAATGTC
ACCCGCAAGGCCTACTGGCAGGTC
(134 bp sequenced)

Figure F. Significant sequences from BLAST search of sequence in Fig. E.

Significant sequence alignment to:

Acc.No.	Species	Description	Identities	Score (bits)	E value
M11233	Human	Cathepsin-D	134/134 (100%)	266	1e-68
X53337	Murine	Cathepsin-D	112/133 (84%)	98	5e-18
AB055312	Bovine	Cathepsin-D	72/84 (85%)	72	3e-10

APPENDIX A7: CATHEPSIN-L

Figure A. Available Cathepsin-L sequences.

No.	Acc.No.	Species
1)	X91755	Bovine
2)	D37917	Porcine
3)	X06086	Murine

Figure B. Multiple alignment of sequences for Cathepsin-L. PCR target region and primer locations are included.

```
1)CATGCGTTCCGCATGGCAATGAATGCCTTTGGTGACATGACCAATGAAGA
2)CATGGCTTCAGCATGGCCATGAATGCCTTTGGTGACATGACCAATGAAGA
3)CACGGCTTTTCCATGGAGATGAACGCCTTTGGTGACATGACCAATGAGGA
  ** *  **   *****  ***** ********************** **

1)ATTTAGGCAGGTGATGAATGGTTTTCAAAATCAGAAGCATAAGAAGGGGA
2)ATTCAGGCAGGTGATGAATGGCTTTCAAAACCAGAAGCACAAGAAGGGGA
3)ATTCAGGCAGGTGGTGAATGGCTATCGCCACCAGAAGCACAAGAAGGGGA
  *** ********** ******* * **   * ******** **********

1)AACTGTTTCATGAACCTCTCCTTGTTGACGTCCCCAAATCTGTGGATTGG
2)AAGTGTTCCACGAATCTCTGGTTCTTGAGGTCCCCAAATCGGTAGATTGG
3)GGCTTTTTCAGGAACCGCTGATGCTTAAGATCCCCAAGTCTGTGGACTGG
    * ** ** *** * **  *  ** *  ******* ** ** ** ***

1)ACTAAGAAAGGCTATGTAACTCCTGTGAAGAATCAGGGTCAGTGTGGTTC
2)AGAGAAAAAGGCTATGTCACTGCCGTGAAGAATCAGGGTCAGTGTGGTTC
3)AGAGAAAAGGGTTGTGTGACTCCTGTGAAGAACCAGGGCCAGTGCGGGTC
  *   * ** ** * *** *** * ******** ***** ***** ** **

1)TTGTTGGGCGTTTAGTGCCACTGGTGCTCTTGAAGGACAGATGTTCCGGA
2)TTGTTGGGCTTTTAGTGCCACCGGCGCCCTCGAAGGACAGATGTTCCGGA
3)TTGTTGGGCGTTTAGCGCATCGGGTTGCCTAGAAGGACAGATGTTCCTTA
  ********* ***** **  * **    ** ***************  *

1)AAACTGGCAAACTTGTTTCACTGAGTGAGCAAAACCTGGTGGACTGCTCT
2)AAACCGGCAAGCTTGTTTCACTGAGTGAGCAGAACCTGGTGGACTGTTCT
3)AGACCGGCAAACTGATCTCACTGAGTGAACAGAACCTTGTGGACTGTTCT
  * ** ***** **  * ********** ** ***** ******** ***
```

Figure C1. PCR Conditions.

Fwd. primer- 21 bp
(TGACATGACCAATGAAGAATT)

Start- 333 of 1388 bp sequence (1).

Rev. primer- 21 bp
(TTTCCGGAACATCTGTCCTTC)

Finish- 552 of 1388 bp sequence (1).

Amplicon size- 220 bp

Annealing temp.- 59°C

Cycles- 35

Perkin Elmer Amplitaq Gold polymerase/ Promega taq polymerase

Figure D. Cathepsin-L purified PCR product run on a 1.5% agarose gel, alongside a 100bp marker.

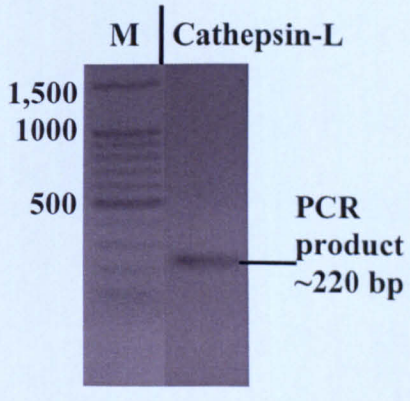

Figure E. DNA sequencing of cloned cDNA insert.

TGACATGACCAATGAAGAATTCAGGCAGGTGATG
AATGGCTTTCAAAACCAGAAGCACAAGAAGGGGA
AAGTGTTCCACGAATCTCTGGTTCTTGAGGTCCCC
AGATCGGTAGATTGGAGAGAAAAAGGCTATGTCA
CTGCCGTGAAGAATCAGGGTCAGTGTGGTTCTTGT
TGGGCTTTTAGTGCCACCGGCGCCCTTGAAGGACA
GATGTTCCGGAAA
(220 bp sequenced)

Figure F. Significant sequences from BLAST search of sequence in Fig. E.

Significant sequence alignment to:

Acc.No.	Species	Description	Identities	Score (bits)	E value
D37917	Porcine	Cathepsin-L	218/220 (99%)	420	e-115
NM_001912	Human	Cathepsin-L	197/219 (89%)	260	1e-66
X91755	Bovine	Cathepsin-L	194/220 (88%)	230	9e-58

APPENDIX A8: CATHEPSIN-H

Figure A. Available Cathepsin-H sequences.

No.	Acc.No.	Species
1)	U06119	Murine
2)	Y00708	Rat
3)	X07549	Human
4)	AF001169	Porcine

Figure B. Multiple alignment of sequences for Cathepsin-H. PCR target region and primer locations are included.

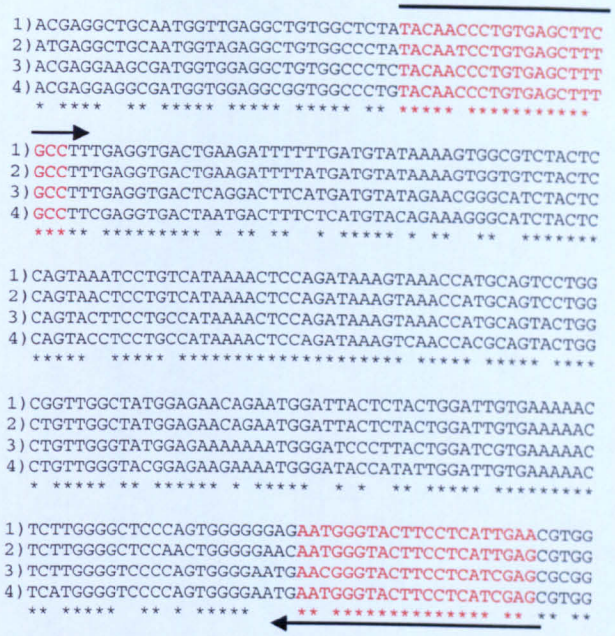

Figure C1. PCR Conditions.

Fwd. primer- 21 bp
(TACAACCCTGTGAGCTTCGCC)

Start- 762 of 1149 bp sequence (4).

Rev. primer- 21 bp
(CTCGATGAGGAAGTACCCATT)

Finish- 974 of 1149 bp sequence (4).

Amplicon size- 213 bp

Annealing temp.- 59°C

Cycles- 35

Perkin Elmer Amplitaq Gold Polymerase/ Promega

Figure D. Cathepsin-H purified PCR product run on a 1.5% agarose gel, alongside a 100bp marker.

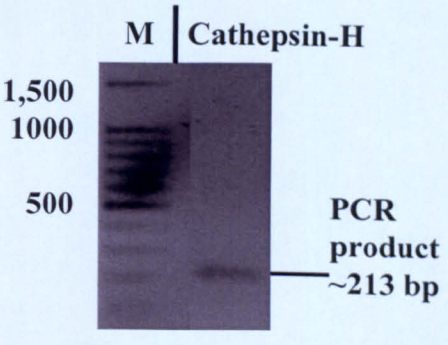

Figure E. DNA sequencing of cloned cDNA insert.

TGAGGAAGTACCCATTCATTCCCCACTGGGGACCC
CATGAGTTTTTCACAATCCAATATGGTATCCCATTT
TCTTCTCCGTACCCAACAGCCAGTACTGCGTGGTT
GACTTTATCTGGAGTTTTATGGCAGGAGGTACTGG
AGTAGATGCCCTTTCTGTACATGAGAAAGTCATTA
GTCACCTCGAAGGCGAAGCTCACAGGGTTGTA
(208 bp of antisense strand sequenced)

Figure F. Significant sequences from BLAST search of sequence in Fig. E.

Significant sequence alignment to:

Acc.No.	Species	Description	Identities	Score (bits)	E value
AF001169	Porcine	Cathepsin-H	207/208 (99%)	404	e-110
X07549	Human	Cathepsin-H	188/208 (90%)	254	6e-65
U06119	Murine	Cathepsin H	175/208 (84%)	151	7e-34

APPENDIX A9: E2G1 (Ubiquitin Conjugating Enzyme)

Figure A. Available E2G1 sequences.

No.	Acc.No.	Species
1)	AK013902	Murine
2)	D78514	Human
3)	AF099093	Rat

N.B. No Porcine sequence data available.

Figure B. Multiple alignment of sequences for E2G1. PCR target region and primer locations are included.

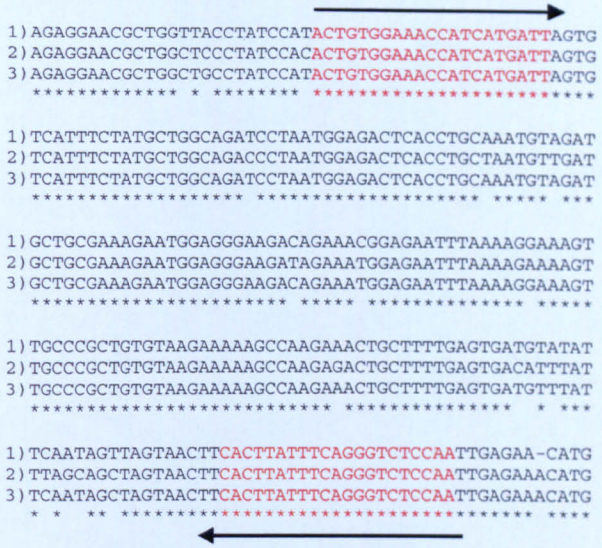

Figure C1. PCR Conditions.

Fwd. primer- 21 bp (ACTGTGGAAACCATCATGATT)

Start- 364 of 617 bp sequence (2).

Rev. primer- 21 bp (TTGGAGACCCTGAAATAAGTG)

Finish- 576 of 617 bp sequence (2).

Amplicon size- 213 bp

Annealing temp.- 56°C

Cycles- 35

Perkin Elmer Amplitaq Gold polymerase/ Promega taq polymerase

Figure D. E2G1 purified PCR product run on a 1.5% agarose gel, alongside a 100bp marker.

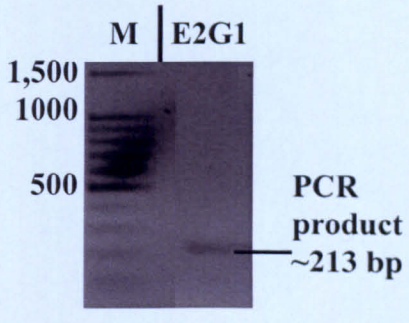

Figure E. DNA sequencing of cloned cDNA insert.

ACTGTGGAAACCATCATGATTAGTGTCATTTCTAT
GCTGGCAGACCCTAACGGCGACTCGCCTGCTAAT
GTGGACGCTGCGAAAGAATGGAGAGAAGACAGAA
ATGGAGAATTCAAAAGGAAAGTCGCCCGCTGTGTA
AGAAAAAGCCAAGAGACTGCTTTTGAGTGACATTT
ATTCAACAGCTGTAACTTCACTTATTTCAGGGTCTC
CAA
(212 bp of sequenced)

Figure F. Significant sequences from BLAST search of sequence in Fig. E.

Significant sequence alignment to:

Acc.No.	Species	Description	Identities	Score (bits)	E value
D78514	Human	E2G1	200/213 (93%)	311	3e-82
AF099093	Rat	E2G1	198/213 (92%)	295	2e-77
AK013902	Murine	E2G1	192/213 (91%)	272	3e-70

APPENDIX A10: C8 (Proteasomal Subunit)

Figure A. Available C8 sequences.

No.	Acc.No.	Species
1)	AF055983	Murine
2)	X55985	Rat
3)	D00762	Human

N.B. No Porcine sequence data available.

Figure B. Multiple alignment of sequences for C8. PCR target region and primer locations are included.

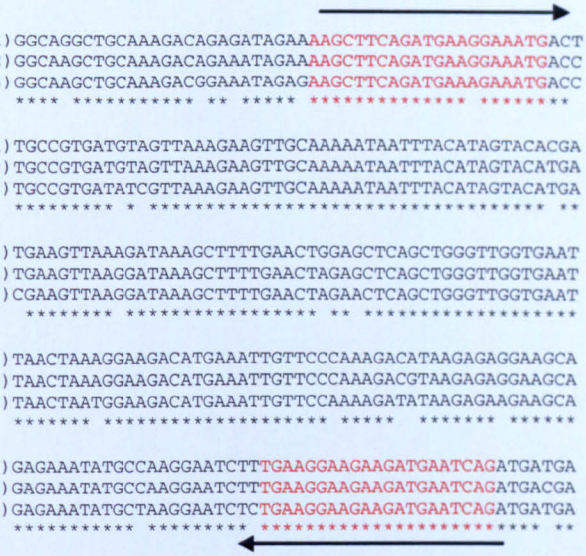

Figure C1. PCR Conditions.

Fwd. primer- 21 bp (AAGCTTCAGATGAAAGAAATG)

Start- 577 of 938 bp sequence (1).

Rev. primer- 21 bp (CTGATTCATCTTCTTCCTTCA)

Finish- 793 of 938 bp sequence (1).

Amplicon size- 217 bp

Annealing temp.- 52°C

Cycles- 35

Perkin Elmer Amplitaq Gold polymerase/ Promega taq polymerase

Figure D. C8 purified PCR product run on a 1.5% agarose gel, alongside a 100bp marker.

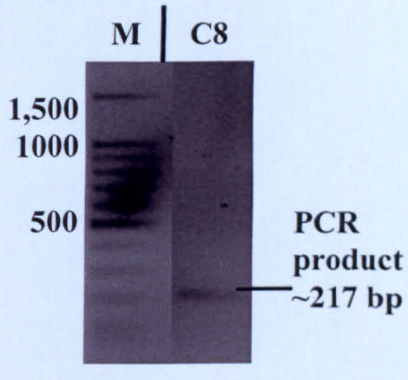

Figure E. DNA sequencing of cloned cDNA insert.

CTGATTCATCTTCTTCCTTCAAAGATTCCTTAGCG
TATTACTCTGCCTCTTCCCTTATATCTTTTGGAAC
AATTTCATGTCTTCCTTTTGTTATTTCACCAACCC
AGCTGAGCTCTAGTTCAAAAGCTTTATCCTTAAC
TTCATCATGTACTATGTAAATTATTTTTGCAACTT
CTTTAACAACATCACGGCAGGTCATTTCTTTCAT
CTGAAGCTT
(217 bp of antisense strand sequenced)

Figure F. Significant sequences from BLAST search of sequence in Fig. E.

Significant sequence alignment to:

Acc.No.	Species	Description	Identities	Score (bits)	E value
D00762	Human	C8	205/217 (94%)	335	2e-89
X55985	Rat	C8	204/217 (94%)	327	5e-87
AF055983	Murine	C8	201/217 (92%)	303	8e-80

APPENDIX A11: UBIQUITIN

Figure A. Available Ubiquitin mRNA sequences.

No.	Acc.No.	Species
1)	M18159	Porcine
2)	M62428	Bovine
3)	M26880	Human

Figure B. Multiple alignment of sequences for Ubiquitin. PCR target region and primer locations are included.

```
1)GAGTCCACCCTGCACCTGGTCCTCCGCCTCAGAGGTGGGATGCAGATCTTCGTGAAGACC
2)GAGTCCACTCTGCACCTGGTCCTCCGCCTCAGAGGTGGGATGCAGATCTTCGTGAAGACC
3)GAGTCTACCCTGCACCTGGTGCTCCGTCTCAGAGGTGGGATGCAGATCTTCGTGAAGACC
  ***** ** ********** ***** **********************************

1)TTGACTGGTAAGACCATCACCCTGGAAGTGGAGCCCAGCGACACCATCGAGAACGTCAAG
2)TTGACCGGCAAGACCATCACCCTGGAGGTGGAGCCCAGTGACACCATCGAGAACGTCAAG
3)CTGACTGGTAAGACCATTACCCTCGAGGTGGAGCCCAGTGACACCATCGAGAATGTCAAG
   **** ** ******** ***** ** ********** ********************** ******

1)GCGAAGATCCAGGACAAGGAAGGCATCCCCCCAGACCAGCAGAGGCTGATCTTTGCCGGG
2)GCCAAGATCCAAGACAAAGAGGGCATCCCCCCAGACCAGCAGAGGCTGATCTTTGCCGGG
3)GCAAAGATCCAAGATAAGGAAGGCATCCCTCCTGATCAGCAGAGGTTGATCTTTGCTGGG
  ** ******** ** ** ** ******** ** ** ********* ********** ***

1)AAGCAGCTGGAAGATGGGCGCACCCTGTCTGACTACAACATCCAGAAGGAGTCCACCCTG
2)AAACAGCTGGAAGATGGCCGCACCCTGTCTGACTACAACATCCAGAAAGAGTCCACTCTG
3)AAACAGCTGGAAGATGGACGCACCCTGTCTGACTACAACATCCAGAAAGAGTCCACTCTG
  ** ********************************** ********** ***

1)CACTTGGTCCTGCGCTTGAGGGGAGGT-TTCTAAGTTCTCCCTTTTAAGCTTTCAACAAA
2)CACTTGGTCCTGCGCTTAAGGGGAGGTGTTTTAAGTTCTCCCTTTTAAGCTTTCGATAAG
3)CACTTGGTCCTGCGCTTGAGGGGGGGT-GTCTAAGTTTCCCCTTTTAAGGTTTCAACAAA
  ****************** ***** *** * ****** ********** **** * **
```

Figure C1. PCR Conditions.

Fwd. primer- 21 bp
(TCAGAGGTGGGATGCAGATCT)

Start- 524 of 832 bp sequence (1).

Rev. primer- 20 bp
(AAGCGCAGGACCAAGTGCAG)

Finish- 752 of 832 bp sequence (1).

Amplicon size- 229 bp

Annealing temp.- 61°C

Cycles- 35

Expand high fidelity system

Figure D. Ubiquitin purified PCR product run on a 1.5% agarose gel, alongside a 100bp marker.

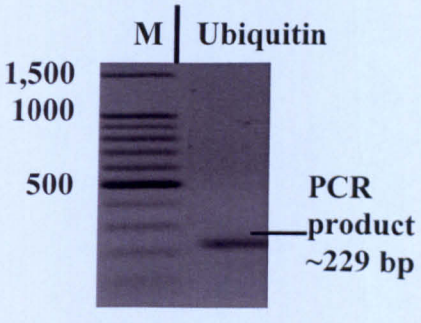

Figure E. DNA sequencing of PCR product.

GTGGAGCCCAGCGACACCATCGAGAATGTCAAGG
CGAAGATCCAAGACAAAGAAGGCATCCCCCCAGA
CCAGCAGAGGCTGATCTTTGCCGGGAAGCAGCTGG
AAGATGGGCGCACCCTGTCTGACTACAACATCCAG
AAGGAGTCCACCCTGCACTTGGGTCCTGCGC
(169 bp sequenced)

Figure F. Significant sequences from BLAST search of sequence in Fig. E.

Significant sequence alignment to:

Acc.No.	Species	Description	Identities	Score (bits)	E value
M18159	Porcine	Ubiquitin	155/156 (99%)	301	2e-79
M62428	Bovine	Ubiquitin	160/169 (94%)	256	1e-65
M26880	Human	Ubiquitin	155/169 (91%)	216	1e-53

APPENDIX A12: ATROGIN-1 (specific E3, Ubiquitin Ligase)

Figure A. Available Atrogin-1 sequences.

No.	Acc.No.	Species
1)	AY059628	Rat
2)	AY059629	Human

N.B. No Porcine sequence data available

Figure C1. PCR Conditions.

Fwd. primer- 20 bp
(CTTGAAGACCAGCAAAACAT)

Start- 469 of 1068 bp sequence (2).

Rev. primer- 21 bp
(TCTGCATGATGTTCAGTTGTA)

Finish- 715 of 1068 bp sequence (2).

Amplicon size- 247 bp

Annealing temp.- 54°C

Cycles- 35

Perkin Elmer Amplitaq Gold Polymerase

Figure B. Multiple alignment of sequences for Atrogin-1. PCR target region and primer locations are included.

```
1)AAAGTAGTACTGAAAGTTCTTGAAGACCAGCAAAACATAAGACTCATACG
2)AAAGTGGTACTGAAAGTCCTTGAAGACCAGCAAAACATTAGACTAATAAG
  ***** ********** ********************** ***** *** *

1)GGAACTTCTCCAGACCCTCTACACATCCTTATGCACGCTGGTCCAGAGAG
2)GGAACTACTCCAGACCCTCTACACATCCTTATGTACACTGGTCCAAAGAG
  ****** *************************** ** ******** ****

1)TCGGCAAGTCCGTGCTGGTGGGCAACATCAACATGTGGGTGTATCGAATG
2)TCGGCAAGTCTGTGCTGGTCGGGAACATTAACATGTGGGTGTATCGGATG
  ********** ******** ** ***** ****************** ***

1)GAGACCACTCTACACTGGCAACAGCAGCTGAACAGCATCCAGATCAGCAG
2)GAGACGATTCTCCACTGGCAGCAGCAGCTGAACAACATTCAGATCACCAG
  ***** * *** ******** ************** *** ******** ***

1)GCCGGCCTTCAAAGGTCTCACGATCACCGACCTGCCTGTGTGCTTACAAC
2)GCCTGCCTTCAAAGGCCTCACCTTCACTGACCTGCCTTTGTGCCTACAAC
  *** ********** *****  **** ********* ***** ******

1)TGAACATCATGCAGAGGCTGAGCGATGGGCGGGACCTGGTCAGCCTGGGC
2)TGAACATCATGCAGAGGCTGAGCGACGGGCGGGACCTGGTCAGCCTGGGC
  ************************* ************************
```

Figure D. Atrogin-1 purified PCR product run on a 1.5% agarose gel, alongside a 100bp marker.

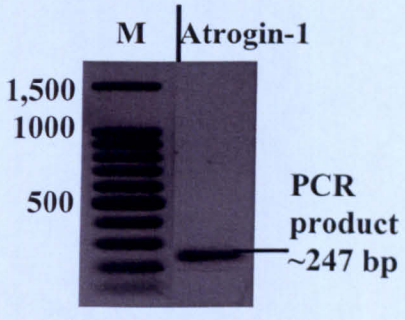

Figure E. DNA sequencing of cloned cDNA insert.

CTTGAAGACCAGCAAAACATCAGACTGATAAGGG
AACTCCTCCAGACCCTCTACACGTCCCTGTGCACA
CTGGTCCAGAGAGTCGGCAAGTCCGTGCTGGTCGG
GAACATTAACATGTGGGTGTATCGGATGGAGACGA
TTCTACACTGGCAGCAGCAGCTGAACAACATCCAG
ATCACCAGGCCTGCCTTCAAAGGCCTCACCTTCAC
CGACCTGCCTCTGTGTTTACAACTGAACATCATGC
AGA
(247 bp sequenced)

Figure F. Significant sequences from BLAST search of sequence in Fig. E.

Significant sequence alignment to:

Acc.No.	Species	Description	Identities	Score (bits)	E value
AY059629	Human	Atrogin-1	232/247 (93%)	371	e-100
AF441120	Murine	Atrogin-1	227/247 (91%)	331	4e-88
AY059628	Rat	Atrogin-1	224/247 (90%)	307	6e-81

APPENDIX A13: μ-CALPAIN

Figure A. Available μ-Calpain sequences.

No.	Acc.No.	Species
1)	AF263610	Porcine (Isoform-A)
2)	AF263609	Porcine (Isoform-B)
3)	AF221129	Bovine
4)	X04366	Human

Figure B. Multiple alignment of sequences for μ-Calpain. PCR target region and primer locations are included.

```
1)GGTCAGTACCCGCTTCCGCCTGCCGCCCGGCGAGTACGTGGTGGTGCCTT
2)GGTCAGTACCCGCTTCCGCCTGCCGCCCGGCGAGTACGTGGTGGTGCCTT
3)GGTCAGCACCCGCTTCCGCCTGCCGCCTGGGGAGTACGTGGTGGTGCCCT
4)GGTCAGCACCCGCTTCCGCCTGCCACCCGGGGAGTATGTGGTGGTGCCCT
  ****** ****************** ** ** ***** *********** *

1)CCACCTTCGAGCCCAACAAGGAGGGCGACTTTGTGCTGCGTTTCTTCTCA
2)CCACCTTCGAGCCCAACAAGGAGGGCGACTTTGTGCTGCGTTTCTTCTCA
3)CCACCTTCGAGCCCAACAAGGAAGGTGACTTTGTGCTGCGTTTCTTCTCA
4)CCACCTTCGAGCCCAACAAGGAGGGCGACTTCGTGCTGCGCTTCTTCTCA
  ********************** ** ***** ******** *********

1)GAGAAGAAAGCCGGGACCCAAGAGCTGGACGACCAGGTCCAGGCCATTCT
2)GAGAAGAAAGCCGGGACCCAAGAGCTGGACGACCAGGTCCAGGCCATTCT
3)GAGAAGAGCGCAGGGACCCAAGAGCTGGATGACCAGGTCCAGGCCAATCT
4)GAGAAGAGTGCTGGGACTGTGGAGCTGGATGACCAGATCCAGGCCAATCT
  ******* ** *****    ******** ****** ********* ***

1)CCCCGACGAGCAAGTGCTCTCGGAAGAGGAGATTGATGAGAACTTCAAAG
2)CCCCGACGAGCAAGTGCTCTCGGAAGAGGAGATTGATGAGAACTTCAAAG
3)CCCCGACGAGCAAGTGCTCTCAGAAGAGGAGATTGATGAGAACTTCAAGT
4)CCCCGATGAGCAAGTGCTCTCAGAAGAGGAGATTGACGAGAACTTCAAGG
  ****** ************** ************** ***********

1)CGCTCTTCAGACAGCTGGCAGGGGAGGACATGGAGATCAGCGTCAGGGAG
2)CGCTCTTCAGACAGCTGGCAGGGGAGGACATGGAGATCAGCGTCAGGGAG
3)CCCTCTTCAGACAACTGGCAGGGGAGGACATGGAGATCAGCGTCAAGGAG
4)CCCTCTTCAGGCAGCTGGCAGGGGAGGACATGGAGATCAGCGTGAAGGAG
  * ******** ** ********************************* * ****
```

Figure C1. PCR Conditions.

Fwd. primer- 20 bp
(CTTCCACCTTCGAGCCCAAC)

Start- 1633 of 2994 bp sequence (1).

Rev. primer- 20 bp
(CCCTGACGCTGATCTCCATG)

Finish- 1833 of 2994 bp sequence (1).

Amplicon size- 201 bp

Annealing temp.- 55°C

Cycles- 35

Perkin Elmer Amplitaq Gold Polymerase

Figure C2.

PCR problematic; long 883bp μ-Calpain probe[990-1872bp region of sequence(1)] used as template; target region 100% alignment to (1).

Figure D. μ-Calpain-1 purified PCR product run on a 1.5% agarose gel, alongside a 100bp marker.

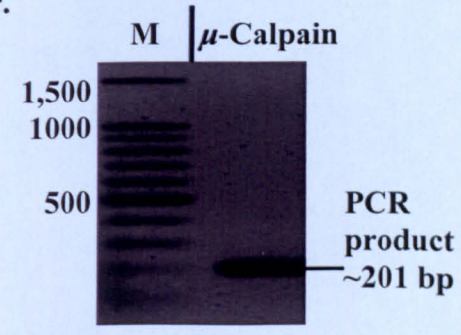

Figure E. DNA sequencing of PCR product.

TTGTGCTGCGTTTCTTCTCAGAGACGAAAGCCGGG
ACCCAAGAGCTGGACGACCAGGTCCAGGCCATTCT
CCCCGACGAGCAAGTGCTCTCGGAAGAGGAGATT
GATGAGAACTTCAAAGCGCTCTTCAGACAGCTGGC
AGGGGAGGACATGGAGATCAGCGTCAGGGACTT
(172 bp sequenced)

Figure F. Significant sequences from BLAST search of sequence in Fig. E.

Significant sequence alignment to:

Acc.No.	Species	Description	Identities	Score (bits)	E value
AF263610 /09	Porcine	μ-Calpain	168/169 (99%)	327	4e-87
AF221129	Bovine	μ-Calpain	154/165 (93%)	240	7e-61
X04366	Human	μ-Calpain	143/161 (88%)	176	9e-42

APPENDIX A14: *m*-CALPAIN

Figure A. Available *m*-Calpain sequences.

No.	Acc.No.	Species
1)	U01181	Porcine
2)	M23254	Human
3)	U07850	Bovine
4)	NM_009794	Murine
5)	BC065306	Rat

Figure B. Multiple alignment of sequences for *m*-Calpain. PCR target region and primer locations are included.

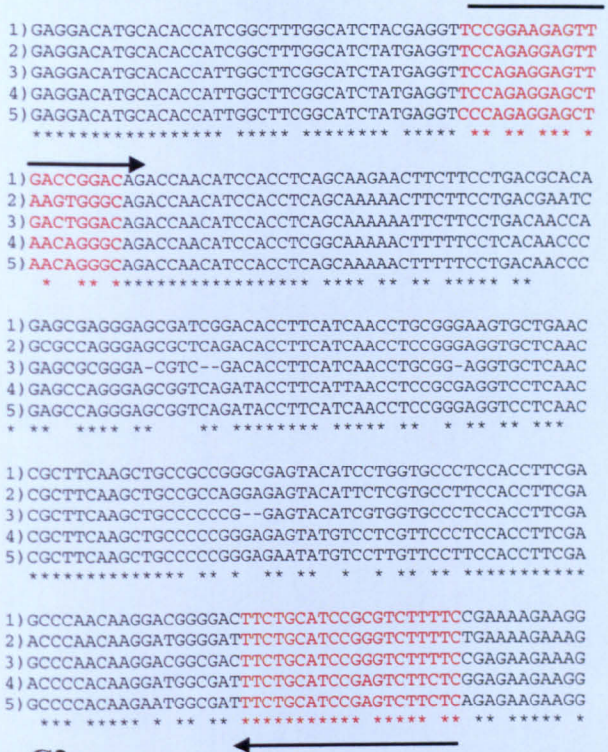

Figure C1. PCR Conditions.

Fwd. primer- 20 bp
(TCCGGAAGAGTTGACCGGAC)

Start- 1438 of 3213 bp sequence (2).

Rev. primer- 20 bp
(GAAAAGACGCGGATGCAGAA)

Finish- 1638 of 3213 bp sequence (2).

Amplicon size- 201 bp

Annealing temp.- 62°C

Cycles- 35

Perkin Elmer Amplitaq Gold Polymerase

Figure C2.

PCR problematic; long 732bp *m*-Calpain probe[1016-1747bp region of sequence(2)] used as template; target region 100% alignment to (1).

Figure D. *m*-Calpain purified PCR product run on a 1.5% agarose gel, alongside a 100bp marker.

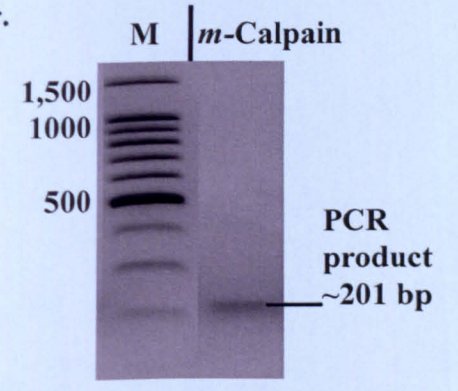

Figure E. DNA sequencing of PCR product.

TCGTCTTGTTGGGCTCGAAGGTGGAGGGC
ACCAGGATGTACTCGCCCGGCGGCAGCTT
GAAGCGGTTCAGCACTTCCCGCAGGTTGA
TGAAGGTGTCCGACCGCTCCCTCGCTCTG
TGCGTCAGGAAGAAGTTCTTGCTGAGGTG
GATGTTGGTCTGTCCGGT
(163 bp sequenced)

Figure F. Significant sequences from BLAST search of sequence in Fig. E.

Significant sequence alignment to:

Acc.No.	Species	Description	Identities	Score (bits)	E value
U01181	Porcine	*m*-Calpain	158/159 (99%)	307	4e-81
U07850	Bovine	*m*-Calpain	138/156 (88%)	204	4e-50
M23254	Human	*m*-Calpain	136/153 (88%)	168	2e-39

APPENDIX A15: CALPAIN-3

Figure A. Available Calpain-3 sequences.

No.	Acc.No.	Species
1)	AF087569	Bovine
2)	AF043295	Porcine
3)	AF127764	Human

Figure B. Multiple alignment of sequences for Calpain-3. PCR target region and primer locations are included.

```
1)TGGCCTGTGGGCTGGTCAAAGGCCATGCCTACTCAGTCACTGGGCTGGAGGAGGCCCTGT
2)TGGCCTGTGGGCTGGTCAAAGGCCACGCCTATTCGGTTACTGGGCTGGAGGAGGCCCTGT
3)TGGCCTGCGGGCTGGTCAGAGGTCACGCCTACTCTGTCACGGGGCTGGATGAGGTCCCGT
  ******* ********** *** ** ***** ** ** ** ******** **** ** **

1)ACAAGGGTGAGAAAGTGAAGCTGGTGCGGCTGCGGAACCCCTGGGGCCAGGTGGAGTGGA
2)TCAAGGGTGAAAAGGTGAAGCTTGTGCGGCTGCGGAACCCCTGGGGCCAGGTGGAGTGGA
3)TCAAAGGTGAGAAAGTGAAGCTGGTGCGGCTGCGGAATCCGTGGGGCCAGGTGGAGTGGA
   *** ***** ** ******** ********** ** ********** ********** **

1)ATGGCTCCTGGAGTGACAGCTGGAAGGACTGGAGCTATGTGGACAAGGACGAGAAGGCCC
2)ATGGCTCCTGGAGTGACAGTTGGAAGGACTGGAGCTTTGTGGACAAAGATGAGAAGGCCC
3)ACGGTTCTTGGAGTGATAGATGGAAGGACTGGAGCTTTGTGGACAAAGATGAGAAGGCCC
  * ** ** ******** ** ********** ********** ** **********

1)GTTTGCAGCACCAGGTCACTGAGGATGGAGAGTTCTGGATGTCCTACGATGATTTTATCT
2)GTCTGCAGCACCAGGTCACTGAGGATGGAGAGTTCTGGATGTCTTATGATGATTTCATCT
3)GTCTGCAGCACCAGGTCACTGAGGATGGAGAGTTCTGGATGTCCTATGAGGATTTCATCT
  ** ********** ********** ** ** ***** ****
```

Figure C1. PCR Conditions.

Fwd. primer- 19 bp
(GCCTGTGGGCTGGTCAAAG)

Start- 1020 of 2512 bp sequence (2).

Rev. primer- 20 bp
(CTGAGTGACCTGGTGCTGCA)

Finish- 1220 of 2512 bp sequence (2).

Amplicon size- 201 bp

Annealing temp.- 62°C

Cycles- 35

Perkin Elmer Amplitaq Gold Polymerase

Figure C2.

PCR problematic; long 1122 bp Calpain-3 probe[869-1990bp region of sequence(2)] used as template; target region 100% alignment to (2).

Figure D. Calpain-3 purified PCR product run on a 1.5% agarose gel, alongside a 100bp marker.

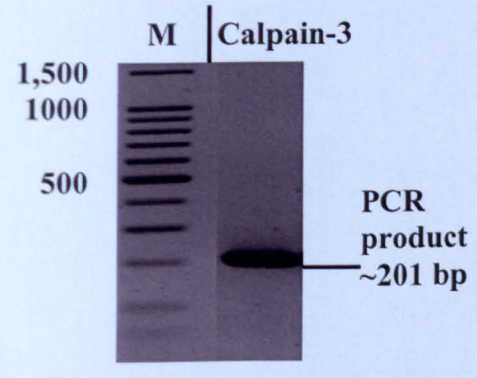

Figure E. DNA sequencing of PCR product.

TGGGCTGGAGGAGGCCCTGTTCAAGGGTGA
AAAGGTGAAGCTTGTGCGGCTGCGGAACCC
CTGGGGCCAGGTGGAGTGGAATGGCTCCTG
GAGTGACAGTTGGAAGGACTGGAGCTTTGT
GGACAAAGATGAGAAGGCCCGTCTGC
(146 bp sequenced)

Figure F. Significant sequences from BLAST search of sequence in Fig. E.

Significant sequence alignment to:

Acc.No.	Species	Description	Identities	Score (bits)	E value
AF043295	Porcine	Calpain-3	146/146 (100%)	289	7e-76
AF087569	Bovine	Calpain-3	134/142 (94%)	218	2e-54
X85030	Human	Calpain-3	131/145 (90%)	176	8e-42

APPENDIX A16: CALPASTATIN

Figure A. Available Calpastatin sequences.

No.	Acc.No.	Species
1)	AY555195	Porcine
2)	M20160	Porcine (Heart)
3)	D16217	Human
4)	L14450	Bovine

Figure B. Multiple alignment of sequences for Calpastatin. PCR target region and primer locations are included.

Figure C1. PCR Conditions.

Fwd. primer- 21 bp
(CGTCTCTGAAGTGGTTTCCCA)

Start- 1741 of 4038 bp sequence (2).

Rev. primer- 22 bp
(CAGGCGGGATAGTGTCATCTCT)

Finish- 1976 of 4038 bp sequence (2).

Amplicon size- 236 bp

Annealing temp.- 55°C

Cycles- 35

Perkin Elmer Amplitaq Gold Polymerase

Figure C2.

PCR problematic; long 808 bp Calpastatin probe[1409-2216 bp region of sequence(2)] used as template; target region 100% alignment to (2).

Figure D. Calpastatin purified PCR product run on a 1.5% agarose gel, alongside a 100bp marker.

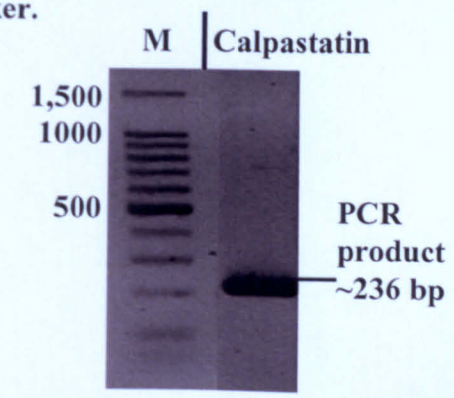

Figure E. DNA sequencing of PCR product.

CTTCAGCTTTTTCCTTGACTTTATCCTCTATGGGC
TTGTTCTCATCTGGGTCAGGCTGTCTTTGCCCCA
GACTGTCAGAAAGCTGATCCAGGGCATCGTCAA
GTTTTTTGTCATCACTCACAGTGTCAGGGGGTGG
ACCTGCAGAGTGGGTGGTTGGAGCTGAGGTTTG
GGAAA
(174 bp sequenced)

Figure F. Significant sequences from BLAST search of sequence in Fig. E.

Significant sequence alignment to:

Acc.No.	Species	Description	Identities	Score (bits)	E value
AY555195 /M20160	Porcine	Calpastatin	174/174 (100%)	345	2e-92
L14450	Bovine	Calpastatin	147/169 (86%)	161	6e-37
D50827	Human	Calpastatin	81/93 (87%)	90	2e-15

APPENDIX A17: CALPAIN-10

Figure A. Available Calpain-10 sequences.

No.	Acc.No.	Species
1)	BQ057475	Human (Image clone)
2)	AF089088	Human (Calpain-10a)

N.B. No Porcine, Bovine or Ovine sequence data available. Rat and Murine sequences variable in PCR target region.

Figure B. Multiple alignment of sequences for Calpain-10. PCR target region and primer locations are included.

```
1) GGCTGCCGGAACAACAGCGGCTTTCCCAGCAACCCCAAATTCTGGCTGCG
2) GGCTGCCGGAACAACAGCGGCTTTCCCAGCAACCCCAAATTCTGGCTGCG
   **********************************************

1) GGTCTCAGAACCGAGTGAGGTGTACATTGCCGTCCTGCAGAGATCCAGGC
2) GGTCTCAGAACCGAGTGAGGTGTACATTGCCGTCCTGCAGAGATCCAGGC
   **********************************************

1) TGCACGCGGCGGACTGGGCAGGCCGGGCCCGGGCACTGGTGGGTGACAGT
2) TGCACGCGGCGGACTGGGCAGGCCGGGCCCGGGCACTGGTGGGTGACAGT
   **********************************************

1) CATACTTCGTGGAGCCCAGCGAGCATCCCGGGCAAGCACTACCAGGCTGT
2) CATACTTCGTGGAGCCCAGCGAGCATCCCGGGCAAGCACTACCAGGCTGT
   **********************************************

1) GGGTCTGCACCTCTGGAAGGTAGAGAAGCGGCGGGTCAATCTGCCTAGGG
2) GGGTCTGCACCTCTGGAAGGTAGAGAAGCGGCGGGTCAATCTGCCTAGGG
   **********************************************

1) TCCTGTCCATGCCCCCCGTGGCTGGCACCGCGTGCCATGCATACGACCGG
2) TCCTGTCCATGCCCCCCGTGGCTGGCACCGCGTGCCATGCATACGACCGG
   **********************************************

1) GAGGTCCACCTGCGTTGTGAGCTCTCACCGGGCTACTACCTGGCT
2) GAGGTCCACCTGCGTTGTGAGCTCTCACCGGGCTACTACCTGGCT
   **********************************************
```

Figure C1. PCR Conditions.

Fwd. primer- 21 bp
(CGGAACAACAGCGGCTTTCCC)

Start- 1243 of 2620 bp sequence (2).

Rev. primer- bp
(GTAGTAGCCCGGTGAGAGCTCACAA)

Finish- 1575 of 2620 bp sequence (2).

Amplicon size- 333 bp

Annealing temp.- ~57°C

Cycles- 35

Perkin Elmer Amplitaq Gold Polymerase

Figure C2.

PCR from porcine template problematic; Human Image Clone:-5813098, acc.no:-BQ057475,(1048 bp), used as template; target region 100% alignment to (2).

Figure D. Calpain-10 PCR product run on a 1.5% agarose gel, alongside a 100bp marker.

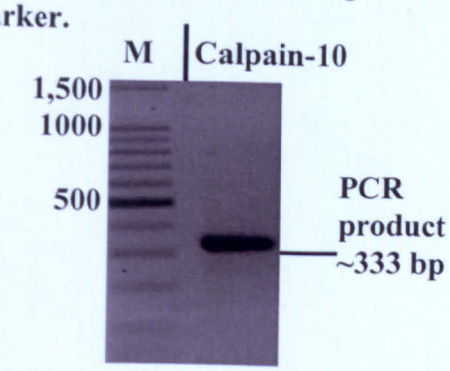

Figure E. DNA sequencing of PCR product.

AATTCTGGCTGCGGGTCTCAGAACCGAGTGAGGTG
TACATTGCCGTCCTGCAGAGATCCAGGCTGCACGC
GGCGGACTGGGCAGGCCGGGCCCGGGCACTGGTG
GGTGACAGTCATACTTCGTGGAGCCCAGCGAGCAT
CCCGGGCAAGCACTACCAGGCTGTGGGTCTGCACC
TCTGGAAGGTAGAGAAGCGGCGGGTCAATCTGCCT
AGGGTCCTGTCCATGCCCCCCGTGGCTGGCACCGC
GTGCCATGCATACGACCGGGAGGTCCACCTGCGTT
GTGAGCTCT
(288 bp sequenced)

Figure F. Significant sequences from BLAST search of sequence in Fig. E.

Significant sequence alignment to:

Acc.No.	Species	Description	Identities	Score (bits)	E value
AF089088	Human	Calpain-10a	288/288 (100%)	571	e-160
AF089089	Murine	Calpain-10	115/138 (83%)	92	8e-16
AF227909	Rat	Calpain-10	115/138 (83%)	92	8e-16

APPENDIX A18: ACTIN

Figure A. Available Actin sequences.

No.	Acc.No.	Species
1)	U16368	Porcine (alpha-actin gene)
2)	J00068	Human (alpha-actin)
3)	M12866	Murine (alpha-actin)
4)	U39357	Ovine (beta-actin)
5)	AF035774	Equine (beta-actin)

Figure B. Multiple alignment of sequences for Actin. PCR target region and primer locations are included.

```
1)CCATCTATGAGGGCTACGCGCTGCCACACGCCATCATGCGCCTGGACCTGGCCGGCCGCG
2)CCATTTATGAGGGCTACGCGCTGCCGCACGCCATCATGCGCCTGGACCTGGCGGGCCGCG
3)CCATCTATGAGGGCTATGCCCTGCCACACGCCATCATGCGTCTGGACCTGGCCGGTCGCG
4)CCATCTACGAGGGGTACGCCCTCCCCCACGCCATCCTGCGTCTGGACCTGGCTGGCCGGG
5)CCATCTACGAGGGGTACGCCCTCCCCCACGCCATCCTGCGTCTGGACCTGGCTGGCCGGG
  **** ** ***** ** ** ** ** ********* **** ********** ** ** *

1)ATCTCACCGACTACCTGATGAAGATCCTCACCGAGCGTGGCTACTCCTTCGTGACCACAG
2)ATCTTACCGACTACCTGATGAAGATCCTCACTGAGCGTGGCTACTCCTTCGTGACCACAG
3)ACCTCACTGACTACCTGATGAAAATCCTCACTGAGCGTGGCTATTCCTTCGTGACCACAG
4)ACCTGACGGACTACCTCATGAAGATCCTCACGGAGCGTGGCTACAGCTTCACCACCACGG
5)ACCTGACGGACTACCTCATGAAGATCCTCACGGAGCGTGGCTACAGCTTCACCACCACGG
  * ** ** ******** ***** ******** ********** **** ***** *

1)CTGAGCGCGAGATCGTGCGCGACATCAAGGAGAAGCTATGCTACGTGGCCCTGGACTTCG
2)CTGAGCGCGAGATCGTGCGCGACATCAAGGAGAAGCTGTGCTACGTGGCCCTGGACTTCG
3)CTGAACGTGAGATTGTGCGCGACATCAAAGAGAAGCTGTGCTATGTGGCCCTGGACTTCG
4)CCGAGCGGGAAATCGTCCGTGACATCAAGGAGAAGCTCTGCTACGTGGCCCTGGACTTCG
5)CCGAGAGGGAAATCGTGCGTGACATCAAGGAGAAGCTCTGCTATGTCGCCCTGGACTTCG
  * **  * ** ** ** ** ** ******** ******** ***** ** **********

1)AGAACGAGATGGCCACCGCCGCCTCCTCCTCCTCCCTGGAGAAGAGCTACGAGCTGCCAG
2)AGAACGAGATGGCGACGGCCGCCTCCTCCTCCTCCCTGGAAAAGAGCTACGAGCTGCCAG
3)AGAATGAGATGGCCACCGCTGCCTCTTCCTCCTCCCTGGAGAAGAGCTATGAGCTGCCCG
4)AGCAGGAGATGGCCACCGCGGCCTCCAGCTCCTCCCTGGAGAAGAGCTACGAGCTGCCGG
5)AGCAGGAGATGGCCACCGCGGCCTCCAGCTCTTCCCTGGAGAAGAGCTACGAGCTGCCCG
  ** * ******** ** ** *****  *** ******** ******** ******** *
```

Figure C1. PCR Conditions.

Fwd. primer- 19 bp
(CCATCATGCGCCTGGACCT)

Start- 630 of 1374 bp sequence (2).

Rev. primer- 22 bp
(CGTAGCTCTTCTCCAGGGAGGA)

Finish- 830 of 1374 bp sequence (2).

Amplicon size- 201 bp

Annealing temp.- 62°C

Cycles- 35

Perkin Elmer Amplitaq Gold Polymerase

Figure D. Actin PCR product run on a 1.5% agarose gel, alongside a 100bp marker.

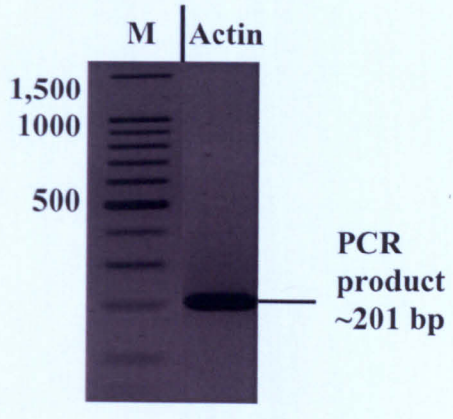

Figure E. DNA sequencing of PCR product.

GACTACCTGATGAAGATCCTCACCGAGCGTGGCTACTCCTTCG
TGACCACAGCTGAGCGCGAGATCGTGCGCGACATCAAGGAGA
AGCTATGCTACGTGGCCCTGGACTTCGAGAACGAGATGGCCA
CCGCCGCCTCCTCCTCCTCCC
(148 bp sequenced)

Figure F. Significant sequences from BLAST search of sequence in Fig. E.

Significant sequence alignment to:

Acc.No.	Species	Description	Identities	Score (bits)	E value
J00068	Human	α-Actin	144/148 (97%)	262	2e-67
NM_174225	Bovine	α-Actin	142/148 (95%)	246	1e-62
U16368	Porcine	α-Actin gene	99/99 (100%)	196	9e-48

APPENDIX A19: ALPHA-TUBULIN

Figure A. Available Alpha-tubulin sequences.

No.	Acc.No.	Species
1)	AU059326	Porcine (clone, EST)
2)	AF251146	Ovine
3)	AF081484	Human
4)	K00558	Human

Figure B. Multiple alignment of sequences for Alpha-tubulin. PCR target region and primer locations are included.

```
1) GTGCACAGGTCTTCAGGGCTTCTTGGTTTTCCACAGCTTTGGCGGGGGAA
2) ATGCACAGGTCTTCAAGGCTTCTTGGTTTTCCACAGCTTTGGTGGGGGAA
3) GTGCACCGGTCTTCAGGGCTTCTTGGTTTTCCACAGCTTTGGTGGGGGAA
4) GTGCACCCGTCTTCAGGGCTTCTTGGTTTTCCACAGCTTTGGTGGGGGAA
   *****  ******* ********************************* *******

1) CGGGTTCTGGGTTCACCTCCCTGCTGATGGAACGTCTCTCTGTCGATTAT
2) CTGGTTCTGGGTTCACCTCCCTGCTGATGGAACGCCTCTCTGTCGATTAT
3) CTGGTTCTGGGTTCACCTCCCTGCTCATGGAACGTCTCTCAGTTGATTAT
4) CTGGTTCTGGGTTCACCTCCCTGCTCATGGAACGCCTGTCAGTTGATTAT
   * ************************ ******** ** ** ** ******

1) GGCAAGAAGTCCAAGCTGGAGTTCTCCATTTACCCAGCCCCCCAGGTTTC
2) GGCAAGAAGTCCAAGCTGGAGTTCTCCATTTACCCAGCCCCCCAGGTTTC
3) GGCAAGAAGTCCAAGCTGGAGTTCTCCATTTACCCAGCACCCCAGGTTTC
4) GGCAAGAAATCCAAGCTGGAGTTCTCCATTTACCCGGCACCCCAGGTTTC
   ******** ************************** ** ***********

1) CACAGCTGTAGTTGAGCCCTACAACTCCATCCTCACCACCCACACCACCC
2) CACAGCTGTCGTTGAGCCCTACAACTCTATCCTCACCACCCACACCACCC
3) CACAGCTGTAGTTGAGCCCTACAACTCCATCCTCACCACCCACACCACCC
4) CACAGCTGTAGTTGAGCCCTACAACTCCATCCTCACCACCCACACCACCC
   ********* ***************** ************************

1) TGGAGCACTCTGATTGTGCCTTCATG------------------------
2) TGGAGCACTCTGATTGTGCCTTCATGGTAGACAATGAGGCCATCTATGAC
3) TGGAGCACTCTGATTGTGCCTTCATGGTAGACAATGAGGCCATCTATGAC
4) TGGAGCACTCTGATTGTGCCTTCATGGTAGACAATGAGGCCATCTATGAC
   *************************
```

Figure C1. PCR Conditions.

Fwd.primer- 19 bp
(GTCTTCAGGGCTTCTTGGT)

Start- 26 of 243 bp sequence (1).

Rev.primer- 20 bp
(CATGAAGGCACAATCAGAGT)

Finish- 243 of 243 bp sequence (1).

Amplicon size- 218 bp.

Annealing temp.-54°C

Cycles- 35

Promega Taq Polymerase

Figure D. Gel purified α-Tubulin PCR product run on a 1.5% agarose gel, alongside a 100bp marker.

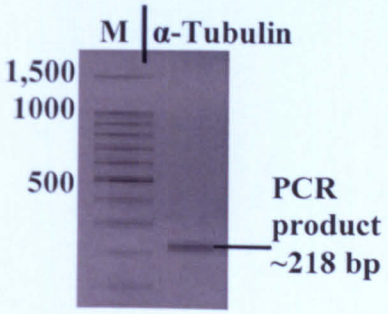

Figure E. DNA sequencing of PCR product.

GGGGGACGGGTTCTGGGTTCCCTCCCTGC
TGATGGAACGTCTCTCTGTCGATTATGGC
AAGAAGTCCAAGCTGGAGTTCTCCATTTA
CCCAGCCCCCCAGGTTTCCACAGCTGTAG
TTGAGCCCTACAACTCCATCCTCACCACC
CACACCACCCTGGAGCACTCT
(166 bp sequenced)

Figure F. Significant sequences from BLAST search of sequence in Fig. E.

Significant sequence alignment to:

Acc.No.	Species	Description	Identities	Score (bits)	E value
AF251146	Ovine	α-Tubulin	155/159 (97%)	276	1e-71
AF081484	Human	α-Tubulin	154/158 (96%)	268	3e-69
AB099045	Bovine	α-Tubulin (partial cds clone)	134/138 (97%)	226	1e-56

APPENDIX A20: TFIID (Transcription Factor II D)

Figure A. Available TFIID sequences.

No.	Acc.No.	Species
1)	D01034	Murine
2)	M55654	Human

N.B. No Porcine sequence data available.

Figure B. Multiple alignment of sequences for TFIID. PCR target region and primer locations are included.

```
1)AAAGACCATTGCACTTCGTGCAAGAAATGCTGAATATAATCCCAAGCGATTTGCTGCAGT
2)AAAGACCATTGCACTTCGTGCCCGAAACGCCGAATATAATCCCAAGCGGTTTGCTGCGGT
  ********************  **** ** ****************** ******** **

1)CATCATGAGAATAAGAGAGCCACGGACAACTGCGTTGATTTTCAGTTCTGGAAAAATGGT
2)AATCATGAGGATAAGAGAGCCACGAACCACGGCACTGATTTTCAGTTCTGGGAAAATGGT
  ******** ************** ** ** **  ***************** ********

1)GTGCACAGGAGCCAAGAGTGAAGAACAATCCAGACTAGCAGCAAGAAAATATGCTAGAGT
2)GTGCACAGGAGCCAAGAGTGAAGAACAGTCCAGACTGGCAGCAAGAAAATATGCTAGAGT
  **************************** ******** ************************

1)TGTGCAGAAGTTGGGCTTCCCAGCTAAGTTCTTAGACTTCAAGATCCAGAACATGGTGGG
2)TGTACAGAAGTTGGGTTTTCCAGCTAAGTTCTTGGACTTCAAGATTCAGAACATGGTGGG
  *** *********** ** ************** *********** ****************

1)GAGCTGTGATGTGAAGTTCCCCATAAGGCTGGAAGGCCTTGTGCTGACCCACCAGCAGTT
2)GAGCTGTGATGTGAAGTTTCCTATAAGGTTAGAAGGCCTTGTGCTCACCCACCAACAATT
  ******************** ** ****** * ************** ******** ** **
```

Figure C1. PCR Conditions.

Fwd. primer- 19 bp (AAGACCATTGCACTTCGTG)

Start- 782 of 1876 bp sequence(2).

Rev. primer- 20 bp (ACATCACAGCTCCCCACCAT)

Finish- 1032 of 1876 bp sequence (2).

Amplicon size- 251 bp

Annealing temp.- 53°C

Cycles- 35

Promega Taq Polymerase

Figure. Gel Purified TFIID PCR product, run on a 1.5% agarose gel, alongside a 100bp marker.

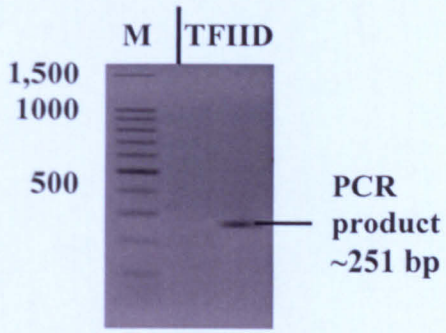

Figure E. DNA sequencing of PCR product.

TCCCAGCGATTTGCTGCTGTAATCATGAGAATAAGAGAACCC
CGGACCACCGCACTGATATTCAGCTCTGGGAAAATGGTGTGC
ACGGGAGCCAAGAGTGAAGAACAGTCCAGACTAGCAGCAAG
AAAATATGCCAGAGTTGTACAGAAGTTGGGTTTTCCAGCTAA
ATTCTTGGACTTCAAGATTCAGAACATG
(195 bp sequenced)

Figure F. Significant sequences from BLAST search of sequence in Fig. E.

Significant sequence alignment to:

Acc.No.	Species	Description	Identities	Score (bits)	E value
M55654	Human	TFIID	178/191 (93%)	276	2e-71
D01034	Murine	TFIID	171/191 (89%)	220	8e-55
XM_217785	Rat	TFIID	168/191 (87%)	196	1e-47

APPENDIX B. CLOSE-MATCHED RELATED SEQUENCES

Sequence information listed in Appendix B links directly to 5.3 Northern Blot Radioactive Probe Testing section within Chapter 5, cDNA Probe Development.

As explained within the cDNA Probe Development section, no porcine data exists for many sequences, and multiple band signals/ unexpected band sizes on Northern test-blots (using porcine RNA) was observed. Therefore, additional closely-related mRNA sequences of interest were searched for, by performing BLAST searches, on those specific cDNA probe sequences generated, and used in Northern blot probing.

mRNA sequences of similar sizes to Northern band signals,- with high bit scores, E Values and sequence similarity values; that may explain band identities were searched for, and listed in figure. A: Probe number and name (abbreviated); related sequence accession number, species, description, size and sequence identity value is included.

Figure A-B-1. Close-matched mRNA sequences (related to cDNA-probe/expressed gene). *Similar-sized to band signals produced in porcine RNA Northern test-blots (see 5.3 Northern Blot Radioactive Probe Testing), are presented below. Abbreviations = Casp-3 (Caspase-3), Ubiq (Ubiquitin), At-1 (Atrogin-1) and Calp-3 (Calpain-3). Seq. Id. (Sequence Identities), in bp and %.*

cDNA Probe	Related sequences of interest: Acc.No. - Species	Description of related sequences (mRNA).	Size (Bp)	Seq. Id.
(3) Casp-3	NM 032991 - Human	Caspase-3 transcript variant beta.	2479	186/206 (90%)
	NM 004346 - Human	Caspase-3 transcript variant alpha.	2646	186/206 (90%)
	U13737 - Human	Caspase-3 isoform alpha.	2635	186/206 (90%)
(9) E2G1	NM 003342 - Human	E2G1 transcript variant 1.	2626	200/213 (93%)
(11) Ubiq	AF038129 - Ovine	Polyubiquitin, UbB.	1102	141/156 (90%)
	AF506969 - Equine	Ubiquitin.	1157	144/156 (92%)
	NM 018955 - Human	Ubiquitin B.	971	153/169 (90%)
	AB009010 - Human	Polyubiquitin, UbC.	2192	143/153 (93%)
	D17296 - Rat	Polubiquitin, UbC.	2545	152/166 (91%)
	NM 019639 - Murine	Ubiquitin C.	2661	141/153 (92%)
(12) At-1	NM 058229 - Human	F-box protein 32 transcript variant 1.	1530	232/247 (93%)
	AJ420108 - Human	F-box protein 32.	1391	232/247 (93%)
(15) Calp-3	AF087569 - Bovine	Skeletal muscle-specific calpain.	2955	134/142 (94%)
	AF087570 - Ovine	Skeletal muscle-specific calpain.	3165	134/142 (94%)
	NM 212465 - Human	Calpain-3 transcript variant 7.	3243	131/145 (90%)

APPENDIX C. OLIGONUCLEOTIDE PROBES AND PRIMERS FOR REAL-TIME PCR

Gene of interest	cDNA sequence accession no. and species	Start and finish bp no. of amplicon	Amplicon size	Forward and Reverse oligonucleotide primer and Taqman probe sequences.
Calpain-1	AF263610, porcine	Start = 1104 bp Finish = 1204 bp	101 bp	Fwd. (16 bp): CGGGAGCCAGCTCCGGG Rev. (20 bp): GGTGTCAGGTTGCAGATCTC
Calpain-2	M23254,human	Start = 1355 bp Finish = 1455 bp	101 bp	Fwd. (19 bp): GTGGGCCTCATCCAGAAGC Rev. (19 bp): CCAGTCAACTCCTCTGGAA
Calpain-3	AF087569, bovine	Start = 1538 bp Finish = 1640 bp	103 bp	Fwd. (19 bp): GGAGGAAGGACCGGAAGCT Rev. (19 bp): TCCTTCTGCAGGTGCTGCT Taqman-probe (28 bp): FAM-TCGCCATCTACGAGGTTCCCAAAGAGAT-TAMRA
Calpastatin	L14450, bovine	Start = 1606 bp Finish = 1713 bp	108 bp	Fwd. (21 bp): CGTCTCTGAAGTGGTTTCCCA Rev. (18 bp): AGCTGATCCAGGGCATCGT
Actin	J00068, human	Start = 764bp Finish = 864 bp	101 bp	Fwd. (18 bp): GTGGCCCTGGACTTCGAG Rev. (19 bp): TTGCCGATGGTGATGACCT
18 s	X03205,human	Start = 898 bp Finish = 998 bp	101 bp	Fwd. (20 bp): *TTCGGAACTGAGGCCATGAT* Rev. (20 bp): TTTCGCTCTGGTCCGTCTTG Taqman-probe (26 bp): FAM-TTGCGCCGCTAGAGGTGAAATTCTTG-TAMRA

Using the Primer Express package (ABI Biosystems), oligonucleotide primers and dual labelled fluorescent probes were designed specifically for those expressed genes of interest: μ- and *m*- calpains, calpain -3, calpastatin, actin and 18 S. The computer package searched for optimal sequence and amplicons, with the optimal amplicon size set at 100 bp. Indicated are the cDNA sequences that were used for designing primers and probes, the region of amplification and primer and probe sequences. Note: for ubiquitous μ- and *m*- calpains non-bovine sequences were inputted into primer express as primer region was identical to bovine sequence.

APPENDIX D. REAL-TIME PCR STANDARD CURVE DATA

As described within Chapters 3 and 4, a standard curve was generated by Real-Time PCR for the ubiquitously expressed μ- and *m*- calpains, muscle-specific calpain-3, calpastatin, actin and 18S. The results are summarised within Chapter 4 and the raw data and curves is as follows for each expressed gene:

Figure A-D-1. Graph to show standard curves for (A) μ-Calpain, (B) *m*-Calpain, (C) Calpain-3, (D) Calpastatin and (E) Actin and (F) 18S. *Table shows amount of total RNA equivalents used to generate 1st strand cDNA using random primers (ng), log total RNA and average Ct value. Identified is the slope of the best fit line for the points plotted.*

(A)

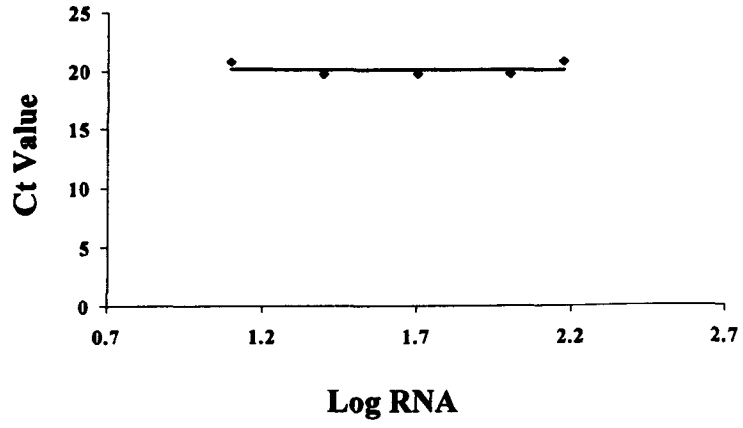

Total RNA (ng)	log RNA	Avg. Ct
150	2.20	20.78
100	2.00	19.76
50	1.70	19.71
25	1.40	19.76
12.5	1.10	20.78

Slope = -0.102

R^2 = 0.0061

(B)

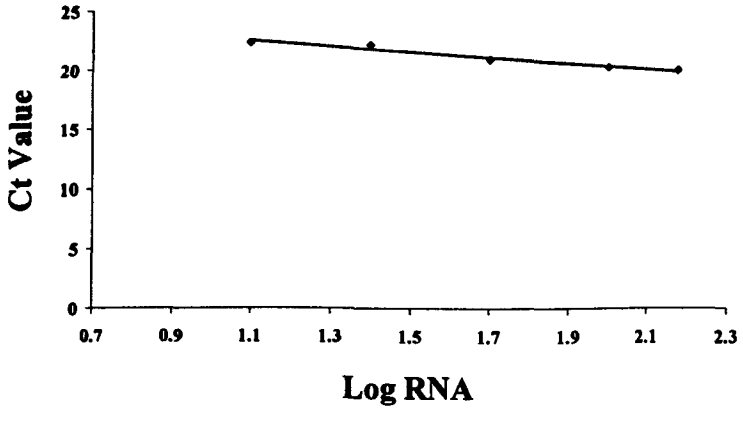

Total RNA (ng)	log RNA	Avg. Ct
150	2.18	19.77
100	2.00	20.11
50	1.70	20.79
25	1.40	22.12
12.5	1.10	22.33

Slope = -2.5887

R^2 = 0.9601

(C)

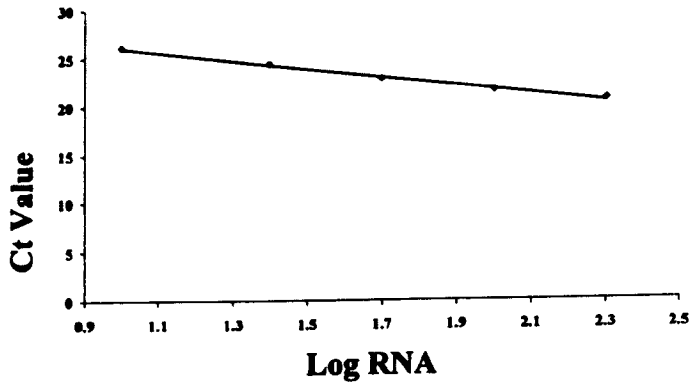

Total RNA (ng)	log RNA	Avg. Ct
200	2.30	20.74
100	2.00	21.71
50	1.70	22.91
25	1.40	24.44
10	1.00	26.08

Slope = -4.1955

R^2 = 0.995

(D)

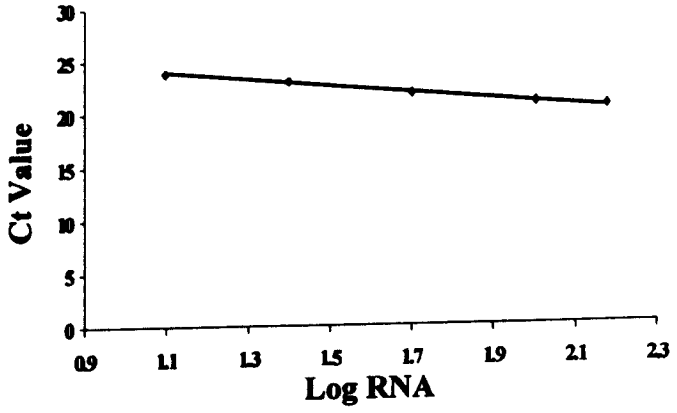

Total RNA (ng)	log RNA	Avg. Ct
150	2.17	20.60
100	2.00	21.00
50	1.70	21.96
25	1.40	23.10
12.5	1.10	23.91

Slope = -3.1455

R^2 = 0.9954

(E)

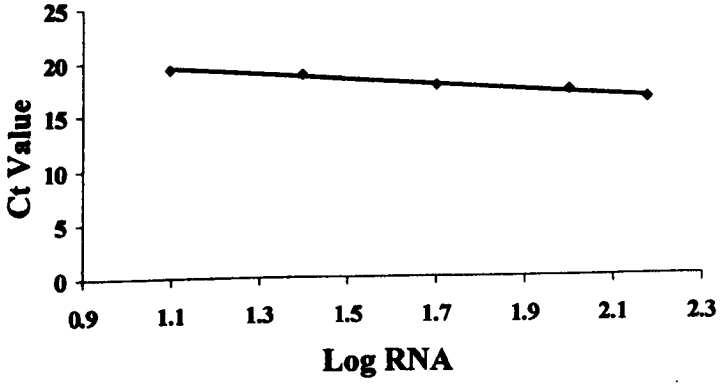

Total RNA (ng)	log RNA	Avg. Ct
150	2.20	16.20
100	2.00	17.00
50	1.70	17.60
25	1.40	18.70
12.5	1.10	19.20

Slope = -2.8118

R^2 = 0.9832

(F)

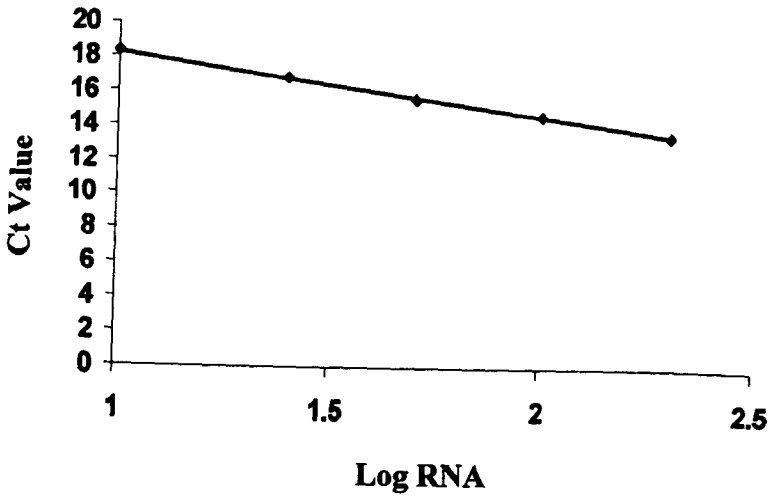

Total RNA (ng)	log RNA	Avg. Ct
200	2.30	13.70
100	2.00	14.80
50	1.70	15.70
25	1.40	16.80
10	1.00	18.30

Slope = -3.4888

R^2 = 0.9988

APPENDIX E. IMAGE CLONES

EST clone match to human Cathepsin-D: Accession No. BM471202, IMAGE Clone No. 5563106, Clone name- 11567-d21. 983 bp insert within 4396 bp pCMV-SPORT6 Ampicillin-resistant vector. EST clone match to human Calpain-10: Accession No. BQ057475, IMAGE Clone No. 5813098, Clone name- CM2064-j11. 1048 bp insert within 1815 bp pOTB7, Chloramphenicol resistant vector. A full vector map for both can be found at http://www.hgmp.mrc.ac.uk/geneservice/rea.../ products/datasheets/MGC/plate_info.shtml). Both clones were Purchased as a 'stab agar' sample, i.e. clones had been streaked onto LB agar containing 50 μg/ml ampicillin/12.5 μg/ml Chloramphenicol. Clones were stored at 4°C and re-streaked onto duplicate LB-agar plates containing ampicillin (100 μg/ml)/Chloramphenicol (12.5 μg/ml). Cathepsin-D clone was incubated overnight at 37°C, Calpain-10 for 24 hr at 33°C.

Single colonies grown on LB-agar plates were picked using sterile pipette and grown in 3 mls LB media containing ampicillin (100 μg/ml) for the Cathepsin-D IMAGE clone and Chloramphenicol (12.5 μg/ml) for Calpain-10 IMAGE clone.

Both IMAGE clones were grown up as described previously (Section 3.9) incubating sterilins overnight at 37°C with shaking and plasmid DNA purified using Promega miniprep method described previously.

IMAGE Clone Digest Procedure

IMAGE clones were linearised using similar RE digest procedure described in Section 3.11. For Cathepsin-D IMAGE Clone, a single Nco I RE digest was performed. The Calpain-10 IMAGE Clone was linearised using EcoR I. Both digested IMAGE Clones were separated by non-denaturing gel electrophoresis (Section 3.6) using a 1.5% agarose in 1X TAE gel and checked for linearisation (see Figure A-E-1).

Figure A-E-1. An example of linearised IMAGE Clones. *Figure below shows examples of un-cut and linearised IMAGE Clones. The samples loaded were IMAGE Clones digested with EcoR I, including Calpain-10, with lambda/hind III DNA markers at either end of gel.*

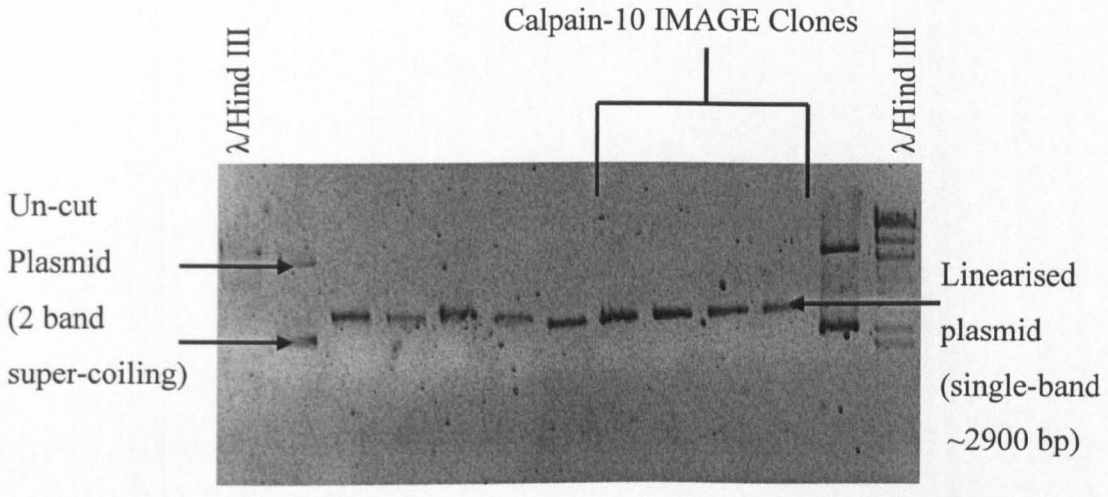

Image clones were subsequently 'cleaned-up' using a routine ethanol precipitation procedure (see Section 3.12)

APPENDIX F. MIDI-PREP PURIFIED PLASMIDS

Large quantities of Caspase-3, -6, Cathepsin-L, -H, E2G1 and Atrogin-1 cDNA probe sequences were grown up from glycerol stocks and purified using plasmid midi-prep procedure. These probes are described in Section 5.2.

cDNA inserts were excised from pGEM®-T Easy Vectors using an EcoR I RE digest (as above). As can be seen from figure all inserts were 200-300 bp, however analysis of the E2G1 sequence suggested it had an internal EcoR 1 cut site, as it was a small size following digest. Another digest was performed using Not 1 (10 U/ µl) RE and Buffer D and samples run by electrophoresis (Figure A-F-1).

Figure A-F-1. Non-denaturing gel electrophoresis of Midi-Prep purified plasmids +inserts. *cDNA inserts excised from pGEM®-T Easy Vectors by RE digest (as above), for E2G1, using Not 1 digest. 100 bp markers are run alongside.*

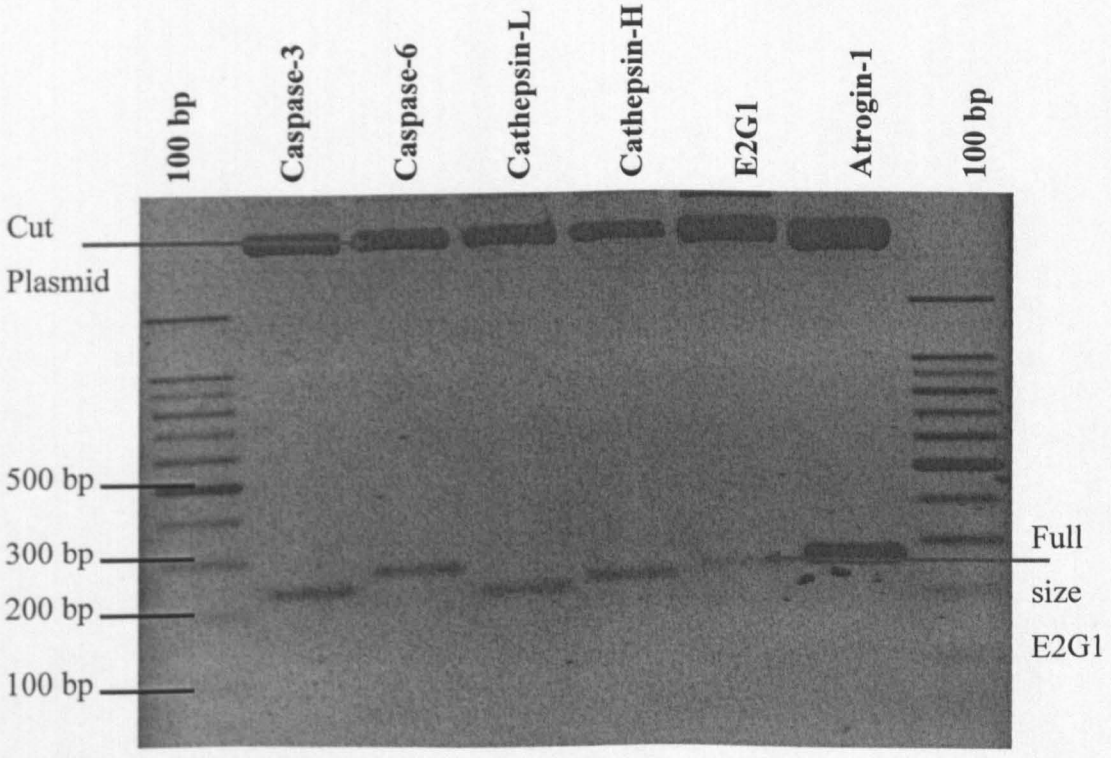

APPENDIX G. CALF DIET

(Calf diet used for the trial outlined in Chapter 4)

BOCM Pauls Beef Super Grade Diet

This diet contains: Wheat, palm kernal explant, low glucosinolate rape seed extract, soya bean hulls, shea nut extract, molasses, calcium carbonate, cocoa hulls, bakery by-product, as declaired by BOCM Pauls.

	g/kg dry matter
Dry Matter (DM)	862
ME	9.05 MJ/kg
Oil	38.8
Protein	129.3
Fibre	103.4
Ash	77.6
Vitamin A	7000 iu/kg
Vitamin D	2000 iu/kg
Vitamin E	25 iu/kg
Sodium Selenite	0.0003 mg/g
Copper Sulphate	0.0350 mg/g

Hay

Measured in the University of Nottingham Laboratory

	g/kg dry matter
Dry Matter (DM)	940.7 g/kg
Gross Energy	16.22 MJ/kg
Nitrogen	9.76 g/kg

APPENDIX H. CALF LD MUSCLE SAMPLES

RNA samples randomly selected were allocated a number (1-24), with 1-12 corresponding to slaughter date 1, and 13-24: slaughter date 2; which was used throughout trial analysis, i.e. for gel loading patterns etc. Note: sample 00534 (21 in table) was missing from sample stocks at the time analysis was performed.

Table A-H-1. Randomly selected LD samples allocated number 1-24. *Table shows corresponding eartag number, treatment group and slaughter date (S): 1/ 2 = 1st/2nd slaughter. Sample 21 in italics as not present during time of sample analysis.*

No.	Eartag No.	Group	S	No.	Eartag. No.	Group	S
1	400149	HIGH	1	13	300141	HIGH	2
2	700039	REFED	1	14	700042	LOW	2
3	02497	HIGH	1	15	600001	REFED	2
4	300007	LOW	1	16	400005	LOW	2
5	400012	LOW	1	17	100031	HIGH	2
6	300004	REFED	1	18	700044	REFED	2
7	300163	REFED	1	19	100161	REFED	2
8	200140	HIGH	1	20	600034	HIGH	2
9	700037	LOW	1	***21***	***00534***	***LOW***	***2***
10	600003	HIGH	1	22	700004	HIGH	2
11	500002	LOW	1	23	500042	REFED	2
12	300045	REFED	1	24	200091	LOW	2

APPENDIX I. PIG DIET

Pig diet used for the trial outlined in Chapter 5

STANDARD FINISHER DIET

Constituent	Kg/tonne
Barley	300
Wheat	393
Hi Pro Soya	275
DCP	9
Mineral 314	12.5
Vitamin E 50	1
Salt	2.7
Limestone	6.8

APPENDIX J. RNA EXTRACTION REAGENTS

Table A-J-1. Chemical reagents used for RNA extraction procedure

Reagent	Composition	Final Conc.
Denaturing Solution	250 g Guanidinium Thiocyanate 293 ml Water 17.6 ml 0.75M Sodium Citrate, pH 7 26.4 ml 10% Sarcosyl	4M 25 mM 0.5%
β-mercaptoethanol	0.36 ml / 50ml Denaturing Solution	0.1M
Sodium Acetate, pH 4		2M
Sodium Acetate, Ph 7		4M
Phenol (water saturated)	Phenol liquefied 80 w/w in water	
Chloroform Isoamyl alcohol	Chloroform and Isoamyl alcohol in ratio of 49:1	
Isopropanol (Propan-2-ol)		
Ethanol		100% and 75%

APPENDIX K. NORTHERN BLOTTING REAGENTS

Table A-K-1. Northern Blotting procedure reagent list

Reagent	Composition	Final Conc.
Sodium Phosphate, pH6.5	15.6g in 1L double-distilled H_2O. DEPC-treated (0.05% w/v), autoclaved X3.	100mM
Sodium Phosphate, pH6.5	made up from 100mM stock with double-distilled, DEPC-treated, autoclaved(X3) water.	10mM
Sodium Phosphate, pH6.5	made up from 100mM stock with double-distilled, DEPC-treated, autoclaved(X3) water.	80mM
RNA Markers	A ladder of nine RNA transcripts. Sizes: 281, 623, 955, 1383, 1908, 2604, 3638, 4981 and 6583.	
Glyoxal DMSO	40% solution deioinised as described below.	
Loading Buffer	50% glycerol 10mM Sodium Phosphate,pH 6.5 Bromophenol Blue	
SSC	175.3 g 3M NaCl 88.2 g 0.3M NaCitrate made to 1L with double-distilled, DEPC-treated, autoclaved(X3) water.	20X
Ammonium Acetate	7.7 g dissolved in 1 L double-distilled de-ionised water	0.1M

Glyoxal-40%: Solution was de-ionised by adding 20 ml to a 50 ml sterile screw capped centrifuge tube (Sarstedt, Numbrecht, Germany), adding 20 g AG501 ion exchange beads (Biorad) and mixed at room temperature by gentle shaking. Beads were centrifuged down for 5 min at 3,000 g, supernatant was removed and added to another 50 ml sterile screw capped centrifuge tube containing 4 g beads. Beads were shaken gently for 30 min at room temperature and same process repeated until beads turned from blue to gold (i.e. beads exhausted).

APPENDIX L. BACTERIAL GROWTH MEDIA

LB MEDIUM (per 100 ml)	
1.0g	Bacto-tryptone (Oxoid, Basingstoke, UK)
0.5g	Yeast extract (Oxoid, Basingstoke, UK)
1.0g	NaCl

Bacto-tryptone, yeast extract and NaCl are mixed in a clean container, with double distilled water added. Whilst solution is stirred continuously, pH is made up to 7.0, by addition of NaOH. Solution is autoclaved and allowed to cool to room temperature.

LB AGAR PLATES WITH AMPICILLIN (200 ml/~7-8 plates)	
2.0g	Bacto-tryptone (Oxoid, Basingstoke, UK)
1.0g	Yeast extract (Oxoid, Basingstoke, UK)
2.0g	NaCl
3.0g	Agar (Oxoid, Basingstoke, UK)
200µl	Ampicillin (100 µg/ml)

Bacto-tryptone, yeast extract, NaCl and Agar are mixed up in a sterile container with double-distilled water (made up to 200 ml final volume), autoclaved, left to cool to room temperature, 100 µg/ml ampicillin added (i.e. 200 µl), mixed and poured equally into 7-8 petri dishes.

SOC MEDIUM (100 ml)	
2.0g	Bacto-tryptone (Oxoid, Basingstoke, UK)
0.5g	Yeast extract (Oxoid, Basingstoke, UK)
1ml	1M NaCl
0.25ml	1M KCl
1ml	2M Mg^{2+} stock, filter-sterilised
1ml	2M glucose, filter-sterilised

Bactotryptone, yeast extract, NaCl and KCl are added to 97 ml double-distilled water, stirred, autoclaved, and left to cool to room temperature. 2M Mg^{2+} stock (20.33 g $MgCl_2.6H_2O$ and 24.65 g $MgSO_4.7H_2O$, made up to 100 ml with double-distilled water) and 2M glucose are added, final volume made up to 100 ml with double-distilled water; filtered through a 0.2 µm filter, and checked final pH is 7.0.